

DISSERTATION SUMMARY

A STRUCTURAL DESIGN PROCEDURE FOR EMULSION TREATED PAVEMENT LAYERS

JOHANNES JACOBUS ERASMUS LIEBENBERG

A dissertation submitted in partial fulfilment of the requirements for the degree of:

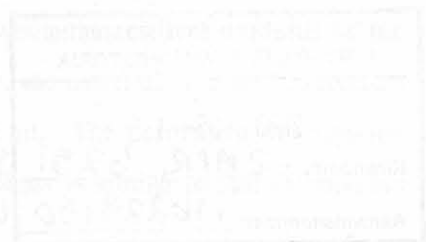
MASTER OF ENGINEERING (TRANSPORTATION ENGINEERING)

In the

**FACULTY OF ENGINEERING, BUILT ENVIRONMENT
AND INFORMATION TECHNOLOGY**

UNIVERSITY OF PRETORIA, PRETORIA

JANUARY 2003



DISSERTATION SUMMARY

A STRUCTURAL DESIGN PROCEDURE FOR EMULSION TREATED PAVEMENT LAYERS

JJE LIEBENBERG

Supervisor: Professor AT Visser
Department: Civil and Biosystems Engineering
University: University of Pretoria
Degree: Master of Engineering (Transportation Engineering)

The use of bitumen emulsion treated pavement layers is well established and is becoming more popular in road building. Current structural design procedures include mainly empirical methods or methods derived from laboratory studies. No design method based on results from accelerated pavement testing of full scale pavements currently exists and no provision for emulsion treated materials exists in the South African Mechanistic Pavement Design Method or the TRH4 structural design guideline document on flexible pavements.

The need therefore existed to provide some guidelines on the structural design of emulsion treated materials based on accelerated pavement testing on a full-scale pavement. The aim of this research was to provide interim guidelines for the structural design from accelerated pavement testing supported by relevant laboratory testing.

A test section, constructed with an emulsion treated ferricrete, was subjected to Heavy Vehicle Simulator testing. Samples from the test site were tested in the laboratory to investigate the engineering properties of the material under different bitumen and cement contents. The laboratory study was used to determine parameters, which are important to the structural design procedure. Results from the laboratory study indicated that the cement content contributes towards the strength of the material, while the bitumen content contributes towards the flexibility of the material.

Results with the Heavy Vehicle Simulator indicated that the test section had a good resistance to permanent deformation. It was determined that the behaviour of the material was two-phased, similar to that of lightly cemented materials. During the first phase, the material demonstrates fatigue properties. The end of the fatigue life phase was defined to be when the resilient modulus of the material reduced to a value of 500 MPa. During the second phase, the material is in an "equivalent granular" phase with a reduced resistance to permanent deformation. The permanent deformation resistance behaviour of an emulsion treated material in its second phase is similar to that of unbound

granular materials. The concept of the stress ratio was introduced to describe the permanent deformation behaviour.

Failure criteria for fatigue and permanent deformation were developed and presented as a transfer function that can be used in the South African Mechanistic Pavement Design Method. The transfer functions were developed for different road categories and a design procedure is proposed.

Finally, a design catalogue for emulsion treated base layers was developed from these transfer functions and is presented.

SAMEVATTING VAN VERHANDELING

STRUKTURELE ONTWERPMETODE VIR EMULSIE BEHANDELDE PLAVEISELLAE

JJE LIEBENBERG

- Promotor:** Professor AT Visser
- Departement:** Siviele en Biosistiem Ingenieurswese
- Universiteit:** Universiteit van Pretoria
- Graad:** Magister in Ingenieurswese (Vervoeringenienswese)

Die gebruik van bitumen emulsie behandelde plaveisellae is goed gevestig en word al hoe meer populêr in die bou van paaie. Huidige ontwerpprosedures bestaan meestal uit empiriese metodes, of metodes ontwikkel uit suiwer laboratoriumstudies. Geen ontwerpmetode wat gebaseer is op volskaalse plaveiseltoetse bestaan tans vir emulsie behandelde materiale nie. Daar word ook nie voorsiening gemaak in die Suid-Afrikaanse Meganitiese Plaveiselontwerpmetode, of die TRH4, vir die gebruik emulsie behandeling nie.

Daar bestaan dus 'n behoefte na riglyne vir die strukturele ontwerp van emulsie behandelde materiale wat gebaseer is op volskaalse plaveiseltoetse. Die doel van hierdie studie was om voorlopige riglyne daar te stel vir die strukturele ontwerp van hierdie materiale wat verkry is uit die volskaalse plaveiseltoetse en relevante laboratoriumtoetse.

'n Toetsseksie van emulsie behandelde ferrikreet is gebou en onderwerp aan toetse met die Swaarvoertuignabootser. Monsters van die toetsseksie is in die laboratorium getoets om the invloed van verskillende sement en bitumen inhoude op die ingenieurseienskappe van die materiaal te ondersoek. Parameters wat belangrik is vir die strukturele ontwerp van emulsie behandelde materiale is in dié laboratoriumstudie bepaal. Resultate van die laboratoriumstudie dui aan dat die sement hoofsaaklik verantwoordelik is vir die sterkte van die materiaal, terwyl die bitumen bydra tot the buigsaamheid.

Die toetse onder die Swaarvoertuignabootser het daarop gewys dat die materiaal redelike goeie weerstand teen permanente vervormings besit. Dit is verder ontdek dat emulsie behandelde materiale 'n twee fase gedrag het wat soortgelyk is aan die van liggeselementeerde materiale. Gedurende die eerste fase het die materiaal vermoeiingseienskappe getoon. Die einde van dié fase is gedefinieer wanneer die elastiese veerkragsmodulus 'n waarde van 500 MPa bereik. Die tweede fase is 'n "ekwiwalente granulêre fase" waar die materiaal 'n verminderde weerstand teen permanente

vervorming het. Die permanente vervormingsgedrag van die materiaal is dieselfde as die van granulêre materiale. Die konsep van Spanningsverhouding, om die permanente vervormingsgedrag van die materiaal te beskryf, is voorgestel.

'n Swigtingsstandaard vir die vermoeiingsleef tyd en permanente vervorming is ontwikkel in die vorm van oorgangsfunksies, wat in die Suid-Afrikaanse Meganitiese Plaveiselontwerpmetode gebruik kan word. Die oorgangsfunksies is ontwikkel vir die verskillende kategorieë paaie in Suid Afrika.

Laastens is 'n katalogus ontwikkel vanaf die oorgangsfunksies wat die ontwerp van emulsie behandelde materiale kan vergemaklik. Die katalogus is ingesluit.

ACKNOWLEDGEMENTS

I wish to express my appreciation to the following organisations and persons who made this dissertation possible:

1. The dissertation is based on a research project by Oudtrans. Permission to use the material is gratefully acknowledged. The opinions expressed are those of the author and do not necessarily represent the policy of Oudtrans.

2. Oudtrans for the financial support on the laboratory and Heavy Vehicle/Semitrailer testing.

3. CSIR Transportek for the provision of data and the use of their facilities during the course of the study.

4. Gwynn Scott (Pty) and the University of Pretoria for their financial support.

The following persons are gratefully acknowledged for their assistance, interest and guidance during the course of study:

i) Dr. Penelle Lang of CSIR Transportek.

ii) Mr. Hechter Teyssie of CSIR Transportek.

iii) Ms. Elizabeth Sutzka of Oudtrans.

AAN: My ouers

iv) Mr. Berndt Verhaar (the **Lieb en Elsie Liebenberg** opportunity to use the facilities of CSIR Transportek).

v) Dr. Marius de Vries of CSIR Transportek.

vi) Mr. Willie Diedericks of CSIR Transportek who assisted for Heavy Vehicle testing, for his interest and dedication to the project.

vii) Mr. Philip Pothof of Newcast North (Pty) Ltd for the opportunity to use the facilities.

viii) Dr. Peter Swane for the fortunate being allowed to do my share of work in the development of the design catalogue.

ix) Gwynn Scott (Pty) as supervisor for this interesting project.

x) My family and friends for their encouragement, prayers and support during the study.

xi) To God, my creator and saviour, who blessed me with the ability to perform this study.

ACKNOWLEDGEMENTS

I wish to express my appreciation to the following organisations and persons who made this dissertation possible:

- a) This dissertation is based on a research project by Gautrans. Permission to use the material is gratefully acknowledged. The opinions expressed are those of the author and do not necessarily represent the policy of Gautrans.
- b) Gautrans for the financial support on the laboratory and Heavy Vehicle Simulator testing
- c) CSIR Transportek for the provision of data and the use of their facilities during the course of the study.
- d) Stewart Scott (Pty) and the University of Pretoria for their financial support.
- e) The following persons are gratefully acknowledged for their assistance, interest and guidance during the course of study:
 - i) Dr. Fenella Long of CSIR Transportek.
 - ii) Mr. Hechter Theyse of CSIR Transportek, .
 - iii) Ms. Elsbieta Sadzik of Gautrans.
 - iv) Mr. Bernoit Verhaeghe of CSIR Transportek for the opportunity to use the facilities at CSIR Transportek.
 - v) Dr. Morris de Beer of CSIR Transportek.
 - vi) Mr. Willie Diedericks of CSIR Transportek who operated the Heavy Vehicle Simulator, for his interest and devotion to the project
 - vii) Mr. Philip Joubert of Stewart Scott (Pty)Ltd. for the opportunity to do this work.
 - viii) Dr. Fritz Jooste for the software he developed in a very short time to assist in the development of the design catalogue.
- f) Professor AT Visser, my supervisor for his guidance and support.
- g) My family and friends for their encouragement, prayers and support during this study.
- h) To God, my creator and saviour, who blessed me with the ability to perform this study.

TABLE OF CONTENTS

CHAPTER 1 INTRODUCTION AND OBJECTIVES.....	1-1
1.1 Historical background.....	1-1
1.2 The use of bitumen emulsion in base layers.	1-2
1.3 The South African Mechanistic Pavement Design Procedure	1-3
1.4 The need for a formal design procedure for pavements with emulsion treated layers.	1-4
1.5 Objectives of the study	1-4
1.6 Scope and extent of the study	1-4
1.7 Structure of the dissertation.	1-5
1.8 References.....	1-5
 CHAPTER 2 MIX DESIGN AND ENGINEERING PROPERTIES OF EMULSION TREATED MATERIALS	 2-1
2.1 Introduction.....	2-1
2.2 History and background of emulsion treated material mix design	2-1
2.3 Emulsion treated material mix design in South Africa	2-2
2.4 The engineering properties of emulsion treated materials	2-5
2.5 Curing of emulsion treated layers.....	2-8
2.6 Conclusions.....	2-8
2.7 References.....	2-9
 CHAPTER 3 STATE OF THE ART ON THE STRUCTURAL BEHAVIOUR AND DESIGN OF EMULSION TREATED PAVEMENT LAYERS.....	 3-1
3.1 Introduction.....	3-1
3.2 The history and background to structural design of pavements containing emulsion treated materials.....	3-1
3.3 Failure mechanism of emulsion treated layers.....	3-2
3.4 The behaviour of emulsion treated pavement layers	3-3
3.5 Structural design of emulsion treated materials.....	3-7
3.6 References.....	3-21
 CHAPTER 4 MECHANISTIC-EMPIRICAL DESIGN MODELS IN PAVEMENT ENGINEERING.....	 4-1
4.1 Introduction to the Mechanistic – Empirical approach.....	4-1
4.2 Prerequisites for incorporating a new material into the mechanistic-empirical design process	4-1

4.3	Granular materials.....	4-2
4.4	Cemented layers.....	4-6
4.5	Asphalt materials	4-12
4.6	Subgrade materials.....	4-14
4.7	Mechanistic-empirical models applicable to emulsion treated materials.	4-16
4.8	Conclusions.....	4-17
4.9	References.....	4-18
CHAPTER 5 PERFORMANCE OF AN EMULSION TREATED GRAVEL UNDER LABORATORY AND HVS TESTING		5-1
5.1	Introduction.....	5-1
5.2	Experimental design	5-1
5.3	The influence of net bitumen and cement contents on the strength and flexibility of emulsion treated gravel materials	5-12
5.4	Static shear strength.....	5-20
5.5	Laboratory Elastic modulus (M_R)	5-22
5.6	Permanent deformation from dynamic triaxial testing	5-26
5.7	Heavy Vehicle Simulator (HVS)	5-28
5.8	Conclusions.....	5-39
5.9	Recommendations.....	5-41
5.10	References.....	5-42
CHAPTER 6 FATIGUE PROPERTIES OF EMULSION TREATED MATERIALS		6-1
6.1	Introduction.....	6-1
6.2	The end of the fatigue life.....	6-1
6.3	Tensile strain analysis.....	6-2
6.4	The Effective fatigue life of emulsion treated materials.....	6-5
6.5	Confidence limits.....	6-9
6.6	Fatigue life damage factor	6-11
6.7	Conclusions.....	6-12
6.8	References.....	6-12
CHAPTER 7 PERMANENT DEFORMATION PROPERTIES OF EMULSION TREATED MATERIALS		7-1
7.1	Introduction.....	7-1
7.2	Factors influencing the development of permanent deformation under repetitive loading	7-1
7.3	Permanent deformation model from Heavy Vehicle Simulator Data	7-1
7.4	Mechanistic analysis of Heavy Vehicle Simulator pavement for permanent deformation.....	7-2

7.5	Permanent deformation transfer function	7-7
7.6	Permanent deformation damage factor	7-12
7.7	Conclusions.....	7-13
7.8	References.....	7-13
CHAPTER 8 THE STRUCTURAL DESIGN OF EMULSION TREATED MATERIALS.....		8-1
8.1	Introduction.....	8-1
8.2	General pavement behaviour	8-3
8.3	Behaviour of emulsion treated materials	8-4
8.4	Material classification.....	8-5
8.5	Mechanistic analysis of emulsion treated pavement.....	8-9
8.6	Design catalogue.....	8-14
8.7	References.....	8-18
CHAPTER 9 CONCLUSIONS AND RECOMMENDATIONS.....		9-1
9.1	Conclusions.....	9-1
9.2	Recommendations.....	9-3
APPENDIX A.LABORATORY TEST RESULTS.....		A
APPENDIX B.OPTICAL MICROSCOPE PICTURES.....		B
APPENDIX C.SELECTED HEAVY VEHICLE SIMULATOR RESULTS.....		C
APPENDIX D.CONTOUR PLOTS OF STRESSES UNDER DUAL WHEEL LOAD.....		D
APPENDIX E.CALCULATION SHEETS FOR PAVEMENT STRUCTURES IN		
DESIGN CATALOGUE.....		E

LIST OF TABLES

Table 2.1	Mix design criteria for ETB's in terms of CBR and UCS.....	2-5
Table 3.1	LTPP sections for pavements with emulsion treated layers.....	3-3
Table 3.2	Early cure reduction factors for strength development of emulsion treated layers.....	3-10
Table 3.3	Suggested structural coefficients for recycled layers.....	3-12
Table 3.4	Resilient modulus values of emulsion treated base layers for each quarter for different full cure periods.....	3-13
Table 3.5	Average base temperatures in southern Africa.....	3-13
Table 3.6	Material properties for emulsion treated materials using the modification approach.....	3-15
Table 3.7	Allowable minimum safety factors at various traffic levels.....	3-16
Table 4.1	Allowable safety factors for granular materials at various traffic levels.....	4-3
Table 4.2	Typical effective range of elastic moduli for cement treated materials in various stages of behaviour.....	4-9
Table 4.3	Maximum allowable tensile strain in the bituminous layer according to Dormon and Metcalf (1964).....	4-13
Table 5.1	Tests on different combinations of cement and net bitumen contents.....	5-2
Table 5.2	Summary of HVS testing on sections 410A4, 410B4 and 412A4.....	5-11
Table 5.3	Summary of California Bearing Ratio (CBR) test results (0% cement).....	5-12
Table 5.4	Summary of Unconfined Compressive Strength (UCS) test results.....	5-13
Table 5.5	Summary of Indirect Tensile Strength (ITS) test results.....	5-14
Table 5.6	Summary of flexural beam fatigue test results.....	5-16
Table 5.7	Static triaxial test results calculated directly from M \ddot{o} hr circles.....	5-21
Table 5.8	Elastic modulus test results from the dynamic triaxial tests.....	5-24
Table 5.9	Summary of permanent deformation results from HVS tests.....	5-30
Table 5.10	Maximum deflection at end of test.....	5-31
Table 5.11	Crack development on HVS test sections.....	5-34
Table 5.12	Summary of backcalculated E moduli for HVS test sections.....	5-37
Table 5.13	Proposed values for strain at break for emulsion treated materials.....	5-41
Table 6.1	Life to crack initiation.....	6-4
Table 6.2	Effective fatigue life.....	6-6
Table 6.3	Confidence limits for different road categories.....	6-9
Table 6.4	Fatigue life damage factors for emulsion-treated gravel.....	6-12
Table 7.1	Permanent deformation life damage factors for emulsion-treated gravel.....	7-12
Table 8.1	Definition of main road categories used in pavement design.....	8-2
Table 8.2	Traffic classes according to TRH4:1996.....	8-3
Table 8.3	Proposed Classification of Emulsion treated materials.....	8-6

Table 8.4 Typical composition of emulsion treated material per class8-7

Table 8.5 Proposed emulsion treated material properties for structural design8-8

LIST OF FIGURES

Figure 2.1 Schematic overview of the ETB mix design process	2-4
Figure 2.2 Effect of cement content on CBR for G4 material	2-4
Figure 3.1 Backcalculated E-moduli at various HVS repetitions	3-5
Figure 3.2 Measured deflection basins at various repetitions.....	3-6
Figure 3.3 Design chart for ETB for subgrade modulus of 20 MPa (3 000 psi)	3-8
Figure 3.4 Fatigue criteria for emulsion treated material for 11% bitumen and 5% air voids by volume	3-9
Figure 3.5 Flow diagram for structural design of emulsion treated bases.....	3-14
Figure 3.6 Transfer function for shear failure for granular materials.....	3-16
Figure 3.7 Proposed design catalogue for emulsion treated materials by De Beer and Grobler (1994).....	3-18
Figure 3.8 Proposed design catalogue for emulsion treated materials by Theyse (1998)	3-19
Figure 4.1 Transfer function for granular materials	4-4
Figure 4.2 S-N curves for G1 to G6 materials at a terminal permanent strain of 20 000 $\mu\epsilon$	4-5
Figure 4.3 Comparison of the relationship between maximum tensile strain ratio (ϵ_s/ϵ_b) and number of strain repetitions to initiate effective fatigue cracking in cemented layers.....	4-8
Figure 4.4 Comparison of the fatigue criteria applicable to strongly cemented layers	4-9
Figure 4.5 Shift factor for cemented layers	4-11
Figure 4.5 Criteria for prediction of subgrade performance in Southern Africa	4-15
Figure 4.6 Emulsion treated materials relative to other materials	4-17
Figure 5.1 Typical set-up of the four point static beam test.	5-4
Figure 5.2 Typical Stress-Strain response measured during four-point beam test.	5-4
Figure 5.3 Typical result from the static triaxial test.....	5-6
Figure 5.4 Typical calculated results from a set of dynamic triaxial data	5-7
Figure 5.5 Overall view of the Heavy Vehicle Simulator	5-9
Figure 5.6 Test section layout for sections 410A4a and 410B4	5-10
Figure 5.7 Test section layout for section 412A4A.....	5-10
Figure 5.8 Influence of cement and net bitumen contents on the UCS	5-13
Figure 5.9 Influence of cement and net bitumen contents on the ITS	5-14
Figure 5.10 Influence of cement and net bitumen contents on the strain at break	5-17
Figure 5.11 Influence of cement and net bitumen contents on the stress at break	5-18
Figure 5.12 Influence of cement and net bitumen contents on the dissipated energy	5-18
Figure 5.13 Sample from laboratory (2 % cement, 1.8 % net bitumen), 32x magnification.....	5-19

Figure 5.14 Optical microscope images of emulsion treated materials with different net bitumen contents (0% cement)	5-19
Figure 5.15 $p_f - q_f$ diagram from static triaxial tests	5-22
Figure 5.16 M6hr stress circles representation of the stress ratio concept	5-23
Figure 5.17 Resilient modulus as a function of the various laboratory test variables	5-25
Figure 5.18 Resilient modulus vs. Bulk stress	5-25
Figure 5.19 Typical permanent deformation results as measured in a dynamic triaxial test	5-26
Figure 5.20 Influence of Relative Density, degree of saturation and stress ratio on the number of repetitions to 9 % plastic strain	5-27
Figure 5.21 Permanent deformation on HVS test sections as measured by the straight edge	5-29
Figure 5.22 Permanent deformation on HVS test sections as measured by the laser profilometer	5-29
Figure 5.23 Permanent deformation on HVS test sections as measured by the MDD module at 40 mm.	5-30
Figure 5.24 Maximum RSD elastic deflection per test section	5-31
Figure 5.25 Radius of curvature per test section	5-32
Figure 5.26 Deflection bowls per test section	5-32
Figure 5.27 MDD elastic in-depth deflections at MDD4 of test section 412A4 (40 kN test section).....	5-33
Figure 5.28 MDD maximum elastic deflection at 40 and 80 kN test loads.....	5-34
Figure 5.29 Final crack patterns	5-34
Figure 5.30 Test pit at section 410B4.....	5-35
Figure 5.31 Reduction of E-moduli of C3 material under trafficking	5-37
Figure 5.32 Back calculated E moduli for the different test sections	5-38
Figure 6.1 Tensile strain analysis	6-3
Figure 6.2 Schematic illustration of the initiation of cracks at the MDD at bottom of the layer	6-3
Figure 6.3 Horizontal tensile strains in the emulsion treated layer.	6-4
Figure 6.4 Life to crack initiation for ferricrete tested at HVS site near Vereeniging	6-5
Figure 6.6 Effective fatigue life for HVS tested emulsion treated material.	6-6
Figure 6.5 Reduction in stiffness with increase in load repetitions on HVS test sections.....	6-7
Figure 6.6 Effective fatigue life of an emulsion treated material	6-8
Figure 6.7 Confidence limits represented by a second function drawn parallel to the regression function.....	6-11
Figure 7.1 HVS permanent deformation model	7-2
Figure 7.2 Illustration of tensile strains and stresses developed in the linear elastic theory	7-3
Figure 7.3 M6hr circle with tensile minor principal stress	7-4
Figure 7.4 Adjusted M6hr circle with minor principal stress equals to zero	7-4

Figure 7.5 Contour plot of the stress ratio on the HVS pavement under 40 KN, 620 kPa dual wheel load.....	7-6
Figure 7.6 Contour plot of octahedral shear stress under a 40 kN, 620 kPa dual wheel load in a 250 mm thick emulsion treated layer.....	7-6
Figure 7.7 Recommended positions to calculate the critical Stress Ratio	7-7
Figure 7.8 Comparison between laboratory test results, HVS test results and foam bitumen study.....	7-8
Function 7.9 HVS transfer functions compared to foam bitumen model.....	7-9
Figure 7.10 HVS transfer functions compared to original laboratory data, shifted laboratory data and foam bitumen model.....	7-10
Figure 7.10 Transfer function for permanent deformation of emulsion treated materials.....	7-11
Figure 8.1 General behaviour of pavements.....	8-4
Figure 8.2 Illustration of different types of emulsion treated materials for structural design	8-5
Figure 8.3 Proposed Classification of emulsion treated materials.....	8-6
Figure 8.4 Effective fatigue transfer function for emulsion treated materials.....	8-10
Figure 8.5 Permanent deformation transfer function for emulsion treated materials	8-12
Figure 8.6 Calculating the ultimate pavement life for a pavement structure with emulsion treated layers.....	8-15
Figure 8.7 Structural design catalogue for ET1 emulsion treated base layers.....	8-16
Figure 8.8 Structural design catalogue for ET2 emulsion treated base layers.....	8-17
Figure 9.1 Influence of cement and net bitumen content on main engineering properties.....	9-2

LIST OF ABBREVIATIONS

AASHO	American Association of State Highway Officials
AASHTO	American Association of State Highway Transportation Officials
ASTM	American Standard Test Methods
CBR	California Bearing Ratio
COLTO	Committee of Land Transportation Officials
CSIR	Council for Scientific Industrial Research
CSRA	Committee of State Road Authorities
ETB	Emulsion treated base
GEMS	Granular emulsion mixes
GM	Grading modulus
HVS	Heavy Vehicle Simulator
ICL	Initial Consumption of Lime
ITS	Indirect Tensile Strength
LVDT	Linear Variable Displacement Transducer
MDD	Multi Depth Deflectometer
PI	Plasticity Index
SABITA	Southern Africa Bitumen and Tar Association
SAMPDP	South African Mechanistic Pavement Design Procedure
TRH	Technical Recommendations for Highways
UCS	Unconfined Compressive strength

LIST OF SYMBOLS

a'	structural coefficient for recycled layers used as base
a_1, a_2, a_3	AASTHO layer coefficients
B_V	Proportion of bitumen present in asphalt mix
c	Cohesion (kPa)
CDF	Cumulative damage factor (Miner's law)
c_{term}	Cohesion term
d	Thickness of asphalt layer (mm)
E	Modulus of elasticity (MPa)
e	natural logarithm = 2.718 281 828 46....
E_1	Elastic modulus of base layer (MPa)
E_2	Elastic modulus of subbase layer (MPa)
E_{bend}	Bending stiffness of beam (MPa)
E_i	Initial modulus of elasticity (MPa)
E_{bend}^i	Initial bending stiffness of beam (MPa)
FOS	Factor of safety
h_1	Thickness of base layer (mm or inches)
h_2	Thickness of subbase layer (mm or inches)
K	Constant indication moisture regime when calculating Factor of Safety
K_1, K_2	Constants describing stress sensitivity material
M_f	Final modulus (MPa)
M_R	Resilient modulus (MPa)
M_t	Modulus at specific time after construction @ 23°C (MPa)
N	Number of load repetitions
N_{c1}	Load repetitions to initiate crushing
N_{c2}	Load repetitions to advanced crushing
N_{eff}	Effective fatigue life

N_f	Number of load repetitions to failure
N_{ff}	Fatigue and fracture life
n_i	Damage of i^{th} load repetition
n_i	Number of load repetitions to crack initiation
N_{if}	Initial fatigue life
N_{PD}	Number of load repetitions to certain level of plastic strain
N_{std}	Number of load repetitions of standard wheel load to certain level of distress
N_t	Total number of allowable load repetitions
N_x	Number of load repetitions of wheel load to certain level of distress
Pen	Penetration of recovered bitumen
p_f	normal stress (kPa)
π	pi = 3.141 592 653 59...
P_{std}	Standard wheel load (kN)
P_x	wheel load (kN)
q_f	Shear stress (kPa)
RD	Relative density (%)
RF	Early cure reduction factor
S	Degree of saturation (%)
S	Sand equivalent value (#4 sieve to minus 200 mesh)
SF	Shift factor
SN	Structural number
SR	Stress ratio
t	Thickness of emulsion treated base layer (mm)
V_B	Bitumen content by volume (%)
V_V	Voids content (%)
σ_1^m	Maximum allowable major principal stress (kPa)
σ_1^a	Working or applied major principal stress (kPa)

σ	Applied stress from tri-axial test (kPa)
θ	Bulk stress (kPa)
α	Factor depending on amount of filler voids present in asphalt mix
ϕ	Friction angle (degrees)
ρ	relative density (lb/ft ³ or kg/m ³)
ε	Resilient strain measured (ε)
τ	Shear stress (kPa)
σ_1	Major principal stresses (kPa)
σ_2	Intermediate principal stress (kPa)
σ_3	Minor principal stresses (kPa)
ε_b	Strain at break ($\mu\varepsilon$)
σ_b	Stress at break (kPa)
σ_d	Deviator stress (kPa)
ε_i	Induced tensile strain due to loading ($\mu\varepsilon$)
ε_m	Tensile strain in asphalt mixture ($\mu\varepsilon$)
σ_{max}	Maximum stress (kPa)
ε_{mix}	Bending strain repeatedly applied to asphalt mixture ($\mu\varepsilon$)
ε_p	Permanent (plastic) strain (ε)
ε_t	Horizontal tensile strain ($\mu\varepsilon$)
σ_t	Vertical compressive stress on top of base layer \approx tyre contact pressure (kPa)
ϕ_{term}	Internal friction angle term (degrees)
ε_v	Vertical compressive strain ($\mu\varepsilon$)
σ_v	Vertical compressive strain (kPa)

CHAPTER 1 INTRODUCTION AND OBJECTIVES

1.1 HISTORICAL BACKGROUND

1.1.1 Roads

Transportation has been an important aspect of human life since the beginning of mankind. Roads linked ancient cities for purposes of trade. When empires arose, trade routes became a primary concern of kings for the stability of their governments. In ancient times roads served the needs of commerce, the military and the pilgrim.

The Encyclopaedia Britannica (1973) makes reference to Persian, Mesopotamian, Chinese and Indian roads during the pre-Roman time. These roads consisted mainly of clearing and levelling, with cuts and fills restricted to a minimum. Traffic was mainly restricted to pedestrians, horsemen, chariots and caravans.

The first scientific road builders were the Romans between 350BC and 200AD. They constructed roads of high standard for their time, with relatively straight horizontal and vertical alignments, various foundation layers and proper drainage. The pavement layers consisted of gravels with aggregates varying from 600 mm in size to as fine as sand. Stabilisation of layers consisting of sand or finer gravel with lime was not uncommon.

With the decline of the Roman, Chinese and Mayan empires, the road system fell into centuries of disrepair. In the last half of the 18th century the fathers of modern road building, Pierre-Marie-Jérôme Trésaguet (1716-1796), John Metcalf, Thomas Telford (1757-1834) and John Loudon MacAdam (1756-1836), applied their trade in France and England.

With the introduction of the motorcar, capable of high speeds, the alignment and road surfaces suitable only for horses and pedestrians were completely inadequate. This brought the importance of roads to the foreground that stimulated the need for research in pavement materials and pavement design. Research into these fields commenced well into the twentieth century and led to major improvements to the concepts developed by the early pioneers.

Most developments in modern pavement design took place in the United States and Europe. The AASHO road test, conducted between 1958 and 1961, provided valuable information on the empirical design of pavement structures, while the work of Westergaard (1926), Burmister (1943) and Ahlvin and Ulery (1962), allowed for the calculation of stresses and strains in elastic layered systems for a more analytical approach. The calculation of stresses and strains in pavement structures, caused by a wheel load, was therefore made possible.

1.1.2 The use of bituminous products in road building

The first recorded use of native bitumen in road construction, appears to be about 700 BC, when Nabopolassar, King of the Babylonians, had a road built of burnt bricks jointed with bitumen (Road Emulsion Association, 1958). After this period the use of bitumen in road-making appears to have been forgotten until the 19th century, except in the work of the Incas of Peru during the 14th and 15th centuries. They constructed the most remarkable system of roads, some of which are said to have been paved using asphalt; unfortunately no details of the work seem to have been recorded.

Bitumen was not used by the early pioneers in road building. Although the Val de Travers deposits of asphalt were discovered as early as 1712, they were not actively exploited until 90 years later. Residues from the distillation of crude oil were being used in surface treatments of roads in the early years of the 20th century in the US. Later on, it was discovered that the addition of suitable volatile solvents to the very viscous residues permitted their cold application. Until the introduction of emulsions in the early 1900's, it was in general necessary for all bitumens and their compounds to be heated prior application, to render them sufficient liquid.

1.2 THE USE OF BITUMEN EMULSION IN BASE LAYERS.

Bitumen emulsions were first manufactured in South Africa in 1927 (Marais and Tait: 1989) and initially used in surface treatments and slurry seals. Over the past 30 years, great success has been achieved by South African road engineers with the technique of adding small quantities of bitumen emulsion to gravels of fair to good quality. Between 1982 and 1992, the South African Bitumen Association (SABITA) sponsored a research programme to develop acceptable mixing, testing and evaluation methodologies for Granular Emulsion Mixes (GEMS). The emphasis of that project was on the upgrading of substandard materials to base layer standards by adding relatively high percentages of emulsion (in excess of 2% net bitumen). In October 1993, SABITA launched a design manual (SABITA: 1993) for GEMS with recommended design procedures for both stabilised GEMS (high emulsion contents) and modified GEMS (low emulsion contents). While ETB (Emulsion Treated Bases) includes the use of bitumen emulsion for upgrading substandard materials, the term GEMS also covers the addition of emulsion to other types of granular material such as:

- Substandard materials
- Granular materials of better quality
- Recycled granular, cement- and lime treated bases or a combination thereof.

A number of shortcomings in the above-mentioned manual resulted in the project launched by SABITA in 1996 to broaden the range of application of Emulsion Treated Bases (ETB's) as a

competitive base course material. This was done by extending the design scope of the current technology and entrenching it in practice. This project provided economic guidelines as well as material design and construction guidelines (SABITA, 1999). Although this project provided guidelines on the structural design of ETB's, it was mostly based on the experience of road engineers.

The advantages of emulsion treated layers are well known and documented (Horak et al: 1992, Lewis et al 1999 and SABITA 1999), but little scientific knowledge on the performance and failure mechanism of emulsion treated layers are available.

1.3 THE SOUTH AFRICAN MECHANISTIC PAVEMENT DESIGN PROCEDURE

The first simplified mechanistic design procedure in South Africa was developed by Van Vuuren, Otte and Paterson in the early 1970's (Van Vuuren et al: 1974). At the International Conference on the Structural Design of Asphalt Pavements in 1977 in Michigan, Walker et al. (1977) published the first comprehensive statement on the state of the art of mechanistic pavement design in South Africa. The procedure was refined and improved since then, and in 1995 it was updated by Theyse (1995) and Theyse et al (1995) for the purpose of revising the TRH4:1985 (CSRA: 1985).

The procedure provides values for the characterisation of pavement materials and includes the following features (Maree and Freeme: 1981 and Theyse: 1996):

- Transfer functions for thin asphalt surfacing (continuously and gap graded) layers as a function of the maximum horizontal tensile strain at the bottom of the layer,
- Transfer functions for thick asphalt base layers as a function of the maximum horizontal tensile strain at the bottom of the layer for a range of stiffness values from 1 000 to 8 000 MPa,
- Fatigue transfer functions for crack initiation of cemented material as a function of the maximum tensile strain at the bottom of the layer,
- Transfer functions for crushing failure of cemented material as a function of the vertical compressive stress at the top of the cemented base.
- Transfer functions for granular materials (crushed stones and natural gravels) as a function of the safety factor against shear failure.
- Transfer functions for in situ subgrades as a function of the maximum vertical compressive strain at the top of the subgrade.

The existing South African Mechanistic Pavement Design Procedure is being used extensively in new pavement design and rehabilitation in South Africa and was used to develop the

TRH4:1996 (CSRA: 1996). It does not however include any transfer functions or failure criteria for layers treated with small quantities of bitumen emulsion.

1.4 THE NEED FOR A FORMAL DESIGN PROCEDURE FOR PAVEMENTS WITH EMULSION TREATED LAYERS.

Previous research (Kari: 1969, Marais and Tait: 1989, SABITA: 1993, SABITA: 1999 and Santucci: 1977) provides valuable knowledge on the material design, construction techniques and quality control of GEMS and ETB's.

The structural design methods available for emulsion treated layers are mostly based on experience by road engineers. Although some indication exists that the behaviour of an emulsion treated layer should be similar to that of a cement treated layer, no performance prediction model exists for emulsion treated material (Theyse: 1997). Due to the fact that emulsion treated layers are being used more frequently, the need for a rational structural design method based on the principles of the South African Mechanistic Pavement Design Method, arise and need to be developed.

1.5 OBJECTIVES OF THE STUDY

The main objectives of this study are to define the life cycle behaviour and failure criteria of pavement layers treated with bitumen emulsion and to develop transfer functions for the relative mode of failure to load repetitions for emulsion treated layers.

A secondary aim of the study would be to provide input into the development of a structural design manual for emulsion treated layers based on the principles of the South African Mechanistic Pavement Design Procedure.

1.6 SCOPE AND EXTENT OF THE STUDY

The scope and extent of the study includes a detailed literature review, detailed laboratory testing on emulsion treated materials as well as additional tests with the Heavy Vehicle Simulator (HVS).

The literature study will review historical data from previous HVS- and laboratory tests on emulsion treated materials where possible.

The laboratory tests in this study were performed on a ferricrete with various cement and net bitumen content. The cement was below 2 % while the net bitumen content never exceeded 3 %. The HVS tests in this study were conducted on ferricrete stabilised with 3 % bitumen emulsion (1.8% net bitumen) and 2 % cement.

Results from the literature review, laboratory- and field tests will be utilised to define the life cycle behaviour and failure mechanism of pavement layers treated with bitumen emulsion.

Transfer functions will be developed to serve as an input into a structural design manual and the South African Mechanistic Pavement Design Method. A design catalogue will be proposed for the use as a design aid according to the principles of the TRH4 structural design guide.

1.7 STRUCTURE OF THE DISSERTATION.

In Chapter 2 a literature review on the mix design and engineering properties of emulsion treated layers are given. Information obtained from this literature review is used to define aspects relevant to the structural design process.

Chapter 3 is a literature review to determine the state of knowledge on the structural properties and existing structural design procedures for pavements containing emulsion treated layers. Historical data from previous laboratory and HVS tests are evaluated.

Chapter 4 discusses developments towards mechanistic-empirical design models.

Chapter 5 comprises an experimental program that includes laboratory and field tests. Laboratory tests include static and dynamic triaxial tests while the field tests include tests with the HVS under various wheel loads. The results from these tests and the performance of the emulsion treated material under laboratory and Heavy Vehicle Simulator testing are presented and discussed.

Chapter 6 discusses the fatigue life properties of the emulsion treated materials from the data obtained from the laboratory and field tests. A failure criteria are developed for fatigue life and design curves for the fatigue life of emulsion treated materials are proposed.

Chapter 7 discusses the permanent deformation properties of and emulsion treated material and the data from chapter 5 are used to develop transfer functions and design curves for permanent deformation.

Chapter 8 discusses the structural design of pavements with emulsion treated layers. A design method based on the South African Mechanistic Pavement Design Method is proposed as well as a design catalogue according to the principles of the TRH4.

Chapter 9 contains the conclusions of the main findings of the study and demonstrate that the study objectives were fulfilled. Recommendations for further research are also made.

1.8 REFERENCES

Ahlvin RG and Ulery HH, 1962, *Tabulated values for the determining the complete pattern of stresses, strains and deflections beneath a uniform circular loading on a homogeneous half space*, Highway Research Board Bulletin no 342, Transportation Research Board, Washington DC, Unites States.

Burmister DM, 1945, *The general theory of stresses and displacements in layered systems I, II and III*, Journal of Applied Physics, Vol. 16, no. 2.

Committee of Land Transportation Officials (COLTO), 1996, TRH4: *Structural design of interurban and rural road pavements*, TRH4, Department of Transport, Pretoria, South Africa.

Committee of State Road Authorities (CSRA), 1985, TRH4: *Structural design of interurban and rural road pavements*, TRH4, Department of Transport, Pretoria, South Africa.

Horak E and Rust FC, 1992, *The performance and behaviour of bitumen emulsion treated road bases in South Africa*, Proceedings of the 7th International Conference on Asphalt Pavements, Nottingham, United Kingdom.

Lewis AJN and Collings DC, 1999, *Cold in-place recycling: a relevant process for road rehabilitation and upgrading*, Proceedings of the 7th Conference on Asphalt Pavements in Southern Africa, Victoria Falls, Zimbabwe.

Marais CP and Tait MI, 1989, *Pavements with bitumen emulsion treated bases: Proposed material specification, mix design criteria and structural design procedures for South African conditions*, Proceedings of the 5th Conference on Asphalt Pavements in Southern Africa, Swaziland.

Road Emulsion Association, 1958, *Modern road emulsions*, 3rd ed., Road Emulsion Association Ltd., London.

SABITA, 1993, *GEMS: The design and use of granular emulsion mixes*, Manual 14, SABITA, Cape Town, South Africa.

SABITA, 1999, *ETB: The design and use of emulsion treated bases*, Manual 21, SABITA, Cape Town, South Africa.

Santucci LE, 1977, *Thickness design procedure for asphalt and emulsified asphalt mixes*, Proceedings of the 4th International Conference on the Structural Design of Asphalt Pavements, An Arbor, United States, pp 424 – 456.

Theyse HL, 1995, *TRH4 Revision 1995, Phase II: Mechanistic Design of the Pavement Structures in the TRH4 Pavement Design Catalogue*, National Service Contract NSC24/2, Transportek, CSIR, Pretoria, South Africa.

Theyse HL, de Beer M, Prozzi J and Semmelink CJ, 1995, *TRH4 Revision 1995, Phase I: Updating the Transfer functions for the South African Mechanistic Design Method*, National Service Contract NSC24/1, Transportek, CSIR, Pretoria, South Africa.

Theyse HL, de Beer M and Rust FC, 1996, *Overview of the South African Mechanistic Pavement Design Analysis Method*, Divisional Publication DP-96/005, Transportek, CSIR, Pretoria, South Africa.

Van Vuuren DJ, Otte E and Paterson WDO, 1974, *The Structural Design of Flexible Pavements in South Africa*, Proceedings of the 2nd Conference on Asphalt Pavements in South Africa, Durban, South Africa.

Walker RN, Paterson WDO, Freeme CR and Marais CP, 1977, *The South African Pavement Design Procedure*, Proceedings of the 4th International Conference on the Structural Design of Asphalt Pavements, University of Michigan, Ann Arbor, Michigan, United States.

Westergaard HM, 1926, *Stresses in Concrete pavement computed by theoretical analysis*, Public Roads Vol. 7, no. 2, United States.

2.2 HISTORY AND BACKGROUND OF EMULSION TREATED MATERIAL MIX DESIGN

Whether emulsion was initially added to granular materials to increase the water resistance of materials, to serve as a compaction aid and to improve the durability of the base layer of roads or to reduce potholes after construction (Black et al. 1984). The formal design procedure was still left at that stage and the design relied on the experience and judgement of the engineer. Zeng (1969) published a mix design procedure for emulsion treated materials to prevent permanent deformation. Three laboratory tests were adopted, namely:

- *Microscopic water susceptibility (mws) test*: This test subjects the emulsion treated base to the damaging effects of water in the vapour state.
- *Confidence Rating test*: This test provides an index of shear strength of the mix after exposure to water vapour.
- *Coarse Aggregate Crushing Test*: This test is an index of mix tensile strength and is used to evaluate the extent of cohesion failure and stripping of the mix after exposure to water vapour.

Spethwords (1976) presented results from a study where the mix design of emulsion treated materials was based on CBR and UCS tests. Because low percentages of binder were used, it was anticipated that the emulsion treated materials would exhibit properties closer to granular or cemented materials than bituminous materials, hence the use of CBR and UCS tests. He presented the influence of density, curing and temperature on the UCS and CBR (Spethwords 1976).

Marais and Lee (1987) published proposals on emulsion treated base mix design in 1989. They view the following properties critical to the design:

- *Initial shear strength* to prevent deformation in the base layer under traffic and varying environmental temperature conditions.
- *Permeability to moisture and air*.

CHAPTER 2 MIX DESIGN AND ENGINEERING PROPERTIES OF EMULSION TREATED MATERIALS

2.1 INTRODUCTION

This chapter contains a literature review of mix design methods and the properties of emulsion treated mixes. Mix design has an influence on the structural properties and –design of emulsion treated pavement layers. Only aspects of mix design that have an influence on the structural properties, structural behaviour and structural design of emulsion treated layers will be reviewed.

2.2 HISTORY AND BACKGROUND OF EMULSION TREATED MATERIAL MIX DESIGN

Bitumen emulsion was initially added to granular materials to improve the water resistance of materials, to serve as a compaction aid and to improve the durability of the base layer if opened to traffic soon after construction (Horak et al: 1984). No formal design procedure was available at that stage and the designs relied on the experience and judgement of the engineer. Kari (1969) published a mix design procedure for emulsion treated materials to prevent permanent deformation. Three laboratory tests were adopted, namely:

- Moisture-vapour-susceptibility (mvs) test: This test subjects the emulsion treated base to the damaging effects of water in the vapour state.
- Resistance R-value test: This test provides an index of shear strength of the mix after exposure to water vapour.
- Cohesimeter C-value test: This test is an index of mix tensile strength and is used to evaluate the extent of cohesion failure and stripping of the mix after exposure to water vapour.

Spottiswoode (1979a) presented results from a study where the mix design of emulsion treated materials was based on CBR and UCS tests. Because low percentages of bitumen were added, it was anticipated that the emulsion treated materials would exhibit properties closer to granular or cemented materials than bituminous materials, hence the use of CBR and UCS tests. He presented the influence of density, curing and temperature on the UCS and CBR (Spottiswoode: 1979b).

Marais and Tait (1989) published proposals on emulsion treated base mix design in 1989. They view the following properties critical to the design:

- Initial shear strength to prevent deformation in the base layer under traffic and varying environmental temperature conditions.
- Permeability to ingress of subsoil water

- Brittleness

They suggested that the Marshall method should be modified to accommodate the particular characteristics of emulsion treated materials. It was proposed that the properties of the treated layers be evaluated at higher temperatures to ensure that under summer conditions and at an early cured state, it will not deform under the action of traffic.

Other mix design methods for emulsion treated materials are described by Louw (1996) and include the following:

- Modified Hveem method (similar to method described by Kari (1969))
- Asphalt Institute
- Retread method
- Abecol method
- Chevron method
- Illinois method, and
- Texas triaxial test method

In 1993 SABITA published the GEMS manual (SABITA: 1993) where formal mix design methods are described for granular materials treated with bitumen emulsion. The publication was based on a research project sponsored by SABITA. The research included extensive laboratory testing and evaluation of the mixes in the field by Heavy Vehicle Simulator testing.

2.3 EMULSION TREATED MATERIAL MIX DESIGN IN SOUTH AFRICA

The SABITA manual 14 (SABITA: 1993), distinguishes between a modification and stabilisation approach in mix design. The modification approach applies to materials with net bitumen contents of less than 1.5 % by mass of the dry aggregate, while the stabilisation approach applies to materials with more than 2 % net bitumen by mass. The binder content between 1.5 % and 2 % is considered to be a “grey” area where either the modification or stabilisation approach might be applicable. The quality of the parent material should play the decisive role in this case.

In 1999 the SABITA manual 21 (SABITA: 1999) was published. It provides clear guidelines on mix design for the modification approach.

The definitions *modification* and *stabilisation* described in this study and in SABITA manuals 14 and 21, differs from the commonly used definitions where *modification* implies the alteration of the physical properties of a material, while *stabilisation* implies the chemical alteration of a material.

2.3.1 Mix design for the stabilisation approach (net bitumen > 1.5 %)

A formal mix design method for materials with net bitumen contents in excess of 1.5 % are recommended in SABITA manual 14 (SABITA: 1993). The document is based on the research initially conducted by Marais and Tait (1989). The purpose of mix design is to determine the correct composition of components and to provide design parameters for the structural design. SABITA manual 14 provides guidelines on emulsion, aggregates, lime and cement and curing.

The optimum binder content is determined by using the Marshall method on samples prepared with different residual bitumen contents. A minimum stability of 2.2 kN at 23°C is required while the stability at 40°C should not be less than 1 kN.

Indirect tensile strength (ITS), carried out at 23°C and 40°C, at a loading rate of 50 mm/min, should not be less than 100 kPa, and if exposed to water, not less than 50 kPa. The ITS is not normally used to determine the optimum binder content.

The stiffness (E-value) of the material could be determined by the methods recommended in SABITA manual 14. The E-value should not be less than 1 000 MPa at 23°C.

Voids should be less than 15 % to prevent excessive strength loss due to water ingress and not less than 5% to allow the emulsion to break and cure.

2.3.2 Mix design for the modification approach (net bitumen < 2.0 %)

A design method for the modification approach was recommended in SABITA manual 14, but after additional research (Louw: 1996, Louw: 1997, Verhaeghe: 1998a and Verhaeghe: 1998b) it was replaced by the method recommended in SABITA manual 21 (SABITA: 1999). A schematic overview of the mix design for the modification approach is presented in Figure 2.1.

Materials with low percentages of bitumen (less than 2%) can hardly be described as visco-elastic and their behaviour will primarily be similar to that of treated gravels. The use of the Marshall method is therefore not realistic and the materials should rather be characterised in terms of CBR and UCS. SABITA (1999) recommends, after research by Verhaeghe (1998b), that 1% cement should be added to assist in the breaking process and adhesion of the emulsion, and to increase the early strength development where the layer is to be opened to traffic soon after construction. The effect of cement on a G4 material is illustrated in Figure 2.2.

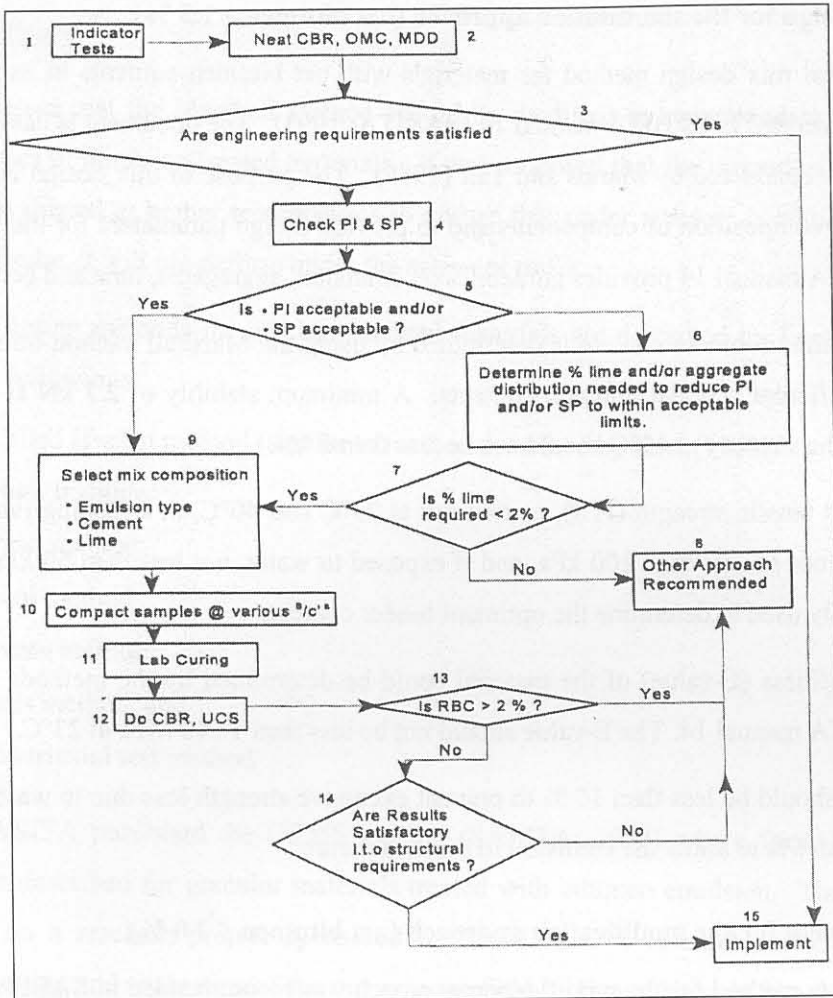


Figure 2.1 Schematic overview of the ETB mix design process (Verhaeghe: 1998a)

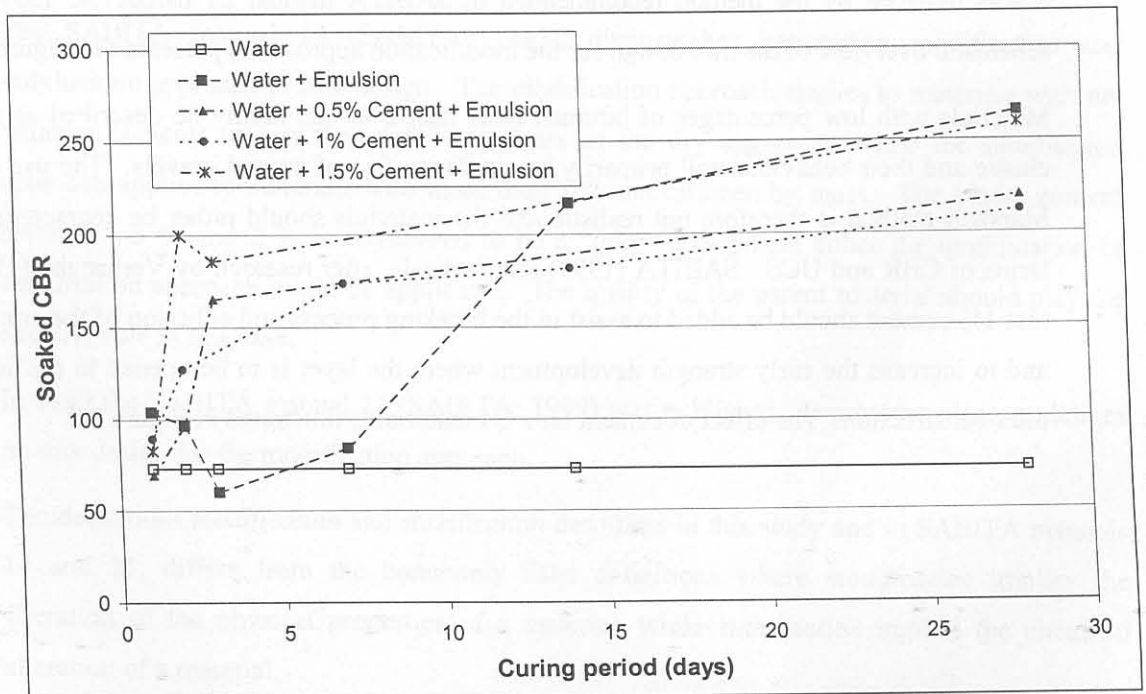


Figure 2.2 Effect of cement content on CBR for G4 material (Verhaeghe: 1998b)

The optimum bitumen content is determined by CBR and/or UCS testing on samples with different residual bitumen contents. The mix design criteria for emulsion treated materials according to the modification approach are outlined in Table 2.1. No ITS tests are being recommended in the modification approach.

Table 2.1 Mix design criteria for ETB's in terms of CBR and UCS (SABITA: 1999)

Material Code	Minimum CBR	Minimum UCS
E1	150 at 100% mod. AASHTO compaction	1 200 kPa
E2	100 at 100% mod. AASHTO compaction	750 kPa

2.4 THE ENGINEERING PROPERTIES OF EMULSION TREATED MATERIALS

As with other road building materials, the engineering properties of emulsion treated materials should be taken into account during the structural design process. The important engineering properties are:

- Stiffness
- Resistance to fatigue cracking
- Resistance to permanent deformation
- Durability

The curing of emulsion treated materials has a major influence on the stiffness of the layer in its early life (up to the first two years). The failure mechanism will therefore be dictated by the stiffness state of the emulsion treated layer during that period. Permanent deformation or fatigue cracking may initially be the prominent failure mechanism, with shear deformation or fatigue cracking dominant thereafter. This needs to be properly defined to develop a structural design model.

2.4.1 Stiffness and resilient modulus

The stiffness of the pavement layer is an important aspect of the structural design. Stiffness of emulsion treated layers depends on the following:

- Curing
- Temperature (more important for higher bitumen contents)
- Rate of loading (more important for higher bitumen contents)

Kari (1969) made use of dynamic triaxial tests to determine the resilient modulus from the following expression:

$$M_R = \frac{\sigma}{\varepsilon} \quad (2.1)$$

where M_R = Resilient modulus

σ = applied axial (deviator) stress

ε = resilient (recoverable) axial strain

He reported values between 60 000 psi (410 MPa) and 900 000 psi (6 200 MPa) with an average value of 300 000 psi (2 000 MPa). It was noted that the upper values approach that of values typical for hot mix asphalt at 77°F (25°C). An increase in relative density of as little as 8% resulted in an increases in excess of 90% for resilient modulus, while curing after 28 days resulted in a 25 % increase in resilient modulus.

Kari (1969) proposed the following empirical relationship to estimate the field resilient modulus:

$$\ln(M_R * 10^{-3}) = 0.4\rho + 2.46S - 0.15Pen \quad (2.2)$$

where: M_R = Resilient modulus (psi)

ρ = density in lb/cu.ft

S = Sand fraction (#4 (4.72 mm) to minus 200 mesh (75 μ m))

Pen = Penetration of recovered bitumen at 77°F (25 °C)

He reported a reasonable fit from the empirical data and adequate for estimating purposes.

Santucci (1977) indicated that the ultimate design modulus might be reached after six months to two years depending on the climate.

According to Marais and Tait (1989) the resilient modulus may be estimated from Indirect Tensile Strength by Equation 2.3, if equipment to determine the modulus accurately is not available.

$$M_R = 5.123 * ITS - 75 \quad (2.3)$$

where: M_R = Resilient modulus in MPa

ITS = Indirect Tensile Strength in kPa at 23°C

SABITA (1993) proposes the following relationship between stiffness and CBR for estimation purposes:

$$E = k.CBR \quad (2.4)$$

where: E = Stiffness in MPa

CBR = California Bearing Ratio (%) at the required compaction

k = constant: 5 for G1 and G2 parent materials

6 for G3 and G4 parent materials

7 for G5 parent materials

De Beer and Grobler (1994) reported values for elastic moduli of 800 MPa after construction to values of approximately 3 000 MPa after 10 months. The highest rate of increase in stiffness was observed between three to four months after construction. Indirect Tensile Strength values also increased from around 300 kPa to approximately 900 kPa.

A reduction of the elastic moduli of approximately 50% was reported by de Beer and Grobler (1993) after 10 000 to 20 000 repetitions by the Heavy Vehicle Simulator at various wheel loads. This can be attributed to the development of fatigue cracks within the emulsion treated layer.

2.4.2 Resistance to fatigue cracking

Repeated loading progressively reduces the tensile strength of emulsion treated materials. Fatigue resistance increases as the emulsion content increases. It is however not as sensitive to bitumen content as asphalt mixes. Small variations will not have a big influence on the fatigue properties. Fatigue characteristics are not generally measured for design purposes according to the SABITA manual 14. (SABITA: 1993). Experiments on road S12 between Witbank and Johannesburg by Marais and Otte (1979), showed that after 9 years and approximately 3.5 million E80's, no cracks were visible on the surface of the section treated with emulsion. Only one other section constructed with other pavement materials could match this performance.

2.4.3 Resistance to permanent deformation

Permanent deformation is the result of the accumulation of repeated plastic strains due to traffic loading. It is caused by a combination of consolidation and shear movement. Proper compaction prevents consolidation to a large extent, while shear deformation could be minimised by proper mix design. Emulsion treated layers are sensitive to permanent deformation in its early life, mainly because of the fact that the curing process is not completed. Once curing has been more or less completed, permanent deformation is rarely the primary

mode of failure (Marais and Otte: 1979). The addition of cement greatly prevents the early sensitivity to permanent deformation.

2.4.4 Durability

Bitumen emulsion was first used in South Africa to allow traffic on the finished base layer soon after construction to reduce or prevent ravelling (Bergh: 2001). This proved to be successful with a minimum disruption to traffic. Emulsion treated materials show greater resistance to the damaging effects of water in the layer than granular or cemented material. (SABITA: 1993, SABITA: 1999). Maree et al (1982) reported that four times less fines were brushed off during a brushing durability test, compared to untreated material. Horak et al (1984) found that the rate of permanent deformation did not change with the addition of water into a pavement recycled with a bitumen emulsion base layer.

Tests done by Spottiswoode (1979a) indicated that the permeability of the material is reduced by the addition of emulsion at high compaction (100 % mod. AASHTO). Horak et al (1984) measured permeability that was three to five times higher than for good compacted crushed stone layers.

2.5 CURING OF EMULSION TREATED LAYERS

The ultimate stability and related properties (stiffness, etc.) of emulsion treated materials are not reached until a major portion of the water in the material has evaporated. Under field conditions this may take several months, or even up to two years (Louw: 1996).

Curing is important to prevent permanent deformation in the early part of the life of an emulsion treated layer. Smaller amounts of emulsion will require shorter periods for full curing, but the length of curing is mainly influenced by the climatic region. Wetter climatic regions will result in slower curing while curing in dry climates may be substantially faster. The addition of lime or cement can assist in the speeding up of the curing process. Lime or cement acts as a catalyst to enhance the breaking process and uses the free water in the material.

Louw (1996) indicated that approximately 70% of the strength of emulsion treated layers is gained within the first two weeks, and that the increase in strength after 18 months is minimal.

2.6 CONCLUSIONS

The following conclusions, which are of importance in the structural design process, can be drawn from the literature study on mix design and engineering properties of emulsion treated materials.

- Mix design processes for emulsion treated materials are well researched, documented and established. The need is for a mechanistic structural design method that will enable

design engineers to bring together the principles of pavement design and the outputs available from the mix design processes.

- The failure mechanism of emulsion treated materials is dependant on the state of curing of the material. Young uncured layers could accumulate permanent deformation that would result in excess rutting, while cured layers could fail in fatigue and/or shear.
- Emulsion treated materials provide better resistance to fatigue cracking than cemented layers. An emulsion treated layer can withstand more elastic movement before failure occurs.
- The increased durability of emulsion treated materials makes it less sensitive to water and has the advantage that an emulsion treated layer may be opened to traffic, for a limited period of time, soon after construction without an overlay or seal.
- Curing of emulsion treated materials is an important aspect to ensure proper strength development and the addition of lime or cement may assist in early strength development.

2.7 REFERENCES

Bergh AO, 2001, *Personal correspondence and communication, Pretoria, South Africa.*

Committee of State Road Authorities (CSRA), 1987, *Guidelines for Road construction Materials*, TRH14:1987, Department of Transport, Pretoria, South Africa.

De Beer M, Grobler JE, 1993, *ETB's: Heavy Vehicle Simulator (HVS) evaluation of the Heilbron sections*, Service contract report PR92/2/1, Transportek, CSIR, Pretoria, South Africa.

De Beer M, Grobler JE, 1994, *Towards improved structural design criteria for granular emulsion mixes*, Proceedings of the 6th Conference on Asphalt Pavements in Southern Africa, Cape Town, South Africa.

Horak E, Myburgh PA and Rose DA, 1984, *Rehabilitation of a cement treated base pavement*, Proceedings of the 4th Conference on Asphalt Pavements in Southern Africa, Cape Town, South Africa.

Kari WJ, 1969, *Design of emulsified asphalt treated base courses*, Proceedings of the 1st Conference on Asphalt Pavements in Southern Africa, Durban, South Africa.

Louw L, 1996, *Mix design methods for GEMS: A literature study*, Contract report CR96/041, Transportek, CSIR, Pretoria, South Africa.

Louw L, 1997, *ETB mix design: Summary of best practices*, Contract report CR96/079, Transportek, CSIR, Pretoria, South Africa.

Marais CP and Tait MI, 1989, *Pavements with bitumen emulsion treated bases: Proposed material specification, mix design criteria and structural design procedures for South African*

conditions, Proceedings of the 5th Conference on Asphalt Pavements in Southern Africa, Swaziland.

Maree JH, Viljoen CBL, Gibson R, 1982, *Aspekte van die behandeling van gebreekteklipkroonlae met klein persentasies bitumenemulsie of teer*, Technical report RP/10/82, NITRR, CSIR, Pretoria, South Africa.

SABITA, 1993, *GEMS: The design and use of granular emulsion mixes*, Manual 14, SABITA, Cape Town, South Africa.

SABITA, 1999, *ETB: The design and use of emulsion treated bases*, Manual 21, SABITA, Cape Town, South Africa.

Santucci LE, 1977, *Thickness design procedure for asphalt and emulsified asphalt mixes*, Proceedings of the 4th International Conference on the Structural Design of Asphalt Pavements, An Arbor, Michigan, United States, pp 424 – 456.

Spottiswoode BH, 1979a, *Emulsion treatment of crushed stone bases*, Proceedings of the 3rd Conference on Asphalt Pavements in Southern Africa, Vol 1, Durban, South Africa.

Spottiswoode BH, 1979b, *Discussions on treated materials*, Proceedings of the 3rd Conference on Asphalt Pavements in Southern Africa, pp 50-51, Vol 2, Durban, South Africa.

Verhaeghe BMJA, Napier RC, Kong Kam Wa NJ, 1998a, *A revised approach to mix design of emulsion treated base materials*, Contract report CR-97/056, Transportek, CSIR, Pretoria, South Africa.

Verhaeghe BMJA, Napier RC and Kong Kam Wa NJ, 1998b, *A revised approach to mix design of emulsion treated base materials: Laboratory investigations*, Contract Report CR-97/057, Transportek, South Africa.

CHAPTER 3 STATE OF THE ART ON THE STRUCTURAL BEHAVIOUR AND DESIGN OF EMULSION TREATED PAVEMENT LAYERS

3.1 INTRODUCTION

Mechanistic design procedures for the structural design of pavements are well established in pavement design. The South African Mechanistic Pavement Design Procedure (SAMPDP) (Maree and Freeme: 1981, Jordaan: 1994 and Theyse et al: 1996) provides guidelines on the structural design for pavements with granular, cement treated and hot mix asphalt pavement layers. The TRH4 (COLTO: 1996) pavement design catalogue was based on the SAMPDP and provides a catalogue of pavements for new roads and rehabilitation (COLTO: 1997) for different road categories, climate types and traffic classifications. The structural design for new roads and rehabilitation of pavements containing emulsion treated layers, are not included in the TRH4 or the SAMPDP and are limited to papers published and the experience of practitioners.

3.2 THE HISTORY AND BACKGROUND TO STRUCTURAL DESIGN OF PAVEMENTS CONTAINING EMULSION TREATED MATERIALS

Emulsion was added to pavement layers initially to enhance the water resisting properties of the layer and to improve cohesion on the surface to allow the road to be opened to traffic soon after construction to prevent or limit ravelling of the base layer. In the first experiments in South Africa (Otte and Marais: 1979), no cement was added to the emulsion treated layer and it was treated as a granular layer during the structural design process.

In 1969 Kari (1969) presented a design procedure based on layer equivalency. He calculated the stresses and strains to determine the thickness of the emulsion treated layer to limit the subgrade strain.

Santucci (1977) published a design procedure for bitumen and emulsion treated materials. His research was done on high bitumen contents (11% by volume or 5 to 5.5% by mass). He developed transfer functions for emulsion treated as well as emulsion and cement treated materials. The maximum horizontal tensile strain at the bottom of the treated layer and the maximum vertical compressive strain at the top of the subgrade were used to determine the thickness of the pavement. The method assumed that the properties of the emulsion treated layer were similar to that of asphalt.

Marais and Tait (1989) made some adjustments to the method of Santucci (1977) to allow for South African conditions.

In 1993 SABITA published manual 14 (SABITA: 1993), and provided different approaches for modification and stabilisation. The structural design for the stabilisation approach was based on the work of Santucci (1977) and Marais and Tait (1989). In the modification approach, the emulsion treated material was treated similarly to a granular material.

De Beer and Grobler (1994) developed transfer functions based on research done on the Heilbron test sections. The method was regarded as too conservative because it proposed thick structures contrary to the experience of practitioners.

Theyse (1998) provided guidelines and a proposed design catalogue for pavements containing emulsion treated materials with low bitumen contents (less than 1.8% net bitumen) based on the DCP design approach.

The SABITA manual 21 (SABITA: 1999), provided guidelines on the mix design and construction of emulsion treated layers. It only proposed the use of a catalogue included in the document for structural design purposes.

3.3 FAILURE MECHANISM OF EMULSION TREATED LAYERS

The bitumen content greatly dictates the failure mechanism of emulsion treated materials. Emulsion treated materials with high bitumen contents tend to behave more like asphalt materials with the dominant failure mechanism being fatigue cracking at the bottom of the layer. Santucci (1977) and Marais and Tait (1989) used fatigue cracking at the bottom of the layer for the failure mechanism on the materials with a high bitumen content (11% by volume and 5% air voids). The SABITA manual 14 (SABITA: 1993), distinguishes between the failure mechanisms of stabilised and modified emulsion treated materials. The theory of Santucci is used for net bitumen contents exceeding 2%. For low bitumen contents, the visco-elastic behaviour of the material will be less evident and the behaviour of the material will primarily be similar to that of untreated gravels or aggregates. According to SABITA (1993) the failure mechanism for low bitumen content emulsion treated materials are similar to that of granular material, which is shear failure or gradual deformation at a steady rate under repeated loading. Both these modes of failure are believed to be related to the ratio between the applied shear stresses and the shear strength of the material under prevailing conditions of moisture and density (Theyse: 1998). The cement contents in these materials are only marginal (1 to 1.5%) to assist in the breaking of the emulsion.

De Beer and Grobler (1994) introduced the concept of fatigue cracking followed by the fracturing of the emulsion treated layer. This includes the development of fatigue-like cracking in the layer, starting mainly at the bottom of the layer, and progresses upward through the weak areas and around the larger aggregates. At an advanced stage of cracking, most of the initial fatigue cracks emerge mainly around the larger aggregates and the layer is then transformed

into the fractured or advanced granular state. During this process the elastic moduli of the emulsion treated material reduces to levels known for unbound gravel materials.

Theyse (1998) stated that the general behaviour of emulsion treated materials are most likely to be equivalent to granular and lightly cemented materials.

3.4 THE BEHAVIOUR OF EMULSION TREATED PAVEMENT LAYERS

3.4.1 The Long Term pavement performance of pavements (LTPP) with emulsion treated pavement layers

A number of pavements with emulsion treated base layers in South Africa are being monitored regularly to obtain understanding and knowledge on the performance of these pavements under normal traffic and climatic conditions (Wright et al: 1991 and Steyn: 1997). Some of the sections that are being monitored are outlined in Table 3.1. The pavement structures of these sections consist of an emulsion treated base with thicknesses varying from 100 mm to 200 mm and net binder contents between 0.1 and 2.3%, with the majority below 1%. Unfortunately no reference to the presence of cement in any of these sections could be found. All the sections have cemented subbases except the P66/1 and the N7/7 (Steyn: 1997) which have granular subbases.

Table 3.1 LTPP sections for pavements with emulsion treated layers (Steyn: 1997)

Test section	Description	Construction year	Traffic data		Traffic demand class	Binder content (%) ^a	Cement content (%) ^a
			AADT (year)	% Heavy			
N12/19	S12: Witbank	1974	12 710 (1993)	13.3	ES100	0.7 ^b	0
P66/1	Wepener	1989	486 (1988)	19.0	ES1	0.9	1.5% (lime)
TR13/3	Britstown	1994	496 (1993)	21.1	ES1	2.0	N/A
N7/7	Kamieskroon	1986	715 (1993)	16.6	ES1	1.0	N/A
N1/1	Cape Town	1984	15 900 (1993)	9.9	ES100	1.0	N/A
MR27	Stellenbosch	1988	N/A	N/A	ES100	1.0	N/A
N2/16	East London	1982	3 953 (1993)	11.2	ES3	1.0	1.0
N3/4	Pietermaritzburg bypass	1988	10 743 (1993)	17.9	ES100	1.0	N/A

^a Wright et al (1991)

^b From bitumen extraction test. (Steyn:1997)

Detailed tests were done on most of the sections and are presented elsewhere (Wright et al: 1991, Steyn: 1997 and Laatz: 1990). Most of the sections are still in a sound condition and behave well. During 1997 little permanent deformation was present while the DCP penetration rates compared well with that of good quality crushed stone materials. It seems therefore that after years of service, most of the pavements still have adequate shear strength to withstand the loads applied by traffic.

3.4.2 The behaviour of emulsion treated layers under repeated loading (HVS testing)

Accelerated testing with the Heavy Vehicle Simulator (HVS) system (Freeme et al, 1982) and technology have advanced the understanding of pavement behaviour and modelling in South Africa significantly (Freeme et al, 1987). The HVS is a mobile accelerated pavement testing rig that tests as-built pavements. Acceleration of testing is achieved through the backwards and forward movement of a wheel load over a selected 8m by 1m test section. The wheel load can be loaded with loads that vary from 40 kN to 200 kN. Additional to the test rig, sophisticated response measuring equipment were developed to measure deformation and deflection on the road surface and in depth, crack movement and moisture content.

Tests done on emulsion treated materials by De Beer and Grobler (1993) reported a reduction of the initial modulus after approximately 10 000 HVS repetitions (Figure 3.1) that resulted in a change in the deflection bowl (Figure 3.2). The change in the deflection bowl indicated that the load spreading characteristics of the layer had changed and that more load was being transferred to the lower layers of the pavement. This resulted in a decrease in the radius of curvature and a deeper but smaller deflection bowl. The change of load bearing characteristics was an indication that the layer had reached the end of its fatigue life and was now functioning as a cracked layer in an equivalent granular phase. This behaviour is similar to that of lightly cemented layers as described by de Beer (1989). Similar behaviour was reported by Jordaan and Horak (1991) during HVS tests on emulsion treated base layers in the Eastern Cape. Horak and Viljoen (1981) found that emulsion treated material exhibits behaviour similar to a good quality crushed stone (G1 or G2) rather than that of an asphalt layer.

The expected life in terms of E80's to 20 mm rutting for the emulsion treated layers tested by de Beer and Grobler (1994) were between 4 and 24 million. These tests were done at very high dual wheel loads of 140 kN, that may result in the end of the fatigue life of the layer after only 10 000 repetitions. The emulsion treated layer also showed a strong stress dependency, similar to granular materials, as can be seen in Figure 3.1.

The pavements showed sensitivity to overloading, but that may be as a result of the subbase support that is important to the behaviour of emulsion treated base layers, according to Horak and Viljoen (1981).

Wheel loads applied to a pavement are converted to equivalent 80 kN axle loads (E80's) by using a equivalency factor F_n , where:

$$F_n = \left(\frac{P}{80} \right)^d \quad (3.1)$$

where: F_n = equivalency factor for load P

P = axle load in kN

d = damage coefficient, which is dependent on the pavement type and material state

The damage coefficient (d) is similar to the “ n ” value as established during the AASHO road test. The coefficient n , determined during the AASHO road test as an average of 4.2, relates to the riding quality of a pavement. The coefficient d was later defined and relates to other forms of distress like cracking, rutting, etc. During accelerated pavement testing, the value of d may vary depending on the pavement type, material state, loading history, etc.

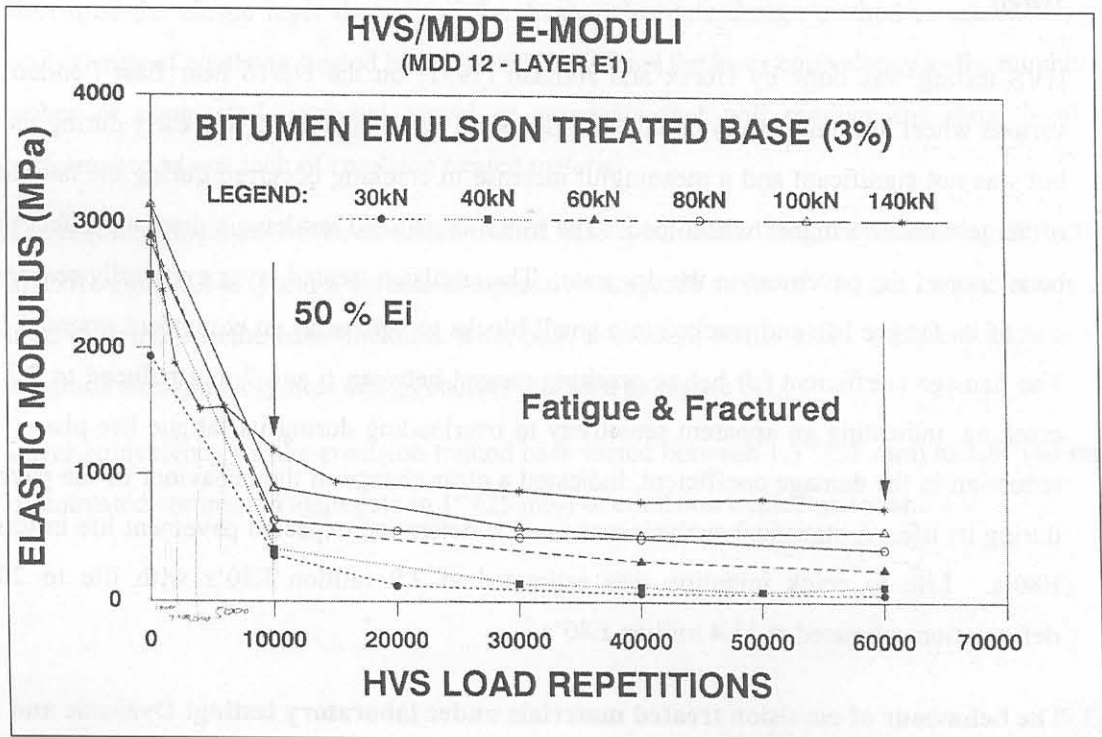


Figure 3.1 Backcalculated E-moduli at various HVS repetitions (De Beer and Grobler: 1993)

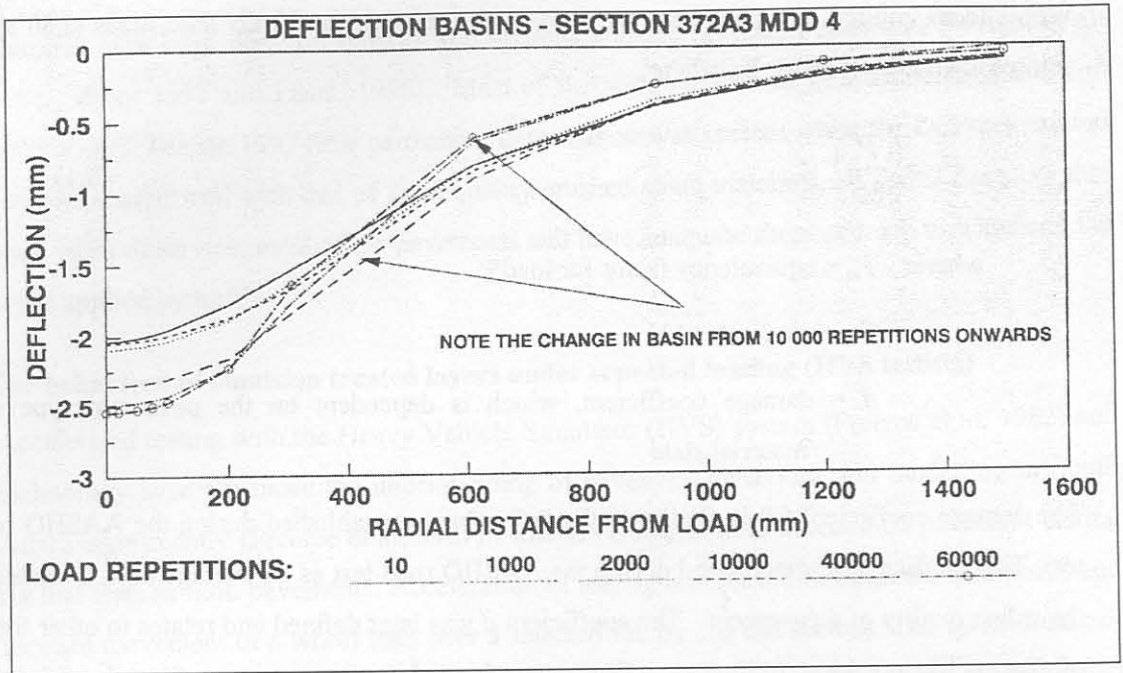


Figure 3.2 Measured deflection basins at various repetitions (De Beer and Grobler: 1993)

HVS testing was done by Horak and Jordaan (1991) on the N2/16 near East London with various wheel loads under dry conditions. Cracking was visible relatively early during the test, but was not significant and a meaningful increase in cracking occurred during the later stages of the test under a higher wheel load. The initial cracks did not have a dramatic effect on the behaviour of the pavement in the dry state. The emulsion treated layer eventually reached the end of its fatigue life and cracked into small blocks to behave as an equivalent granular layer. The damage coefficient (d) before cracking ranged between 6 and 7 and reduced to 2.7 after cracking, indicating an apparent sensitivity to overloading during its fatigue life phase. This reduction in the damage coefficient, indicated a clear change in the behaviour of the pavement during its life. A statistical analysis was used to determine expected pavement life in terms of E80's. Life to crack initiation was estimated at 2.9 million E80's with life to 20 mm deformation estimated at 31.4 million E80's.

3.4.3 The behaviour of emulsion treated materials under laboratory testing: Dynamic and static testing

Maree et al (1982) performed static triaxial tests on crushed stone material stabilised with small percentages of bitumen or tar. They found that the internal angle of friction reduced from values between 57° and 60° to values between 49° and 54° with an increase in emulsion or tar content. This is as a result of the lubricating effect of the bitumen emulsion or tar. The degree of saturation had little effect on the internal friction of the treated material. The treated

material was less sensitive to elastic deformation, than for untreated material and failure occurred after increased axial deformation under a lower maximum deviator stress.

Maree et al (1982) found that the cohesion also reduced with an increase in emulsion content. This was against expectation. The cohesion was however less sensitive to saturation in treated samples than in untreated samples. The lubricating effect could also be responsible for this during testing. The reduction in cohesion is possibly because the curing process had not been completed and that the cohesion would increase to higher values when the material is fully cured.

Horak et al (1984) and Maree et al (1982) reported a stress sensitivity in laboratory tests for the treated materials with a similar slope to that of granular materials but with a higher initial value.

3.5 STRUCTURAL DESIGN OF EMULSION TREATED MATERIALS

3.5.1 Kari (1969)

Kari used the elastic layer theory and the Asphalt Institute design method to establish layer equivalency of emulsion treated base layers. He defined the layer equivalency as the number of inches of compacted untreated gravel or aggregate that will produce the same level of performance as one inch of emulsion treated material.

The required thickness of the emulsion treated base is calculated to satisfy a limiting deflection of 1.016 mm (0.040") and a vertical compressive subgrade strain of 980 $\mu\epsilon$. Design charts are used to determine the base thickness from base E-moduli, traffic class, surface thickness and subgrade strength. A typical design chart is included as Figure 3.3.

Layer equivalency for the emulsion treated base varied between 1.3" (33 mm) to 1.8" (46 mm) of untreated compacted aggregate to 1" (25 mm) of emulsion treated material.

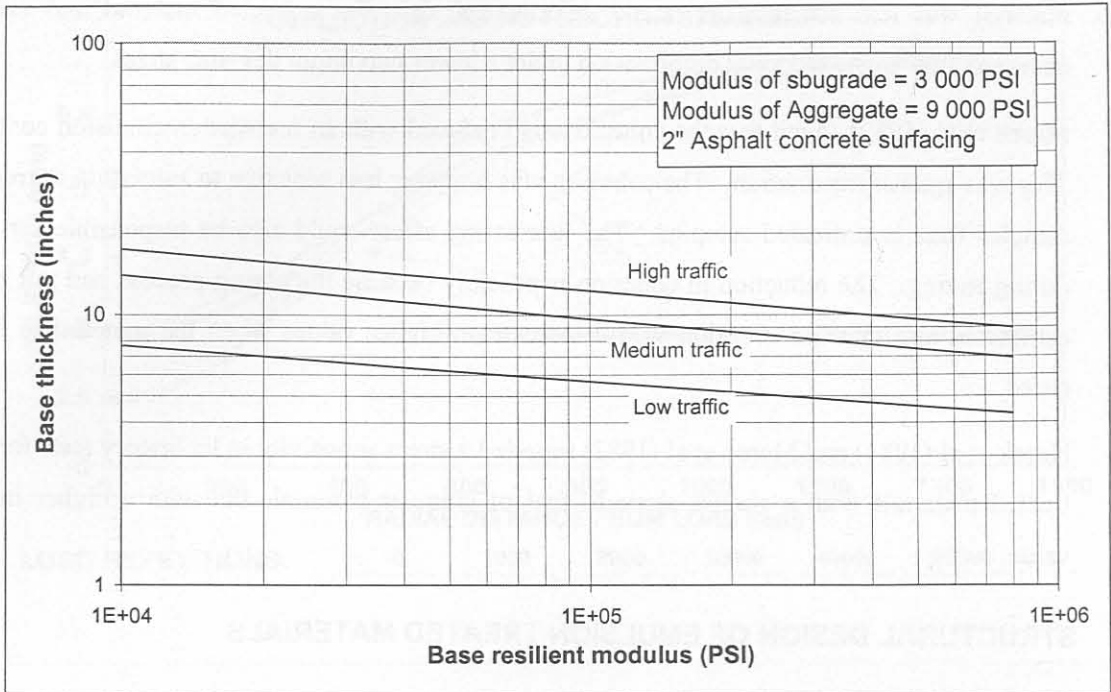


Figure 3.3 Design chart for ETB for subgrade modulus of 20 MPa (3 000 psi) (Kari: 1969)

3.5.2 Santucci (1977)

Santucci used the elastic layer principles to determine required layer thickness using the maximum horizontal tensile strain at the bottom of the emulsion treated layer and the maximum vertical compressive strain at the top of the subgrade. He presented transfer functions for materials treated with emulsion and materials treated with cement and emulsion in terms of the critical parameter (ϵ_t at bottom of layer) and load repetitions to failure (Figure 3.4). Failure of the emulsion treated base layer was defined when the fatigue cracks reflect through to the surface. The fatigue curves were shifted to allow for crack propagation through the layer. These fatigue lines were developed for relatively high emulsion contents (11% by volume or 5 to 6% by mass) and 5% voids.

A correction (Equation 3.2) for different void- and bitumen contents was supplied based on research by Pell and Cooper (1975) as well as Epps (1968).

$$N_c = N_f \cdot 10^M \quad (3.2)$$

with: N_c = Corrected number of repetitions

N_f = Number of repetitions to failure from transfer function

$$M = 4.84 \left(\frac{V_B}{V_V + V_B} - 0.69 \right) \quad (3.3)$$

with: V_B = Bitumen content by volume and V_V = Void content

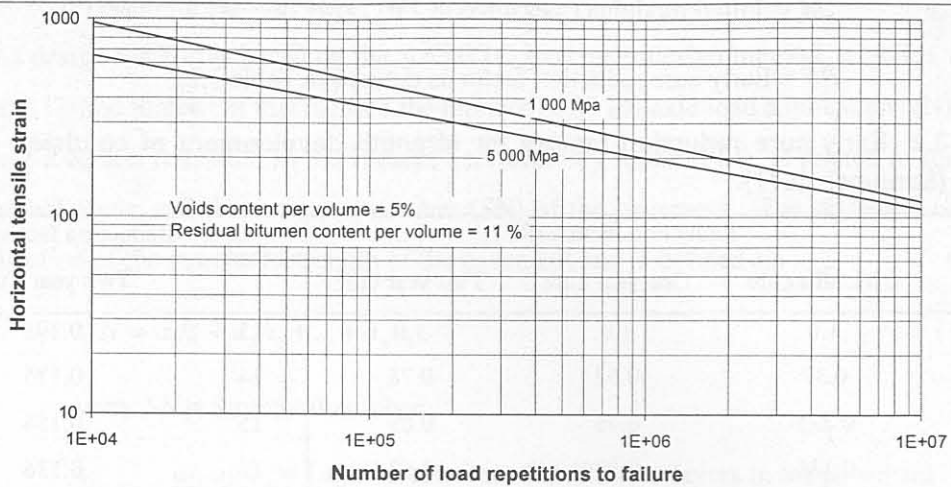


Figure 4.3a Fatigue criteria for granular emulsion mixes

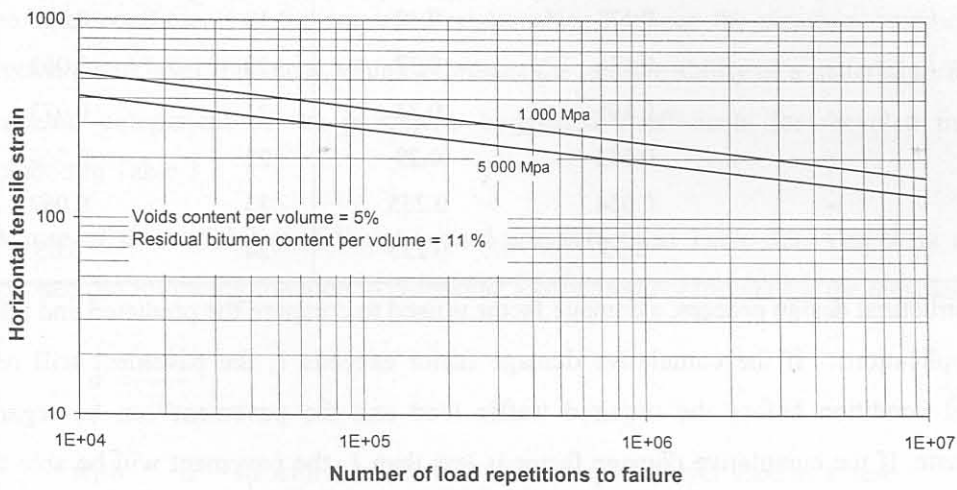


Figure 3.4b Fatigue criteria for cement modified granular emulsion mixes

Figure 3.4 Fatigue criteria for emulsion treated material for 11% bitumen and 5% air voids by volume (Santucci: 1977)

Santucci also provided a detailed procedure to allow for the influence of seasonal temperature effects and curing during the early life of the layer, on the resilient modulus of the material. The resilient modulus for design purposes at a specific time after construction can be calculated by Equation 3.4.

$$M_t = M_f - (M_f - M_i)RF \quad (3.4)$$

with M_t = Modulus at a specific time after construction at 23°C (73°F)

M_f = Final modulus (measured at 23°C after three day air cure and four day vacuum cure at room temperature)

M_i = Initial modulus (measured at 23°C after one day air cure)

RF = Early cure reduction factor as defined in Table 3.2.

Table 3.2 Early cure reduction factors for strength development of emulsion treated layers (Santucci: 1977).

Month	Reduction factors (RF)			Month	Reduction factors (RF)
	6 Months cure	One year cure	Two year cure		Two year Cure
1	1.0	1.0	1.0	13	0.198
2	0.37	0.62	0.78	14	0.175
3	0.225	0.48	0.69	15	0.154
4	0.136	0.37	0.62	16	0.136
5	0.082	0.29	0.545	17	0.120
6	0.05	0.225	0.48	18	0.105
7	-	0.175	0.42	19	0.093
8	-	0.136	0.37	20	0.082
9	-	0.105	0.33	21	0.073
10	-	0.082	0.29	22	0.064
11	-	0.064	0.255	23	0.057
12	-	0.05	0.225	24	0.05

In the structural design process, a damage factor is used to compare the predicted and allowable load applications. If the cumulative damage factor exceeds 1, the pavement will reach its terminal condition before the required traffic load and the pavement can be regarded as inadequate. If the cumulative damage factor is less than 1, the pavement will be able to carry the required load before the terminal condition is reached. The Cumulative damage factor for the i^{th} loading is defined as the number of repetitions (n_i) of a given response parameter divided by the 'allowable' repetitions (N_i) of the response parameter that would cause failure. The Cumulative Damage Factor for the parameter is given by summing the damage factors over all the loadings in the traffic spectrum and is calculated as follows:

$$CDF = \sum_n \frac{n_i}{N_i} \quad (3.5)$$

with: CDF = Cumulative damage factor

n_i = Damage of the i^{th} load repetition

N_i = Total number of allowable load repetitions

This is an iterative process until the required layer thickness is determined. Permanent deformation of the subgrade layer is also considered during the structural design process.

3.5.3 Van Wijk, Yoder and Wood (1984)

This design method is based on the AASHTO pavement design method, which is widely used in the United States. In this method the number of 80 kN axle load applications (N) required to cause a certain reduction in the Present Serviceability Index (PSI) is related to soil support, a regional factor and the structural number (SN) of the pavement. The structural number is an indication of the structural strength of the pavement and is defined as:

$$SN = a_1 h_1 + a_2 h_2 + \dots + a_n h_n \quad (3.6)$$

with: SN = Structural number

a_1, a_2, a_n = Layer coefficients for different layers in the pavement

h_1, h_2, h_n = Respective layer thicknesses

The layer coefficients is the empirical relationships between the structural number (SN) of a pavement and layer thickness, which expresses the relative ability of a material to function as a structural component of the pavement. Suggested coefficients for recycled materials are included in Table 3.3

Because of the variability of the structural coefficients in Table 3.3, Van Wijk et al (1984) proposed the following function to determine a structural coefficient for the recycled layer.

$$a' = \frac{a \cdot h'}{h} \quad (3.7)$$

with: a' = structural coefficient of the recycled layer used as a base

a = structural coefficient of the AASHTO bituminous layer (0.44)

h' = thickness of the recycled layer

h = thickness of the AASHTO asphalt layer to give the same strain, deformation or fatigue life

The method then proceeds to determine the required thickness of the recycled layer to satisfy the required structural number for the pavement

Table 3.3 Suggested structural coefficients for recycled layers (Van Wijk et al: 1984)

Material	Binder(s)	Coefficient	
		Range	Average
Cold recycled asphaltic material	Bitumen emulsion	0.30 – 0.38	-
In-situ recycled bituminous concrete base	Bitumen emulsion	0.22 – 0.39	-
Central plant recycled bituminous concrete used as base	Bitumen emulsion	0.37 – 0.59	-
	Bitumen emulsion	0.22 – 0.49	0.39
In-place recycled bituminous concrete	Lime	-	0.40
	Cement	0.23 – 0.43	0.33
AASHTO surface	-	-	0.44
AASHTO base	-	-	0.35

3.5.4 Marais and Tait (1989)

Marais and Tait published a structural design procedure for emulsion treated materials based on the work done by Santucci (1977). A number of adjustments were made to the method to allow for South African conditions. The influence of curing and seasonal temperature effects on the elastic modulus were included on a quarterly basis rather than on a monthly basis as proposed by Santucci. The value of the resilient modulus for each cured quarter is presented in Table 3.4. Resilient modulus values from laboratory tests at 23°C and 40°C at the initial and fully cured states are used as input into the structural design. The average base temperatures applicable in South Africa for each quarter are outlined in Table 3.5 and the respective moduli should be used in the structural design.

Fatigue cracking initiated at the bottom of the layer and progressed through the layer to the surface was regarded as the mechanism of failure for the layer and the same transfer function published by Santucci (1977) was used. The subgrade strain criteria are the same as those used by Maree and Freeme (1981) for the evaluation of the pavement structures in TRH4 (CSRA, 1980).

Table 3.4 Resilient modulus values of emulsion treated base layers for each quarter for different full cure periods. (Marais and Tait: 1989)

Quarter	Full curing period		
	6 months	1 year	2 years
1	$0.46(M_f - M_i) + M_i$	$0.30(M_f - M_i) + M_i$	$0.18(M_f - M_i) + M_i$
2	$0.94(M_f - M_i) + M_i$	$0.70(M_f - M_i) + M_i$	$0.46(M_f - M_i) + M_i$
3	M_f	$0.88(M_f - M_i) + M_i$	$0.64(M_f - M_i) + M_i$
4	M_f	$0.98(M_f - M_i) + M_i$	$0.74(M_f - M_i) + M_i$
5	M_f	M_f	$0.86(M_f - M_i) + M_i$
6	M_f	M_f	$0.92(M_f - M_i) + M_i$
7	M_f	M_f	$0.96(M_f - M_i) + M_i$
8	M_f	M_f	$0.99(M_f - M_i) + M_i$

With M_f = Resilient modulus at fully cured state

M_i = Resilient modulus at initial cured state

Table 3.5 Average base temperatures in southern Africa (Marais and Tait: 1989)

Quarter	Temperature
Summer	100 % at 40°C
Autumn	50% at 40°C and 50% at 23°C
Winter	100% at 23°C
Spring	50% at 23°C and 50% at 40°C

Table 3.4 Resilient modulus values of emulsion treated base layers for each quarter for different full cure periods. (Marais and Tait: 1989)

Quarter	Full curing period		
	6 months	1 year	2 years
1	$0.46(M_f - M_i) + M_i$	$0.30(M_f - M_i) + M_i$	$0.18(M_f - M_i) + M_i$
2	$0.94(M_f - M_i) + M_i$	$0.70(M_f - M_i) + M_i$	$0.46(M_f - M_i) + M_i$
3	M_f	$0.88(M_f - M_i) + M_i$	$0.64(M_f - M_i) + M_i$
4	M_f	$0.98(M_f - M_i) + M_i$	$0.74(M_f - M_i) + M_i$
5	M_f	M_f	$0.86(M_f - M_i) + M_i$
6	M_f	M_f	$0.92(M_f - M_i) + M_i$
7	M_f	M_f	$0.96(M_f - M_i) + M_i$
8	M_f	M_f	$0.99(M_f - M_i) + M_i$

With M_f = Resilient modulus at fully cured state

M_i = Resilient modulus at initial cured state

Table 3.5 Average base temperatures in southern Africa (Marais and Tait: 1989)

Quarter	Temperature
Summer	100 % at 40°C
Autumn	50% at 40°C and 50% at 23°C
Winter	100% at 23°C
Spring	50% at 23°C and 50% at 40°C

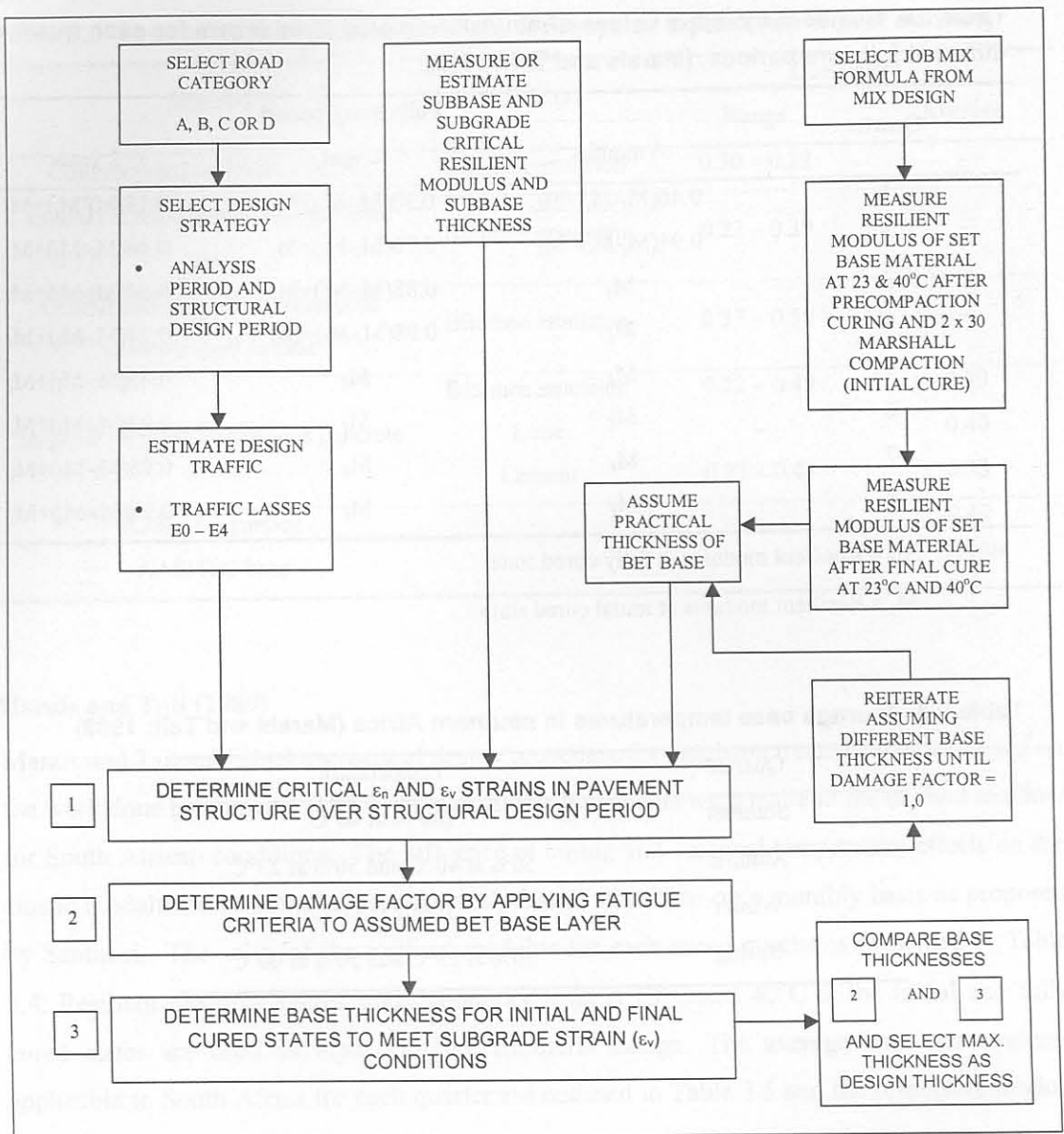


Figure 3.5 Flow diagram for structural design of emulsion treated bases (Marais and Tait: 1989)

3.5.5 SABITA manual 14: GEMS: The design and use of granular emulsion mixes (1993)

The structural design for emulsion treated layers with higher bitumen contents (greater than 2%) are regarded as stabilisation and the approach by Santucci (1977) and Marais and Tait (1985) are followed.

Emulsion treated materials with low bitumen contents (lower than 1.5%) are treated the same as granular materials. For mechanistic analysis the cohesion (c) normally used for the untreated material can be doubled for a modification design of emulsion treated materials. The proposed values for cohesion and internal friction are given in Table 3.6.

Table 3.6 Material properties for emulsion treated materials using the modification approach (SABITA: 1993)

Material code	Moisture state	Apparent Cohesion, c (kPa)	Internal friction, ϕ (°)
G1	Wet	130	55
	Dry	90	55
G2	Wet	110	52
	Dry	80	52
G3	Wet	100	50
	Dry	70	50
G4	Wet	90	48
	Dry	70	48
G5	Wet	80	43
	Dry	60	43

A safety factor against shear failure is calculated as follows:

$$FOS = \frac{\sigma_3 \left(K \cdot \tan^2 \left(45 + \frac{\phi}{2} \right) - 1 \right) + 2K \cdot c \cdot \tan \left(45 + \frac{\phi}{2} \right)}{\sigma_1 - \sigma_3} \quad (3.8)$$

where FOS = Safety factor against shear failure

σ_3 and σ_1 = Calculated major and minor principal stresses acting in the middle of the layer (kPa)

c = Cohesion (kPa)

ϕ = Angle of internal friction (degrees)

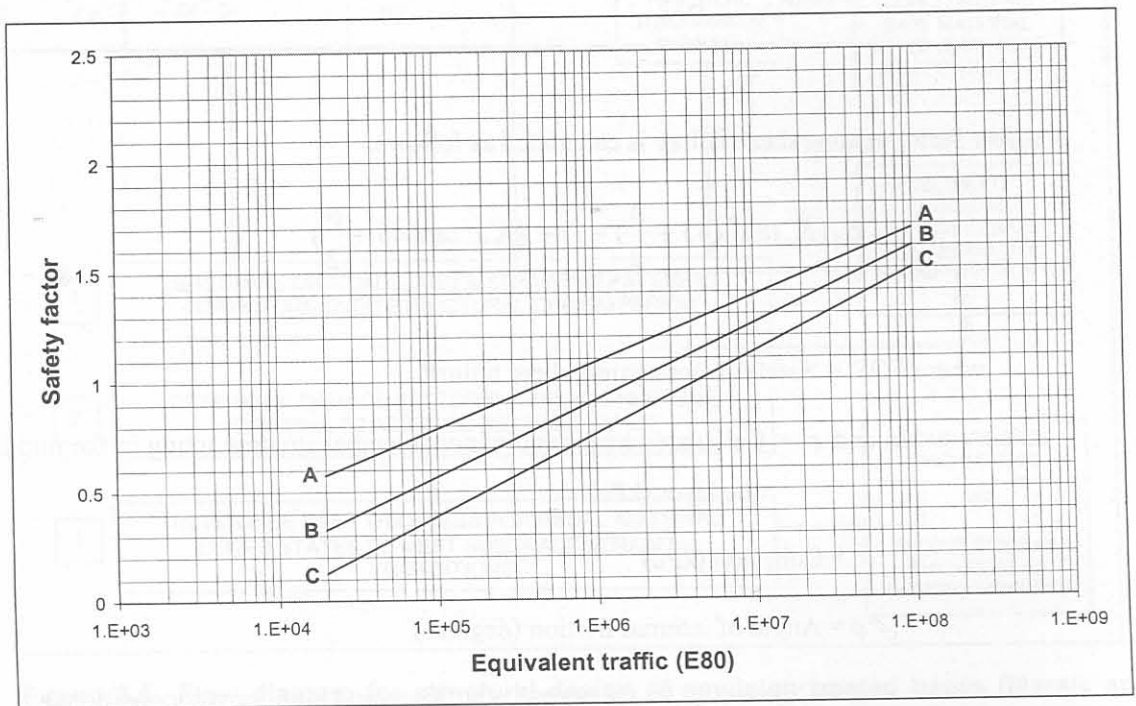
K = Constant (0.95 for normal conditions and 0.65 for wet conditions)

The allowable minimum safety factor for emulsion treated layers at various traffic levels are given in Table 3.7.

The transfer function (Figure 3.6) used to determine the number of load repetitions to shear failure is similar to the one used by Maree and Freeme (1981) for the evaluation of the pavement structures in TRH4 (CSRA: 1980).

Table 3.7 Allowable minimum safety factors at various traffic levels (SABITA: 1993)

Road Category	Design traffic class	Minimum safety factor
A	E4 (12 – 50 million E80's)	1.60
	E3 (3 – 12 million E80's)	1.40
B	E3 (3 – 12 million E80's)	1.30
	E2 (0.8 – 3 million E80's)	1.05
	E1 (0.2 – 0.8 million E80's)	0.85
C	E2 (0.8 – 3 million E80's)	0.95
	E1 (0.2 – 0.8 million E80's)	0.75
	E0 (<0.2 million E80's)	0.50


Figure 3.6 Transfer function for shear failure for granular materials (Maree and Freeme: 1981)

3.5.6 De Beer and Grobler (1994)

Structural design criteria for emulsion treated materials in terms of fatigue cracking and fracturing was developed by de Beer and Grobler (1994) on sections with 3% emulsion (1.8 % net bitumen) and pre-treated with lime. The research was done on weathered dolerites classified as a G4 according to the TRH14 (CSRA, 1987) classification system.

The initial failure point was defined where the initial elastic modulus reduced by 50%. A failure criteria for the fatigue and total fractured (granular) state was also developed. This curve

represents a condition where the maintenance is good and the pavement is in a relatively dry state with approximately 10 mm rutting.

$$\text{Initial fatigue: } N_{if} = 10^{8.6[2.756 - \log(\varepsilon_i)]} \quad (3.9)$$

$$\text{Fatigue and total fracture: } N_{ff} = 10^{4.6[3.435 - \log(\varepsilon_i)]} \quad (3.10)$$

With: N_{if} = Initial fatigue life (Approximately 50% of E_i)

N_{ff} = Fatigue and fracture life (approximately 10 mm rutting)

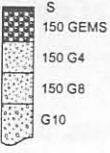
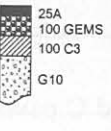
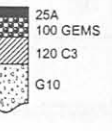
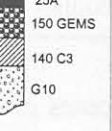
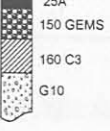
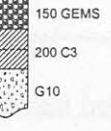
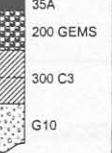
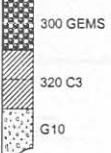
ε_i = Calculated initial horizontal tensile strain at bottom of emulsion treated layer

They recommended that for design purposes of category B and C pavements, the fatigue and total fracture curve (Equation 3.10) be used. A design catalogue was developed from the above transfer functions and is included as Figure 3.7. No provision was made for curing and the early reduced strength of emulsion treated layers.

3.5.7 Theyse (1998)

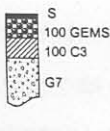
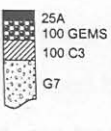
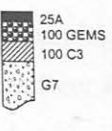
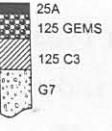
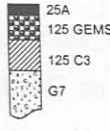

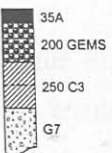
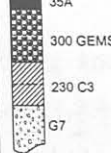
Theyse provides interim guidelines on the structural design of pavements with emulsion treated base layers based on the Dynamic Cone Penetrometer (DCP). The DCP design method is an empirical design method, similar to the CBR cover design approach, mainly developed for the evaluation and design of granular pavements. The DCP is primarily used for the evaluation of existing pavements and the processing and interpretation of DCP data is well advanced in South Africa (Kleyn: 1984 and de Beer: 1991).

The principles of the DCP design method, combined with DCP data measured from various long term pavement performance (LTPP) sections, were used to do some quantitative design analysis (Theyse, 1998). A design catalogue was developed and distributed to practitioners for review. The proposed design catalogue is included as Figure 3.8.

ROAD CATEGORY	EMULSION TREATED BASE LAYERS							
	PAVEMENT CLASS AND DESIGN BEARING CAPACITY (80 kN AXLES/LANE)							
	E0-1 < 0,5 x 10 ³	E0-2 0,5 - 3,0 x 10 ⁴	E0-3 0,3 - 1,0 x 10 ⁵	E0-4 1,0 - 2,0 x 10 ⁵	E1-1 2,0 - 4,0 x 10 ⁵	E1-2 4,0 - 8,0 x 10 ⁵	E2 0,8 - 3,0 x 10 ⁶	E3 3,0 - 10 x 10 ⁶
A: Major interurban freeways and roads. (95% approximate design reliability)								
B: Interurban collectors and major rural roads. (90% approximate design reliability)								
C: Lightly trafficked rural roads and strategic roads. (80% approximate design reliability)								
D: Lightly pavement structures, rural access roads. (80% approximate design reliability)								

Maximum traffic: 10 x 10⁶ E80's
 Symbol A denotes AG, AC or AS
 S denotes Double Surface Treatment (seal or combinations of seal and slurry)

Catalogue of GEMS Designs on a Poor Subgrade (E = 15 Mpa)

ROAD CATEGORY	EMULSION TREATED BASE LAYERS							
	PAVEMENT CLASS AND DESIGN BEARING CAPACITY (80 kN AXLES/LANE)							
	E0-1 < 0,5 x 10 ³	E0-2 0,5 - 3,0 x 10 ⁴	E0-3 0,3 - 1,0 x 10 ⁵	E0-4 1,0 - 2,0 x 10 ⁵	E1-1 2,0 - 4,0 x 10 ⁵	E1-2 4,0 - 8,0 x 10 ⁵	E2 0,8 - 3,0 x 10 ⁶	E3 3,0 - 10 x 10 ⁶
A: Major interurban freeways and roads. (95% approximate design reliability)								
B: Interurban collectors and major rural roads. (90% approximate design reliability)								
C: Lightly trafficked rural roads and strategic roads. (80% approximate design reliability)								
D: Lightly pavement structures, rural access roads. (80% approximate design reliability)								

Maximum traffic: 10 x 10⁶ E80's
 Symbol A denotes AG, AC or AS
 S denotes Double Surface Treatment (seal or combinations of seal and slurry)

Catalogue of GEMS Designs on a Strong Subgrade (E = 90 Mpa)

Figure 3.7. Proposed design catalogue for emulsion treated materials by De Beer and Grobler (1994)

EMULSION TREATED BASE LAYERS											
ROAD CATEGORY	PAVEMENT CLASS AND DESIGN BEARING CAPACITY (80 kN AXLES/LANE)										Foundation
	ES0.003 0,1 - 0,3 x 10 ⁴	ES0.01 0,3 - 1,0 x 10 ⁴	ES0.03 1,0 - 3,0 x 10 ⁴	ES0.1 3,0 - 10 x 10 ⁴	ES0.3 0,1 - 0,3 x 10 ⁶	ES1 0,3 - 1,0 x 10 ⁶	ES3 1,0 - 3,0 x 10 ⁶	ES10 3,0 - 10 x 10 ⁶	ES30 10 - 30 x 10 ⁶	ES100 30 - 100 x 10 ⁶	
A: Major interurban freeways and roads. (95% approximate design reliability)											
B: Interurban collectors and major rural roads. (90% approximate design reliability)											
C: Lightly trafficked rural roads and strategic roads. (80% approximate design reliability)											
D: Lightly pavement structures, rural access roads. (80% approximate design reliability)											

Symbol A denotes AG, AC or AS
 AO, AP may be recommended as a surfacing measure for improved skid resistance when wet to reduce water spray
 S denotes Double Surface Treatment (seal or combinations of seal and slurry)
 S1 denotes Single Surface Treatment
 * is Seal is used, increase C4 and G5 subbase thickness to 200 mm

Most likely combinations of road category and design bearing capacity

Figure 3.8. Proposed design catalogue for emulsion treated materials by Theyse (1998)

3.5.8 SABITA manual 21: ETB: The design and use of emulsion treated bases (1999)

No formal structural design procedure is given in the document and it recommended that the catalogue in the manual be used. The catalogue is the same catalogue proposed by Theyse (1994), which is included above as Figure 3.8.

3.6 Conclusions

This chapter addressed the current state of the art on the structural behaviour and design procedures for pavements with emulsion treated layers. Most of the emulsion treated materials have net bitumen contents between 0.6 and 3%, with cement content generally below 2%. The following conclusions that is of importance to this study may be drawn from this literature study:

- There is general consensus that the behaviour of emulsion treated layers is a two staged behaviour. One stage being the pre-cracked phase where the layer acts as a slab will be governed by fatigue and the other being the equivalent granular phase where the layer will exhibit properties similar to that of granular materials.
- The end of the fatigue life of the treated layer is not yet clearly defined and need to be addressed in this study. The end of the fatigue life may be a function of the emulsion and cement contents and should be done in terms of elastic and plastic parameters, e.g. deflection and horizontal strain. The contribution of the fatigue layer to the total life of the layer is also not clear.
- Emulsion treated materials fail at lower stresses, but at increased deformation than cement treated and crushed stone materials. It is able to withstand more deformation before failure than cemented or granular materials. Higher deflections in emulsion treated layers might therefore not necessarily be an indication of a weak layer. This property needs to be considered when a failure criteria for the end of the fatigue phase is defined.
- The influence of the addition of cement on the structural properties of an emulsion treated material is unknown. The literature suggests that the properties of an emulsion treated layer without cement are similar to that of high quality crushed stone.
- The curing of emulsion treated layers without cement or lime may take several months to complete. This process can be speeded up with the addition of cement or lime. A design modulus for input into the mechanistic design procedure need to be defined.
- Transfer functions that are available are for high bitumen contents in terms of horizontal tensile strain at the bottom of the layer. For low bitumen contents the same transfer function for granular materials in terms of shear strength are used.

- Design catalogues based on DCP tests and experience are available. Their development were limited to some of the long term pavement performance (LTPP) sections in South Africa.
- The influence of cement on the fatigue properties of the emulsion treated layer are not known. In the first phase is it a cement treated layer with emulsion or an emulsion treated layer with cement?

3.6 REFERENCES

Committee of Land Transportation Officials (COLTO), 1996, *Structural design of flexible pavements for interurban and rural roads*, Draft TRH4:1996, Department of Transport, Pretoria, South Africa.

Committee of Land Transportation Officials (COLTO), 1997, *Draft TRH12: Flexible pavement rehabilitation investigation and design*, Draft TRH12:1997, Department of Transport, Pretoria, South Africa.

Committee of State Road Authorities (CSRA), 1980, *Structural design of interurban and rural road pavements*, Draft TRH4:1980, Department of Transport, Pretoria, South Africa.

Committee of State Road Authorities (CSRA), 1987, *Guidelines for Road Construction Materials*, TRH14:1987, Department of Transport, Pretoria, South Africa.

De Beer M, 1989, Aspects of the design and behaviour of road structures incorporating lightly cemented layers, PhD Thesis, University of Pretoria, Pretoria, South Africa.

De Beer M, 1991, *Use of the Dynamic Cone Penetrometer in the design of road structures*, Research Report DPVT-187, Transportek, CSIR, Pretoria, South Africa.

De Beer M and Grobler JE, 1993, *ETB': Heavy Vehicle Simulator (HVS) Evaluation of the Heilbron Sections*, South African Roads Board, Service Contract Report PR92/2/1, Pretoria, South Africa.

De Beer M and Grobler JE, 1994, *Towards improved structural design criteria for granular emulsion mixes*, Proceedings of the 6th Conference on Asphalt Pavements in Southern Africa, Cape Town, South Africa.

Epps JA, 1968, Influence of mixture variables on the flexural fatigue and tensile properties of asphalt concrete, Ph.D Dissertation, University of California, Berkeley, United States.

Freeme CR, Maree JH and Viljoen AW, 1982, *Mechanistic design of asphalt pavements and verification of designs using the Heavy vehicle Simulator*, Proceedings of the 5th International Conference on the Structural Design of Asphalt Pavements, Vol 1 pp 156 – 173, Delft, The Netherlands.

Freeme CR, Maree JH and Viljoen AW, 1987, *The behaviour and mechanistic design of asphalt pavements*, Proceedings of the 6th International Conference on the Structural Design of Asphalt Pavements, Vol. 1, Ann Arbor, Michigan, United States.

Horak E and Rust FC, 1991, *The performance and behaviour of bitumen emulsion treated road bases in South Africa*, Proceedings of the 7th International Conference on Asphalt Pavements, Nottingham, United Kingdom.

Horak E and Viljoen AW, 1981, *Heavy Vehicle Simulator (HVS) testing of experimental sections consisting of recycled materials in Natal*, Technical report RP/4/81, National Institute for Transport and Road Research, CSIR, Pretoria, South Africa.

Jordaan GJ, 1994, *The South African Mechanistic Pavement Rehabilitation Design Method*, Department of Transport, Research Report RR91/242, Pretoria, South Africa.

Kari WJ, 1969, *Design of emulsified asphalt treated base courses*, Proceedings of the 1st Conference on Asphalt Pavements in Southern Africa, Durban, South Africa.

Kleyn EG, 1984, *Aspekte van plaveisevaluering en –ontwerp soos bepaal met behulp van die dinamiese kegelpenetrometer*, MEng Thesis, University of Pretoria, Pretoria, South Africa.

Laatz AJ and du Toit GD, 1990, *Identification and initial performance indicators of emulsion treated bases (ETBs), for long term pavement performance monitoring - Interim report*, Interim report no. IR-88/014, Transportek, CSIR, Pretoria, South Africa.

Marais CP and Tait MI, 1989, *Pavements with bitumen emulsion treated bases: Proposed material specification, mix design criteria and structural design procedures for South African conditions*, Proceedings of the 5th Conference on Asphalt Pavements in Southern Africa, Swaziland.

Maree JH and Freeme CR, 1981, *The mechanistic design method used to evaluate the pavement structures in the catalogue of the draft TRH4:1980*, Report no. RP/2/81, National Institute for Transport and Road Research, CSIR, Pretoria, South Africa.

Maree JH, 1982, *Aspekte van die ontwerp an gedrag van padplaveisels met korrelmateriaalkroonlae*, PhD Thesis, University of Pretoria, Pretoria, South Africa.

Maree JH, Viljoen CBL, Gibson R, 1982, *Aspekte van die behandeling van gebreekteklipkroonlae met klein persentasies bitumenemulsie of teer*, NITRR, CSIR, Technical report RP/10/82, Pretoria, South Africa.

Pell PS and Cooper KE, 1975, *The effect of testing and mix variables on the fatigue performance of bituminous materials*, Proceedings of the Association of Asphalt Paving Technologists, Vol, 44, pp 1 – 37.

SABITA, 1993, *GEMS: The design and use of granular emulsion mixes*, Manual 14, SABITA, Cape Town, South Africa.

SABITA, 1999, *ETB: The design and use of emulsion treated bases*, Manual 21, SABITA, Cape Town, South Africa.

Santucci LE, 1977, *Thickness design procedure for asphalt and emulsified asphalt mixes*, Proceedings of the 4th International Conference on the Structural Design of Asphalt Pavements, Ann Arbor, Michigan, United States, pp 424 – 456.

Steyn WJvdM, 1997, Summary of field and laboratory tests results on selected Emulsion Treated Base (ETB) pavements, Technical Report TR-97/049, Transportek, CSIR, Pretoria, South Africa.

Theyse HL, 1998, Towards guidelines on the structural design of pavements with emulsion treated layers, Transportek, CSIR, (CR-97/045), Pretoria, South Africa.

Theyse HL, de Beer M, Rust FC, 1996, *Overview of the South African Mechanistic Pavement Design Analysis Method*, Divisional Publication DP-96/005, Transportek, CSIR, Pretoria, South Africa.

Van Wijk AJ, Yoder EJ and Wood LE, 1984, *Structural aspects of two cold recycled layers*, 4th Conference on Asphalt Pavements in Southern Africa, Cape Town, South Africa.

Wright BG, Lacante SC, Laatz AJ and du Toit GD, 1991, *Long term performance of emulsion treated base pavements*, Project Report PR 88/014, South African Roads Board, Pretoria, South Africa.

4.2 PREREQUISITES FOR INCORPORATING A NEW MATERIAL INTO THE MECHANISTIC-EMPIRICAL DESIGN PROCESS

The mechanistic-empirical design method allows the designer some latitude in the choice of design inputs within the domain in which the method was developed. The South African Mechanistic Design Procedure was developed in the 1970's through a series of research and was approved and refined in the 1980's and 1990's (Meyer and Pienaar 1981, Ong 1972, Ong 1975, Meyer 1974, Meyer 1982, de Beer 1985, de Beer 1991, Jordaan 1988 and Theyse et al. 1998). The method was developed for South African conditions and South African materials and verified to a large extent with the use of a number of Heavy Vehicle Simulator (HVS) tests.

The incorporation of a new or fairly untried material into a mechanistic design process requires a number of prerequisites. These include:

- The basic behaviour of the particular material should be well understood. This does not imply that the full behaviour pattern over the lifespan of the total life cycle should be known, but requires at least some general description of how the material is expected to behave in terms of response, strength and performance characteristics. If this description

CHAPTER 4 MECHANISTIC-EMPIRICAL DESIGN MODELS IN PAVEMENT ENGINEERING

4.1 INTRODUCTION TO THE MECHANISTIC – EMPIRICAL APPROACH

The first step in the development of mechanistic design procedures took place when Boussinesq (1883) developed a mathematical solution in 1885 to determine stresses and strains in a one layer system subjected to a point load on the surface. The material was assumed to be linear elastic, homogeneous with semi-infinite dimensions. In 1926 Westergaard (1938) developed a two-layer system with the assumption that the upper layer is an elastic plate that bend through but with no vertical deflection within the layer. Timoshenko developed the general theory of elasticity where stresses and strains in a linear elastic system subject to complex loading conditions can be calculated. Burmister (1945) improved this theory for two- and three-layer systems, but it was not user friendly because of complex equations. The work of Acum and Fox (1948), Peattie (1962) and Jones (1962) provided tables for systems with a maximum of three layers. The development of computers from the 1960's provided the opportunity for analyses of systems with five and more layers. Pavement engineers were then able to analyse pavement structures with various number of layers and loading conditions. The calculated stresses and strains could be compared with values obtained from tests or experiments.

4.2 PREREQUISITES FOR INCORPORATING A NEW MATERIAL INTO THE MECHANISTIC-EMPIRICAL DESIGN PROCESS

The mechanistic-empirical design model allows the designer some latitude in the sense that designs slightly outside the domain in which the method was developed, may be investigated. The South African Mechanistic Design Procedure was developed in the 1970's from a wide range of research and was improved and refined in the 1980's and 1990's (Maree and Freeme: 1981, Otte: 1972, Otte: 1978, Maree: 1978, Maree: 1982, de Beer: 1985, de Beer: 1989, Jordaan: 1988 and Theyse et al: 1996). The method was developed for South African conditions and South African materials and verified to a large extent with the use of a number of Heavy Vehicle Simulator (HVS) tests.

The incorporation of a new or fairly unknown material into a mechanistic design process require a number prerequisites. These include:

- The basic behaviour of the particular material should be well understood. This does not imply that the full behaviour pattern nor the timescale of the total life cycle should be known, but requires at least some general description of how the material is expected to behave in terms of resilient, strength and performance characteristics. If this description

agrees with the behaviour model for a well-known material already included in the design method, the process for developing a model for the new material could be simplified and accelerated.

- Once the input parameters have been identified from consideration of the expected behaviour pattern and failure mechanism for a new material, representative values of these parameters should be obtained. These input parameters will typically include the resilient properties of the material and some strength parameters related to the mode of failure of the material.
- A well established performance model (transfer function) relating the calculated stress or strain condition in the different pavement layers to the expected structural performance of the different material types used in these layers, must be available. In this case the structural performance is defined as the number of stress/strain repetitions that can be sustained by the material at that particular stress/strain level until a certain terminal condition is reached.

4.3 GRANULAR MATERIALS

Granular layers deform due to consolidation or densification and gradual shear under repeated loading. The consolidation or densification phase is usually limited to the early life of the layer and is a function of the construction quality, compaction and quality of the material used. Most of this initial deformation can be limited by proper construction and compaction. Research by Maree (1978, 1982) indicated that granular layers fail in shear when the shear strength of the layer is exceeded. He introduced the concept of a safety factor against shear failure for granular materials used in the South African Mechanistic Pavement Design Method. The safety factor against shear failure is based on the Mohr-Coulomb theory for static loading and represents the ratio of the material shear strength to the applied stresses responsible for shear. The principal stresses (σ_1 and σ_3) in the middle of the layer are regarded as the critical parameters used to calculate the safety factor. The safety factor incorporates the cohesion, internal friction, moisture regime and stress condition of the material.

The safety factor against shear is defined by:

$$F = \frac{\sigma_3 \left(K \cdot \tan^2 \left(45 + \frac{\phi}{2} \right) - 1 \right) + 2K \cdot c \cdot \tan \left(45 + \frac{\phi}{2} \right)}{\sigma_1 - \sigma_3} \quad (4.1)$$

where F = Safety factor against shear failure

σ_3 and σ_1 = Calculated major and minor stresses acting in the middle of the layer

c = Cohesion (kPa)

ϕ = Angle of internal friction (degrees)

K = Constant (0.95 for normal conditions and 0.65 for wet conditions)

A safety factor of less than 1 implies that the shear stress exceeds the shear strength of the material and that rapid shear failure will occur under static loading. Under dynamic loading conditions, which is typically what happens on a pavement, the applied shear stress will only exceed the shear strength for a short period of time and shear failure will not occur under one or two load repetitions. The shear failure or deformation will gradually accumulate under a number of load repetitions. The rate of shear deformation of the granular layer is influenced by the magnitude of the safety factor.

Allowable safety factors proposed by Maree (1978, 1982) for different granular materials are summarised in Table 4.1.

Table 4.1 Allowable safety factors for granular materials at various traffic levels (Maree: 1978)

Road Category (TRH4)	Design traffic	Minimum safety factor
A	> 10 million E80's	1.6
	1 – 10 million E80's	1.5
B	3 – 30 million E80's	1.4
	0.1 – 3 million E80's	1.3
C	0.1 – 1 million E80's	1.2
	< 0.1 million E80's	1.0

The transfer function for granular layers to a terminal condition of 20 mm deformation at the surface is presented in Figure 4.1.

The model developed by Maree (1982), which is included in the South African Mechanistic Pavement Design Method, only consider deformation in the layer as a result of shear failure.

Figure 4.1 δ - ϵ curves for G1 to G3 materials to a terminal permanent strain of 20 mm (Went, 1992)

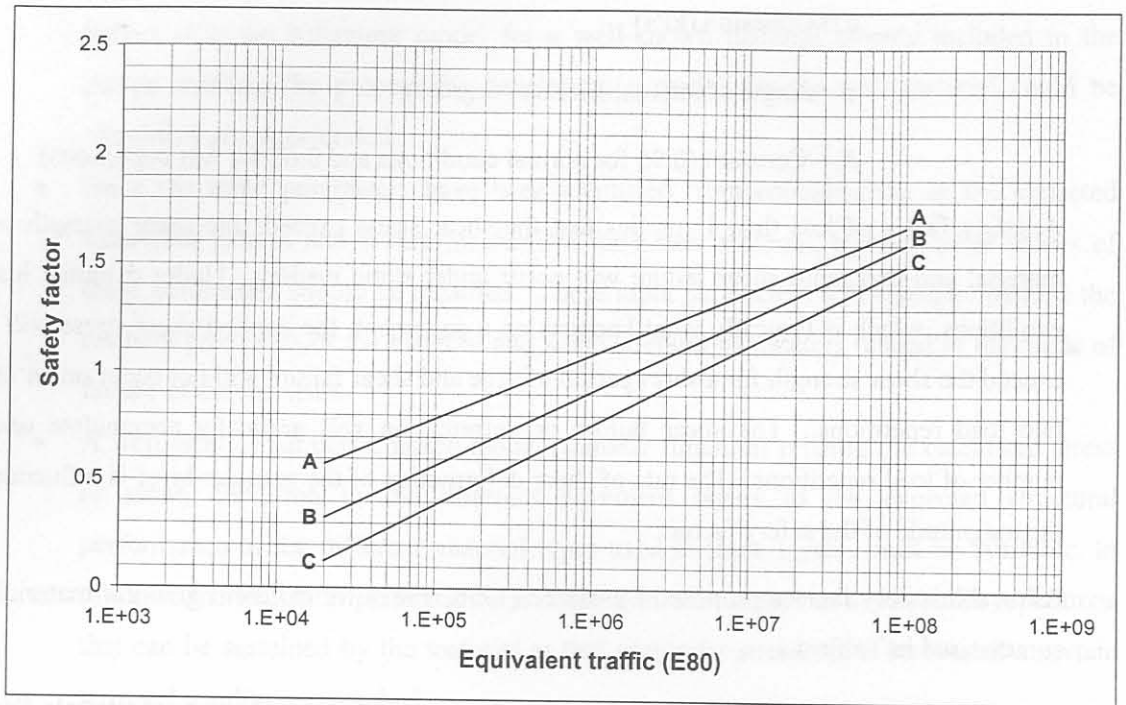


Figure 4.1 Transfer function for granular materials (Maree: 1982)

Wolff (1992) developed a design method that includes the initial rapid deformation as well as the gradual deformation at a constant rate thereafter. He developed design curves for G1 to G6 materials based on SN-curves and expressed the development of permanent deformation by the following function:

$$\varepsilon_p = (mN + a)(1 - e^{-bN}) \quad (4.2)$$

where: ε_p = cumulative permanent deformation or strain

N = number of load repetitions

m , a and b = constants

Properties of the function are described in detail by Wolff (1992) and Shackleton (1995).

The stress state, or bulk stress Θ , in the middle of the layer were used as the critical parameter in the transfer functions developed by Wolff (1992). The bulk stress is defined as the sum of the principal stresses ($\Theta = \sigma_1 + \sigma_2 + \sigma_3$). The shortcomings of the linear modelling of granular materials were addressed by introducing a non-linear elastic analysis. The K-theta model, developed by Biarez (1962), Hicks (1970), Seed et al (1967) and others were used to describe the non-linearity of the granular materials:

$$M_R = K_1 \Theta^{K_2} \quad (4.3)$$

where: M_R = resilient modulus

Θ = bulk stress which is the sum of principle stresses

K_1 and K_2 = constants

The transfer functions developed by Wolff (1992) were based on results from 22 HVS tests on base layers that varied from G1 to G6 quality. The functions were developed for various levels of permanent strains between 10 000 $\mu\epsilon$ and 200 000 $\mu\epsilon$. The relationship between the bulk stress and the number of load repetitions was given, in a non-linear form, as:

$$\Theta = A \left(1 - e^{-\frac{B}{N^m}} \right) \quad (4.4)$$

where: Θ = bulk stress

N = number of load repetitions

m , A and B = regression constants

A typical S-N curve for G1 to G6 materials for a permanent strain of 20 000 $\mu\epsilon$ (equivalent to 3 mm of permanent deformation in a 150 mm layer) is presented in Figure 4.2.

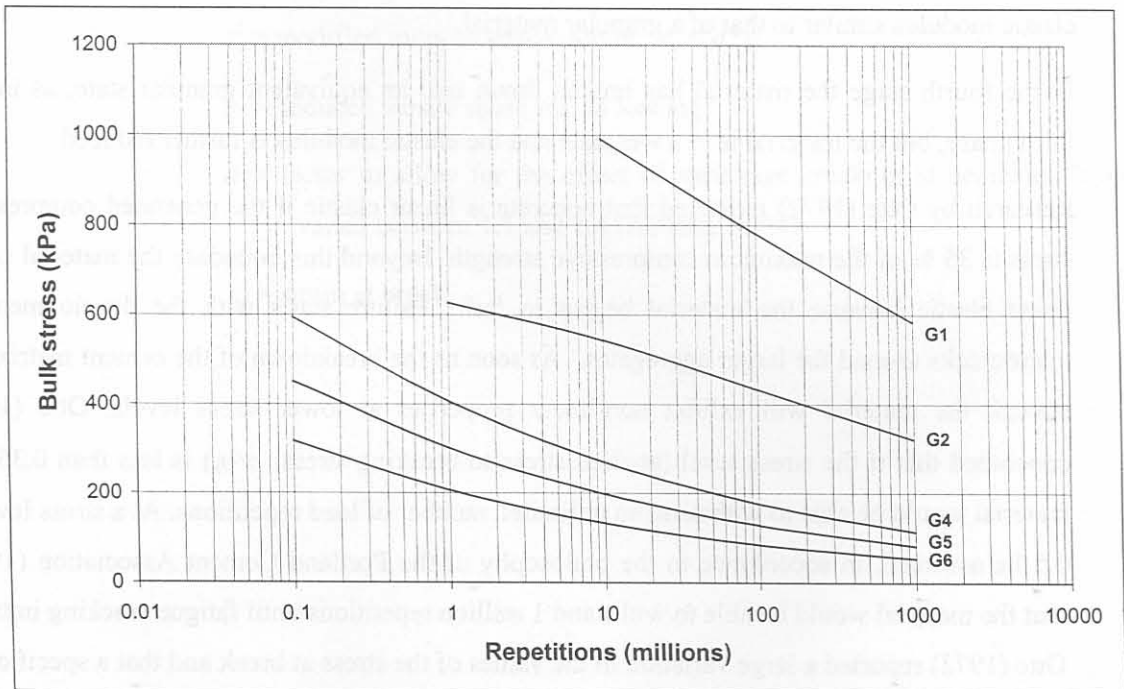


Figure 4.2 S-N curves for G1 to G6 materials at a terminal permanent strain of 20 000 $\mu\epsilon$. (Wolff: 1992)

4.4 CEMENTED LAYERS

Cemented layers are analysed in terms of fatigue cracking and crushing. Fatigue cracking usually starts at the bottom of the layer and progresses upwards through the layer, while crushing occurs at the top (upper 50 to 75 mm) of a lightly cemented base layer.

4.4.1 Fatigue life

De Beer (1985) describes the behaviour of cemented layers as a four staged behaviour that influences the effective elastic moduli of the material.

The first stage, also known as the pre-cracked phase, involves the possible presence of shrinkage cracks but at large block sizes (greater than 5 times layer thickness) and the material acts as a slab similar to a concrete slab.

In the second phase loading and/or the environment have reduced the block size, but the behaviour is still predominantly controlled by the large blocks of material relative to the layer thickness (block size between 1 and 5 times layer thickness). The material still acts as a slab but with a reduced elastic moduli.

In the third phase the material has broken down in small blocks (block size smaller than layer thickness) and the material is equivalent to that of a granular material. The material also has an elastic modulus similar to that of a granular material.

In the fourth stage the material has broken down into an equivalent granular state, as in the third phase, but the material is in a wet state and the elastic modulus is further reduced.

Research by Otte (1972) indicated that concrete is linear elastic if the generated compressive stress is 35 % of the maximum compressive strength. Beyond this boundary the material is not linear elastic because the material begins to fail. Failure starts with the development of microcracks around the larger aggregates. As soon as the breakdown of the cement matrix had started, the material will exhibit non-linear properties at lower stress levels. Otte (1978) concluded that if the stress level (applied stress to breaking stress, σ/σ_b) is less than 0.35, the material would be able to withstand an unlimited number of load repetitions. At a stress level of 0.5 he assumed, in accordance to the philosophy of the Portland Cement Association (1959), that the material would be able to withstand 1 million repetitions until fatigue cracking initiates. Otte (1972) reported a large variation in the values of the stress at break and that a specification in terms of strain at break resulted in less variation. The corresponding strain ratios ($\varepsilon/\varepsilon_b$) for unlimited and 1 million repetitions are 0.25 and 0.33 respectively. The fatigue life function developed by Otte was mainly for strongly (4 to 6 % cement content or C1 and C2) (CSRA: 1986) stabilised materials and is defined in Equation 4.5.

$$N_f = 10^{9.1 \left(1 - \frac{\epsilon}{\epsilon_b}\right)} \quad (4.5)$$

where: N_f = Number of load repetitions to failure

ϵ = Horizontal tensile strain at bottom of the layer

ϵ_b = Strain at break

Otte (1972) determined average values for the strain at break on various projects, with cement stabilised base layers with 4% cement, at $145 \mu\epsilon$. He recommended that a maximum allowable strain of 25 % of the strain at break, should never be exceeded.

Research by de Beer (1989) and Jordaan (1988) point out that the transfer function developed by Otte underestimates the effective fatigue life of lightly cemented layers. An effective fatigue life function for lightly cemented (C3 and C4) materials was developed by de Beer from various HVS tests and is defined in equation 4.6. A comparison between the fatigue life functions developed by Otte and de Beer is presented in Figure 4.3.

$$N_f = 10^{7.19 \left(1 - \frac{\epsilon_s}{8\epsilon_b}\right)} \quad (4.6)$$

where: N_f = Effective fatigue life

ϵ_s = modified induced tensile strain: $\epsilon_s = d * \epsilon_i$

ϵ_i = induced tensile strain due to loading

d = factor to allow for the effect of shrinkage cracking in cemented layers varies between 1.1 and 1.4 (Jordaan: 1994)

ϵ_b = strain at break

Figure 4.3 Comparison of the fatigue curves proposed by Otte (1972) and de Beer (1989)

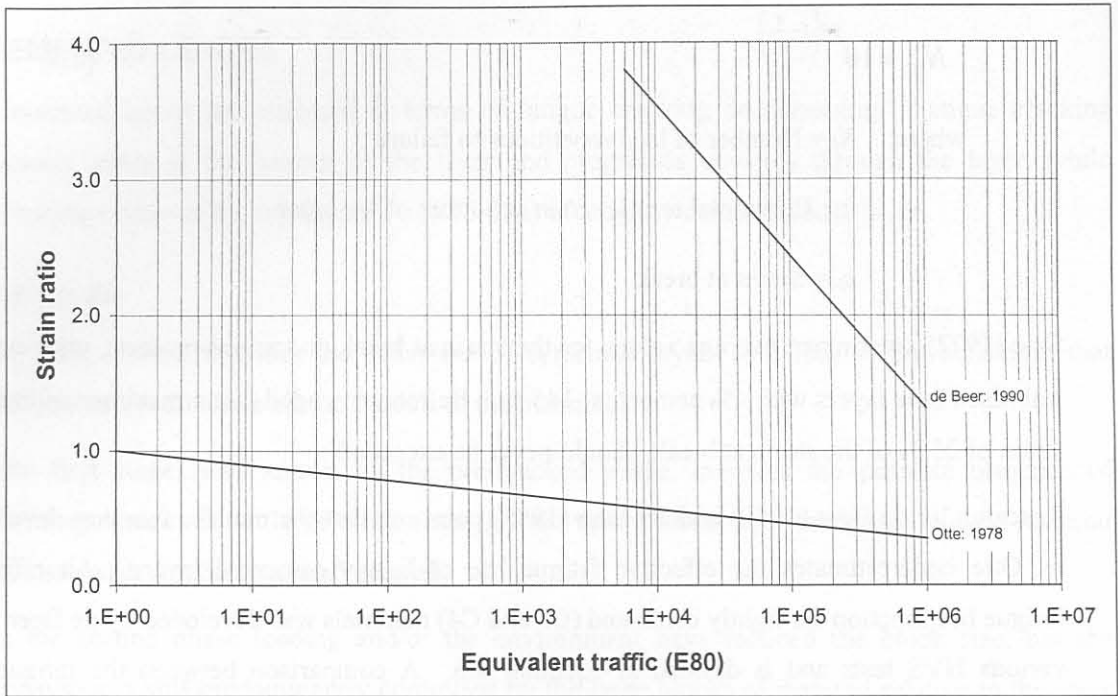


Figure 4.3 Comparison of the relationship between maximum tensile strain ratio (ϵ_s/ϵ_b) and number of strain repetitions to initiate effective fatigue cracking in cemented layers (de Beer: 1989).

According to Jordaan (1988) the layer will be in its transitional (second) phase, still intact but with microcracks present, and with a reduced elastic moduli, if the tensile strain exceeds 25 % of the strain at break. The values for the elastic modulus for cemented material are included in Table 4.2.

The method by Otte was further improved by Jordaan (1988) to allow for the in-situ pavement conditions by adjusting the strain at break (ϵ_b) as determined in the laboratory for strongly cemented layers. This is done by increasing the strain at break by a factor of m which has a value of 4.7. Figure 4.4 presents a comparison between the failure criteria of Otte and the improved one by Jordaan.

It might be possible that the maximum horizontal strain does not occur at the bottom of the cemented layer. Jordaan (1988) derived a method to test if the maximum strain does occur at the bottom of the layer that is similar to the formula recommended by SHELL (1978) for the use on asphalt layers to determine when the maximum horizontal strain shifts from a position at the bottom of the asphalt layer to a position within the asphalt layer.

Table 4.2 Typical effective range of elastic moduli for cement treated materials in various stages of behaviour. (Jordaan: 1994)

Original code	UCS (MPa) Pre-cracked material	Parent material	Phase 1	Phase 2	Phase 3	
			Pre-cracked phase with large shrinkage cracks (MPa)	Transitional phase: Layer intact, but microcracks present (MPa)	Post-cracked phase: layer broken up in equivalent granular state	
					Dry state (MPa)	Wet State (MPa)
C1	5 – 12	Crushed stone G2 – G3	2 500 – 3 000	800 – 1 000	400 - 500	50 – 400
C2	3 – 6	Crushed stone G2 – G3, and Natural Gravel G4	2 000 – 2 500	500 – 800	300 - 800	50 - 300
C3	1.5 – 3	Natural Gravel G4 – G10	1 000 – 2 000	500 - 800	200 - 400	20 - 250
C4	0.75 – 1.5	Natural Gravel G4 – G10	500 – 2000	400 - 600	100 - 350	20 - 200

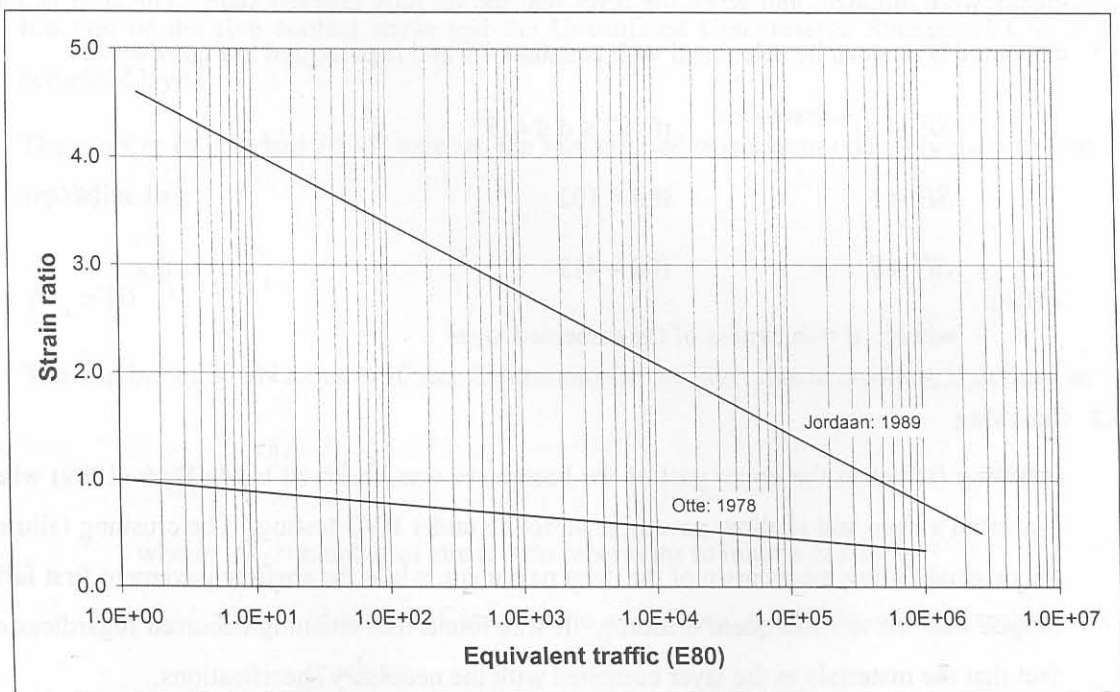


Figure 4.4 Comparison of the fatigue criteria applicable to strongly cemented layers (Jordaan: 1988)

The position of the maximum horizontal strain is at the bottom of the cemented layer when:

$$\left(\frac{E_3}{E_2}\right)^2 h_c < K \quad (4.7)$$

$$\text{where: } h_c = h_1 \left(\frac{E_1}{E_3}\right)^{\frac{1}{3}} + h_2 \left(\frac{E_2}{E_3}\right)^{\frac{1}{3}} \quad (4.8)$$

E_1 = elastic modulus of the asphalt layer (MPa)

E_2 = elastic modulus of the cement treated base layer (MPa)

E_3 = elastic modulus of the subbase layer (MPa)

h_1 = thickness of the asphalt layer (mm)

h_2 = thickness of the cement treated layer (mm)

K = constant = 128

After the initiation of cracks at the bottom of a cemented layer, the crack progresses through the layer with time as the layer is subjected to traffic loading. The progression of cracks through the layer is addressed by means of a shift factor to allow for the time between when the cracks were initiated, and when the layer reached its fully cracked state. The shift factor for cemented layers can be calculated with equation 4.9 and is presented in Figure 4.5.

$$\begin{aligned} SF &= 10^{(0.00285d - 0.293)} && \text{if } 102 \leq d \leq 419 \\ SF &= 1 && \text{if } d < 102 \\ SF &= 8 && \text{if } d > 419 \end{aligned} \quad (4.9)$$

where: d = thickness of the cemented layer

4.4.2 Crushing

Crushing failure in the upper part of the base layer was observed by de Beer (1989) when he evaluated a deep and shallow pavement structure under HVS testing. The crushing failure was the original failure mechanism of the deep pavement, while the shallow pavement first failed in fatigue that led to subsequent crushing. It was found that crushing occurred regardless of the fact that the materials in the layer complied with the necessary specifications.

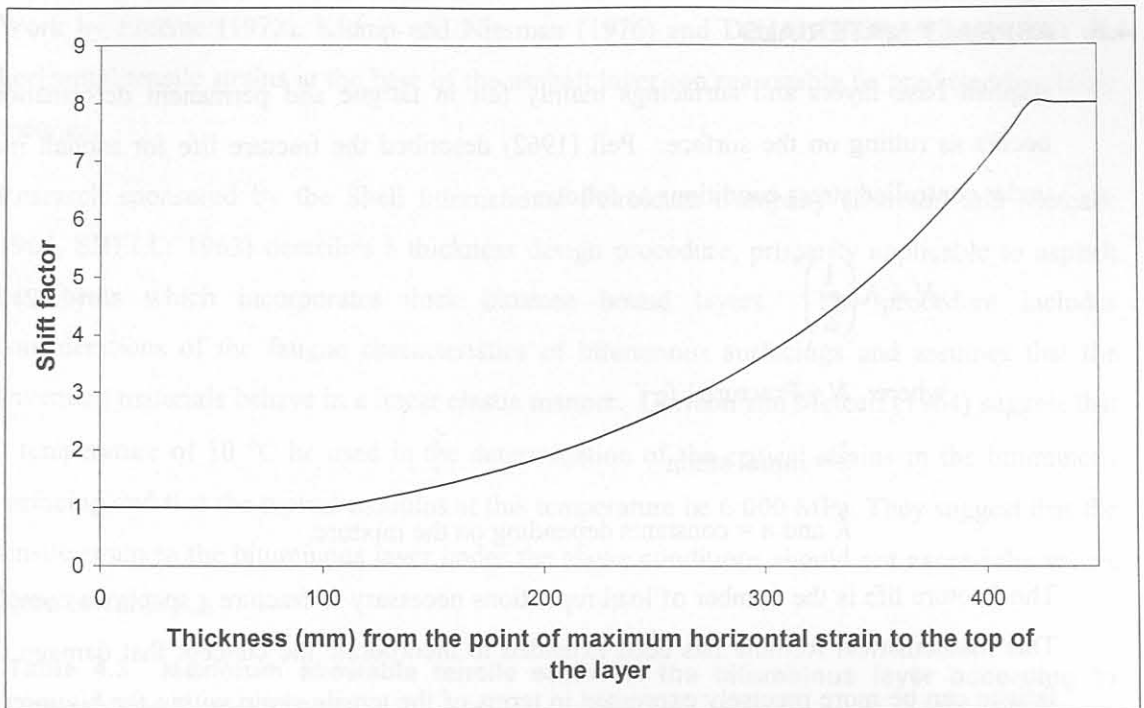


Figure 4.5 Shift factor for cemented layers (Jordaan: 1994)

This failure mechanism differs from the fatigue failure normally associated with cemented materials as described by Otte (1972) and de Beer (1989). This led to the development of the “crushing life” concept for lightly cemented gravel pavement materials. The crushing is a function of the tyre contact stress and the Unconfined Compressive Strength (UCS) of the cemented layer.

The number of standard 80 kN axles to the initiation of crushing in relatively deep pavements are defined as:

$$N_{c1} = 10^{8.21 \left(1 - \frac{\sigma_t}{1.2UCS}\right)} \quad (4.10)$$

The number of 80 kN axles to 10 mm deformation in the layer due to crushing is defined as:

$$N_{c2} = 10^{9.1 \left(1 - \frac{\sigma_t}{1.2UCS}\right)} \quad (4.11)$$

where: N_{c1} = number of stress ratio repetitions to initiate crushing

N_{c2} = number of stress ratio repetitions to 10mm of deformation due to crushing

σ_t = vertical stress at the top of the layer (kPa)

UCS = Unconfined Compressive Strength of the in-situ cementitious material

4.5 ASPHALT MATERIALS

Asphalt base layers and surfacings mainly fail in fatigue and permanent deformation that occurs as rutting on the surface. Pell (1962) described the fracture life for asphalt material under controlled stress conditions as follows:

$$N = K \left(\frac{1}{\varepsilon} \right)^n \quad (4.12)$$

where: N = Fracture life

ε = initial strain

K and n = constants depending on the mixture.

The fracture life is the number of load repetitions necessary to fracture a specimen completely. This mathematical formula has been extended to incorporate the concept that damage due to fatigue can be more precisely expressed in terms of the tensile strain within the bitumen (Pell: 1976), and resulted in the following equation:

$$N = K \left(\frac{\alpha B_v}{\varepsilon_M} \right)^n \quad (4.13)$$

where: N = number of load repetitions to cause crack initiation

α = a factor depending on the amount of filler voids and/or voids present in the mix

B_v = proportion of bitumen present in the total volume of mix

ε_M = tensile strain in the mixture

K and n = constants depending on the mixture.

Epps and Monismith (1969) presented fatigue regression lines from controlled stress laboratory testing for granite mixes graded to meet the extremes, as well as the middle of the State of California 13.2 mm maximum sieve-size grading specifications which contains 6 % bitumen (by mass of aggregate). These regression lines can be presented by the following equation:

$$N_f = 1.15 * 10^{-6} \left(\frac{1}{\varepsilon_{mix}} \right)^{2.92} \quad (4.14)$$

where: N_f = number of load applications to fracture

ε_{mix} = bending strain repeatedly applied

Work by Freeme (1972), Klomp and Niesman (1976) and Dehlen (1969) indicated that the horizontal tensile strains at the base of the asphalt layer can reasonably be predicted by elastic theories.

Research sponsored by the Shell International Petroleum Company (Dormon and Metcalf: 1964, SHELL: 1963) describes a thickness design procedure, primarily applicable to asphalt pavements which incorporates thick bitumen bound layers. The procedure includes considerations of the fatigue characteristics of bituminous surfacings and assumes that the pavement materials behave in a linear elastic manner. Dormon and Metcalf (1964) suggest that a temperature of 10 °C be used in the determination of the critical strains in the bituminous surfacing and that the typical modulus at this temperature be 6 000 MPa. They suggest that the tensile strain in the bituminous layer under the above conditions should not exceed the values given in Table 4.3.

Table 4.3 Maximum allowable tensile strain in the bituminous layer according to Dormon and Metcalf (1964)

Number of equivalent 80 kN axle load applications	Tensile strain in bituminous layer (µε)
10 ⁵	230
10 ⁶	145
10 ⁷	92
10 ⁸	58

The work of Monismith et al (1971), Heukelom and Klomp (1964) and Kingham et al (1972) were used by Freeme and Strauss (1979) to develop the transfer functions included in the South African Mechanistic Pavement Design Method. These researchers all related the crack initiation fatigue life to the tensile strain in the sample.

The transfer function currently included in the South African Mechanistic Design Method for thick asphalt bases is as follows:

$$N_f = 10^{\alpha \left(1 - \frac{\log \epsilon_t}{\beta} \right)} \quad (4.15)$$

where: N_f = Number of 80 kN equivalent axle repetitions to crack initiation

ϵ_t = tensile strain at the bottom of the asphalt layer

α and β = regression constants depending on mix stiffness and percentile level

The transfer function for thin asphalt surfacings is similar to the one for thick asphalt bases and is as follows:

$$N_f = 10^{A \left(1 - \frac{\log \varepsilon_i}{B} \right)} \quad (4.16)$$

where: N_f = Number of 80 kN equivalent axle repetitions to crack initiation

ε_i = tensile strain at the bottom of the asphalt surfacing layer

A and B = regression constants depending on mix type (gap graded, continuous graded etc.) and percentile level

The propagation of cracks through the layer will occur as a result of repeated loading after cracks have been initiated at the bottom of the layer. Factors that accelerate or provide the necessary conditions for cracks to propagate through the layer, are those which induce tensile stress in the material. A shift factor to allow for this crack propagation is proposed by Jordaan (1994) and is as follows:

$$SF = \frac{d}{20} - 0.25 \quad (4.17)$$

where: SF = Shift factor to allow for crack propagation

d = thickness of asphalt layer in mm

Work done by Harvey et al (1995) include the mix properties such as bitumen content, air void content as well as voids filled with bitumen into fatigue life predictions from controlled strain laboratory testing. They indicated that an increase in bitumen content and a decrease in air voids enhance the fatigue life properties of asphalt mixes. An increase in the voids filled with bitumen also benefits the laboratory fatigue life. Maximum bitumen content and minimum void content are for given conditions not only limited by economics, but also by other distress mechanisms such as rutting, instability and bleeding.

The permanent deformation of asphalt materials is not included in the South African Mechanistic Pavement Design Method. It is assumed that proper mix design will prevent excessive permanent deformation before the end of the fatigue life. Asphalt is visco-elastic and permanent deformation is dependent on a number of factors that include time of loading, temperature, magnitude of load and the various mix properties. To accurately model the permanent deformation of asphalt would require complex analysis procedures that are beyond the scope for routine structural design of pavements. These procedures are more useful in the mix design of asphalt materials.

4.6 SUBGRADE MATERIALS

Subgrade soils are usually found at a depth of 450 mm and more in the pavement structure. The dominant failure mechanism assumed is permanent deformation as a result of the

combined action of consolidation and shear. The critical parameter for evaluating this failure mechanism is the vertical compressive strain at the top of the subgrade layer. The first criteria for subgrade performance for South African subgrades, was published by Paterson (1978) and is presented in Figure 4.5. The background for these criteria is the work done by Paterson (Paterson and Maree: 1978) and by the US Army Engineer Waterways Experiment Station (WES) (Brabston et al: 1975). Paterson's criteria was based on the analysis of data from the AASHO road test done by the personnel from SHELL (Dormon: 1962, Dormon and Metcalf: 1965). The AASHO data are the only source of original data for the prediction of performance of subgrade material used as background for the South African Mechanistic Design Method. Criteria were published for three road categories that were applicable for any natural gravel or gravel-soils layers underneath the subbase.

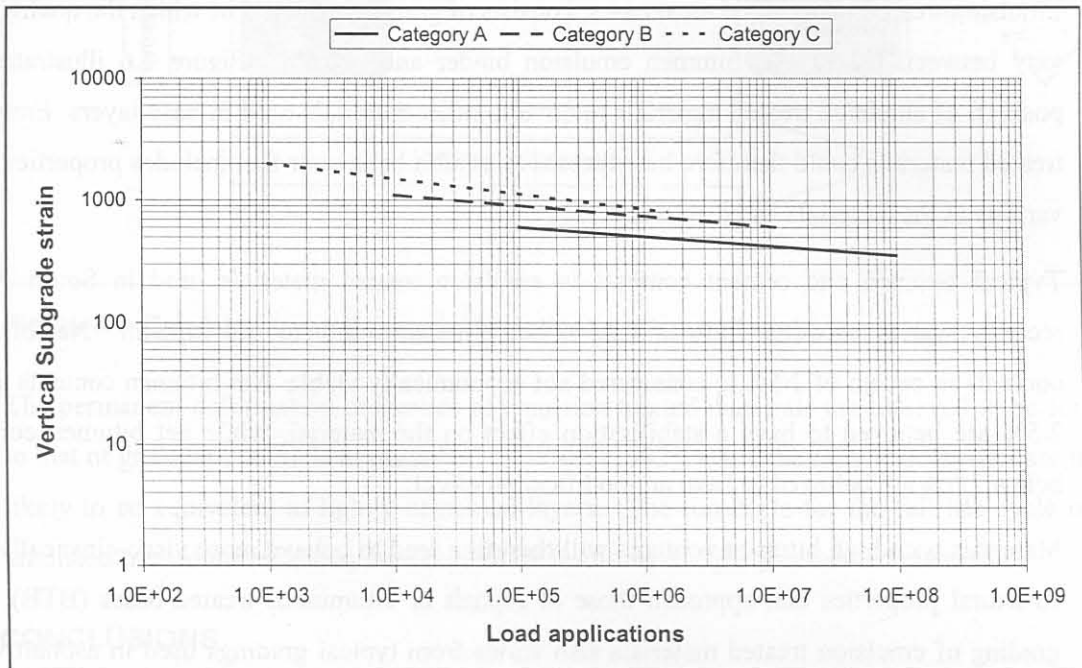


Figure 4.5 Criteria for prediction of subgrade performance in Southern Africa Paterson (1978)

Jordaan (1994) developed a regression equation from the available international literature in which the failure criteria is a function of the adopted terminal rut depth.

$$N = \left(\frac{\varepsilon_v}{20^{2.37} Rut} \right)^{-10} \quad (\text{after Jordaan: 1994}) \quad (4.18)$$

where: ε_v = Maximum vertical compressive strain at the top of the subgrade

Rut = Allowable rutting (mm)

In the revision of the TRH4 Flexible Pavement Design document, (Theyse et al: 1995 and Theyse: 1996) the following failure criteria is included into the SAMPDM that incorporate the terminal rut condition as well as the percentile level required:

$$N = 10^{A-10 \log(\epsilon_v)} \quad (\text{after Theyse et al: 1996}) \quad (4.19)$$

where: ϵ_v = Maximum vertical compressive strain at the top of the subgrade

A = Regression coefficient that includes the percentile level and the terminal rut condition

4.7 MECHANISTIC-EMPIRICAL MODELS APPLICABLE TO EMULSION TREATED MATERIALS.

Emulsion treated material, in most cases, consists of granular material of which the quality may vary between G2 to G7, bitumen emulsion binder and cement. Figure 4.6 illustrates the position of emulsion treated materials relative to other materials used in base layers. Emulsion treated materials could therefore be expected to exhibit behaviour that includes properties from various of the materials listed above.

Typical bitumen and cement contents in emulsion treated materials used in South Africa recently, varies between 1.0% and 2.5% net bitumen and 1 to 2% cement. Net bitumen contents in excess of 2.5% is considered not economically viable. Net bitumen contents above 2.5% are believed to have a stabilisation effect on the material, while net bitumen contents below 2.5% are believed to have an modification effect.

Materials with high bitumen contents will therefore tend to behave more visco-elastically with structural properties that approach those of asphalt or bituminous treated bases (BTB). The grading of emulsion treated materials also varies from typical gradings used in asphalt where the grading requirements of asphalt material are more closely controlled. Materials with lower (less than 2.5%) contents of net bitumen would therefore not behave similar so asphaltic materials.

Materials with low bitumen- and cement contents (typically less than 1%) would tend to behave more according to the Möhr-Coulomb theory with structural properties like unbound granular material. The applicability of the Möhr-Coulomb theory to materials with cement- and net bitumen contents typically expected in emulsion treated materials, is not researched, but is expected to be applicable.

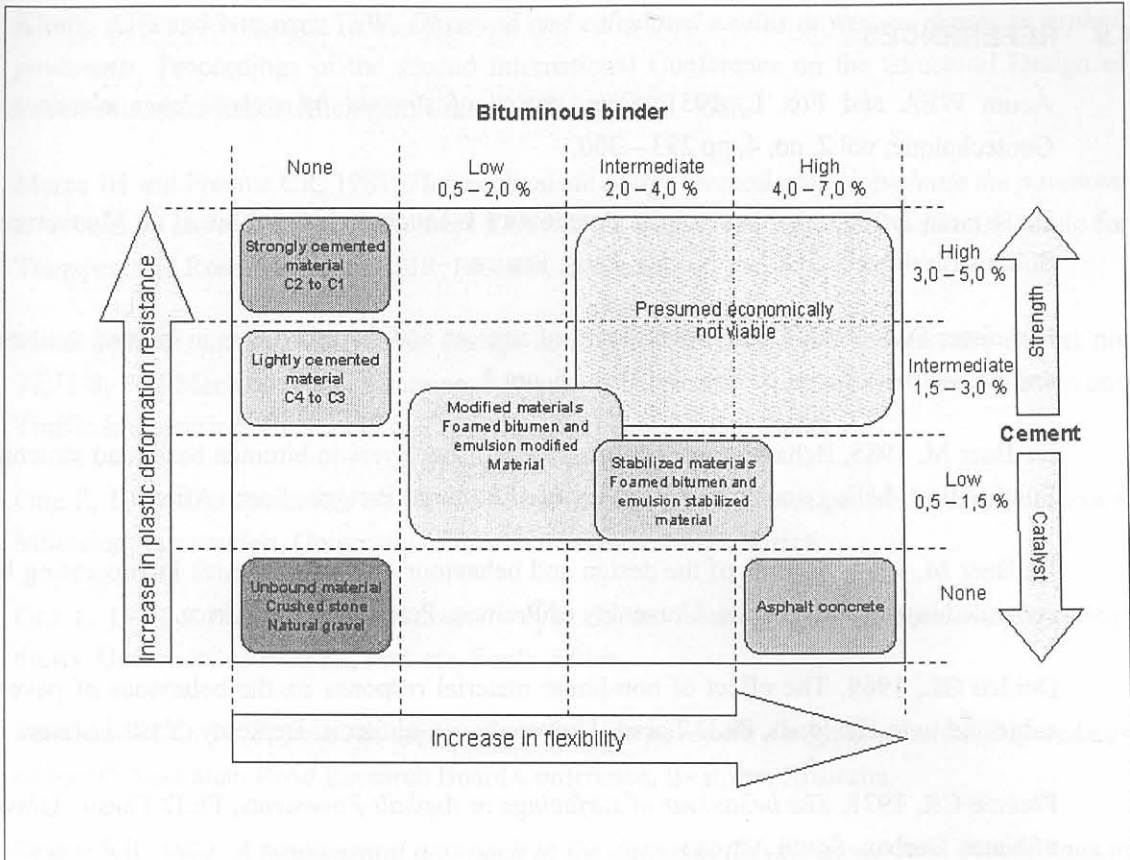


Figure 4.6 Emulsion treated materials relative to other materials

The permanent deformation properties of emulsion treated materials are believed to be similar to that of granular materials as described by Wolff (1992), while the fatigue properties are more likely to be equivalent to lightly cemented layers. The timescale for the full life cycle of an emulsion treated material may however differ from that of lightly cemented materials.

4.8 CONCLUSIONS

The South African Mechanistic Pavement Design Method includes design models for four generic material types commonly used for pavement structural layers in South Africa. These include granular materials, strongly and lightly cemented layers, bituminous surfacings and bases as well as subgrade materials. Of these materials, the lightly cemented material and the granular material, seem to also represent an emulsion treated material, in terms of general behaviour. No transfer function for emulsion treated material is included in the current South African Mechanistic Pavement Design method.

The fatigue life transfer function for lightly cemented material should be evaluated to predict the fatigue life for emulsion treated materials. The transfer functions for permanent deformation developed by Maree (1982) as well as Wolff (1992) should be evaluated for applicability to predict the permanent deformation of emulsion treated layers.

4.9 REFERENCES

- Acum WEA and Fox L, 1951, *Computation of stresses in a three-layer elastic system*, Geotechnique, vol.2, no. 4, pp 293 – 300.
- Boussinesq J, 1883, *Application des Potentials à L'Etude de L'Equilibre et du Mouvement des Solides Elastiques*, Gauthier-Villars, Paris, France.
- Burmister DM, 1945, The general theory of stresses and displacements in layered systems I, II and III, *Journal of applied Physics*, Vol. 16, no. 2.
- De Beer M, 1985, *Behaviour of cementitious subbase layers in bitumen base road structures in South Africa*, MEng dissertation, University of Pretoria, Pretoria, South Africa.
- De Beer M, 1989, *Aspects of the design and behaviour of road structures incorporating lightly cemented layers*, PhD Thesis, University of Pretoria, Pretoria, South Africa.
- Dehlen GL, 1969, *The effect of non-linear material response on the behaviour of pavements subjected to traffic loads*, Ph.D Thesis, University of California, Berkeley, United States.
- Freeme CR, 1971, *The behaviour of surfacings in Asphalt Pavements*, Ph.D Thesis, University of Natal, Durban, South Africa.
- Freeme CR and Strauss JA, 1979, *Towards the Structural Design of More Economical Pavements in South Africa*, Proceedings of the Third Conference on Asphalt Pavements for Southern Africa, Durban, South Africa.
- Harvey JT, Deacon JA, Tsai B and Monismith CL, 1995, *Fatigue performance of asphalt and its relationship to asphalt concrete pavement performance in California*, Asphalt Research Program, CAL/APT Program, Institute of Transportation Studies, Iniversity of California, Berkeley, United States.
- Heukelom W and Klomp AJG, 1964, *Road design and dynamic loading*, Proceedings of the Association of Asphalt Paving Technologists, Vol I pp 92 –123.
- Jones A, 1962, *Tables of stresses in three-layer elastic systems*, Highway Research Board Bulletin 342.
- Jordaan GJ, 1988, *Analysis and developments of some pavement rehabilitation design methods*, PhD thesis, University of Pretoria, Pretoria, South Africa.
- Jordaan GJ, 1994, *The South African Mechanistic Pavement Rehabilitation Design Method*, Department of Transport, Research Report RR91/242, Pretoria, South Africa.
- Kingham IR and Kallas BF, 1972, *Laboratory fatigue and its relationship to Pavement Performance*, Proceedings of the 3rd International Conference on the Structural Design of Asphalt Pavements, Vol I pp 849 – 865, London, United Kingdom.

- Klomp AJG and Niesman ThW, *Observed and calculated strains at various depths in asphalt pavements*, Proceedings of the second International Conference on the Structural Design of Pavements, Ann Arbor, Michigan, United States, pp 671 – 688.
- Maree JH and Freeme CR, 1981, *The mechanistic design method used to evaluate the pavement structures in the catalogue of the draft TRH4:1980*, Report no. RP/2/81, National Institute for Transport and Road Research, CSIR, Pretoria, South Africa.
- Monismith CL and Mclean, 1972, *Design considerations for asphalt pavements*, Report no. TE71-8, Soil Mechanics and Bituminous Research Laboratory, Institute for Transportation and Traffic Engineering, University of California, Berkeley, United States.
- Otte E, 1972, *Die Spannings en Vervormingseienskappe van Sementgestabiliseerde Materiale*, MSc(Eng) dissertation, University of Pretoria, Pretoria, South Africa.
- Otte E, 1978, *A structural design procedure for cement-treated layers in pavements*, DSc(Eng) thesis, University of Pretoria, Pretoria, South Africa.
- Paterson WDO, 1978, *Towards applying mechanistic pavement design in practice*, Proceedings of the 9th Australian Road Research Board Conference, Brisbane, Australia.
- Peattie KR, 1962, *A fundamental approach to the design of flexible pavements*, Proceedings of the First International Conference on the Structural Design of Asphalt Pavements, Ann Arbor, Michigan, United States, p 403.
- Pell PS, 1962, *Fatigue characteristics of bitumen and bituminous mixes*, Proceedings of the First International Conference on the Structural Design of Asphalt Pavements, Ann Arbor, Michigan, United States, pp 310 – 323.
- Pell PS, 1967, *Fatigue of Asphalt Pavement Mixes*, Proceedings of the Second International Conference on the Structural Design of Asphalt Pavements, Ann Arbor, Michigan, United States, pp 577 – 593.
- Portland Cement Association, 1959, *Soil-cement laboratory handbook*, Portland Cement Association, Chicago, United States.
- Shackleton MC, 1995, *Modelling of the permanent deformation of untreated pavement layers*, MEng dissertation, University of Pretoria, Pretoria, South Africa.
- SHELL, 1963, *Charts for flexible pavements*, Shell International Petroleum Company Limited, London, United Kingdom.
- SHELL, 1978, *Shell pavement design manual – asphalt pavements and overlays for road traffic*, Shell International Petroleum Company Limited, London, United Kingdom.

Theyse HL, de Beer M, Prozzi J and Semmelink CJ, 1995, *TRH4 Revision (1995): Phase I: Updating the South African Mechanistic Design Method*, Report no. I/PA/13/95, National Service Contract NSC-24/1, Transportek, CSIR, Pretoria, South Africa.

Theyse HL, de Beer M and Rust FC, 1996, *Overview of the South African Mechanistic Pavement Design Analysis Method*, Divisional Publication DP-96/005, Transportek, CSIR, Pretoria, South Africa.

Theyse HL, 1998, *Towards Guidelines on the Structural Design of Pavements with Emulsion-treated Layers*, Contract Report CR-97/045, Transportek, CSIR, Pretoria, South Africa.

Theyse, HL, 2001, Personal correspondence and communication.

Westergaard HM, 1938, *A problem of elasticity suggested by a problem in Soil Mechanics: Soft material reinforced by numerous strong horizontal sheets*, in *Contribution to the Mechanics of Solids*, Stephan Timoshenko 60th Anniversary Vol., Macmillan, New York, Unites States.

Wolff H, 1992, *The Elasto-plastic behaviour of granular pavement layers in South Africa*, PhD thesis, University of Pretoria, Pretoria, South Africa.

CHAPTER 5 PERFORMANCE OF AN EMULSION TREATED GRAVEL UNDER LABORATORY AND HVS TESTING

5.1 INTRODUCTION

The experimental programme in this study was developed to provide an understanding of the structural behaviour and the engineering properties that influence the structural behaviour of materials treated with bitumen emulsion and cement. Data acquired from the study was used to develop a failure criteria and subsequent transfer functions for emulsion treated materials. The tests consisted of laboratory testing and testing under the Heavy Vehicle Simulator (HVS).

The laboratory testing included an investigation of different contents of cement and bitumen emulsion on the engineering properties as well as the behaviour under static and dynamic triaxial testing. Different bitumen and cement contents were considered in an attempt to provide a classification for emulsion treated material and to define the structural input parameters into the structural design process.

The HVS tests were full-scale tests on an in-service pavement. The HVS tests provided information on the possible modes of distress under HVS testing as well as the behaviour of the emulsion treated materials in the “pre-cracked” and “post-cracked” phases under various wheel loads.

5.2 EXPERIMENTAL DESIGN

5.2.1 Laboratory testing

The following tests were conducted on the material treated with various cement and binder contents:

- California Bearing Ratio tests (CBR)
- Unconfined Compressive tests (UCS)
- Indirect Tensile tests (ITS)
- Static four point flexural beam tests
- Drained unconsolidated static triaxial tests
- Drained unconsolidated dynamic triaxial tests

The UCS, ITS and flexural beam tests were conducted at cement contents of 0, 1 and 2% and net bitumen contents of 0, 0.6, 1.8 and 3%. A minimum of three repetitions for the CBR, UCS and ITS were performed with a minimum number of 4 repetitions for the flexural beam test. Table 5.1 presents a detailed overview of the experimental design for the laboratory testing.

Table 5.1 Tests on different combinations of cement and net bitumen contents

		Net bitumen content (%)			
		0	0.6	1.8	3.0
Cement content (%)	0	CBR	CBR, UCS, ITS, Flexural beam	CBR, UCS, ITS, Flexural beam	CBR, UCS, ITS, Flexural beam
	1	UCS, ITS, Flexural beam	UCS, ITS, Flexural beam	UCS, ITS, Flexural beam	UCS, ITS, Flexural beam
	2	UCS, ITS, Flexural beam, Dynamic triaxial, Static triaxial	-	UCS, ITS, Flexural beam, Dynamic triaxial, Static triaxial, HVS	UCS, ITS, Flexural beam

The static and dynamic triaxial tests were performed at two densities, namely 67% and 73% relative density and at saturation levels of 75% and 45%. For the static triaxial tests confining pressures of 20 kPa, 80 kPa, 140 kPa and 200 kPa were used for each saturation and density level. The dynamic tests were performed at confining pressures of 80 kPa and 140 kPa and at stress ratios of 0.2, 0.55 and 0.9.

The bitumen and cement content for all the static and dynamic triaxial tests were kept at 1.8 % and 2 % respectively, which were the same as used on the HVS site.

The aim of this testing was to determine the influence of different cement and net bitumen contents on some engineering properties. The values reported for the CBR, UCS and ITS are not recommended for use as guidelines in the design of emulsion treated materials and only illustrate the effect of cement and emulsion on them.

Specimen preparation and curing

The mixing process of the cement and bitumen emulsion was not part of this research and mixing was done by hand in the laboratory. All the samples were cured for 28 days at ambient temperature. Different curing methods and curing periods were not considered in this study. This was done in detail by Verhaeghe et al (1998). The curing time and method decided upon was done to enable results from this study to be compared with the results from other studies undertaken on foamed bitumen. (Long: 2001, Robroch: 2001). All the samples for the CBR, UCS, ITS and Flexural beam tests were compacted to 100% of modified AASHTO density, and tested at optimum moisture content.

5.2.2 Laboratory test procedures

California Bearing Ratio (CBR)

The California Bearing Ratio (CBR) was developed to describe the bearing capacity of a material or soil. It is determined by measuring the load required to allow a standard piston to penetrate the surface of a material at a rate of 1.27 mm per minute to depths of 2.54, 5.08 and 7.62 mm. The California load standards are 13.344, 20.016 and 25.354 kN respectively for each penetrated depth.

The CBR test is described in detail as test method A8 in the TMH1 (NITRR: 1986).

Unconfined Compressive Strength Tests (UCS)

The Unconfined compressive test is used to evaluate the strength of stabilised materials in the laboratory. The UCS of a stabilised material is the load in kPa required to crush a specimen with a height of 127 mm and a diameter of 152.4 mm, to total failure, at a constant load application rate of 140 kPa per second.

The UCS test is described as test method A14 in the TMH1 (NITRR: 1986).

Indirect Tensile Strength Tests (ITS)

The Indirect tensile strength is used to evaluate the tensile strength properties of a stabilised material. The test consists of loading a cylindrical specimen with compressive loads distributed along two loading strips, on the sides of the specimen. The load is applied at a constant rate of 140 kPa per second. This results in a relatively uniform tensile stress perpendicular to, and along, the diametric plane of the applied load. Failure usually occurs by splitting along the loaded plane. The details of the test are described as test method A16T in TMH1 (NITRR: 1986).

Static four point beam test

The static four point beam test consists of a beam with dimensions of 75 * 75 * 450 mm which is supported at each edge. Vertical loads are applied at two positions at a distance equal to one third of the length of the beam, away from the end of the beam. The test is performed under controlled strain mode and the magnitude of the load is determined by the resistance of the beam as it is flexed. The vertical displacement of the beam is measured on top of the beam by two Linear Variable Displacement Transducers (LVDT's) on the middle span, halfway between the loading points. The applied load and the vertical displacement of the beam, recorded during the test, are used to calculate the horizontal stress and strain at the bottom of the beam from linear elastic beam theory.

The basic set-up of the static four-point beam test is illustrated in the photograph in Figure 5.1 and a typical example of the stress-strain response measured during the test is shown in Figure 5.2.



Figure 5.1 Typical set-up of the four point static beam test.

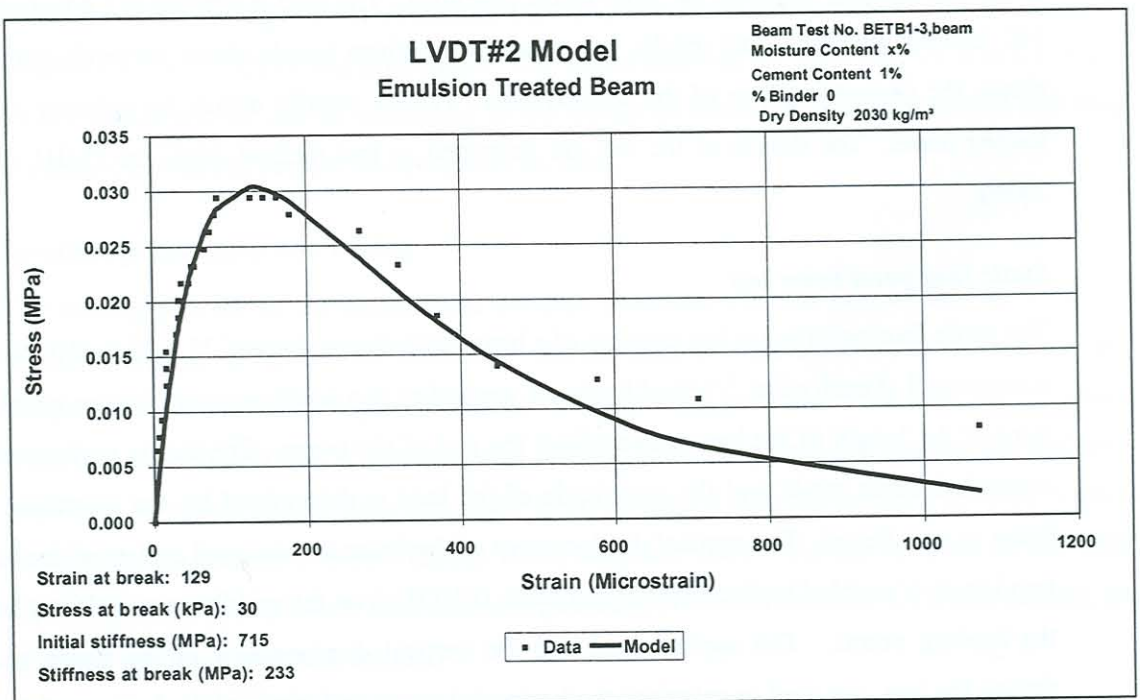


Figure 5.2 Typical Stress-Strain response measured during four-point beam test.

Static triaxial tests

The static triaxial test is widely used to determine the shear strength parameters of soils. In this test, samples of up to 150 mm in diameter and 300 mm in height can be used. The sample is encased by a thin rubber membrane and placed inside a plastic cylindrical chamber that may be filled with water or compressed air to provide a confining pressure. To cause the shear failure of the sample, axial stress is applied through a hydraulic loading ram from the top. A load cell in the loading ram records the applied load, while a LVDT in the loading ram records the displacement of the ram.

The load is applied at a constant rate of 2 mm per minute and the magnitude of the load and displacement of the loading is recorded electronically. The recorded load and displacement may be used to calculate the deviator stress ($\sigma_1 - \sigma_3$) applied to the sample and the vertical uniaxial strain of the sample. A typical stress-strain curve from a static triaxial test is shown in Figure 5.3a. The data obtained from the stress-strain plot may then be used to calculate the slope of the stress-strain curve that is the secant stiffness modulus (E_{sec}) of the sample (Figure 5.3b).

The static triaxial test is better known for determining the shear strength envelope or Möhr-Coulomb failure envelope of granular materials (Das: 1990). This is done by performing a number of static triaxial tests at different confining pressures. The peak stress (yield stress) that a sample can sustain, at a particular confining pressure is obtained from the turning point on the stress-strain curve. By plotting the Möhr stress circles associated with the different confining pressures and respective yield stress values, a failure envelope may be obtained from the tangent drawn to the Möhr stress circles. The shear strength parameters, c and ϕ , may then be determined from the Möhr stress circles.

Dynamic triaxial tests

The dynamic triaxial test is a repeated load test, where a load pulse with a magnitude below the static shear strength of the material is repeatedly applied to the sample with a short rest period between the pulses. The set-up of the dynamic triaxial test is similar to that of the static triaxial test, with the addition of a set of LVDT's that are normally fixed over the middle third of the height of the sample. The elastic and plastic deformation over the middle third of the sample can then be measured. This eliminates the influence of frictional shear forces and edge displacement effects between the load plates and the sample.

STATIC TRIAXIAL TEST

Material: Ferricrete

Emulsion

Sample #: ETF01

Dry Density (kg/cub m): 1870

Confining pressure (kPa): 22

Moisture (%): 10.5

Linear stiffness (MPa): 474

Maximum deviator stress (kPa): 1998

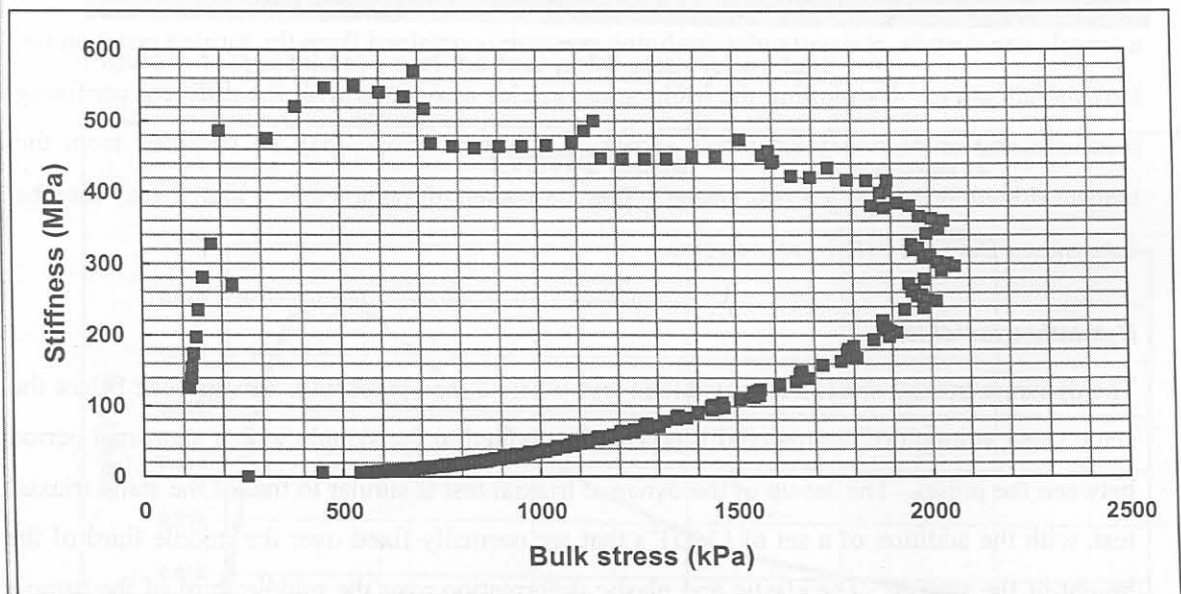
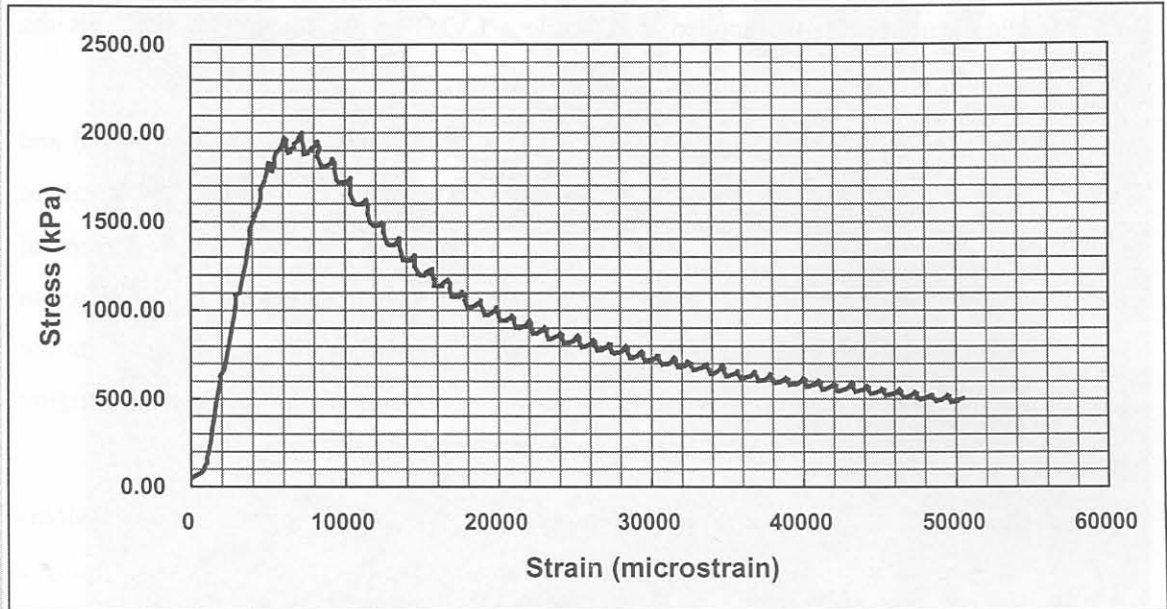
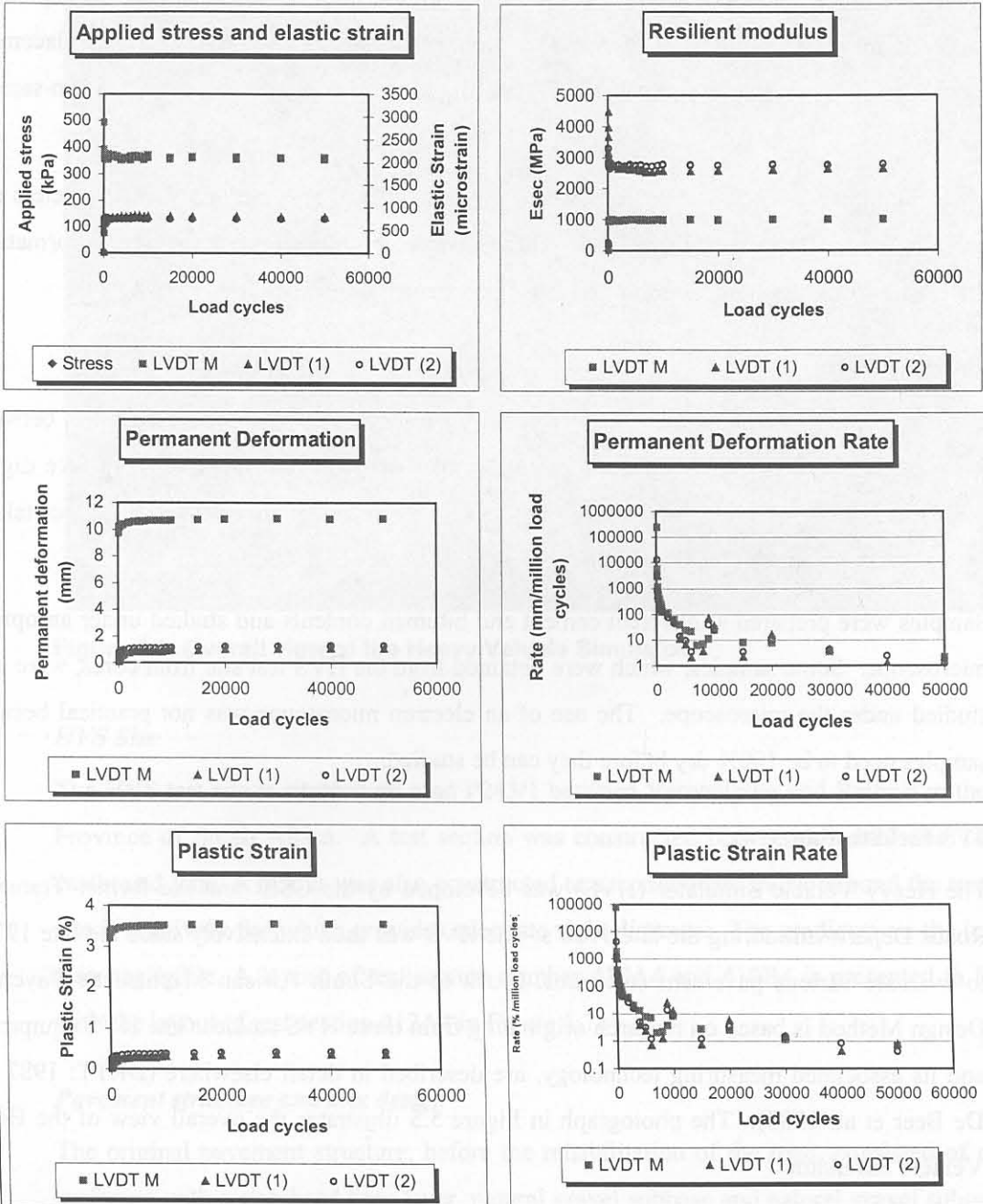


Figure 5.3 Typical result from the static triaxial test.

Material: Ferricrete with cement Sample #: ETF19
 Density: 2062 kg/ cub m Confining pressure: 80.8 kPa
 Moisture: 10.7 % Stress Ratio 90 % of failure stress



Elastic response results

	Average for test		Final values	
	Elastic Strain (microstrain)	Resilient Modulus (MPa)	Elastic Strain (microstrain)	Resilient Modulus (MPa)
LVDT M	2127	939	2065	1004
LVDT #1	726	2667	786	2639
LVDT #2	722	2659	748	2773
	724	2663	767	2706

Plastic response results

	Final values		Permanent Deformation (mm)	Rate of PD (mm/million)	Plastic Strain (%)	Rate of PS (%/million)
	Permanent Deformation (mm)	Rate of PD (mm/million)				
LVDT M	10.78	2.1	10.78	2.1	3.55	0.7
LVDT #1	1.10	2.2	1.10	2.2	0.37	0.8
LVDT #2	1.28	1.2	1.28	1.2	0.43	0.4
	4.38	1.8	4.38	1.8	1.45	0.6

Figure 5.4 Typical calculated results from a set of dynamic triaxial data

A cyclic load with a load- and rest period duration of 0.2 seconds each was selected for this study. The load magnitude for the dynamic tests was set at different levels of the maximum static load and run for 50 000 load cycles. The load-displacement response of the sample was recorded in windows of three load cycles during various stages of the test. Displacement measurements were taken from the LVDT on the loading ram as well as the two on-sample LVDT's.

By combining all the data sampled during a dynamic triaxial test, a number of parameters can be calculated, as shown in Figure 5.4. These parameters include the permanent deformation, the elastic strain, resilient modulus and rate of permanent deformation.

5.2.3 Optical microscope

The microscope consists of an ordinary optical microscope capable of magnifications between 7x and 90x. A digital camera, attached to the microscope, makes it possible to take digital pictures of the samples that are studied. State of the art software provides the feature of taking optical digital pictures at high magnification, which are perfectly in focus.

Samples were prepared at different cement and bitumen contents and studied under an optical microscope. Some samples, which were obtained from the HVS test site from cores, were also studied under the microscope. The use of an electron microscope was not practical because samples need to be 100% dry before they can be studied.

5.2.4 HVS Field testing

The Heavy Vehicle Simulator (HVS) was developed by the CSIR and the former Transvaal Roads Department during the late 1970's. The HVS was used extensively since the late 1970's to evaluate various pavement structures. Much of the South African Mechanistic Pavement Design Method is based on research originating from these HVS studies. The HVS equipment, and its associated measuring technology, are described in detail elsewhere (DRTT: 1987 and De Beer et al: 1988). The photograph in Figure 5.5 illustrates the overall view of the Heavy Vehicle Simulator.

HVS tests on emulsion treated materials were previously undertaken on labour intensive constructed pavements near Cullinan in the Gauteng Province (Mancotywa: 2000(a), 2001). The use of Deep In-Situ Recycling equipment in Southern Africa has become more popular recently for a number of reasons. Two of these reasons are the availability and cost of high quality crushed material and easier traffic accommodation. The HVS tests included in this study (test numbers 410A4, 410B4 and 412A4) were the first HVS tests performed on pavement structures treated with bitumen emulsion and cement and constructed by means of a

deep in-situ recycling machine. A Wirtgen DSR2500 deep in situ recycling machine was used in the rehabilitation of the road which was tested.



Figure 5.5 Overall view of the Heavy Vehicle Simulator

HVS Site

The HVS test site is situated on road P243/1 between Vereeniging and Balfour in the Gauteng Province of South Africa. A test section was constructed between km 14.2 and 14.4 on the eastbound lane. A detour was also constructed to accommodate traffic around the test site. The site is relatively flat which provides adequate sight distances. The gradients on the test site are also negligible. A layout of test section number 410A4 and 410B4 is presented in Figure 5.6 with the layout of test section 412A4 in Figure 5.7.

Pavement structure and mix design

The original pavement structure, before the rehabilitation of the road, consisted of an asphalt surfacing with a stabilised base layer, natural gravel subbase and natural gravel subgrade. The stabilised base layer was understood to be in an equivalent gravel phase and no longer in its fatigue life phase.

The rehabilitation design of the pavement consisted of a 30 mm Asphalt surfacing, 250 mm Deep In-Situ recycled layer stabilised with 2% cement and 1.8% net bitumen using the foam bitumen process. The lower natural gravel layers were left intact. The HVS test section consisted of a section treated with foam bitumen and a section stabilised with bitumen

emulsion. This study will focus on the tests performed on the section treated with bitumen emulsion.

A fountain on the south side of the test section, which was only discovered after the construction of the test section, resulted in the moisture content remaining high during the test. Construction related problems that could have influenced the behaviour of the test, include the presence of loose material on the base before surfacing (Sommelink and Botha: 2000a). The Asphalt surfacing was completed five days after the completion of the base layer.

Existing mix design techniques were used in the design of the emulsion treated layer. The final design however consisted of 1.8% net bitumen and 2% cement.

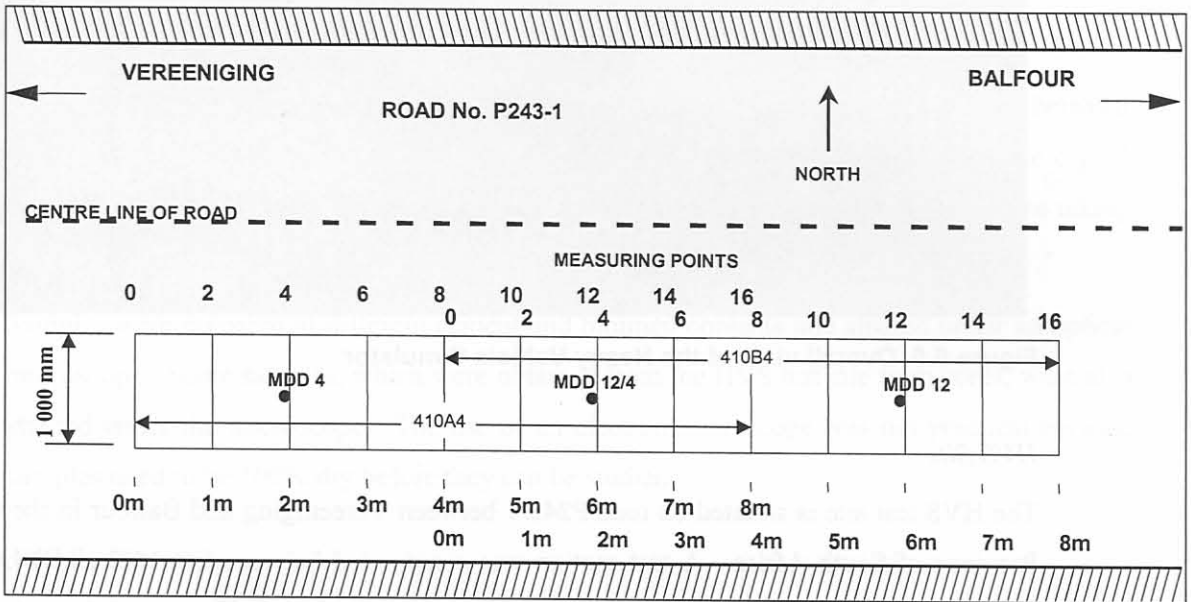


Figure 5.6 Test section layout for sections 410A4a and 410B4

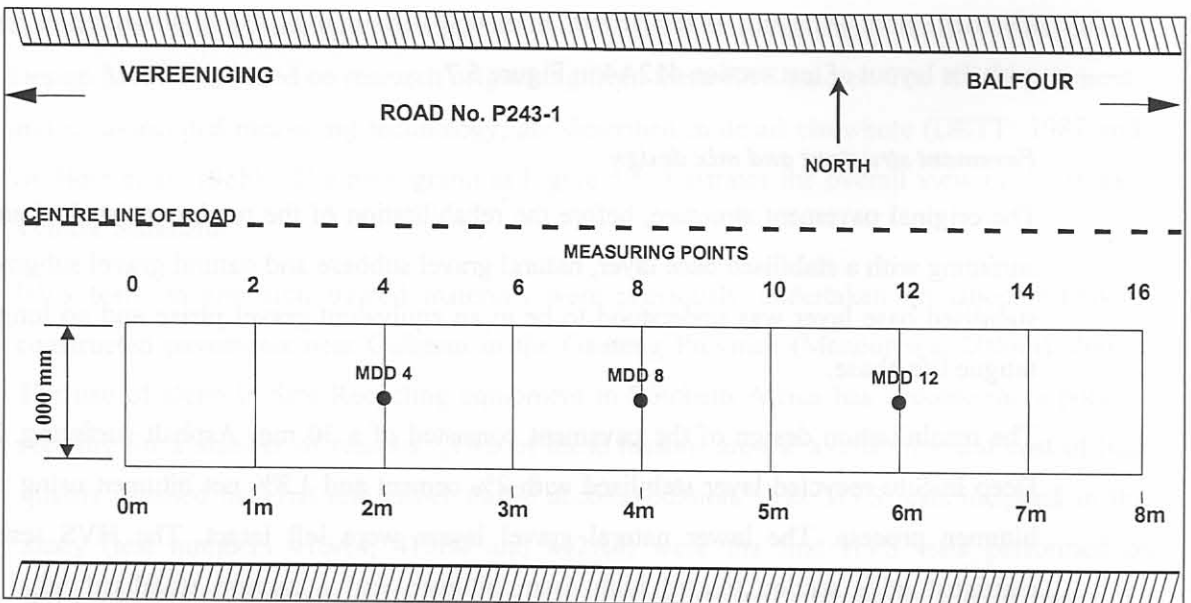


Figure 5.7 Test section layout for section 412A4A

Test programme

The test commenced with a wheel load of 80 kN and tyre inflation pressure of 800 kPa (test 410A4). A tyre inflation pressure of 800 kPa was used to ensure a homogeneous contact area between the tyre and the pavement. After 350 000 repetitions the load was increased to 100 kN and the tyre pressure to 850 kPa. The test was also moved 4 m to ensure that 4 m of the 8 m test section overlapped with 4 m of the previous test, while 4 m was on a new section (test 410B4). The 100 kN test was continued for another 150 000 repetitions after which water was applied to the surface to evaluate the behaviour of the pavement in a wet condition.

A test at the standard axle load of 40 kN (test 412A4) and tyre inflation pressure of 620 kPa was performed to evaluate the performance of the pavement under the legal axle limit as well as determine the damage factors for different distress modes of the higher wheel loads. This test was run for 957 121 repetitions where after the load was increased to 80 kN (800 kPa tyre pressure) for another 268 879 repetitions. The final 95 700 repetitions were undertaken under nominally wet conditions. The detailed test programmes of all the tests are included in Appendix C.

Table 5.2 provides a summary of the test conditions on the test sections

Table 5.2 Summary of HVS testing on sections 410A4, 410B4 and 412A4

Section	Dry/wet	Load applications	Trafficking load (kN)	Tyre inflation pressure (kPa)
410A4	Dry	295 617	80	800
410B4	Dry	171 500	100	850
	Wet	13 907	100	850
412A4	Dry	957 121	40	620
	Dry	268 879	80	800
	Wet	95 700	80	800

All three tests were performed under nominally dry conditions and no testing was permitted during rain. The load was applied at a speed of 8 km/h using a wandering pattern 1 m wide. The wandering pattern was obtained by allowing the test beam to move 50 mm sideways on a side after each load application. This process caused the wandering pattern to simulate a normal distribution of load applications on the test section as would be expected from normal traffic (Blabb and Litzka: 1995).

Pavement response measurement instruments

The standard HVS instruments were used to evaluate the performance of the test section under HVS testing. These include the following:

- Straightedge
- Laser Profilometer
- Road Surface Deflectometer (RSD)
- Multi Depth Deflectometer (MDD)
- Thermocouples

Cracks on the surface were monitored and photographed at various intervals during the test cycle. Response measurements were taken using 40 kN and 80 kN wheel loads with 620 kPa and 800 kPa tyre inflation pressure respectively. Most of the testing effort, however, was concentrated on the 40 kN measurements which were used in the analysis of the data.

5.3 THE INFLUENCE OF NET BITUMEN AND CEMENT CONTENTS ON THE STRENGTH AND FLEXIBILITY OF EMULSION TREATED GRAVEL MATERIALS

5.3.1 Materials

Ferricrete milled from the HVS test site by a Deep In-situ Recycler was used in the laboratory testing. The detailed properties of the materials are included in Appendix A. The maximum dry density of the material was approximately 2 000 kg/m³ with an optimum moisture content of between 11.2% and 12.5%. The material has a Grading Modulus (GM) of 2.13, a Plasticity Index (PI) of 7 and a CBR of 56 at 98%, and 18 at 93% of modified AASHTO compaction. The material can be classified as a G7 material according to the TRH14 (CSRA: 1987) material classification system.

5.3.2 California Bearing Ratio

The CBR tests were performed at 100% modified AASHTO compaction with moisture content as close to the optimum moisture content as possible. The results from the CBR tests are presented in Table 5.2.

Table 5.3 Summary of California Bearing Ratio (CBR) test results (0% cement)

	Net bitumen content (%)			
	0	0.6	1.8	3.0
CBR @ 100%	10	13	12	25

The tested values were lower than the original tests performed on the material, and the reason for this was that the material was compacted wet of optimum in the laboratory. Compacting

the material wetter than optimum usually results in lower values even if the specimen is left in the open to dry out. Although it is not recommended that these values be used as a guideline for design, it can be seen that adding emulsion increases the bearing capacity of the material. The magnitude of this increase can however not be quantified. No reason could be obtained why the specimens were compacted wet of optimum.

5.3.3 Unconfined Compressive Strength

The UCS tests were performed at 100% modified AASHTO compaction with moisture content as close to the optimum moisture content as possible. The samples were cured for 28 days at ambient temperature and sealed to prevent excessive loss of moisture. No special or rapid curing processes were used. The results from the UCS tests are presented in Table 5.4.

Table 5.4 Summary of Unconfined Compressive Strength (UCS) test results

		Net bitumen content (%)			
		0	0.6	1.8	3.0
Cement content (%)	0	-	192	132	316
	1	305	548	545	788
	2	3 198	-	2 375	1 645

Figure 5.8 illustrates the effect of various net bitumen and cement contents on the UCS of the ferricrete material observed in this study.

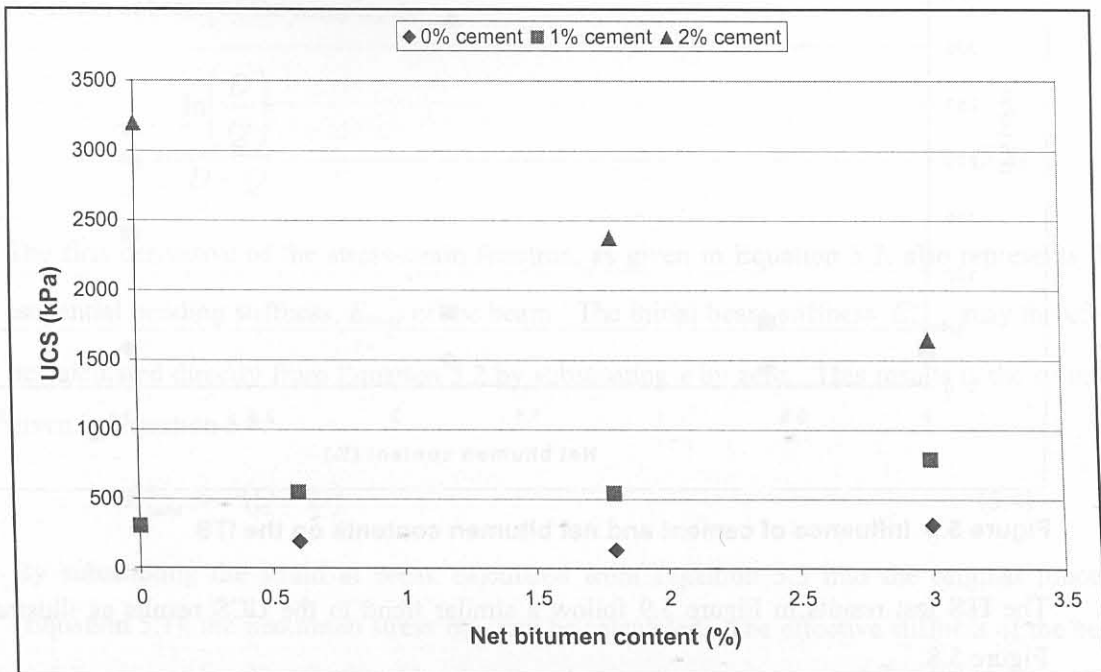


Figure 5.8 Influence of cement and net bitumen contents on the UCS

From the graph it is clear that an increase in bitumen binder has little effect on the UCS of this material at low cement content, but leads to a reduction in the UCS at higher cement content.

5.3.4 Indirect Tensile Strength

The ITS tests were also performed at 100% modified AASHTO compaction with moisture content as close to the optimum moisture content as possible. The samples were cured for 28 days at ambient temperature. The results from the ITS tests are presented in Table 5.5.

Table 5.5 Summary of Indirect Tensile Strength (ITS) test results

		Net bitumen content (%)			
		0	0.6	1.8	3.0
Cement	0	-	16	24	34
content	1	33	56	65	136
(%)	2	409	-	325	230

Figure 5.9 illustrates the effect of various net bitumen and cement contents on the ITS of the ferricrete material as observed in this study.

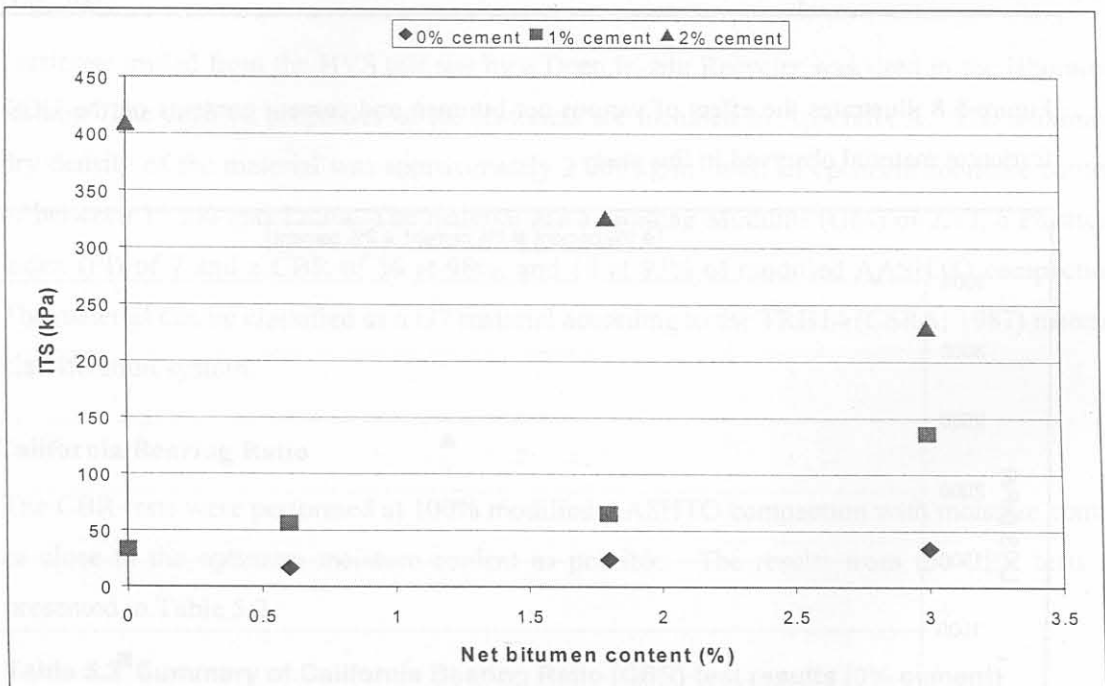


Figure 5.9 Influence of cement and net bitumen contents on the ITS

The ITS test results in Figure 5.9 follow a similar trend to the UCS results as illustrated in Figure 5.8.

5.3.5 Flexural beam tests

The data from the flexural beam test consists of a plot of stress versus strain as shown on the example in Figure 5.2. The turning point on the curve indicates failure of the specimen. The stress at this point is regarded as the stress at break while the strain at this point can be regarded as the strain at break. Theyse (2000) proposed the following mathematical model to fit the data from the beam tests:

$$\sigma = P(e^{-D\varepsilon} - e^{-Q\varepsilon}) \quad (5.1)$$

where: σ = stress

ε = strain

e = natural logarithm

P, D and Q = regression coefficients

The first derivative of the function is as follows:

$$\frac{\partial \sigma}{\partial \varepsilon} = P(Qe^{-Q\varepsilon} - De^{-D\varepsilon}) \quad (5.2)$$

The turning point of the function, where the stress is a maximum, is obtained by setting the derivative (Equation 5.2) to zero and solving for ε . The solution for ε is given in Equation 5.3 and it represents the maximum strain that can be sustained before failure of the sample and is the strain at break of the sample, ε_b .

$$\varepsilon_b = \frac{\ln\left(\frac{D}{Q}\right)}{D - Q} \quad (5.3)$$

The first derivative of the stress-strain function, as given in Equation 5.2, also represents the tangential bending stiffness, E_{bend} of the beam. The initial beam stiffness E_{bend}^i may therefore be calculated directly from Equation 5.2 by substituting ε by zero. This results in the solution given in Equation 5.4.

$$E_{bend}^i = P(Q - D) \quad (5.4)$$

By substituting the strain at break calculated from Equation 5.3 into the original function (Equation 5.1), the maximum stress σ_{max} can be calculated. The effective stiffness of the beam at failure may then be calculated by dividing the maximum stress (σ_{max}) by the strain at break (ε_b).

The amount of energy required to break the beam, that gives an indication of the toughness of the material, can be calculated by the integral of the original function between zero and the strain at break:

$$\text{Energy} = \int_0^{\epsilon_b} \sigma d\epsilon = \int_0^{\epsilon_b} P(e^{-D\epsilon} - e^{-Q\epsilon}) d\epsilon \quad (5.5)$$

$$= P \left(\frac{e^{-Q\epsilon_b} - 1}{Q} - \frac{e^{-D\epsilon_b} - 1}{D} \right) \quad (5.6)$$

Table 5.6 and Figure 5.10 to 5.12 provide a summary of the flexural beam tests.

Table 5.6 Summary of flexural beam fatigue test results

	Net bitumen content (%)			
	0	1.8	3.0	
row 1 = strain at break				
row 2 = stress at break				
row 3 = toughness				
row 4 = Initial stiffness				
row 5 = Stiffness at break				
	0	Samples broke under own weight	Samples broke under 2kg test equipment weight	
Cement content (%)	1	96 $\mu\epsilon$	336 $\mu\epsilon$	677 $\mu\epsilon$
		38 kPa	25 kPa	53 kPa
		2.66 mJ/m^3	6.48 mJ/m^3	41.4 mJ/m^3
		1 428 MPa	235 MPa	275 MPa
		496 MPa	85 MPa	95 MPa
2	183 $\mu\epsilon$	141 $\mu\epsilon$	235 $\mu\epsilon$	
	273 kPa	360 kPa	307 kPa	
	45.1 mJ/m^3	32.2 mJ/m^3	53.2 mJ/m^3	
	4 921 MPa	4 731 MPa	3 919 MPa	
	1 600 MPa	2 655 MPa	2 200 MPa	

The samples with no cement broke under its own weight when tested and no strain at break values could be obtained for them. The samples with only 3 % net bitumen and no cement, broke under the weight of the 2 kg test equipment, and “flowed” slowly to failure. This indicates increased flexibility at higher net bitumen content, but with little or no strength.

In general, an increase in bitumen content resulted in an increase in flexibility or strain at break. It does however not seem to have a significant effect on the stress at break. At lower cement content, an increase in bitumen content contributes positively to the amount of energy required to initiate failure.

An increase in cement content has a significant effect on the strength of the material in the sense that the stress at break increases considerably. It reduce the flexibility of the of the material, with a reduction in strain at break, when bitumen is present in the material. More energy was required to break samples with higher cement content.

An increase in the cement will therefor provide strength to the material, but adding too much will sacrifice the flexibility. This should be borne in mind when specifying the Unconfined Compressive Strength in the mix design process, and whether the objective of the structural designer is strength or flexibility.

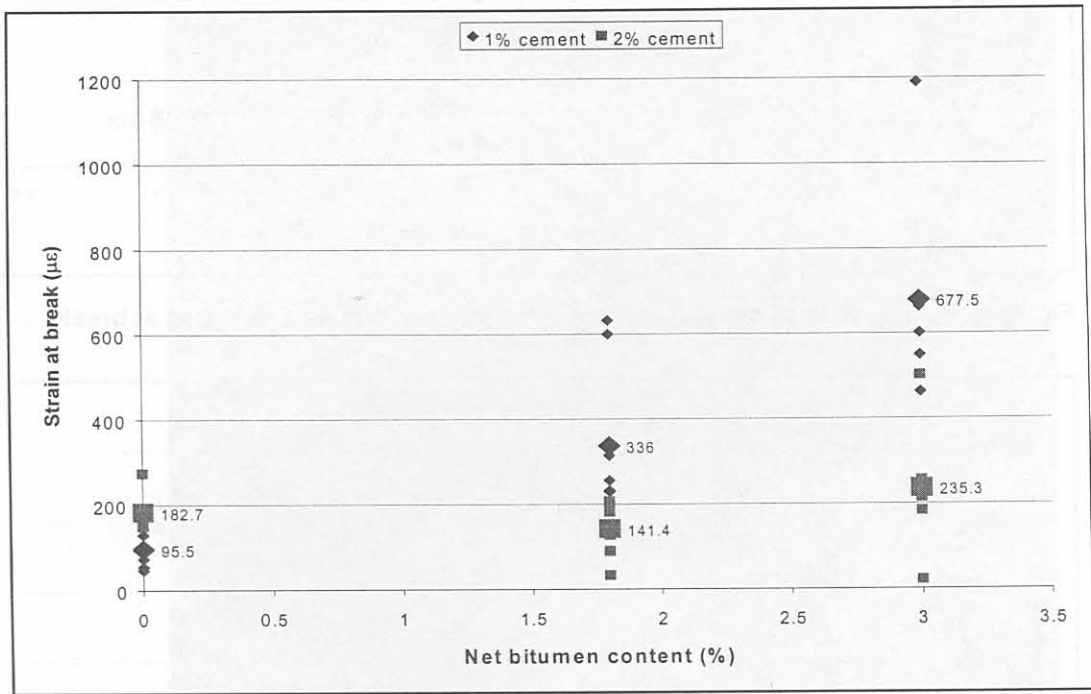


Figure 5.10 Influence of cement and net bitumen contents on the strain at break

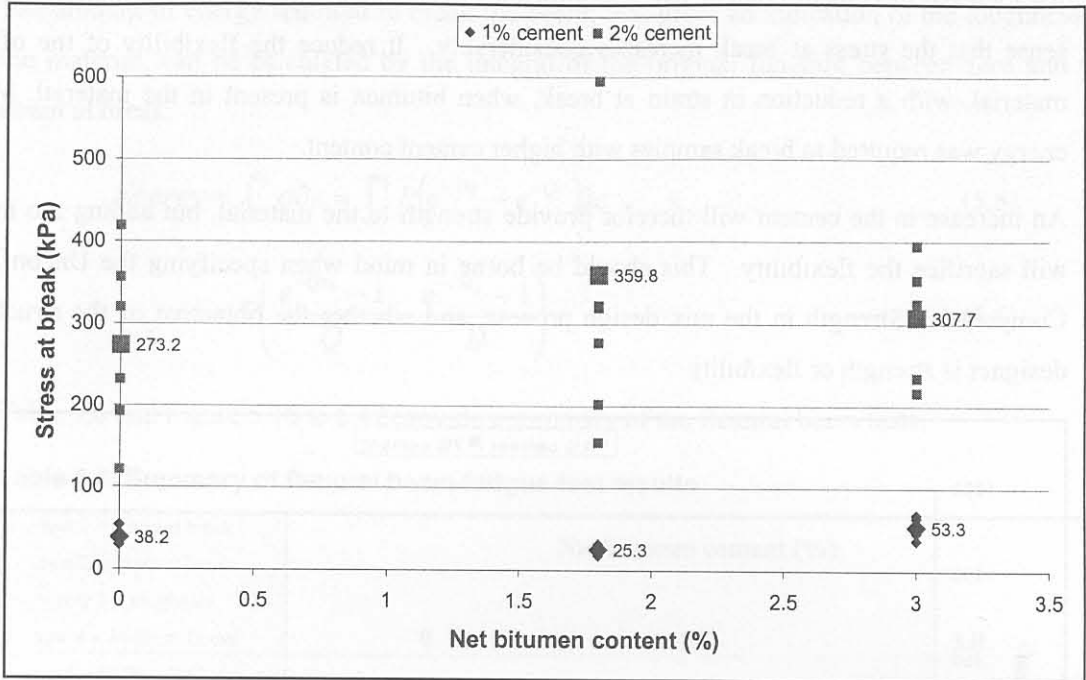


Figure 5.11 Influence of cement and net bitumen contents on the stress at break

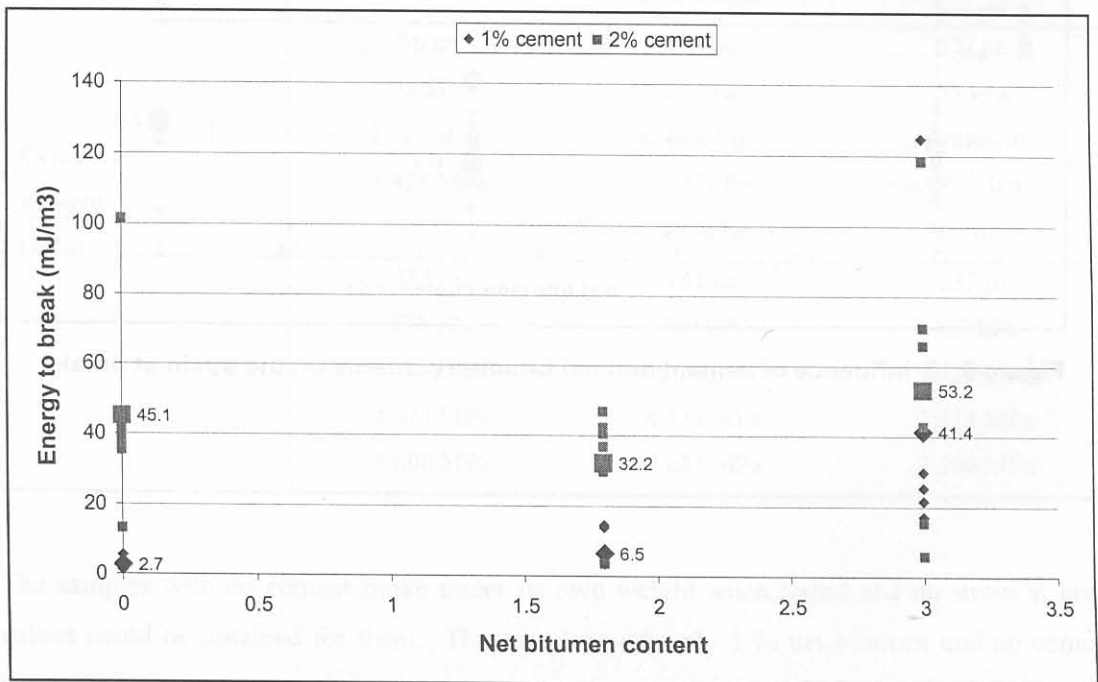


Figure 5.12 Influence of cement and net bitumen contents on the dissipated energy

5.3.6 Observations under the optical microscope

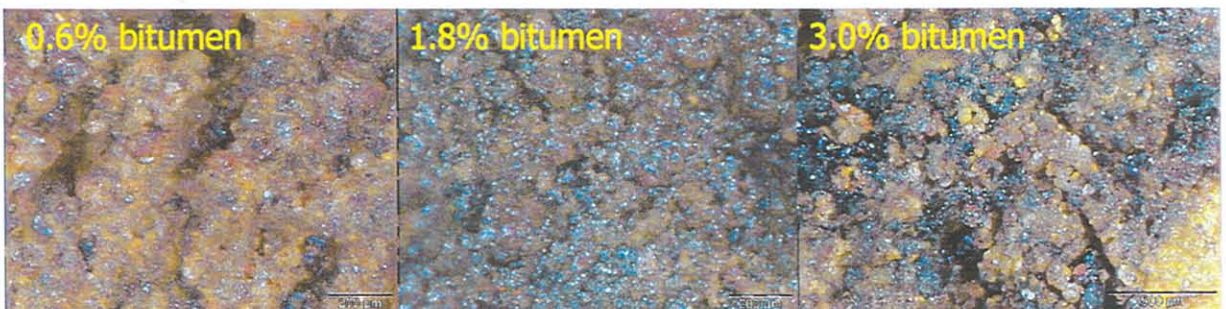
The observations under the optical microscope did not provide much more information other than the distribution of bitumen through the sample. The increased amount of bitumen present is clearly visible on the different samples, but no distinction could be made as to whether the bitumen tended to stick to the finer or coarser particles. The influence of the bitumen on the

cement particles could also not be observed. On samples from the HVS site, a film of bitumen around the larger particles was clearly visible.

Figure 5.13 presents a photograph of a laboratory sample with 2% cement and 1.8 % net bitumen under 32x magnification. The black dots on the photograph are the bitumen, with the white threads on the left of the picture, the cement. It can be seen that the bitumen is thoroughly mixed into the material. No blobs of bitumen could be observed in the samples. Figure 5.14 presents a comparison of samples with 0.6, 1.8 and 3.0 % net bitumen contents. More detailed pictures of the observations under the microscope are attached as Appendix B.



Figure 5.13 Sample from laboratory (2 % cement, 1.8 % net bitumen), 32x magnification



50x magnification

Figure 5.14 Optical microscope images of emulsion treated materials with different net bitumen contents (0% cement)

5.3.7 Discussion

Initial Consumption of Lime (ICL) tests on the material indicated that the ICL value of the material was 1.5 %. The ICL is an indication of the minimum amount of cement or lime that is required to satisfy conditions for the cement-hydration reaction to commence (Eades and Grimm: 1964).

From the tests done in this study it appears that the cement dominates the UCS and ITS at high cement content (above ICL) and that the addition of bituminous binder reduces the UCS and ITS of the material. At lower cement content (lower than ICL) the effect of the cement is much less and an increase in bitumen tends to have a slight increase in the UCS and/or ITS. The cement has little strengthening effect on the material when the ICL requirement is not met, and could therefore describe the greater effect of the bituminous binder on the material at low cement content. This effect could however be dependent on the type of material, but similar findings were reported to the author by Van Vuuren (2001) and Verwey (2001). An increase in binder content in excess of 3% might have a positive influence on the ITS value regardless of the cement content. The material could then behave in a visco-elastic manner with similar properties to that of asphalt materials. Additional research is however required to prove this theory.

The increase in flexibility at low cement content can be ascribed to the fact that the ICL of the material was not met and that the cement reaction, which will contribute to the brittleness of the material, has not commenced. A delicate balance between cement and bitumen content should be aimed for during the mix design process.

No comparison or relationship could be observed between the test results from the Indirect Tensile Strength and the four point flexural beam test

5.4 STATIC SHEAR STRENGTH

The static shear strength of the material was determined from static triaxial tests. The complete test results are documented by Long and Theyse (2001). Table 5.7 presents a summary of these results.

For the cement treated material, it is clear that the cohesion and friction angle is insensitive to the degree of saturation. This could be explained by the fact that the shear strength is more dependent on the chemical bonding from the cement than on the suction generated by negative pore water pressures.

Table 5.7 Static triaxial test results calculated directly from Mohr circles (Long and Theyse: 2001)

Cement content (%)	Net Bitumen content (%)	Relative density (%)	Saturation (%)	Cohesion (kPa)	Friction angle (degrees)
0	0	86	79	20	43.1
0	0	86	56	37	39.7
0	0	96	79	31	41.0
0	0	96	56	126	40.1
2	0	70	73	333	50.9
2	0	70	63	337	50.5
2	1.8	70	64	543	32.5
2	1.8	70	59	329	46.5
2	1.8	73	64	458	48.3
2	1.8	73	59	370	54.8

For the emulsion treated material it appears that the cohesion and the internal angle of friction tend to influence each other. If the cohesion increases, the internal angle of friction decreases, regardless of the increase or decrease in relative density and saturation. Due to this model effect no relationship between relative density, saturation and the two shear strength parameters could be obtained.

The values of c and ϕ can also be calculated from the K_f -line parameters a and α from a $p_f - q_f$ diagram. The relationships for c and ϕ are as follows (Lambe et al: 1996 and Das: 1990):

$$q_f = a + p_f \tan \alpha \quad (5.7)$$

$$\sin \phi = \tan \alpha \quad (5.8)$$

$$c = \frac{a}{\cos \phi} \quad (5.9)$$

where $q_f = \frac{\sigma_1 - \sigma_3}{2}$ = shear stress

$$p_f = \frac{\sigma_1 + \sigma_3}{2}$$
 = normal stress

c = cohesion (kPa)

ϕ = angle of internal friction (degrees)

The $p_f - q_f$ diagram (Figure 5.15) is obtained from the results of static triaxial tests. A straight-line regression may be performed on the results from the maximum shear stress (τ) values at each stress state, to obtain the relevant parameters a and α from which c and ϕ can be calculated, by using Equations 5.7 to 5.9.

The cohesion (c) and internal friction angle (ϕ) calculated by the indirect method for the ferricrete material tested were 308 kPa and 50.9° respectively for all the saturation and relative densities within the stress conditions tested. These values are dependant on the parent material, and because the ferricrete tested was of high quality, the values for other types of materials are expected to be lower.

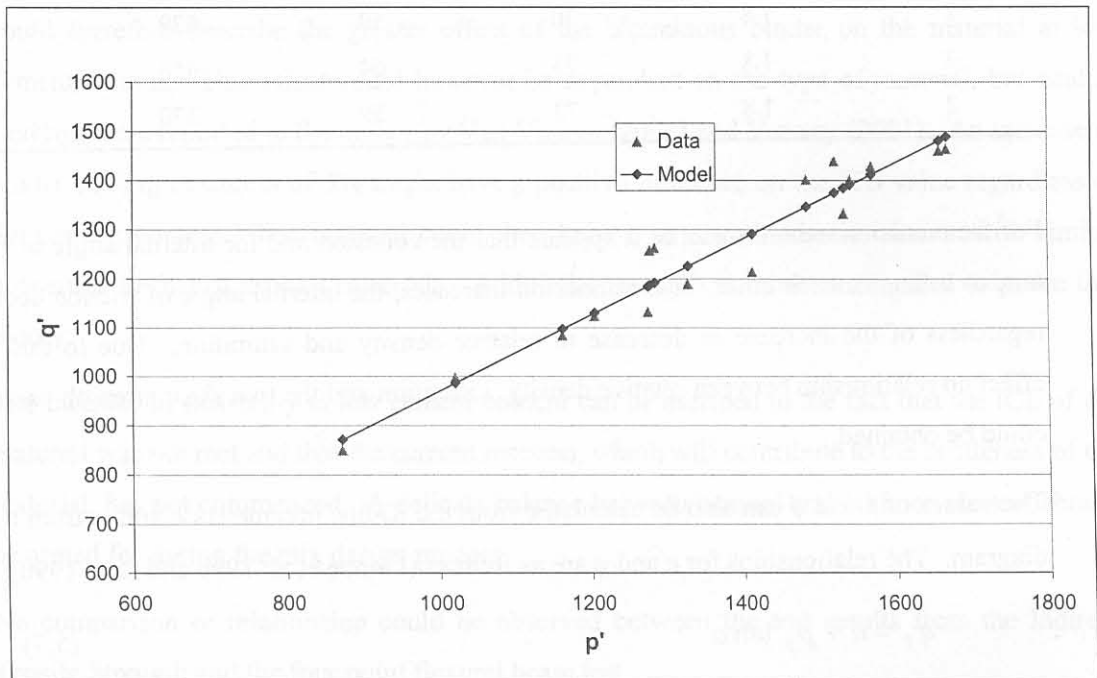


Figure 5.15 $p_f - q_f$ diagram from static triaxial tests

5.5 LABORATORY ELASTIC MODULUS (M_R)

The dynamic triaxial test results were used to calculate the elastic or resilient stiffness of the materials. Specimens were prepared for each material at two compaction levels and two degrees of saturation. The tests were performed at stress ratios of 0.20, 0.55 and 0.9 with confining pressures of 80 and 140 kPa for each stress ratio.

The stress ratio of a material is the ratio between the applied stress and the maximum shear strength at the failure envelope of the material. Theyse (2000) derived Equation 5.10 for the calculation of the stress ratio. It is graphically presented in Figure 5.16.

$$SR = \frac{\sigma_1^a - \sigma_3}{\sigma_1^m - \sigma_3} = \frac{\sigma_1^a - \sigma_3}{\sigma_3 \left[\tan^2 \left(45^\circ + \frac{\phi}{2} \right) - 1 \right] + 2.c. \tan \left(45^\circ + \frac{\phi}{2} \right)} \quad (5.10)$$

where: SR = Stress ratio

σ_3 = minor principal stress or confining pressure (kPa)

c = cohesion (kPa)

ϕ = internal angle of friction (degrees)

σ_1^a = working or applied major principal stress (kPa)

σ_1^m = maximum allowable major principal stress for given ϕ , c , and σ_3 (kPa)

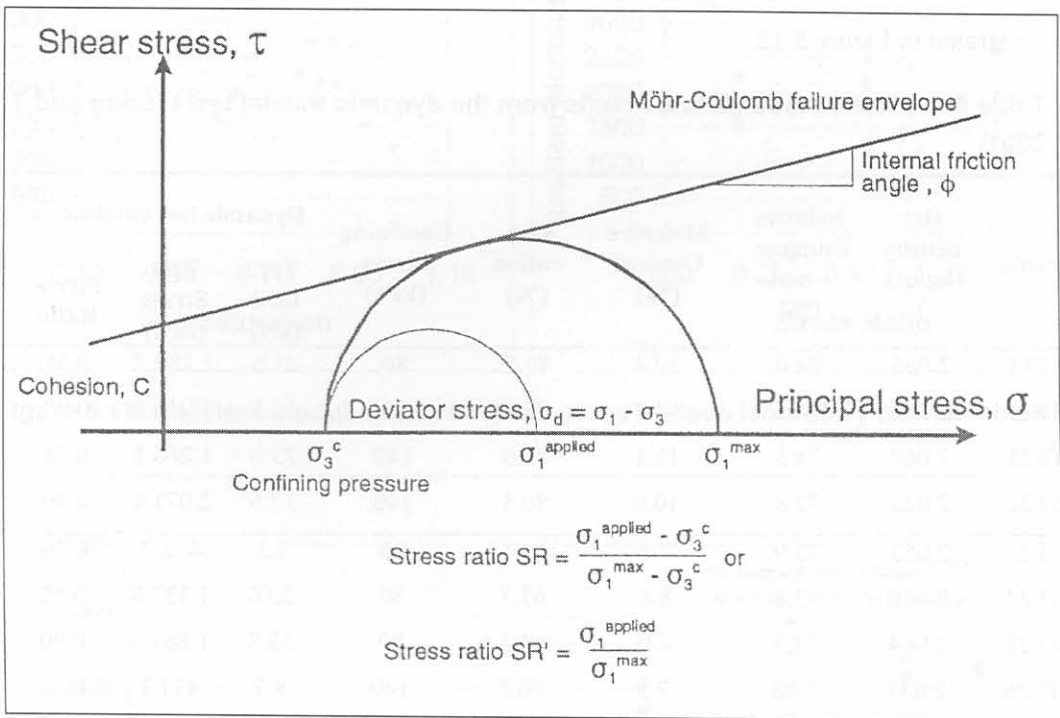


Figure 5.16 Möhr stress circles representation of the stress ratio concept (Theyse: 2000)

The complete results of the dynamic triaxial tests were documented in detail by Long and Theyse (2001).

A summary of the elastic modulus results from the dynamic triaxial tests on the emulsion treated ferricrete are presented in Table 5.8. The tests were done with 2.0 % cement and 1.8% net bitumen.

The elastic modulus ranged between 1 200 MPa and 2 700 MPa with an average of 2 039 MPa, a standard deviation of 450 MPa and a coefficient of variation of 22 %.

The resilient modulus as determined by the dynamic triaxial test is essentially a compressive elastic modulus. The values give an indication of the compressive behaviour of the material and do not necessarily describe the flexibility, tensile, or permanent deformation response of the material. It is however assumed that the flexibility, tensile and permanent deformation behaviour will be similar.

Figure 5.17 presents the influence of different parameters on the resilient modulus.

The only parameter that demonstrated some influence on the resilient modulus was the stress ratio. The confining pressure, relative density and degree of saturation produced a large amount of scatter and no definite relationship could be observed.

The bulk stress (σ) can be calculated from the applied stress ratio and confining pressure. A plot with the bulk stress against the resilient modulus revealed some stress dependency as illustrated in Figure 5.18.

Table 5.8 Elastic modulus test results from the dynamic triaxial tests (Long and Theyse: 2001)

Sample	Dry density (kg/m ³)	Relative Compaction (%)	Moisture Content (%)	Saturation (%)	Confining Stress (kPa)	Dynamic test conditions			Elastic Modulus (MPa)
						Test load (kN)	Test Stress (kPa)	Stress Ratio	
ETF18	2 055	74.0	10.4	82.2	80	21.6	1 189.7	0.55	2 160
ETF19	2 062	74.3	10.7	85.7	80	35.3	1 946.8	0.90	2 721
ETF21	2 068	74.5	11.1	89.9	140	23.0	1 266.1	0.55	2 657
ETF22	2 023	72.8	10.8	80.5	140	37.6	2 071.9	0.90	2 712
ETF23	2 053	73.9	7.8	61.4	80	7.5	413.7	0.20	1 607
ETF24	2 050	73.8	8.6	67.3	80	20.6	1 137.8	0.55	2 224
ETF25	2 064	74.3	8.0	64.3	80	33.8	1 861.8	0.90	1 964
ETF26	2 077	74.8	7.3	60.2	140	8.7	477.1	0.20	1 615
ETF27	2 070	74.5	8.3	67.5	140	23.8	1 311.9	0.55	2 507
ETF28	2 088	75.2	7.3	61.4	140	39.0	2 146.8	0.90	2 594
ETF29	2 164	77.9	9.4	92.2	80	10.4	575.6	0.20	1 530
ETF30	2 181	78.5	8.1	82.3	80	28.7	1 582.9	0.55	1 857
ETF31	2 143	77.2	10.5	98.6	80	47.0	2 590.2	0.90	1 615
ETF32	2 114	76.1	11.2	99.2	140	11.7	646.4	0.20	1 662
ETF33	2 104	75.8	11.3	98.1	140	32.3	1 777.6	0.55	1 223
ETF35	2 150	77.4	8.2	78.1	80	11.1	610.0	0.20	2 249
ETF36	2 152	77.5	9.0	86.1	80	30.4	1 677.5	0.55	2 102
ETF38	2 148	77.3	8.5	80.6	140	13.0	717.4	0.20	1 830
ETF39	2 152	77.5	7.9	75.5	140	35.8	1 972.9	0.55	1 970

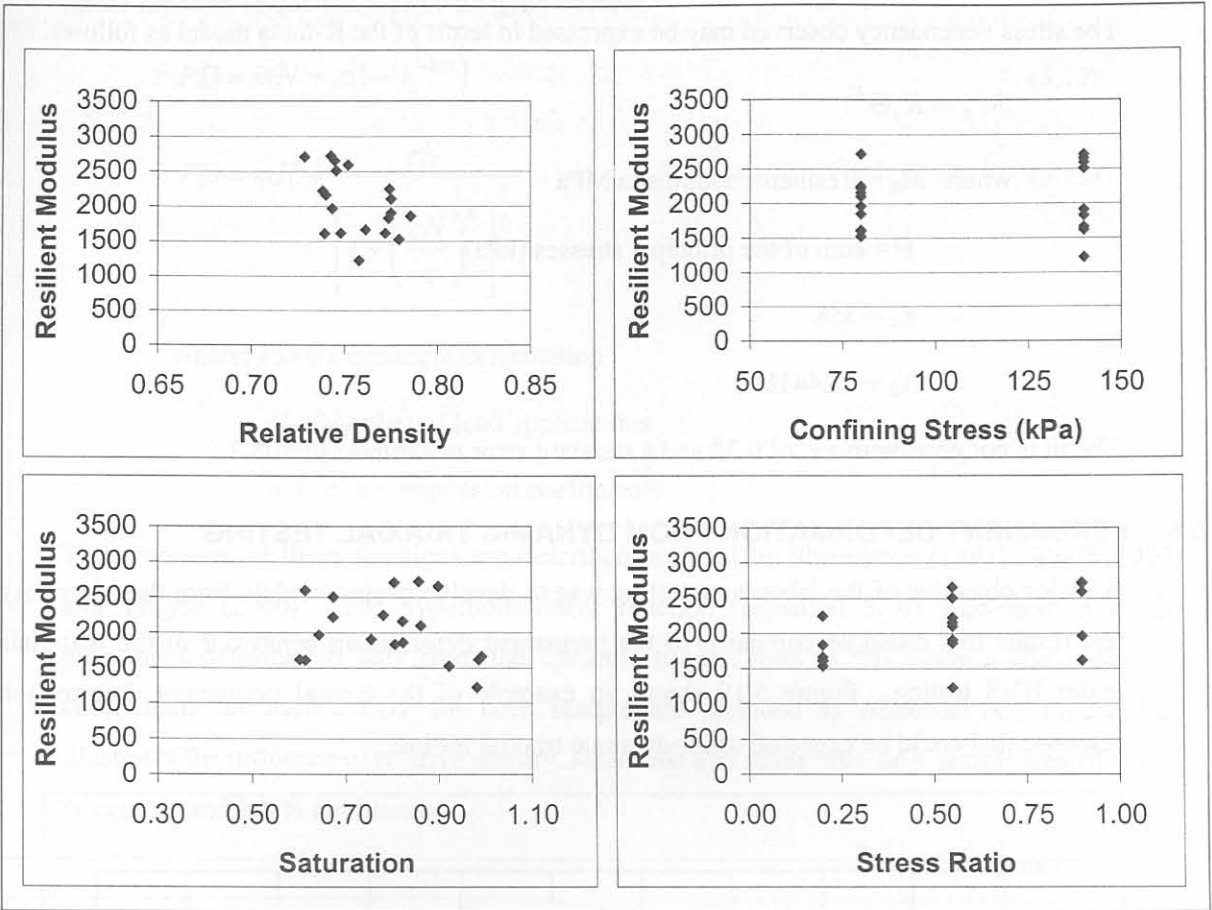


Figure 5.17 Resilient modulus as a function of the various laboratory test variables

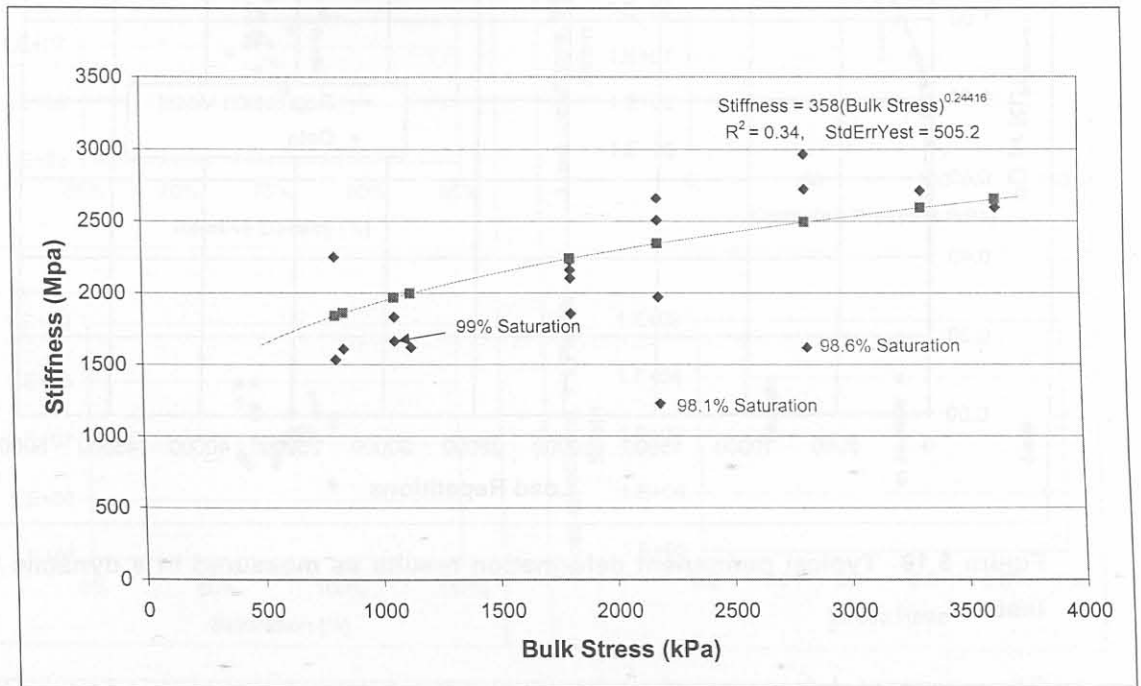


Figure 5.18 Resilient modulus vs. Bulk stress

The stress dependency observed may be expressed in terms of the K-theta model as follows:

$$M_R = K_1 \Theta^{K_2} \quad (5.11)$$

where: M_R = Resilient modulus in MPa

Θ = sum of the principal stresses (kPa)

$K_1 = 358$

$K_2 = 0.24416$

The fit is not good with a r^2 of 0.34 and a standard error of estimate of 505.2.

5.6 PERMANENT DEFORMATION FROM DYNAMIC TRIAXIAL TESTING

A major objective of the laboratory testing was to develop design models from the laboratory test results that could be compared to the permanent deformation behaviour of the materials under HVS testing. Figure 5.19 shows an example of the typical permanent deformation response that could be expected under dynamic triaxial testing.

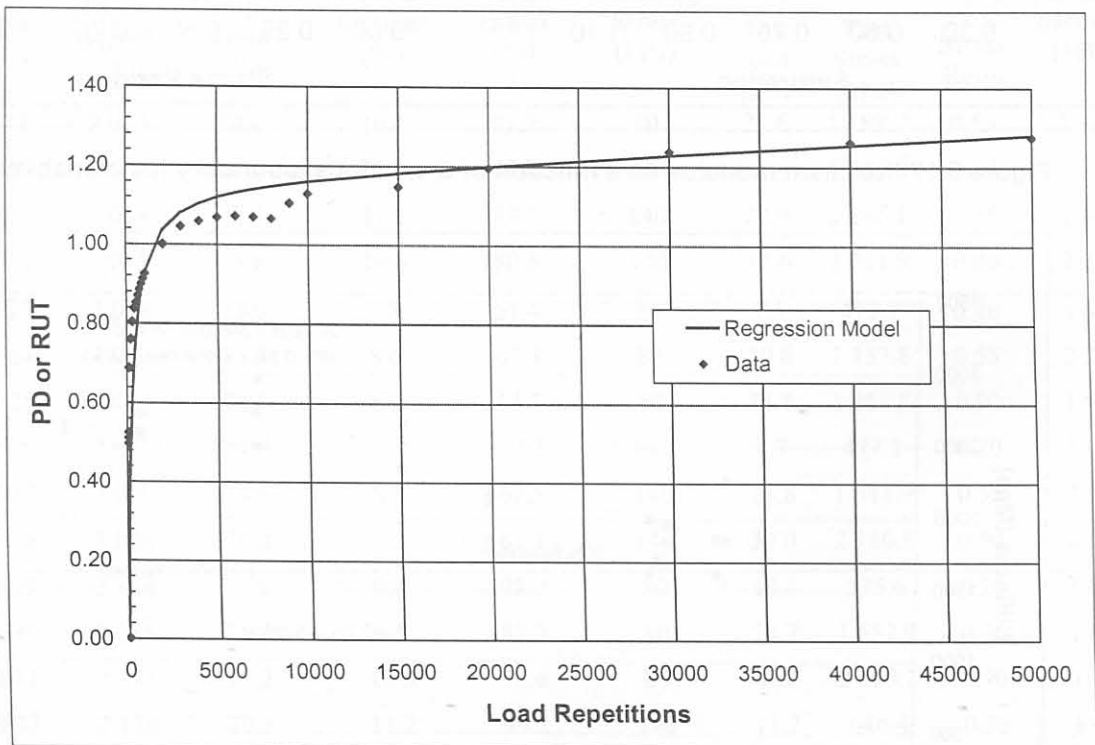


Figure 5.19 Typical permanent deformation results as measured in a dynamic triaxial test

The permanent deformation of all the samples tested entered a stable condition, where the permanent deformation increased linearly with increasing cycles. The permanent deformation

data can be fitted with either the exponential-linear function (Equation 5.12) or the hyperbolic-linear function (Equation 5.13) with good success.

$$PD = mN + a(1 - e^{-bN}) \quad (5.12)$$

$$PD = mN + \frac{cN}{\left[1 + \left(\frac{cN}{a}\right)^b\right]^{\frac{1}{b}}} \quad (5.13)$$

where: PD = Permanent deformation

N = Number of load applications

a, b, c, n = regression coefficients

The properties of these functions are described in detail by Shackleton (1995), Wolff (1992) and Theyse (2000). The hyperbolic-linear function (Equation 5.10) was used to fit the permanent deformation data from the dynamic triaxial tests in this study. The regression coefficients for each LVDT for each sample are included as Appendix A. Figure 5.20 illustrates the influence of relative density, saturation and stress ratio on a sample treated with 2 % cement and 1.8 % net bitumen.

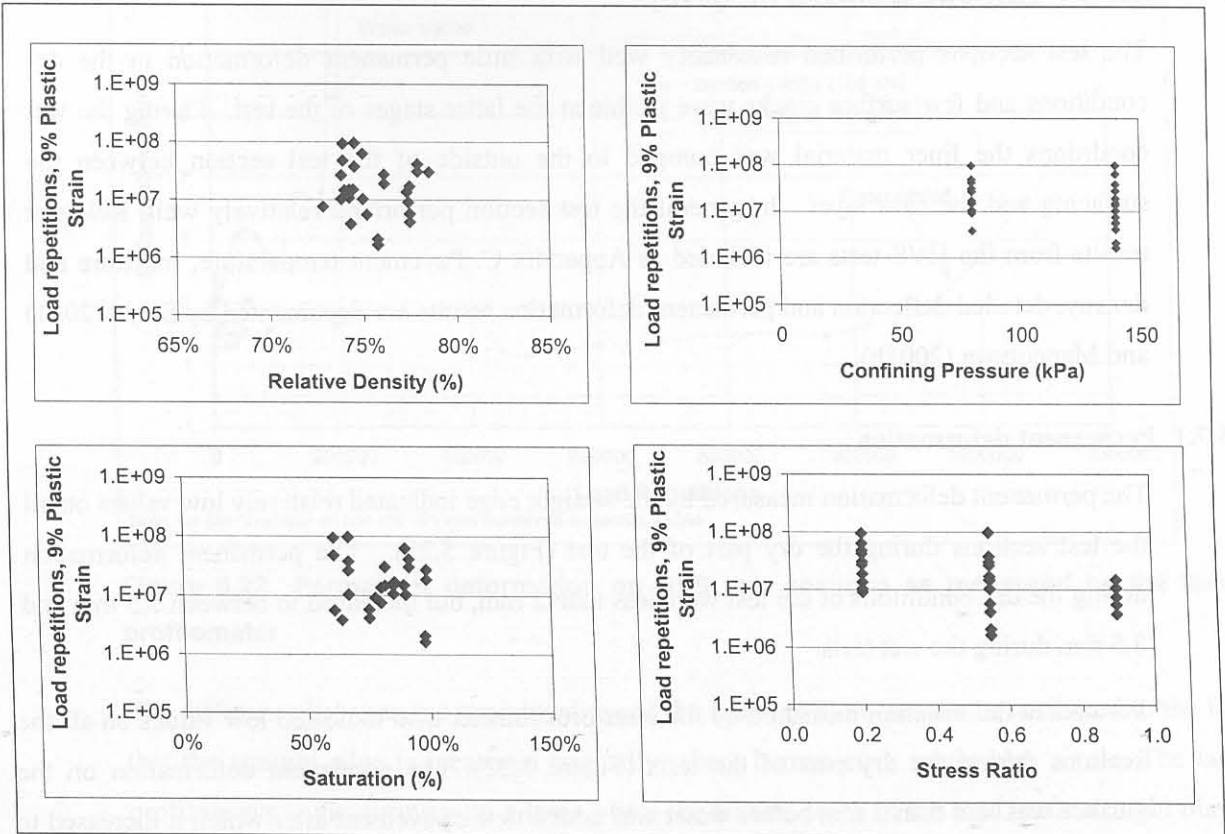


Figure 5.20 Influence of Relative Density, degree of saturation and stress ratio on the number of repetitions to 9 % plastic strain

The number of load repetitions is largely insensitive to the relative density and degree of saturation when bitumen emulsion is added to the sample. The results for an untreated ferricrete, as documented by Long and Theyse (2001), shows a sensitivity towards relative density and degree of saturation for untreated samples. The stress ratio however seems to have some influence on the number of load repetitions to 9% plastic strain, although a large amount of scatter is present. Long and Theyse (2001) developed the following statistical relationship between the various parameters in which only the plastic strain (*PS*) and strain ratio (*SR*) are statistically significant:

$$\log N = 4.78 + 0.07PS - 0.68SR \quad (r^2 = 0.30) \quad (5.14)$$

where: N = Number of load repetitions

PS = Plastic strain (%)

SR = Stress ratio as defined in Equation 5.7

According to Long and Theyse (2001) there was no significant improvement in the permanent deformation resistance of the ferricrete by the addition of bitumen emulsion when compared to the untreated and cement treated samples as tested under dynamic triaxial tests.

5.7 HEAVY VEHICLE SIMULATOR (HVS)

The test sections performed reasonably well with little permanent deformation in the dry conditions and few surface cracks were visible at the latter stages of the test. During the wet conditions the finer material was pumped to the outside of the test section between the surfacing and the base layer. In general the test section performed relatively well. Relevant results from the HVS tests are included as Appendix C. Pavement temperature, moisture and density, detailed deflection and permanent deformation results are documented by Steyn (2001) and Mancotywa (2001b).

5.7.1 Permanent deformation

The permanent deformation measured by the straight edge indicated relatively low values on all the test sections during the dry part of the test (Figure 5.21). The permanent deformation during the dry conditions of the test were less than 2 mm, but increased to between 5.5 mm and 8.5 mm during the wet tests.

Permanent deformation measured by the laser profilometer also indicated low values on all the sections during the dry part of the tests (Figure 5.22). The permanent deformation on the surface was less than 2 mm before water was added to the pavement after which it increased to between 5 and 6 mm.

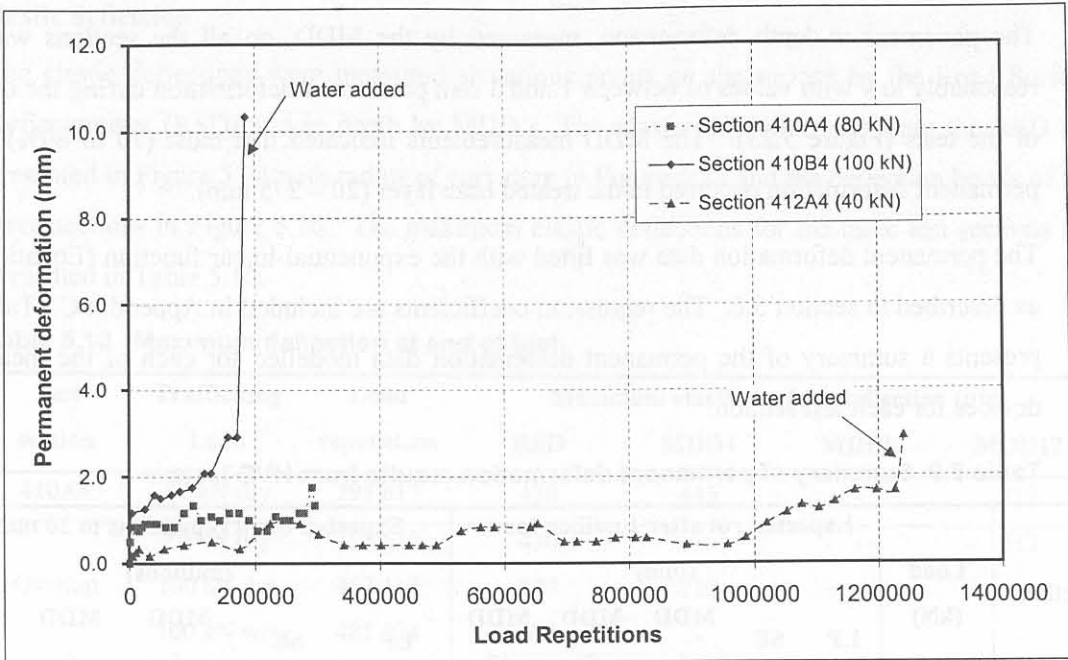


Figure 5.21 Permanent deformation on HVS test sections as measured by the straight edge

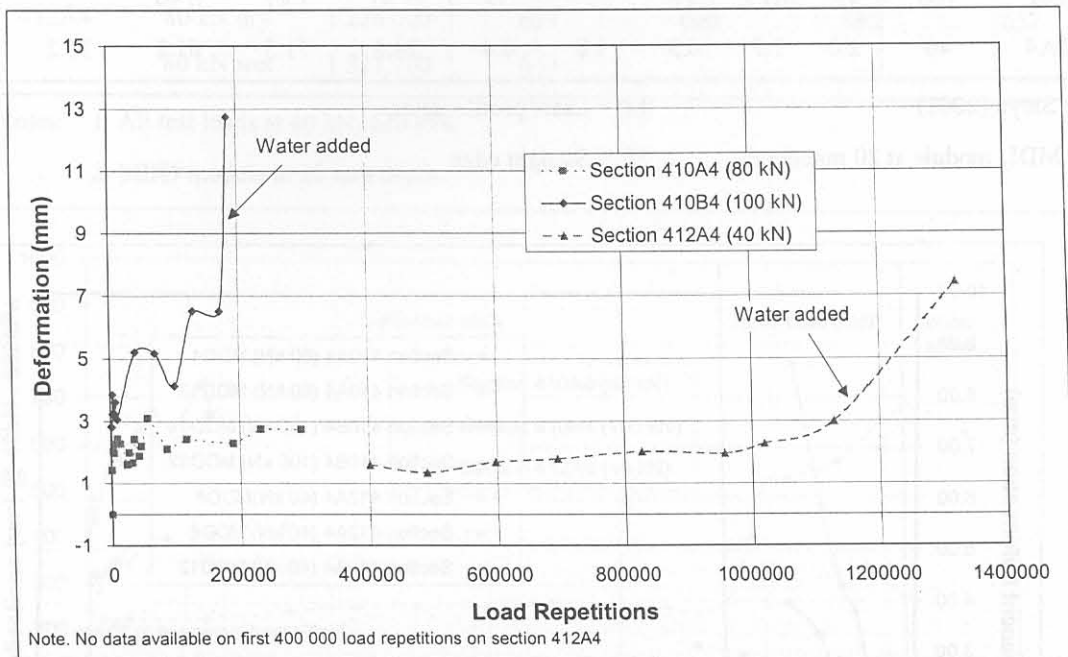


Figure 5.22 Permanent deformation on HVS test sections as measured by the laser profilometer

The difference between the straight edge and the laser profilometer can be attributed to the fact that the straight edge is measured manually where human error might play a role. The laser profilometer is measuring with a laser where the texture depth of the road surface might play a role.

The pavement in-depth deformation, measured by the MDD, on all the sections was also reasonably low with values of between 1 and 3 mm permanent deformation during the dry part of the tests (Figure 5.23). The MDD measurements indicated that most (70 to 80%) of the permanent deformation occurred in the treated base layer (20 – 275 mm).

The permanent deformation data was fitted with the exponential-linear function (Equation 5.9) as described in section 5.6. The regression coefficients are included in Appendix C. Table 5.9 presents a summary of the permanent deformation data modelled for each of the measuring devices for each test section.

Table 5.9 Summary of permanent deformation results from HVS tests

Section	Load (kN)	Expected rut after 1 million loads (mm)					Expected Load repetitions to 20 mm rut (millions)				
		LP	SE	MDD	MDD	MDD	LP	SE	MDD	MDD	MDD
				4	8	12			4	8	12
410A4*	80	11.1	2.2	8.9	-	7.8	1.80	9.09	1.12	-	1.28
Overlap*	80/100	3.3	10.2	-	-	-	6.06	1.96	-	-	-
410B4*	100	9.1	10.7	17	-	32	2.20	1.87	0.59	-	0.31
412A4	40	2.0	1.7	0.3	1.8	0.4	24.8	71.5	61.2	33.2	50.7

*After Steyn (2001)

LP = Laser profilometer

Note: MDD module at 20 mm depth

SE = Straight edge

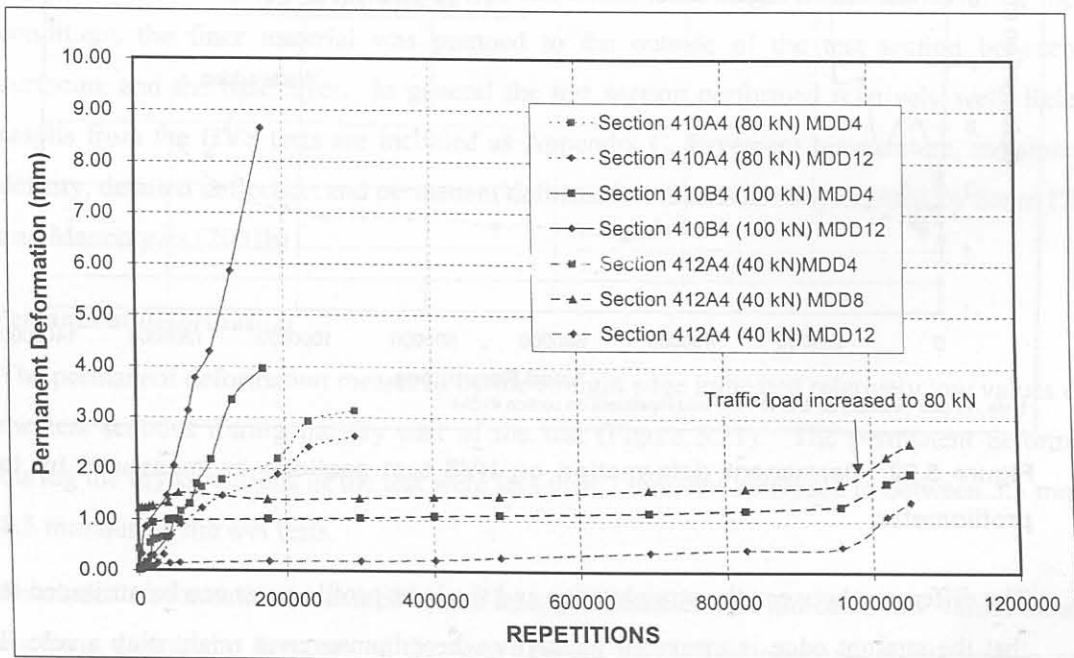


Figure 5.23 Permanent deformation on HVS test sections as measured by the MDD module at 40 mm.

5.7.2 Elastic deflection

The elastic deflections were measured at various points on the surface by the Road Surface Deflectometer (RSD) and in depth by MDD's. The maximum deflections from the RSD are presented in Figure 5.24 with radius of curvature in Figure 5.25 and the deflection bowls of the three sections in Figure 5.26. The maximum elastic deflections for the three test sections are presented in Table 5.10.

Table 5.10 Maximum deflection at end of test

Test section	Trafficking Load	Load repetitions	Maximum elastic surface deflection (μm)			
			RSD	MDD4	MDD8	MDD12
410A4	80 kN dry	295 617	430	443	-	517
	80 kN dry	295 617	430	-	-	517
Overlap	100 kN dry	467 117	728	717	-	-
	100 kN wet	481 024	678	-	-	-
410B4	100 kN dry	171 500	778	-	-	848
	100 kN wet	185 407	646	-	-	-
412A4	40 kN dry	957 121	268	281	311	237
	80 kN dry	1 226 000	687	660	680	637
	80 kN wet	1 321 700	637	-	-	-

- Notes: 1. All test loads at 40 kN, 620 kPa
 2. MDD module at 20 mm depth

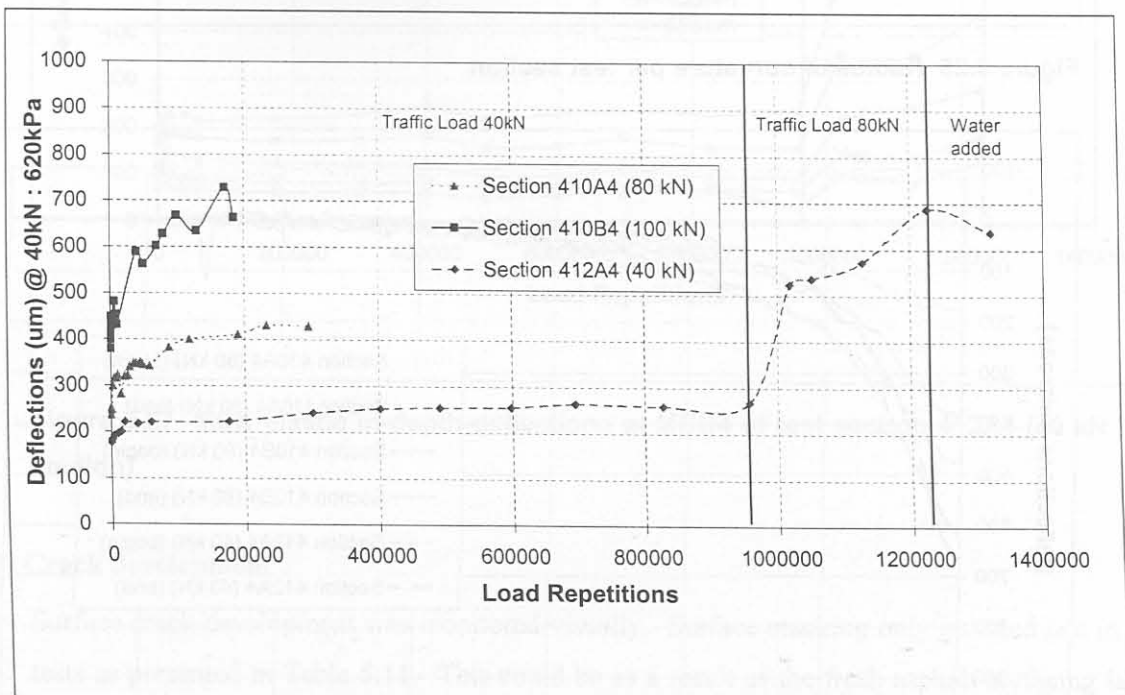


Figure 5.24 Maximum RSD elastic deflection per test section

For the 80 kN and 100 kN tests, the maximum deflection increased sharply during the test and when the tests were terminated the maximum deflections were almost twice their original value. For the 40 kN test, the maximum deflection did not show an increase during the duration of the 40 kN test. It increased sharply when the trafficking load was increased to 80 kN and terminated at values similar to that of the 100 kN test. This indicates that the pavement is sensitive to overloading.

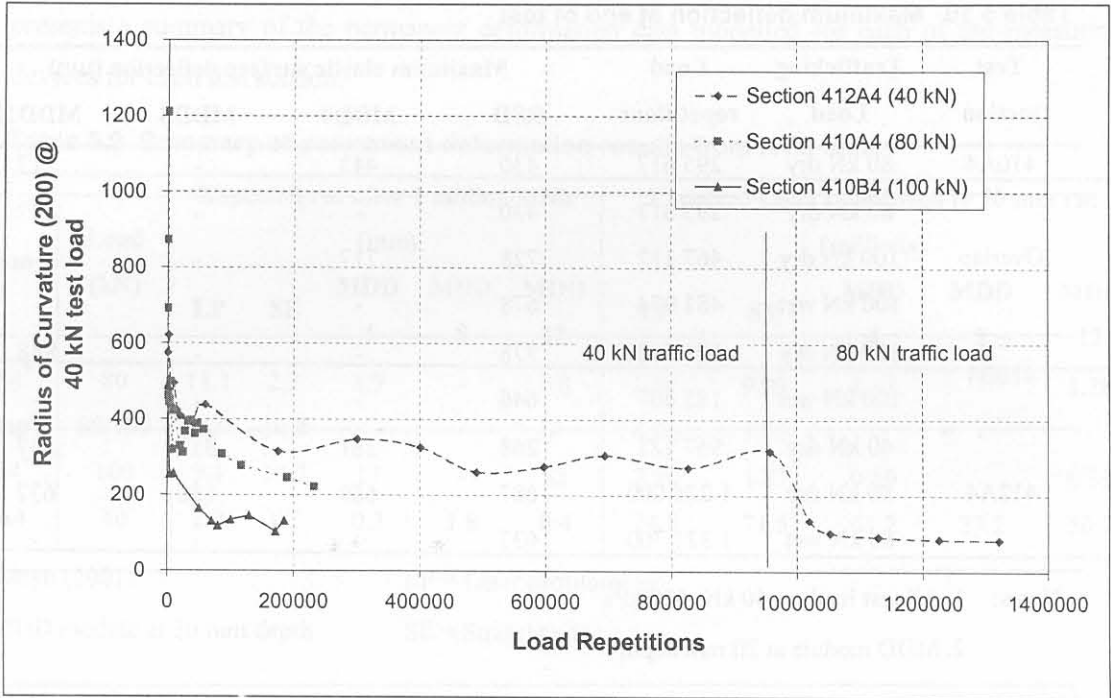


Figure 5.25 Radius of curvature per test section

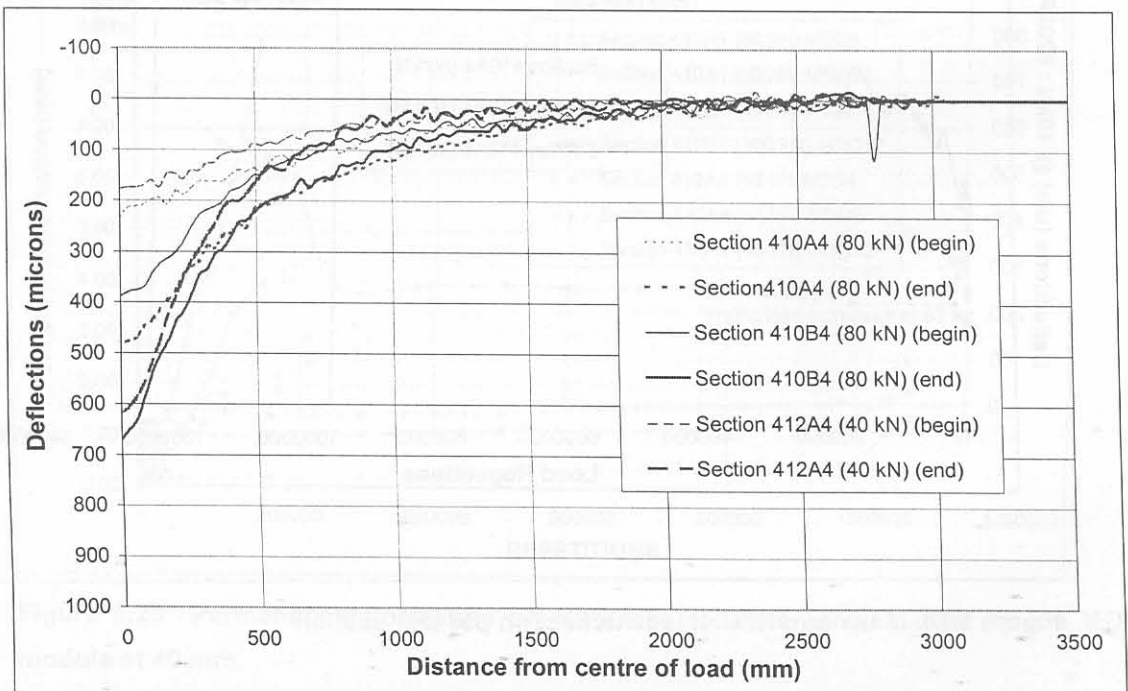


Figure 5.26 Deflection bowls per test section

The deflection bowls from the RSD data indicated the influence of an increasing wheel load on the maximum deflection and shape of the deflection bowl. The shape of the deflection bowls and the radius of curvature (*ROC*) showed that there was a change in the elastic behaviour of the pavement structure during trafficking. This change in elastic behaviour is not as distinct as in the case with cement treated layers, and it appears that layers treated with emulsion change their elastic behaviour more gradually during trafficking. The *ROC* also decreases when the trafficking wheel load is increased which indicates that the pavement structure tends to reduce its load spreading capability in the upper layers.

Figure 5.27 shows the elastic in-depth deflections at MDD 4 of section 412A4 (40 kN test section). This data indicated that the elastic in-depth deflections were equally distributed between the layers shallower than 650 mm. It also appears that the material reacted in a linear elastic fashion, as the increased elastic deflection measured is similar to the increased test wheel load (Figure 5.28).

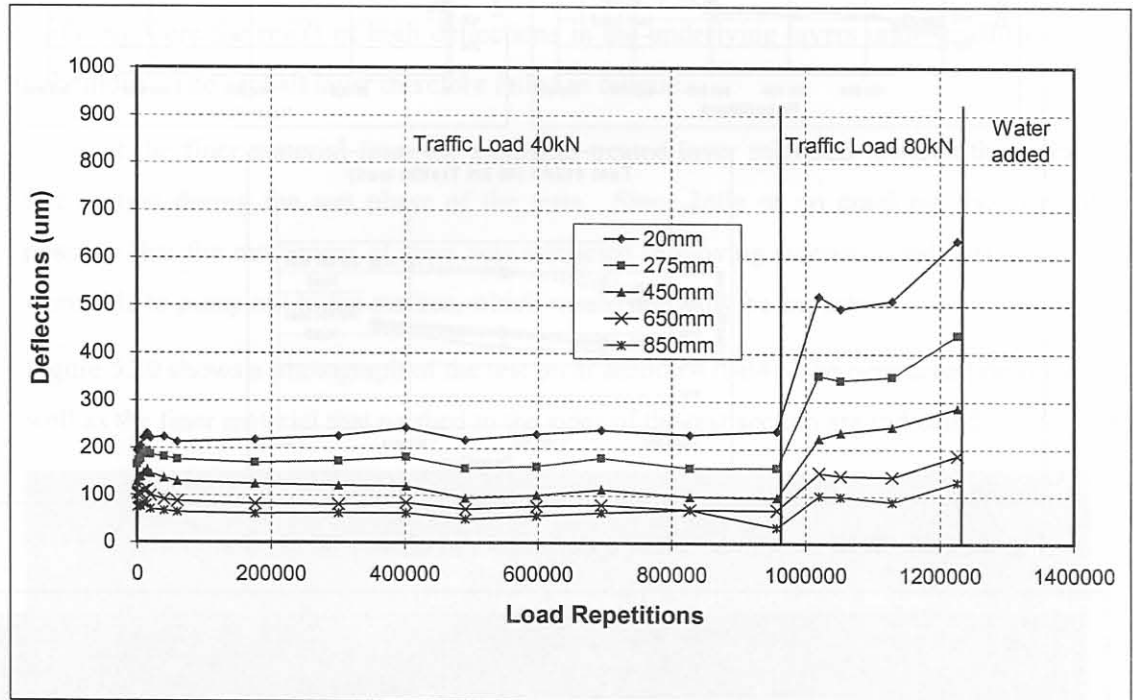


Figure 5.27 MDD elastic in-depth deflections at MDD4 of test section 412A4 (40 kN test section)

5.7.3 Crack development

Surface crack development was monitored visually. Surface cracking only initiated late in the tests as presented in Table 5.11. This could be as a result of the fresh asphalt surfacing layer over the emulsion treated base layer.

The crack development for sections 410B4 and 412A4 are shown in Figure 5.29. The figures show the final crack patterns of the test sections. A detailed record of the crack patterns for all the test sections is included in Appendix C.

Table 5.11 Crack development on HVS test sections

Test section	Number of repetitions before surface cracking was detected
410A4	No cracking developed before test was terminated at 295 617
410B4	129 544
412A4	1 226 000*

* First 957 121 repetitions were at 40 kN and the last 268 879 at 80 kN

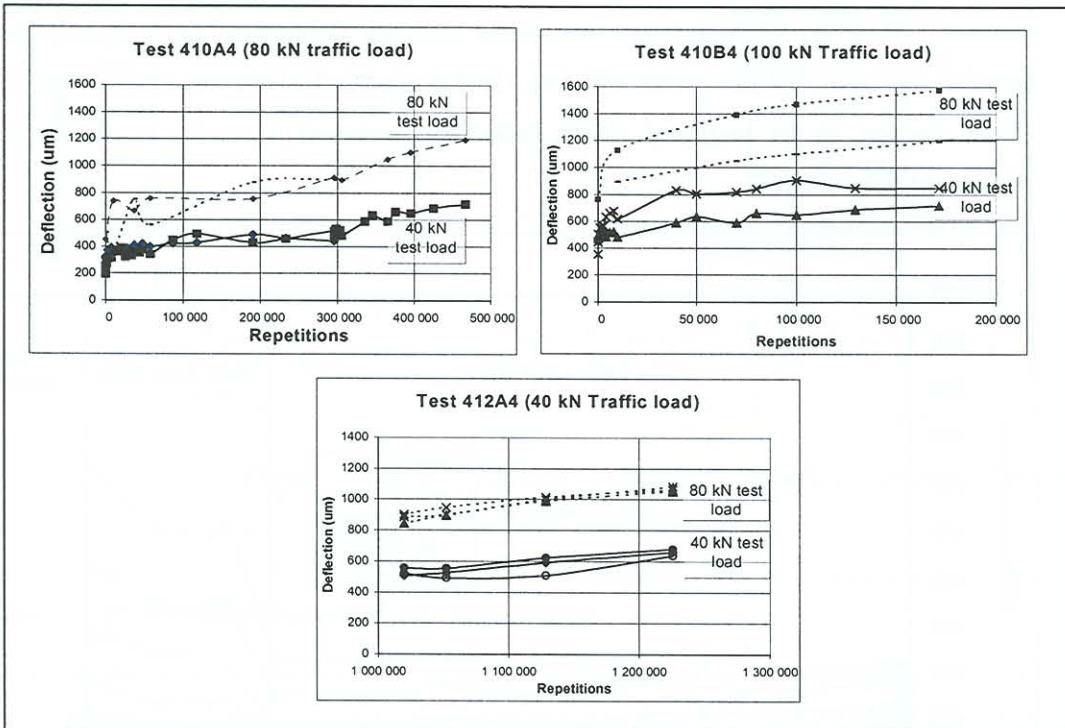


Figure 5.28 MDD maximum elastic deflection at 40 and 80 kN test loads

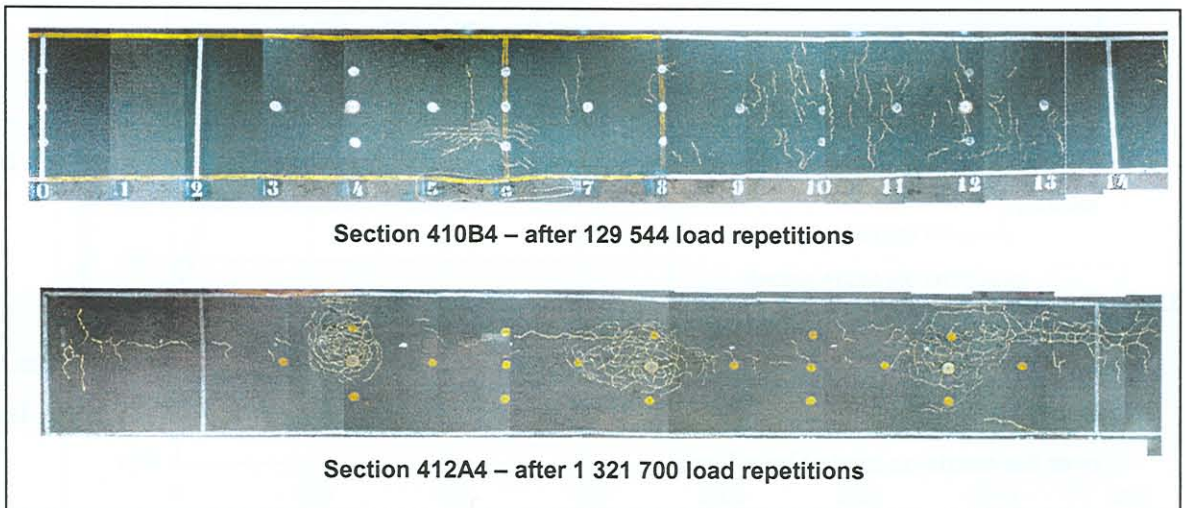


Figure 5.29 Final crack patterns

5.7.4 Test pits

Test pits were opened at the test sections as described by Steyn (2001) and Mancotywa (2001b). The objective of the test pits was to observe the behaviour and condition of the various layers after trafficking. On sections 410A4 and 410B4 the first test pit was opened to a depth of 600 mm, the second only through the base layer (300 mm) and for the third only the surfacing was removed. On section 412A4 only one test pit to a depth of 800 mm was opened.

The emulsion treated layer broke down into large lumps during the 80 and 100 kN tests (sections 410A4 and 410B4) but no indication of this could be found during the 40 kN test (section 412A4).

On the 40 kN test, no cracks in the emulsion treated layer could be observed to the full depth profile of the test pit. The cracks that reflected on the surface of the road were only in the asphalt layer and none of these cracks could be followed into the emulsion treated layer. As most of the cracking started during the wet period of the tests, the cracks in the asphalt surfacing were the result of high deflections in the underlying layers under trafficking in wet conditions. The asphalt layer therefore failed in fatigue.

Some of the finer material from the emulsion treated layer migrated towards the sides of the test section during the wet phase of the tests. Since little or no cracking was present it is possible that the movement of fines was restricted to moving sideways and very few of them were able to pump out to the surface, which would normally be expected.

Figure 5.30 shows a photograph of the test pit at section 410B4. The permanent deformation as well as the finer material that washed to the sides of the test section are indicated on the photo.

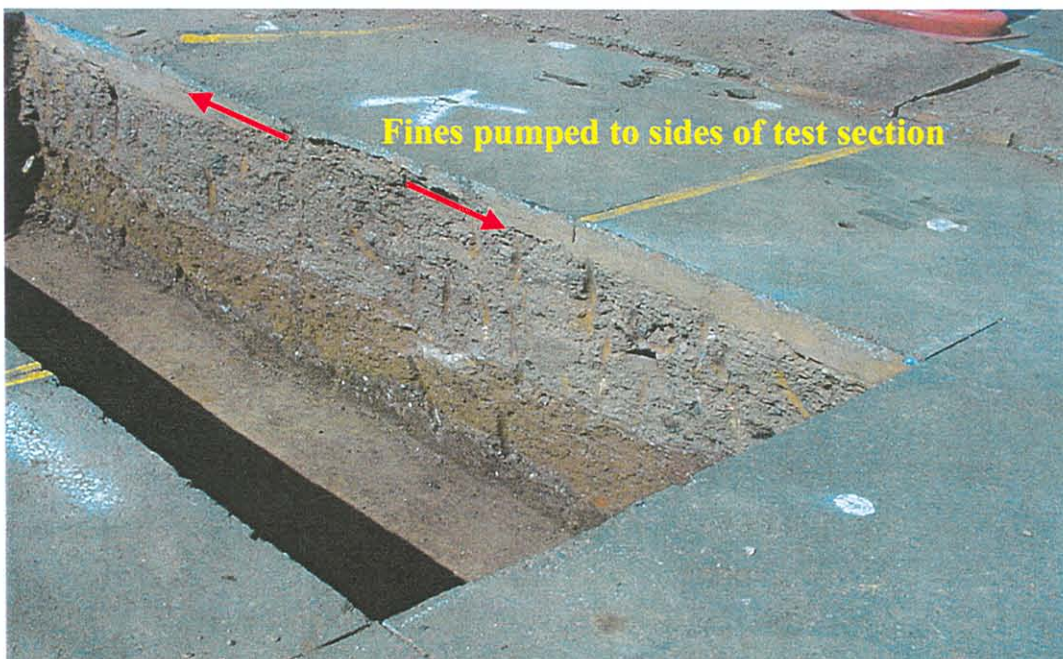


Figure 5.30 Test pit at section 410B4

5.7.5 Effective elastic stiffness

The depth deflection profiles were used to back-calculate the effective elastic moduli (E – moduli) for the different layers at various stages of trafficking. The subgrade was assumed to be of infinite depth i.e. an elastic half space. The dual wheels were spaced at 350 mm and the effective moduli were calculated directly under one of the wheels. It was found that more realistic E moduli were obtained from this approach because the linear elastic theory calculate unrealistically low moduli for the base layer if calculated between the wheels. These results compared favourably with the method used by de Beer (1989) where the wheel spacing was reduced to ensure that the contact areas met. A Poisson's ratio of 0.35 was used in the backcalculation and an analysis at different Poisson's ratios indicated that the stiffness was not sensitive to small variations. This was also found by Fossberg (1970) and Otte (1972) on cement stabilised base layer materials. Work by Semmelink (2001) and Semmelink et al (2000b), however, indicated values for the Poisson's ratio of the emulsion treated ferricrete as low as 0.1.

The results show that the E moduli of the emulsion treated base layer decreases gradually with trafficking. For higher wheel loads this reduction is more rapid than for lower wheel loads. It is believed that this reduction in E moduli, together with the change in the shape of the deflection bowl, as discussed in section 5.7.2, will enhance the understanding of the behaviour of emulsion treated layers.

Concepts of the reduction in E moduli for cement treated layers were introduced into South Africa as early as 1978 (Otte: 1978). Freeme (1983) proposed the concept of "effective stiffness or moduli" which states that a bound (bituminous or cementitious) layer cracks in fatigue or breaks down, then the layer ceases to behave as a homogeneous continuum in the way normally assumed in theoretical analysis. The concept of pre-cracked and post-cracked phases was introduced by Freeme (1983) and is illustrated in Figure 5.31.

Research by de Beer and Grobler (1993), Mancotywa (2001a) as well as results from this study indicated a similar reduction of E moduli in emulsion treated layers.

The effective E moduli on the 40 and 80 kN started at between 1 500 and 2 700 MPa while the E moduli on the 100 kN section started at 1 000 MPa. Table 5.12 and Figure 5.32 present the backcalculated E moduli for the three test sections at the beginning and end of each test.

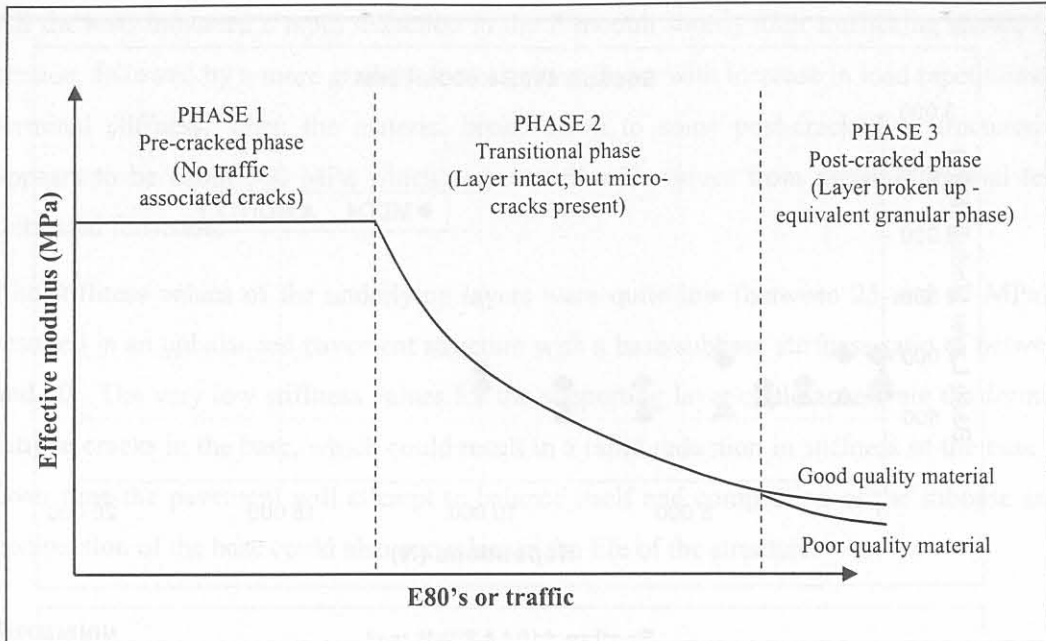


Figure 5.31 Reduction of E-moduli of C3 material under trafficking (Freeme: 1983)

Table 5.12 Summary of backcalculated E moduli for HVS test sections.

Section	Trafficking load	Initial Stiffness (MPa)	Final stiffness (MPa)	Number of repetitions
410A4	80 kN	2 000 – 2 700	1 100	295 617
Overlap	80 kN	2 000 – 2 700	1 000	295 617
	100 kN	1 000	850	467 117
410B4	100 kN	1 000	750	171 500
412A4	40 kN	1 750 – 2 250	750 – 1 250	957 121
	80 kN		350 – 500	1 226 000

All the tests commenced at an initial effective E modulus of between 1 750 and 2 700 MPa which agree well with the dynamic triaxial test results. The 100 kN test, however, started at a stiffness of 1 000 MPa. It is assumed that the 100 kN trafficking load caused the reduction in E modulus from the start of the test and could also be the reason for the scatter in the data and for the E modulus not to decrease with increase in load repetitions (Figure 5.32b). This was also the case at MDD4 in the 80 kN test (Figure 5.32a). The reduction of E moduli with increase in load repetitions was clearly evident on the 40 kN test as can be seen in Figure 5.32c. The stiffness after 957 121 repetitions at 40 kN was in the range of between 750 and 1 250 MPa and reduced further when the wheel load was increased to 80 kN to a value of around 500 MPa. Dynamic triaxial tests done on the untreated ferricrete indicated that the average resilient modulus of the untreated ferricrete was about 660 MPa. This relatively high value for natural gravel can be attributed to the well-graded material obtained from the deep in situ recycling.

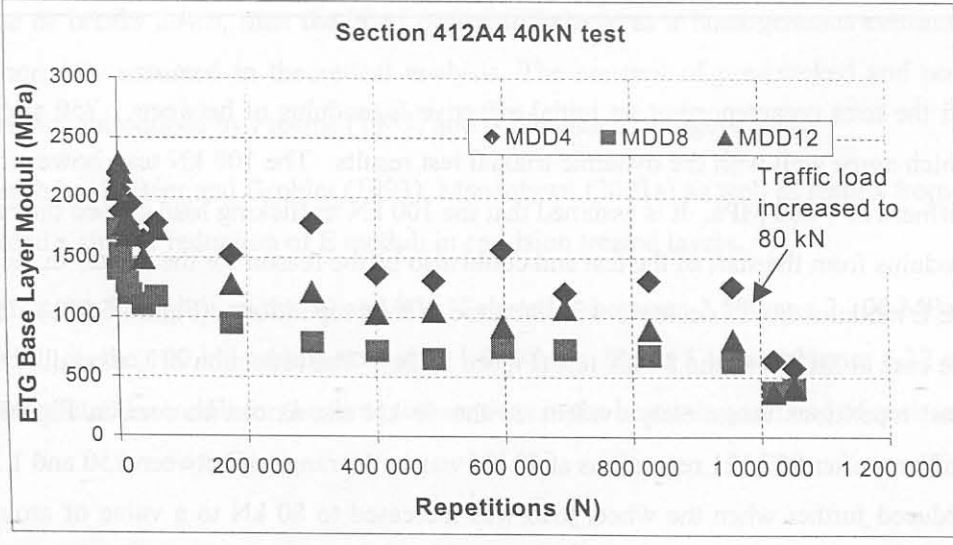
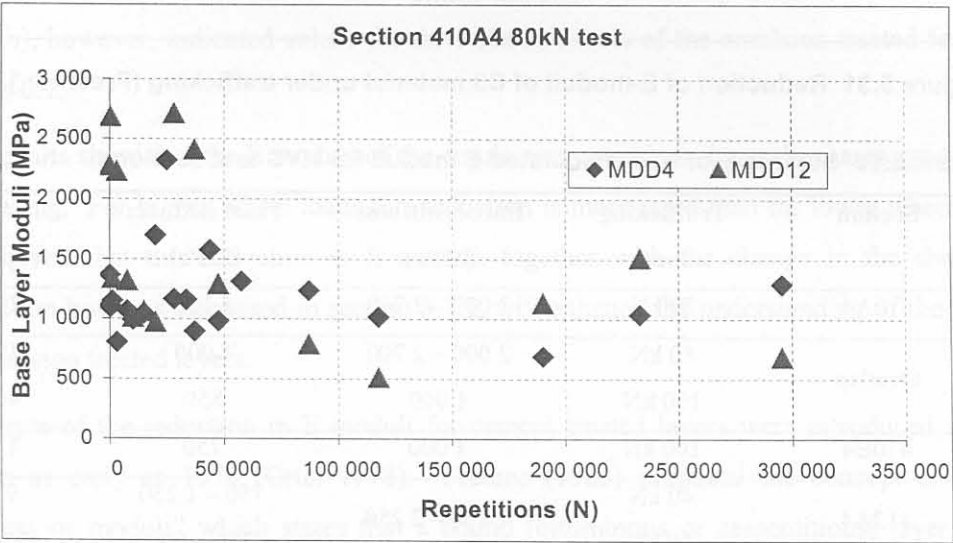
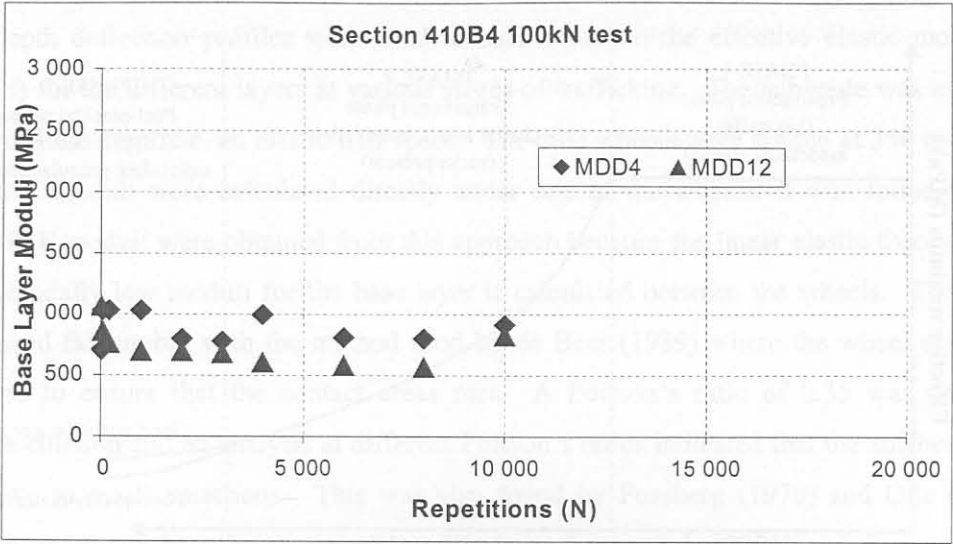


Figure 5.32 Back calculated E moduli for the different test sections

All the tests indicated a rapid reduction in the E moduli shortly after trafficking started on the section, followed by a more gradual decrease in stiffness with increase in load repetitions. The terminal stiffness, when the material broke down to some post-cracked or fractured state appears to be about 500 MPa which agrees well with values from dynamic triaxial tests of untreated ferricrete.

The stiffness values of the underlying layers were quite low (between 25 and 45 MPa), and resulted in an unbalanced pavement structure with a base/subbase stiffness ratio of between 11 and 20. The very low stiffness values for the supporting layer could accelerate the forming of fatigue cracks in the base, which could result in a rapid reduction in stiffness of the base layer. Over time the pavement will attempt to balance itself and compaction of the subbase and de-compaction of the base could also occur late in the life of the structure.

5.7.6 Discussion

The emulsion treated test sections performed well during the HVS tests. The thickness of the treated recycled layer (250 mm) could have contributed to this performance of the pavement. Very little permanent deformation was measured at the surface, throughout the dry phases of the tests, with crack development mainly restricted to the wet tests. Although most of the permanent deformation occurred within the emulsion treated layer, the amount of permanent deformation was small. The small contribution of the lower layers to the permanent deformation as well as the elastic deflection, indicate that the emulsion treated layer provided good protection for the subgrade and other lower lying layers.

The reduction in the E moduli and gradual change in the deflection bowl, confirm that the behaviour of emulsion treated layers are a phased behaviour. The test pits however revealed that the second phase might not necessarily be a so called “equivalent granular” phase, but rather a phase with a reduced stiffness in which the permanent deformation of the layer (as a base layer) might be the dominant failure mechanism. The mechanism of the permanent deformation could be similar to that present in unbound granular base layers, which is a combination of gradual shear failure and densification or compaction during the initial bedding in phase.

5.8 CONCLUSIONS

The following conclusions could be drawn from the laboratory and HVS test results included in this study:

- The Initial Consumption of Lime (ICL) requires to be satisfied to enable the cement to add significant strength to the mix. Bitumen emulsion alone does not necessarily add strength to the material when the net bitumen content is less than 3 %.

- The cement contributes to the brittleness of the material while the bitumen emulsion contributes to the flexibility of the mix. The quantities of cement and net bitumen in the mix tend to cause the behaviour of the material to be more like a lightly cemented material than an asphalt material.
- There exists a fine balance between the cement and emulsion content in the mix to ensure the optimal strength and flexibility that would be required in the structural design.
- The compaction method, compaction moisture and curing method applied to the laboratory samples may influence the results from the different laboratory tests. This experiment attempted to simulate field conditions as closely as possible by 28 day curing at ambient temperature.
- The static compressive shear strength parameters (c and ϕ) were estimated for the material in this study at 308 kPa and 50.9° , respectively.
- The initial resilient modulus of the emulsion treated material from both the laboratory testing and backcalculation from HVS in depth elastic deflections, was in the order of 2 000 MPa. The good grading of the material from the deep in-situ recycler may have contributed to the relative high stiffness value.
- The material has a stress sensitivity in the sense that the stiffness increases slightly with an increase in the bulk stress or stress condition within the material.
- The laboratory tests indicated that the permanent deformation of the untreated ferricrete was not significantly improved by the addition of emulsion and cement. The HVS, however, resulted in very low permanent deformation results, even after a high number of load repetitions.
- There is a definite phased behaviour in the elastic response of the material, although it was not as drastic as was the case with cement treated material. There seems to be a more gradual change in the elastic response as opposed to a rapid change at some stage during the life of the material.
- The HVS section showed very little cracking and most of the cracking was initiated only after the wet testing commenced. Most of the cracking appears to be limited to the asphalt surfacing of the pavement rather than in the emulsion treated layer.
- During the wet test, fine material was pumped to the sides of the test section, outside the trafficking section. Most of the fines were trapped between the base layer and the asphalt surfacing.

The behaviour of emulsion treated layers is at least a two phase behaviour with the first phase being a fatigue life phase with a high modulus of elasticity and a layer that would mainly fail in fatigue. Although no cracks were visible during the inspection of the test pits, it is reasonable

to believe that microcracks were present in the layer, which resulted in the reduced stiffness after a number of load applications. The second phase would be an “equivalent granular phase” with a reduced stiffness. This “equivalent granular phase” does not mean that the material is truly an unbound material in the complete sense, but rather that the stiffness properties of the material are similar to that of a granular material and that the failure mechanism of this phase would be permanent deformation due to gradual shear deformation.

5.9 RECOMMENDATIONS

The following recommendations are given regarding the structural design of emulsion treated layers:

- The initial stiffness or E moduli proposed for emulsion treated layers constructed by means of a *deep in-situ recycling machine* were 2 000 MPa, with the second phase (equivalent granular phase) stiffness of 500 MPa. It is important to note that these numbers referred to a parent material that is well graded and which fits the G6 material specification.
- The Poisson’s ratio (μ) of the material, as used in the structural evaluation in both the fatigue life and post fatigue life phases, be 0.35. The use of this value is proposed until further formal research proves otherwise.
- The structural evaluation of an emulsion treated material be done as a two phase behaviour similar to that of cement treated material with a fatigue life phase as first phase and an “equivalent granular” phase as second phase.
- The strain at break (ϵ_b) should be obtained from four point flexural beam tests. The values from the results in this study approximate the values for cement treated materials, provided that the ICL is met. For estimation, the strain at break values assumed in Table 5.13, should be used. These values were averaged from the laboratory study for the possible different combinations of cement and emulsion contents and are valid for parent material of G5 to G7 quality. Special curing should be allowed for layers constructed without cement or at low cement contents below the ICL on parent materials of G4 to G7. This is however not recommended. The designer should keep in mind that the strain at break will reduce if more than the required amount of cement is added.

Table 5.13 Proposed values for strain at break for emulsion treated materials

		Net bitumen content	
		1% to 2 %	2% to 3.5%
Cement- content	Below ICL	325 $\mu\epsilon$	500 $\mu\epsilon$
	Slightly above ICL	145 $\mu\epsilon$	230 $\mu\epsilon$

- The compressive shear parameters should be obtained from static triaxial testing, but for estimation, values of 200 - 300 kPa for the cohesion (c) and 45° - 50° for the angle of internal friction (ϕ) can be assumed.

5.10 REFERENCES

- Basson JEB, Wijnberger OJ and Skultety J, 1981, *The multi depth deflectometer: A multistage sensor for the measurements of resilient deflections and permanent deformations at various depths in road pavements*, Technical report RP/3/81, National Institute for Transport and Road Research, CSIR, Pretoria, South Africa.
- Blabb R and Litzka J, 1995, *Measurements of the lateral distribution of heavy vehicles and its effects on the design of road pavements*, Proceedings of the Fourth International Symposium on Heavy Vehicles and Dimensions, edited by CB Winkler, University of Michigan Transportation Research Institute, Ann Arbor, United States, pp 389 – 395.
- Das BM, 1990, *Principles of Geotechnical Engineering*, 2nd ed., PWS-KENT Publishing Company, Boston, United States.
- De Beer M, Horak E and Visser AT, 1988, *The multi depth deflectometer (MDD) system for determining the effective elastic moduli of pavement layers*, First International Symposium on non-destructive testing of pavement and back calculation of moduli, ASTM STP 1026, Baltimore, United States.
- De Beer M, 1989, *Aspects of the design and behaviour of road structures incorporating lightly cementitious layers*, PhD thesis, University of Pretoria, Pretoria, South Africa.
- De Beer M and Grobler JE, 1993, *ETB's: Heavy Vehicle Simulator (HVS) evaluation of the heilbron sections*, Report RSC92/2/1, Division of Roads and Transport Technology, CSIR, Pretoria, South Africa.
- Division of Roads and Transport Technology (DRTT), 1987, *Accelerated testing; 1: The Heavy Vehicle Simulator*, Information Brochure, CSIR, Pretoria, South Africa.
- Eades JL and Grim RE, 1964, *A quick test to determine the lime requirements for lime stabilisation*, Highway research Record no. 139, Washington DC, United States.
- Fossberg PE, 1970, *Load-deformation characteristics of three layer pavements containing cement-stabilised bases*, PhD Thesis, University of Berkeley, California, United States.
- Freeme CR. 1983, *Evaluation of pavement behaviour for major rehabilitation of roads*, Technical Report RP/19/83, National Institute for Transport and Road Research, CSIR, Pretoria, South Africa.
- Lambe TW and Whitman RV, 1969, *Soil Mechanics*, Massachusetts Institute of Technology, John Wiley and Sons Inc., New York, United States

Long FM and Theyse HL, 2001, *Laboratory testing for the HVS Sections on Road P243-1*, Contract Report CR-2001/32, Transportek, CSIR, Pretoria, South Africa.

Mancotywa WS, 2000, *First level analysis report: Phase 1 HVS testing of experimental sections on road R2388 near Cullinan*, Contract Report CR-99/011, CSIR Transportek, Pretoria, South Africa, South Africa.

Mancotywa WS, 2001a, *First level analysis report: Phase 2 HVS testing of the Emulsion Treated natural gravel base section on road R2388 near Cullinan*, Contract Report CR-2000/47, CSIR Transportek, Pretoria, South Africa, South Africa.

Mancotywa WS, 2001b, *First level analysis report: 2nd Phase HVS testing of the Emulsion Treated Gravel and Foam Bitumen Gravel base sections on road P243/1 near Vereeniging*, Contract Report CR-2000/53, CSIR Transportek, Pretoria, South Africa, South Africa.

National Institute for Transport and Road Research (NITRR), 1986, *TMH1: Standard Methods of testing Road Construction Materials*, 2nd ed., CSIR, Pretoria, South Africa.

Otte E, 1972, *Die spannings- en vervormingseienskappe van sementgestabiliseerde materiale*, MSc dissertation, University of Pretoria, Pretoria, South Africa.

Otte E, 1978, *A structural design procedure for cement treated layers in pavements*, DSc thesis, University of Pretoria, Pretoria, South Africa.

Robroch S, 2001, *laboratory testing on foamed bitumen and cement treated material from the HVS test section on road P243/1*, Contract Report CR-2001/69, Transportek, CSIR, Pretoria, South Africa.

Semmelink CJ and Botha PB, 2000(a), *Evaluation of foam bitumen and emulsion treated ferricrete material on the new HVS site in the initial stages*, Contract report LR-2000/1/JR38794, Transportek, CSIR, Pretoria, South Africa.

Semmelink CJ and Botha PB, 2000(b) *Strength of foamed-cement and emulsion cement stabilised ferricrete base material from HVS site at Heidelberg as measured with K-mould*, Technical Report TR2001/14, Transportek, CSIR, Pretoria, South Africa.

Semmelink CJ, 2001, *Personal communication and correspondence*, Pretoria, South Africa.

Shackleton MC, 1995, *Modelling of the permanent deformation of untreated pavement layers*, MEng dissertation, University of Pretoria, Pretoria, South Africa.

Steyn WJvdM, 2001, *Level one data analysis of HVS tests on Foam Treated Gravel and Emulsion Treated Gravel on road P243-1: 80 kN and 100 kN test sections*, Contract report CR-2001/5, Transportek, CSIR, Pretoria, South Africa.

Theyse HL, 2000, *Laboratory design models for materials suited to labour-intensive construction: Volume I: Report*, Contract Report CR-99/038, Transportek, CSIR, Pretoria, South Africa.

Theyse HL, 2000, *The stiffness, strength and performance of unbound aggregate*, Contract report CR-2000/35, Transportek, CSIR, Pretoria, South Africa.

Van Vuuren H, 2001, *Personal communication and correspondence*, Bloemfontein, South Africa.

Verhaeghe BMJA, Napier RC and Kong Kam Wa NJ, 1998, *A Revised Approach to Mix Design of Emulsion Treats Base Materials: Laboratory Investigations*, Contract Report CR-97/057, CSIR Transportek, Pretoria, South Africa.

Verwey G, 2001, *Personal communication and correspondence*, Pretoria, South Africa.

Wolff H, 1992, *The Elasto-plastic behaviour of granular pavement layers in South Africa*, PhD thesis, University of Pretoria, Pretoria, South Africa.

CHAPTER 6 FATIGUE PROPERTIES OF EMULSION TREATED MATERIALS

6.1 INTRODUCTION

Most materials bound by cement and/or bitumen show fatigue resistance properties that will resist the formation of tensile failure areas (cracks) when subjected to tensile stresses or strains. Fatigue has been defined as “*the process of progressive localised permanent structural change occurring in a material subjected to conditions which produce fluctuating stresses and strains at some point or points and which may culminate in cracks or complete fracture after a sufficient number of fluctuations*” (ASTM: 1964). Fatigue will therefore start when the material is repeatedly subjected to a load that induces a tensile strain in the material. Early in their life, as a component in a pavement structure, treated materials act similarly to a loaded beam. Tensile strains develop mainly at the bottom of these layers and will initiate the breaking up of the bonds formed by cement and bitumen. This will lead subsequently to the formation of cracks, which may in some cases be of microscopic size.

Cracking in pure cementitious layers can be divided into non-traffic associated cracking and traffic associated cracking. The non-traffic associated cracking involves cracking due to environmental conditions such as temperature and moisture content. Research on non-traffic associated cracking in emulsion treated layers is limited, but the performance from emulsion treated layers with cement in the field has proved that there is less non-traffic associated cracking than in pure cement treated layers.

Cracking in bituminous bases and surfacings, usually occurs due to the combined effect of traffic loading and ageing of the bituminous binder.

The scope of this chapter includes the analysis of the fatigue properties observed of the emulsion treated material tested. A failure criterion for the effective fatigue life is also developed for the use in structural design.

6.2 THE END OF THE FATIGUE LIFE

The fatigue life of a treated pavement material is normally characterised by a high modulus of elasticity, low elastic deflections and virtually no permanent deformation. The end of the fatigue life resulted in a non-linear behaviour because of the non-homogeneity from the presence of cracks, a reduced modulus of elasticity, increased elastic deflection and a decrease in the resistance to permanent deformation. The initiation of cracks in a layer will lead to a reduction in the stiffness that will lead to a further reduction as the cracks progress through the layer. The end of the fatigue life of a bound pavement layer will therefore consists of two

phases, namely the crack initiation phase and crack progression phase. The progression of cracks through the layer may not necessarily be linear through the layer and the speed of crack propagation may vary as the balance and stress state of the pavement vary.

The effective fatigue life is defined as the stage in the life of the layer where the crack (whatever its size) progresses through the layer and the effective stiffness of the layer is reduced to similar values as found in granular or unbound layers.

The effective stiffness of the ferricrete at Vereeniging seems to converge to a terminal stiffness value of around 500 MPa after a number of load repetitions. The point at which the effective stiffness reaches a value of 500 MPa, is approximately 25% of the initial stiffness in this case, and is assumed to be the end of the fatigue life phase of the ferricrete material. The layer is then in a reduced stiffness phase equivalent to a granular layer although the layer may still be largely intact and only broken down in large blocks.

6.3 TENSILE STRAIN ANALYSIS

Horizontal tensile strains at the bottom of the layer were calculated at various load repetitions during the HVS tests. The strains were calculated using a linear elastic multilayer software package with stiffnesses as backcalculated in Chapter 5. Figure 6.1 contains a plot from the analysis on a linear-log scale.

The horizontal tensile strain at the bottom of the layer showed a relatively stable increase in strain up to a point where it starts to oscillate. This was consistent at all the test sections and MDD's where no load history was present. A closer look at the elastic deflections, as well as the backcalculated stiffness, revealed that both these parameters entered an unstable phase although it is not easily visible. The elastic deflection decreased immediately after this point, while the resilient modulus increased. The point is preceded by a sharper increase in tensile strain as indicated in Figure 6.1.

This behaviour indicated that there were some changes in the behaviour of the pavement at this point, which is caused by the development of cracks in the close vicinity of the MDD module at the bottom of the emulsion treated layer. After the formation of the cracks there was a redistribution of the stresses around the MDD module at the bottom of the layer that lead to the reduction in the elastic deflection. The horizontal strains at the bottom of the layer were then concentrated around the cracks as shown in Figure 6.2.

Figure 6.3 presents the maximum horizontal tensile strain before crack initiation, at various positions within the layer. The tensile strains were determined using a multi-layer linear elastic software program, and it confirms that the maximum horizontal strain for the pavement structure under consideration is at the bottom of the layer.

The life to crack initiation for each of the HVS tests is summarised in Table 6.1 and Figure 6.4 presents a transfer function to determine the life to crack initiation.

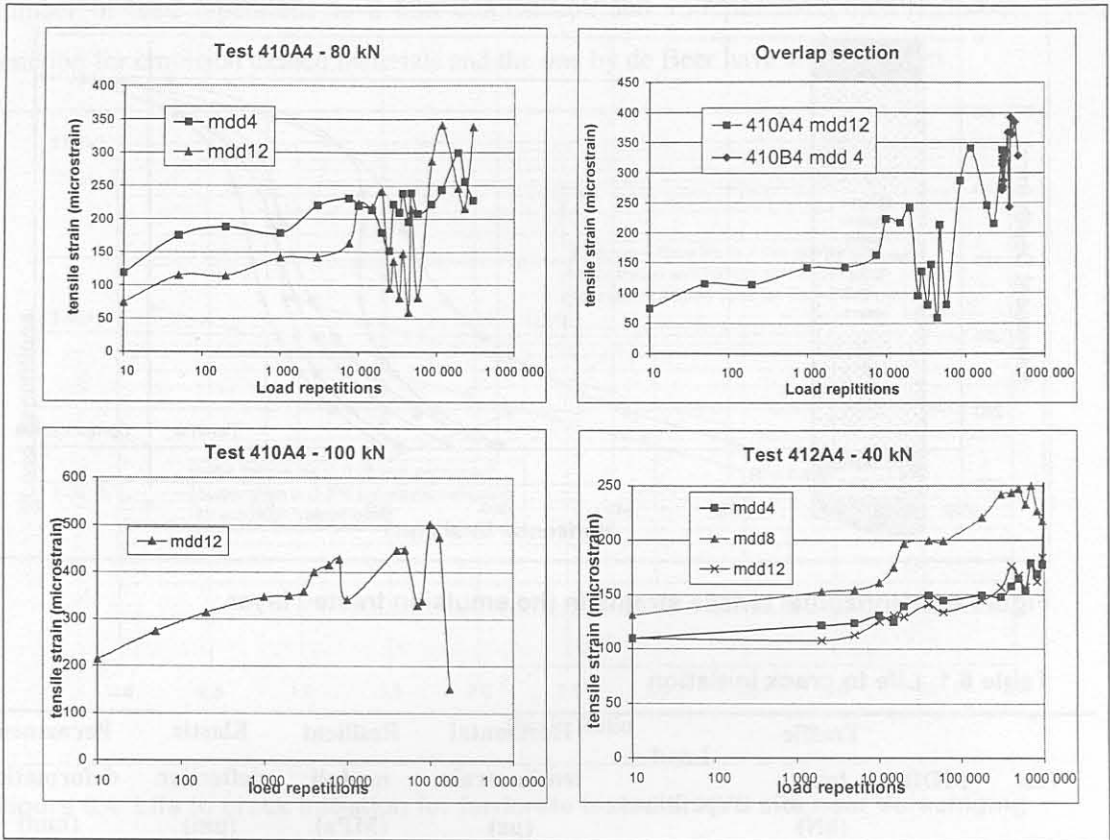


Figure 6.1 Tensile strain analysis

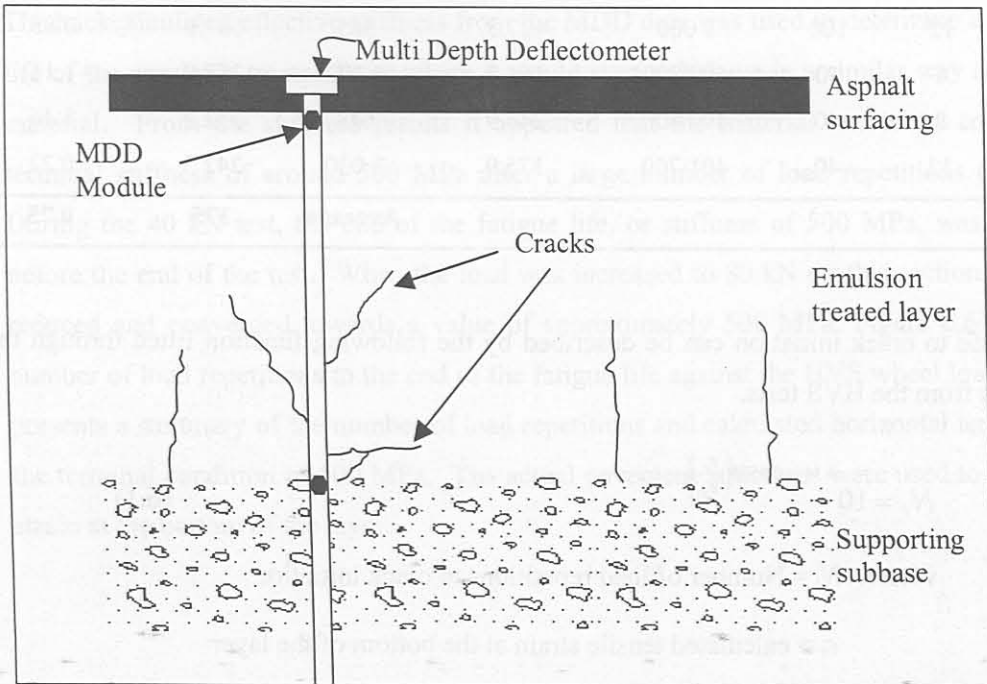


Figure 6.2 Schematic illustration of the initiation of cracks at the MDD at bottom of the layer

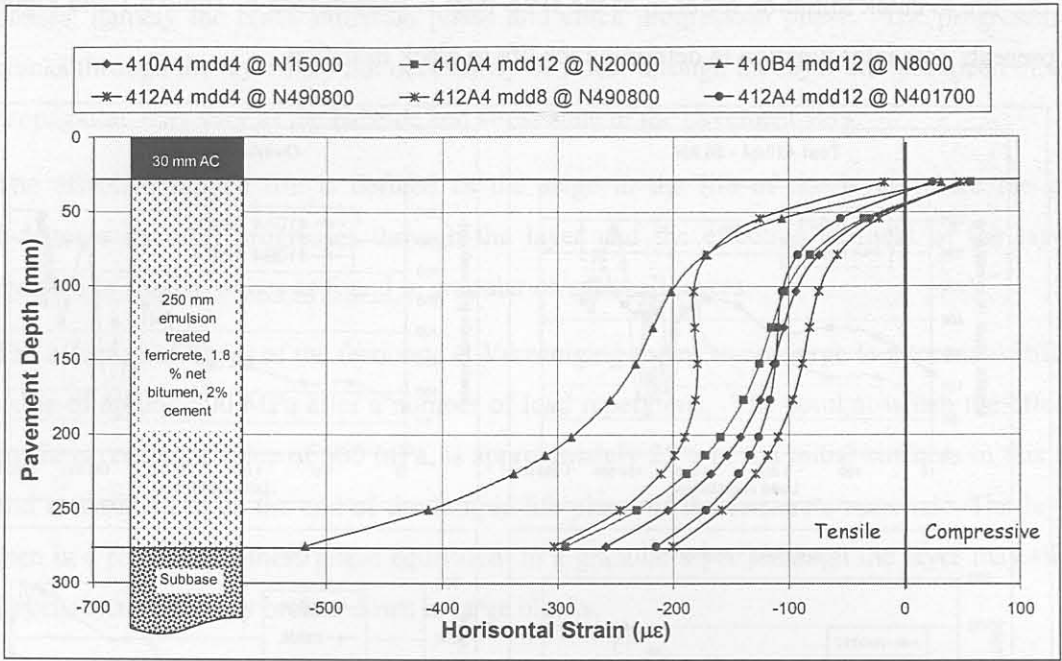


Figure 6.3 Horizontal tensile strains in the emulsion treated layer.

Table 6.1 Life to crack initiation

Test	MDD	Traffic load (kN)	Load repetitions	Horizontal tensile strain (µε)	Resilient moduli (MPa)	Elastic deflection (µm)	Permanent deformation (mm)
410A4	4	80	15 000	213.5	1 042	361.4	0.53
410A4	12	80	20 000	241.6	969	391.3	0.28
410B4	12	100	8 000	427.5	565	667.0	0.85
412A4	4	40	490 800	164.8	1 302	258.0	1.11
412A4	8	40	490 800	246.9	648	332.2	1.46
412A4	12	40	401 700	175.9	1 030	242.5	0.22
Average						375	0.75

The life to crack initiation can be described by the following function fitted through the data points from the HVS tests.

$$N_i = 10^{6.344 - 0.8573 \left(\frac{\epsilon_t}{\epsilon_b} \right)} \quad (6.1)$$

where: N_i = Number of load repetitions to crack initiation

ϵ_t = calculated tensile strain at the bottom of the layer

ϵ_b = strain at break

This equation is similar to the one developed by de Beer (1989) for crack initiation in lightly cemented materials. De Beer defined crack initiation in lightly cemented materials as the number of load repetitions to 2 mm deformation and 750 μm maximum deflection. The function for emulsion treated materials and the one by de Beer have similar slopes.

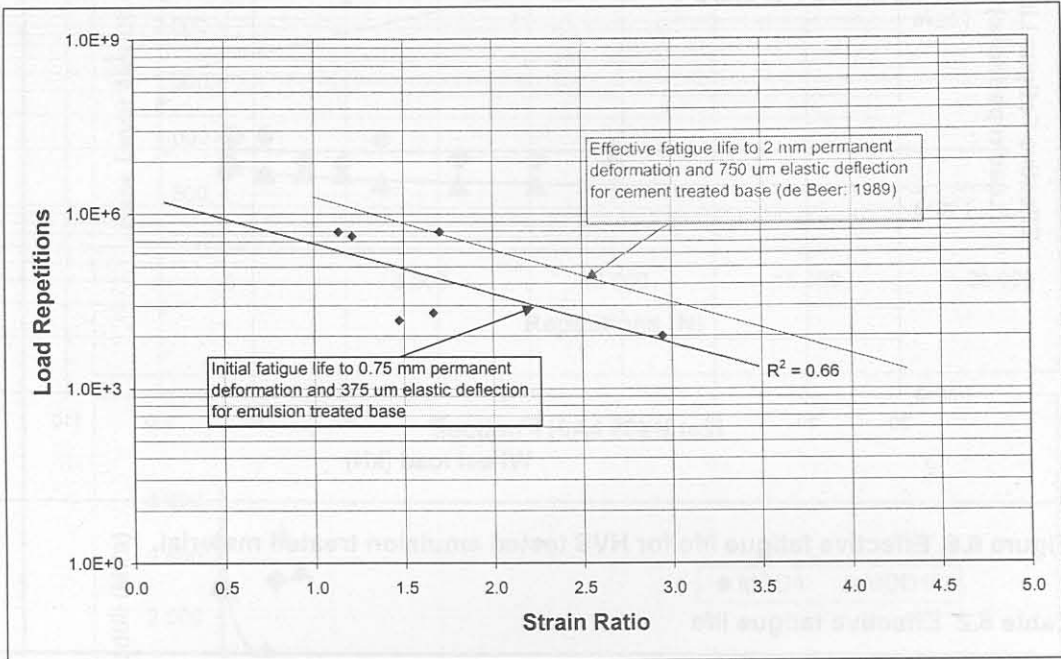


Figure 6.4 Life to crack initiation for ferricrete tested at HVS site near Vereeniging

6.4 THE EFFECTIVE FATIGUE LIFE OF EMULSION TREATED MATERIALS

The backcalculated effective stiffness from the MDD data was used to determine a point in the life of the emulsion treated layer where it would start to behave in a similar way as a granular material. From the stiffness results it appeared that the material tended to converge to a terminal stiffness of around 500 MPa after a large number of load repetitions (Figure 6.5). During the 40 kN test, the end of the fatigue life, or stiffness of 500 MPa, was not reached before the end of the test. When the load was increased to 80 kN on this section the stiffness reduced and converged towards a value of approximately 500 MPa. Figure 6.6 presents the number of load repetitions to the end of the fatigue life against the HVS wheel load. Table 6.2 presents a summary of the number of load repetitions and calculated horizontal tensile strain at the terminal condition of 500 MPa. The actual pavement structures were used to calculate the strain at the bottom of the layer.

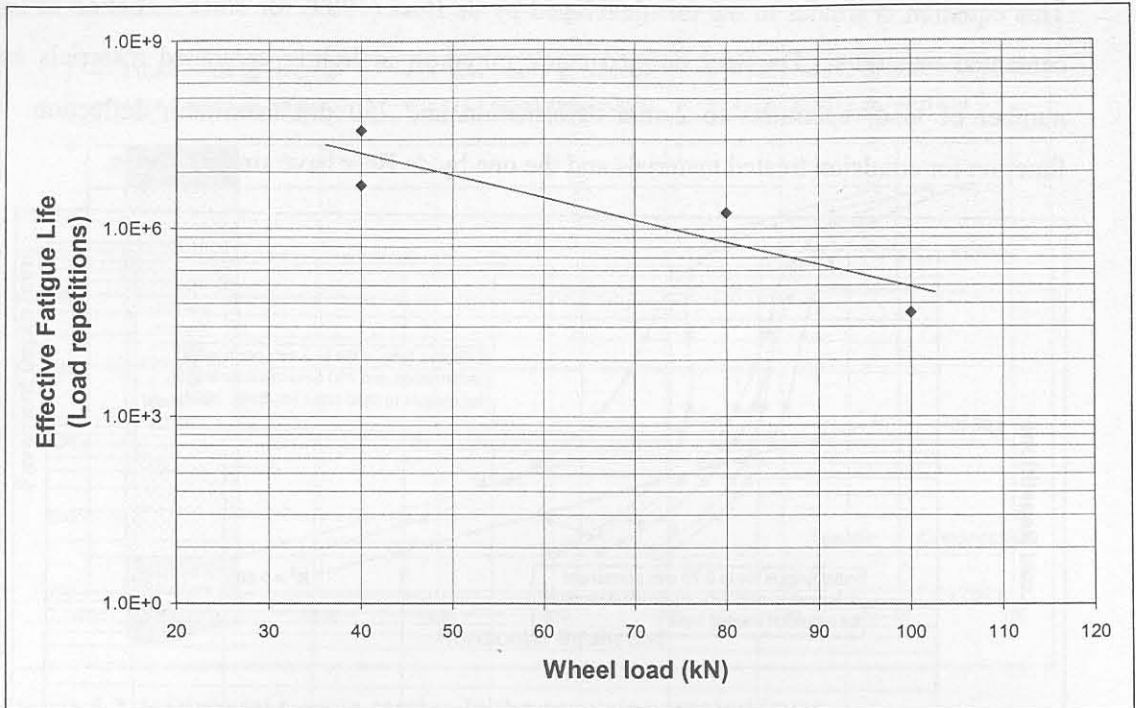


Figure 6.6 Effective fatigue life for HVS tested emulsion treated material.

Table 6.2 Effective fatigue life

Test	MDD	Load	ϵ_t	ϵ_b	Strain ratio (ϵ_t/ϵ_b)	N
410A4*	4	80	270.0	145	2.048	$3.53 * 10^6$
410A4	12	80	301.3	145	2.078	$1.8 * 10^6$
410B4	12	100	437.0	145	3.013	$45.4 * 10^3$
412A4	4	40	133.2	145	0.918	$3.2 * 10^9$
412A4	8	40	135.3	145	0.933	$5.0 * 10^6$
412A4	12	40	119.6	145	0.825	$37.2 * 10^6$

A curve was fitted through the data above which included various strain at break values. The effective fatigue life for the material tested, can be expressed as follows:

$$N_{eff} = 10^{8.5066 - 1.2774 \left(\frac{\epsilon_t}{\epsilon_b} \right)} \quad (6.2)$$

where: N_{eff} = Effective fatigue life

ϵ_t = calculated tensile strain at the bottom of the layer

ϵ_b = strain at break

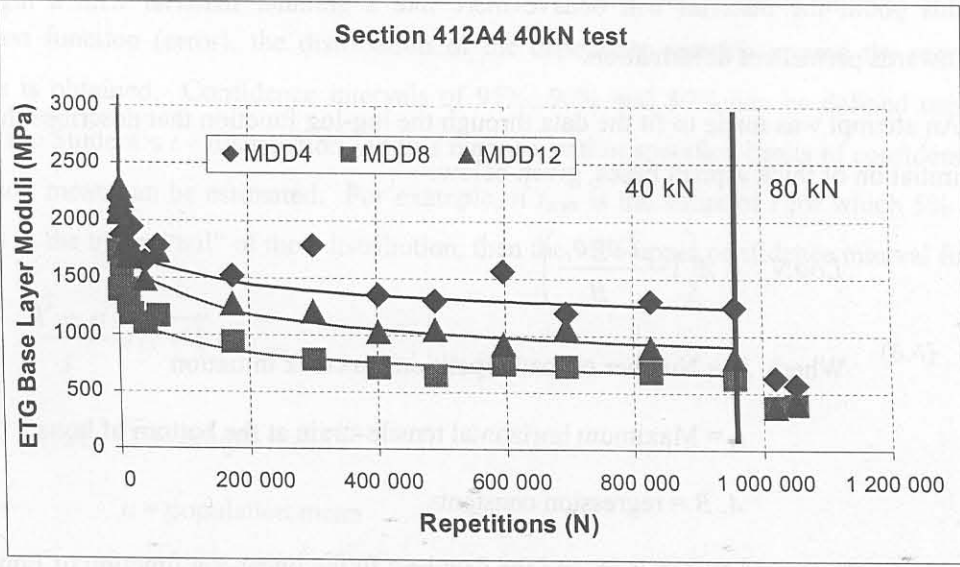
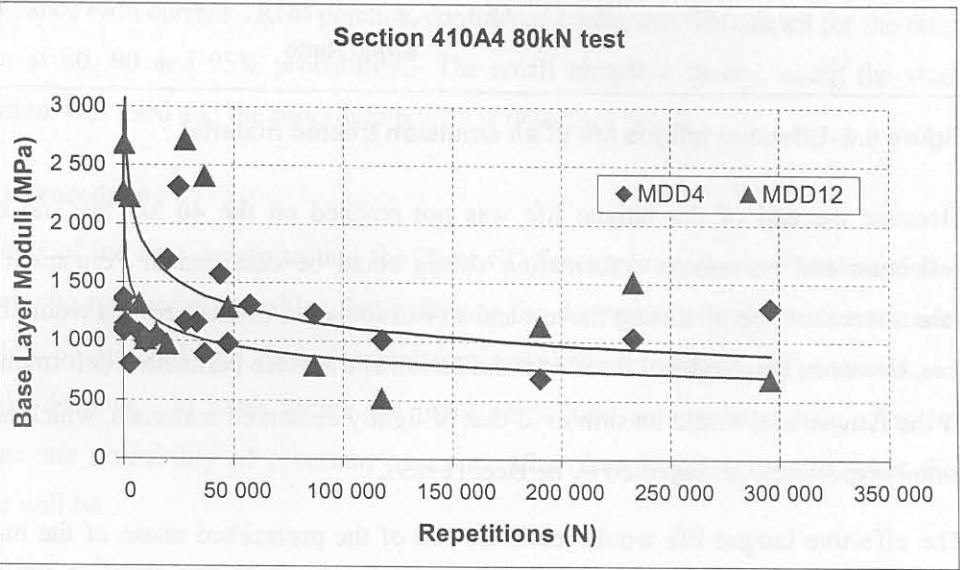
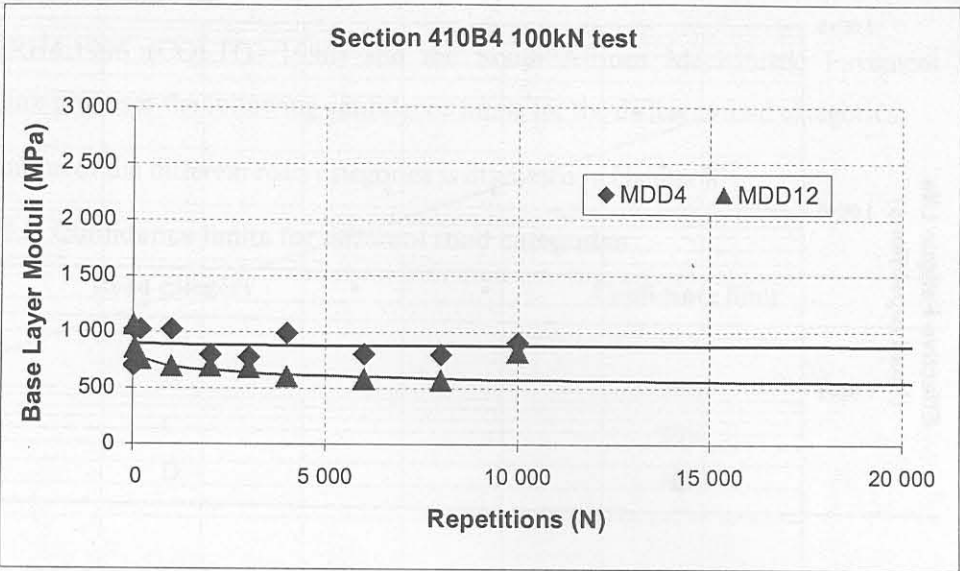


Figure 6.5 Reduction in stiffness with increase in load repetitions on HVS test sections

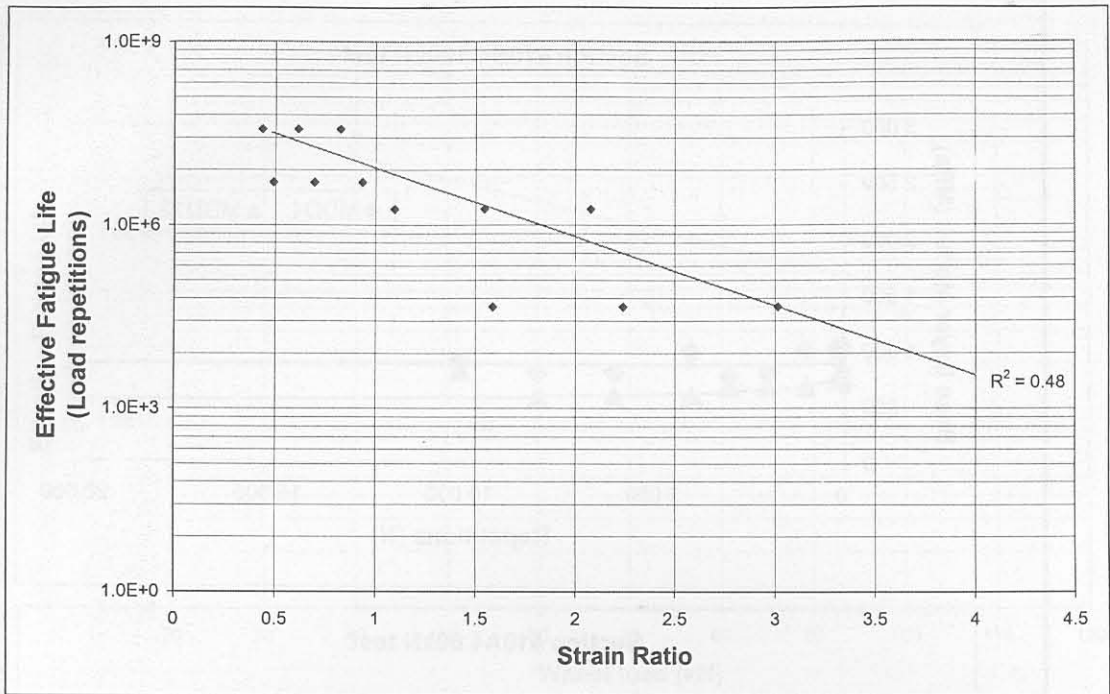


Figure 6.6 Effective fatigue life of an emulsion treated material

Because the end of the fatigue life was not reached on the 40 kN test, no actual elastic deflection and permanent deformation values could be determined. Permanent deformation values were very small during the test and an extrapolation of these results would be inaccurate. It is, however, believed that the elastic deflection and surface permanent deformation at the end of the fatigue life, would be similar to that of lightly cemented materials, which is 750 μm and 2 mm respectively, as reported by de Beer (1989).

The effective fatigue life would mark the end of the precracked phase of the material. After this point, the material will behave more like a granular material with a higher tendency towards permanent deformation.

An attempt was made to fit the data through the log-log function that describes the life to crack initiation of thick asphalt bases, given below.

$$\text{Log}N_f = A \left(1 - \frac{\text{Log}\varepsilon_t}{B} \right) \quad (6.3)$$

Where: N_f = Number of load repetitions to crack initiation

ε_t = Maximum horizontal tensile strain at the bottom of layer

A, B = regression constants

No good fit could be obtained, and the data best fit the linear-log function of Equation (6.2).

6.5 CONFIDENCE LIMITS

The TRH4:1996 (COLTO: 1996) and the South African Mechanistic Pavement Design Procedure proposes the following confidence limits for the different road categories.

A definition of the different road categories is discussed in chapter 8.

Table 6.3 Confidence limits for different road categories

Road category	Confidence limit
A	95%
B	90%
C	80%
D	50%

In accordance with current TRH4 practice, confidence limits were calculated for the fatigue life function at 80, 90 and 95% probability. The small sampling theory, using the student's t distribution, was used and the procedure briefly is described below.

6.5.1 Analysis Procedure

The scatter of the data points around the "best fit" function is to be expected, and indirectly represents the number of variables that influence the dependant variable under consideration. Variability of material and design parameters makes the prediction of a specific outcome extremely difficult. In cases where the input parameters are variable, it is often better to determine the probability of a certain outcome rather than to try to predict what the exact outcome will be.

By plotting a histogram of the number of sample points per distance interval from the regression function (error), the distribution of the dependant variable around the regression function is obtained. Confidence intervals of 95%, 90% and 80% can be defined using the table of the Student's t - distribution. In this manner, within specified limits of confidence, the population mean can be estimated. For example, if $t_{0,95}$ is the value of t for which 5% of the area lies in the upper "tail" of the t distribution, then the 95% upper confidence interval for t is:

$$\frac{\bar{X} - \mu}{s} \sqrt{N - 1} < t_{0,95} \quad (6.4)$$

where: \bar{X} = sample mean

μ = population mean

s = standard deviation

N = Sample size

From which we can see that μ is estimated to lie in the interval:

$$\mu < \bar{X} + t_{0.95} \frac{s}{\sqrt{N-1}} \quad (6.5)$$

with 95% confidence (i.e. probability of 0.95). It therefore means that there is a 95% confidence that the distance interval from the regression function, or “error”, will be lower than determined in Equation 6.5.

In general, we can represent the upper confidence limit for population means by:

$$\bar{X} + t_c \frac{s}{\sqrt{N-1}} \quad (6.6)$$

where the value t_c , called the *critical value* or *confidence coefficients*, depends on the level of confidence desired and the sample size. They can be read of the tables for the student’s t distribution.

The transfer function sample data consists of small samples seldom including repeat tests. It was therefor necessary to make the assumption that there was no “lack of fit” error in the regression functions for the transfer function data and that the variation of the dependant variable around the regression function was not influenced by the value of the independent variable. Under this assumption the confidence limits for the dependant variable will be equal distances from the regression function regardless of the value of the independent variable. A second function representing the confidence limit may therefor be drawn equal distances from the regression function. This is illustrated in Figure 6.7.

6.5.2 Transfer functions for fatigue life for different road categories

Applying the confidence intervals as described above, the transfer functions for fatigue life for the different road categories can be presented as follows:

$$\text{Category A: } N_{f_A} = 10^{7.9183 - 1.2775 \left(\frac{\epsilon_t}{\epsilon_b} \right)} \quad (6.7a)$$

$$\text{Category B: } N_{f_B} = 10^{8.0331 - 1.2775 \left(\frac{\epsilon_t}{\epsilon_b} \right)} \quad (6.7b)$$

$$\text{Category C: } N_{f_C} = 10^{8.1747 - 1.2775 \left(\frac{\epsilon_t}{\epsilon_b} \right)} \quad (6.7c)$$

$$\text{Category D: } N_{f_D} = 10^{8.5066 - 1.2775 \left(\frac{\epsilon_t}{\epsilon_b} \right)} \quad (6.7d)$$

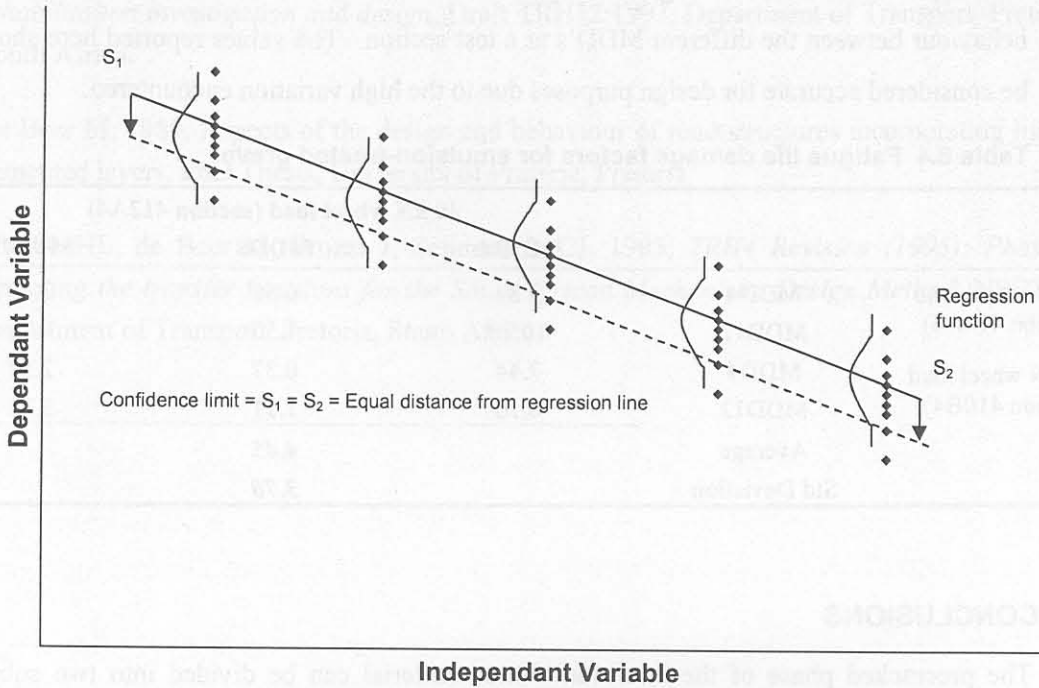


Figure 6.7 Confidence limits represented by a second function drawn parallel to the regression function

6.6 FATIGUE LIFE DAMAGE FACTOR

The HVS data can also be used to determine the load sensitivity and damage factors for a material. The damage factor, n , is used in Equation 6.8 to determine the damage caused by a particular wheel load relative to the damage caused by a standard wheel load.

$$\left(\frac{N_x}{N_{std}} \right) = \left(\frac{P_x}{P_{std}} \right)^n \quad (6.8)$$

where: N_x = load repetitions at wheel load

N_{std} = load repetitions at standard wheel load

P_x = wheel load

P_{std} = standard wheel load

n = damage factor

Damage factors were calculated by relating a certain defect under a 80 kN and 100 kN wheel load, to that under a 40 kN wheel load. The 40 kN HVS wheel load is equivalent to a 80 kN standard axle load. The damage factors calculated for fatigue life are presented in Table 6.3.

The high variation in the fatigue damage factor is the result of the difference in the fatigue behaviour between the different MDD's at a test section. The values reported here should not be considered accurate for design purposes due to the high variation encountered.

Table 6.4 Fatigue life damage factors for emulsion-treated gravel

		40 kN wheel load (section 412A4)		
		MDD4	MDD8	MDD12
80 kN wheel load (section 410A4)	MDD4	9.84	0.50	3.40
	MDD12	10.70	1.50	4.36
100 kN wheel load (section 410B4)	MDD4	7.44	0.37	2.57
	MDD12	8.16	1.11	3.31
Average			4.45	
Std Deviation			3.70	

6.7 CONCLUSIONS

The precracked phase of the emulsion treated material can be divided into two subphases, namely, the life to crack initiation and the effective fatigue life. The life to crack initiation is the phase before traffic induced cracking started in the layer and the layer is still intact with a relatively high stiffness. When microcracks start to develop at the bottom of the layer, these cracks will start to propagate through the layer. The material is then in a crack propagation phase. When the cracks have propagated through the layer, the stiffness of the layer is reduced to a value in the order of 500 MPa. The end of the effective fatigue life was defined to be when the layer reaches a stiffness of approximately 500 MPa. The layer will then behave similar to good quality granular material, although the layer is not physically in a granular state. Permanent deformation of the emulsion treated layer will then become the dominant failure mechanism. No definite value for the damage factor could be obtained and it is recommended that until further research develops more reliable values, a value of 4 should be used as normally used in pavement analysis (COLTO: 1996).

6.8 REFERENCES

ASTM, 1964, STP 91A: *Tentative guide for fatigue testing and the structural analysis of fatigue data*, 2nd edition, American Standard Test Methods, West Conshohocken, PA, Unites States.

Committee of Land Transportation Officials (COLTO), 1996, *Draft TRH4: Structural design of flexible pavements for interurban and rural roads*, Draft TRH4:1996, Department of Transport, Pretoria, South Africa.

Committee of Land Transportation Officials (COLTO), 1997, *Draft TRH12: Flexible pavement rehabilitation investigation and design*, Draft TRH12:1997, Department of Transport, Pretoria, South Africa.

De Beer M, 1989, Aspects of the design and behaviour of road structures incorporating lightly cemented layers, PhD Thesis, University of Pretoria, Pretoria.

Theyse HL, de Beer M, Prozzi J, Semmelink CJ, 1995, *TRH4 Revision (1995): Phase I: Updating the transfer functions for the South African Mechanistic Design Method*, NSC24/1, Department of Transport, Pretoria, South Africa.

The permanent deformation models developed from the laboratory study and the Heavy Vehicle Simulator, are presented in this chapter and a recommendation is made on the use of a permanent deformation model in the mechanistic analysis of emulsion treated materials.

7.2 FACTORS INFLUENCING THE DEVELOPMENT OF PERMANENT DEFORMATION UNDER REPETITIVE LOADING

A number of factors are important and influence the development of permanent deformation under repetitive loading. These factors are well researched and not described in detail, but they are described. Most researchers (Marsar, 1975; Benzenberg, 1971; Frost, 1972) agreed that the following factors are important when defining the permanent deformation behaviour of an unbound granular material:

- degree of saturation of the material at the time when the load is applied
- the density to which the material was compacted
- the magnitude of the applied load, which influences the stress state in the material,
- the grading of the material, and
- the load history of the material.

7.3 PERMANENT DEFORMATION MODEL FROM HEAVY VEHICLE SIMULATOR DATA

The regression model fitted through the Heavy Vehicle Simulator data in chapter 5 (section 5.7.1) was used to develop a model for permanent deformation. The model is similar to the laboratory model from section 5.6 in Equation 5.14, but is expressed in terms of wheel load or contact stress ratio. The model is presented in Figure 7.1.

CHAPTER 7 PERMANENT DEFORMATION PROPERTIES OF EMULSION TREATED MATERIALS

7.1 INTRODUCTION

The development of permanent deformation in emulsion treated materials with cement is assumed to be similar to that of granular materials. The same principles therefore apply for emulsion treated materials as for granular unbound materials in terms of permanent deformation. The development of a permanent deformation model in this study is based on the linear elastic theory.

The permanent deformation models developed from the laboratory study and the Heavy Vehicle Simulator, are presented in this chapter and a recommendation is made on the use of a permanent deformation model in the mechanistic analysis of emulsion treated materials.

7.2 FACTORS INFLUENCING THE DEVELOPMENT OF PERMANENT DEFORMATION UNDER REPETITIVE LOADING

A number of factors are important and influences the development of permanent deformation under repeated loading. These factors are well researched and the mechanism behind them fully described. Most researchers (Maree: 1978, Barenberg: 1971, Wolff 1992) reported that the following factors are important when defining the permanent deformation behaviour of an unbound granular material:

- degree of saturation of the material at the time when the load are applied
- the density to which the material was compacted,
- the magnitude of the applied load, which influences the stress state in the material,
- the grading of the material, and
- the load history of the material.

7.3 PERMANENT DEFORMATION MODEL FROM HEAVY VEHICLE SIMULATOR DATA

The regression model fitted through the Heavy Vehicle Simulator data in chapter 5 (section 5.7.1) was used to develop a model for permanent deformation. The model is similar to the laboratory model from section 5.6 in Equation 5.14, but is expressed in terms of wheel load and not stress ratio. The model is presented in Figure 7.1.

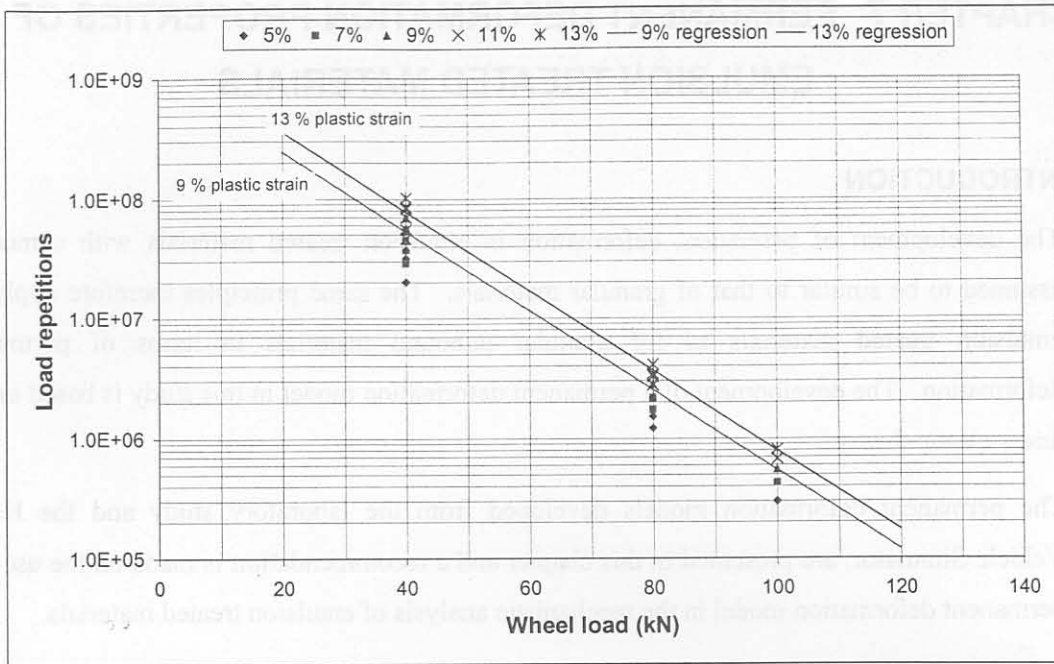


Figure 7.1 HVS permanent deformation model

The model presented in Figure 7.1 is only applicable to the pavement structure and conditions of the HVS site and is in terms of wheel load and not an engineering parameter (e.g. stress ratio).

7.4 MECHANISTIC ANALYSIS OF HEAVY VEHICLE SIMULATOR PAVEMENT FOR PERMANENT DEFORMATION

In order to use the results from this research in different pavement structures and load conditions, it is necessary to have a generic function in terms of an engineering parameter that can be easily calculated. In the current South African Mechanistic Pavement Design Method, pavement structures are modelled using the multi-layer linear elastic theory. This theory cannot directly predict the behaviour of unbound materials and the permanent deformation response of these materials. It also can not accommodate the non-linear behaviour of unbound materials. More appropriate advanced models have not yet been calibrated and are complex to use. These complex models are difficult to use and are not widely used in pavement engineering yet. To fit in with the current South African Mechanistic Pavement Design Method, the structural design models for permanent deformation of emulsion treated materials are also based on the multi-layer linear elastic theory.

The engineering parameter used in the permanent deformation models for emulsion treated materials is the Stress Ratio as described by Theyse (1999).

The stress ratio is a function of the principal stresses and the shear stress parameters and is the Inverse of the Factor of Safety as defined by Maree (1978). Theoretically, a stress ratio in

excess of 1 will lead to failure although such a stress condition cannot exist in practice. It is however possible that the Stress Ratio can exceed 1.0 if the time of loading is very short. In such a case the stresses in a soil mass cannot be redistributed timeously and the maximum shear strength may be exceeded for a fraction of time.

7.4.1 Stress ratio

The calculation of the stress ratio is given in Equation 5.10, and is repeated below:

$$SR = \frac{\sigma_1^a - \sigma_3}{\sigma_1^m - \sigma_3} = \frac{\sigma_1^a - \sigma_3}{\sigma_3 \left[\tan^2 \left(45^\circ + \frac{\phi}{2} \right) - 1 \right] + 2.c. \tan \left[45^\circ + \frac{\phi}{2} \right]} \quad (7.1)$$

where: SR = Stress ratio

σ_3 = minor principal stress or confining pressure

c = cohesion

ϕ = internal angle of friction

σ_1^a = working or applied major principal stress

σ_1^m = maximum allowable major principal stress for given ϕ , c , and σ_3

One of the major shortcomings of the linear elastic theory is that tensile stresses are allowed in the material. For asphalt and cemented materials it may be applicable, but unbound materials are not able to withstand tensile stresses. This is illustrated in the beam in Figure 7.2 below.

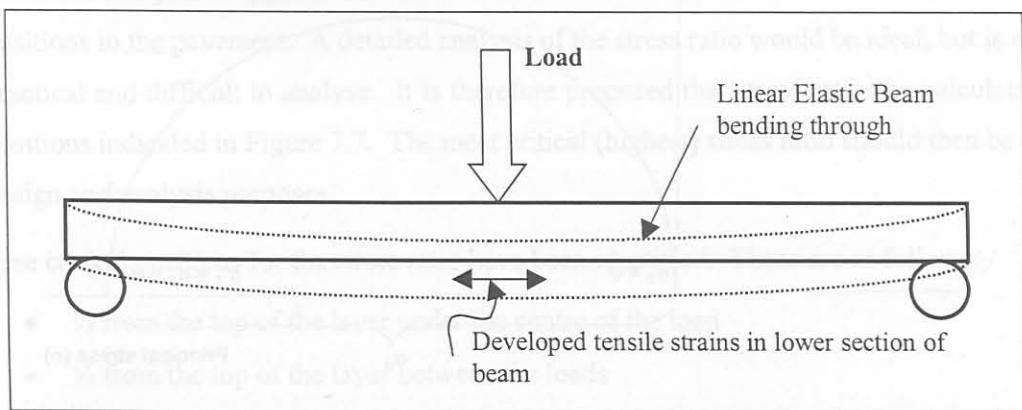


Figure 7.2 Illustration of tensile strains and stresses developed in the linear elastic theory

From the Figure above, the development of tensile strains at the bottom of the beam are indicated clearly. Since $\sigma = \epsilon.E$, where E is the modulus of elasticity, the stress (σ) will be negative if strain (ϵ) is negative (E is always positive). In practice, granular materials will

“redistribute” the stresses so that the tensile stresses at the bottom are eliminated. Models to effectively model this behaviour are not widely in use.

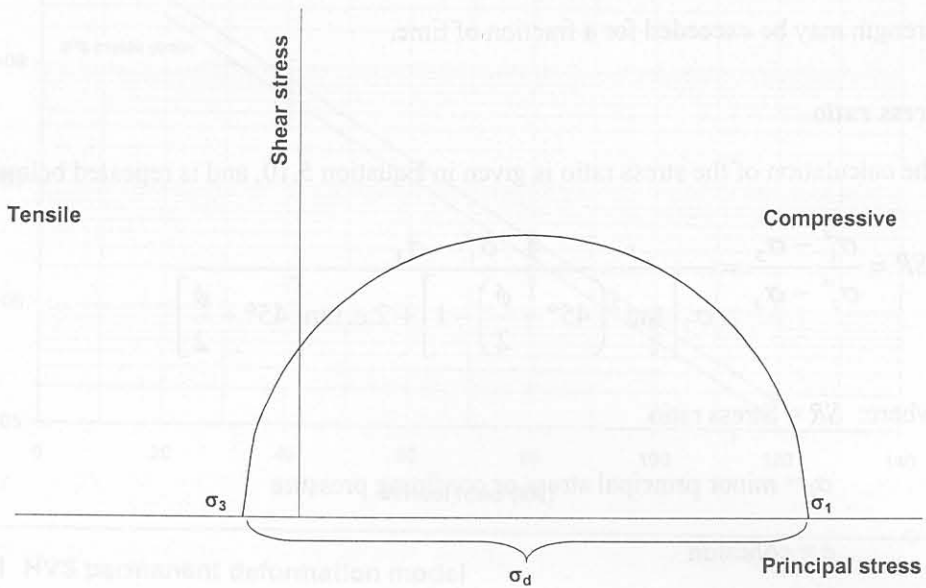


Figure 7.3 Mohr circle with tensile minor principal stress

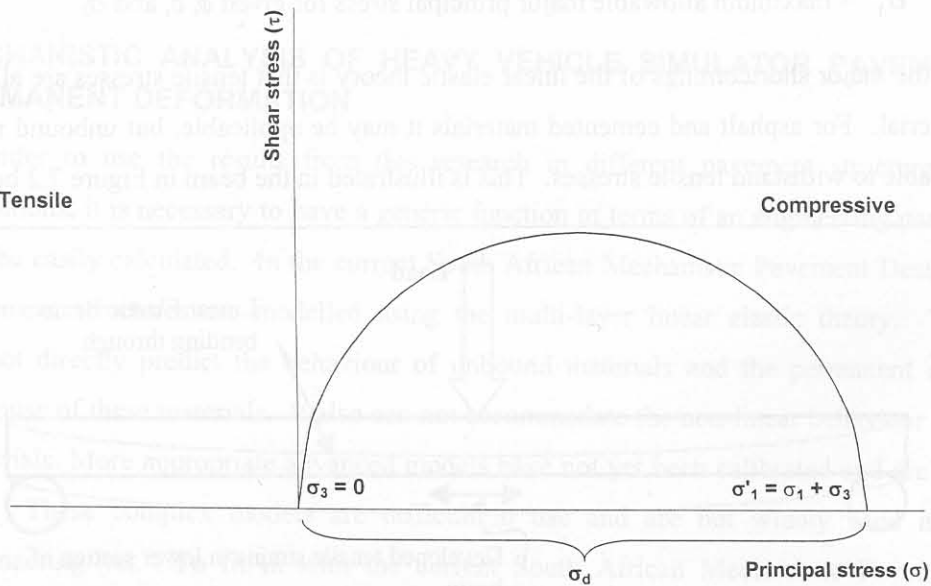


Figure 7.4 Adjusted Mohr circle with minor principal stress equals to zero

The current practice in the South African Mechanistic Pavement Design Method, is to “shift” the Mohr circle that the minor principal stress (σ_3) became zero, and increase the major principal stress (σ_1) by the same magnitude. The radius of the Mohr circle remains the same, which means that the deviator stress (σ_d) remains the same.

This adjustment gives a more reasonable result and is a better approximation of the stress state in an unbound pavement layer. It is recommended that the same practice be followed in the analysis of emulsion treated materials.

Critical positions of the Stress Ratio

The current practice in the South African Mechanistic Pavement Design Method is to calculate the critical parameter in the centre of the layer, either under the load or between the loads, in the case of a dual wheel load. Figure 7.5 shows a contour plot of stress ratio for the HVS pavement under a 40 kN, 620 kPa dual wheel load. The contour plots were determined using a linear elastic software program by calculating the stresses and strains at a grid in the layer under consideration. Areas with the same stress or strain were connected to form a contour of stresses or strains.

Unbound materials fail when the shear strength of the materials is exceeded. An analysis of the deviator stress and octahedral shear stress indicated that the critical shear stresses are in the upper quarter of the layer underneath the load (Figure 7.6). The octahedral shear stress is a stress invariant that provides an indication of the total shear distortion applied by any given stress state. The risk of the shear strength being exceeded is critical at these points. The analysis shows that the stress ratio at the centre of the layer is actually the lowest and not the critical location (Figure 7.5). The critical stress ratio is in most cases in the upper quarter of the layer between the centre of the load and the edge of the load. The position of the critical stress ratio varies as the composition of pavement structures varies.

From the analysis it appears that the critical stress ratio varies between a number of definite positions in the pavement. A detailed analysis of the stress ratio would be ideal, but is not often practical and difficult to analyse. It is therefore proposed that stress ratios be calculated at the positions indicated in Figure 7.7. The most critical (highest) stress ratio should then be used for design and analysis purposes.

Five critical positions for the stress ratio have been identified. These are as follows:

- $\frac{1}{4}$ from the top of the layer under the centre of the load
- $\frac{1}{4}$ from the top of the layer between the loads
- $\frac{1}{4}$ from the top of the layer at the outer edge of the load
- $\frac{1}{4}$ from the bottom of the layer under the centre of the load
- $\frac{1}{4}$ from the bottom of the layer between the loads

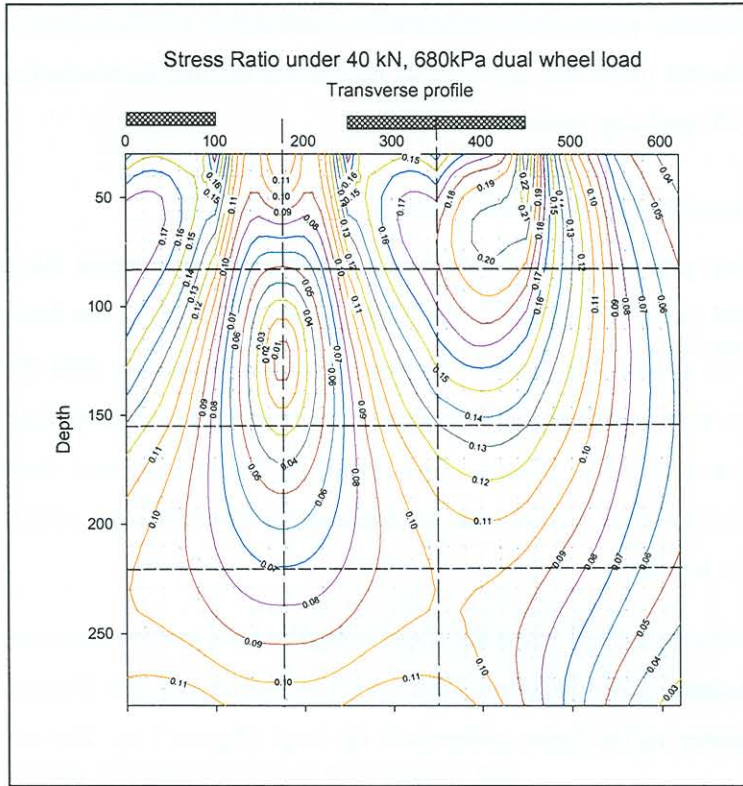


Figure 7.5 Contour plot of the stress ratio on the HVS pavement under 40 kN, 620 kPa dual wheel load.

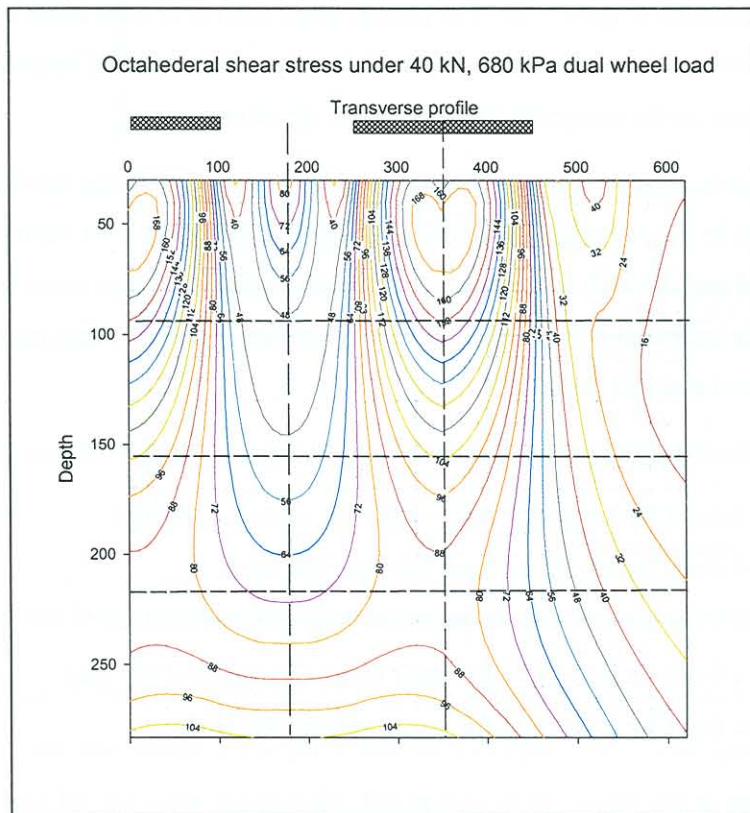


Figure 7.6 Contour plot of octahedral shear stress under a 40 kN, 620 kPa dual wheel load in a 250 mm thick emulsion treated layer.

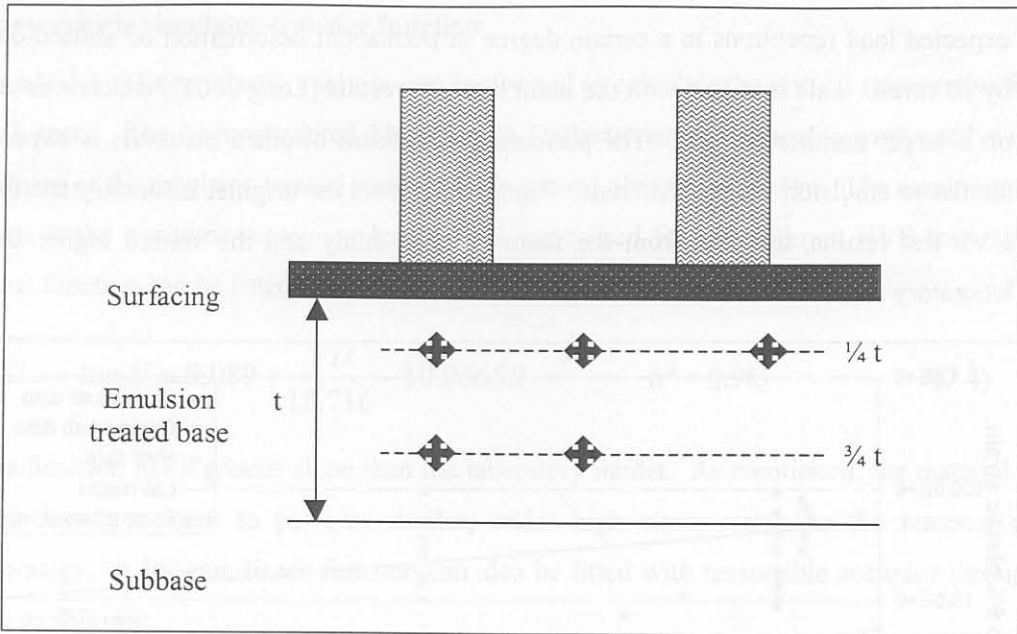


Figure 7.7 Recommended positions to calculate the critical Stress Ratio

7.5 PERMANENT DEFORMATION TRANSFER FUNCTION

7.5.1 Laboratory transfer function

The laboratory transfer function was developed from different saturation, relative densities and stress ratios. The function was developed from the dynamic triaxial test results described in chapter 5. At low stress ratios the results were similar to that of the Heavy Vehicle Simulator, but at high stress ratios the laboratory model gives more repetitions to a certain level of plastic strain than measured under the HVS. The dynamic triaxial test, tests only one layer with ideal confinement and support conditions. It is assumed that these factors played a role at high stress ratios. The function in Equation 7.2 could be fitted through the laboratory data in terms of stress ratio. The degree of saturation and relative density did not provide a significant influence on the permanent deformation to be included in the equation.

$$\log N = 7.4266 + \frac{PD}{25.2465} - \frac{SR}{1.2415} \quad (r^2 = 0.51) \quad (7.2)$$

where: N = Number of repetitions to certain degree of permanent deformation

PD = degree of permanent deformation (%)

SR = Stress ratio calculated according to equation (7.1)

At high stress ratios, the number of repetitions to a certain degree of permanent deformation, is approximately 20 times higher than expected for the Heavy Vehicle Simulator data. This coincides with the observations, described by Long (2002), during the testing of the adjacent foam bitumen section. It was therefore proposed that at higher stress ratios (0.55 and 0.9) the

expected load repetitions to a certain degree of permanent deformation be shifted downwards by 20 times. This is in line with the foam bitumen results (Long 2002), which was undertaken on a larger number of tests. The performance of foam bitumen materials is expected to be similar to emulsion treated materials. Figure 7.8 shows the original laboratory test results, the HVS test results, the data from the foam bitumen study and the shifted higher stress ratio laboratory results.

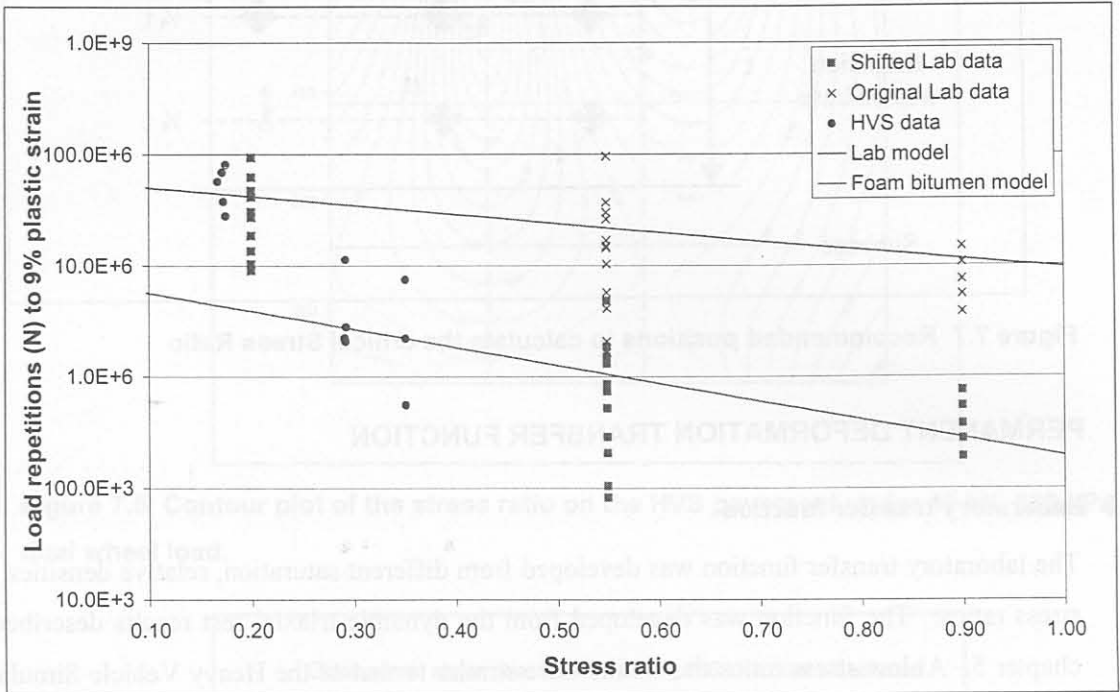


Figure 7.8 Comparison between laboratory test results, HVS test results and foam bitumen study.

The number of load repetitions to a certain degree of permanent deformation can also be plotted against the bulk stress. This indicates that there is a decrease in the number of load repetitions to permanent deformation with an increase in bulk stress. This approach does not allow the material properties to be taken into account, and only considers the stress condition. From the complexity of the equation it is difficult to write it in terms of load repetitions and this should be solved by iterations.

$$\Theta = 4780.935 * \left(1 - e^{-\frac{181.534}{N^{0.379701}}} \right) \quad (7.3)$$

Where: Θ = bulk stress ($\Theta = \sigma_1 + \sigma_2 + \sigma_3$)

N = Load repetitions to 9 % plastic strain

This equation is similar to the one proposed by Wolff (1992) for the elasto-plastic analyses of granular material.

7.5.2 Heavy vehicle simulator transfer function

A multi layer linear elastic analysis was performed to calculate the critical stress ratios for the HVS tests. The backcalculated Multi Depth Deflectometers stiffnesses were used with the stiffness of the emulsion treated material in its second phase as 500 MPa. The maximum stress ratios at the positions recommended in 7.5.1 were used for the different HVS tests. A log-linear function can be fitted through the data as follows:

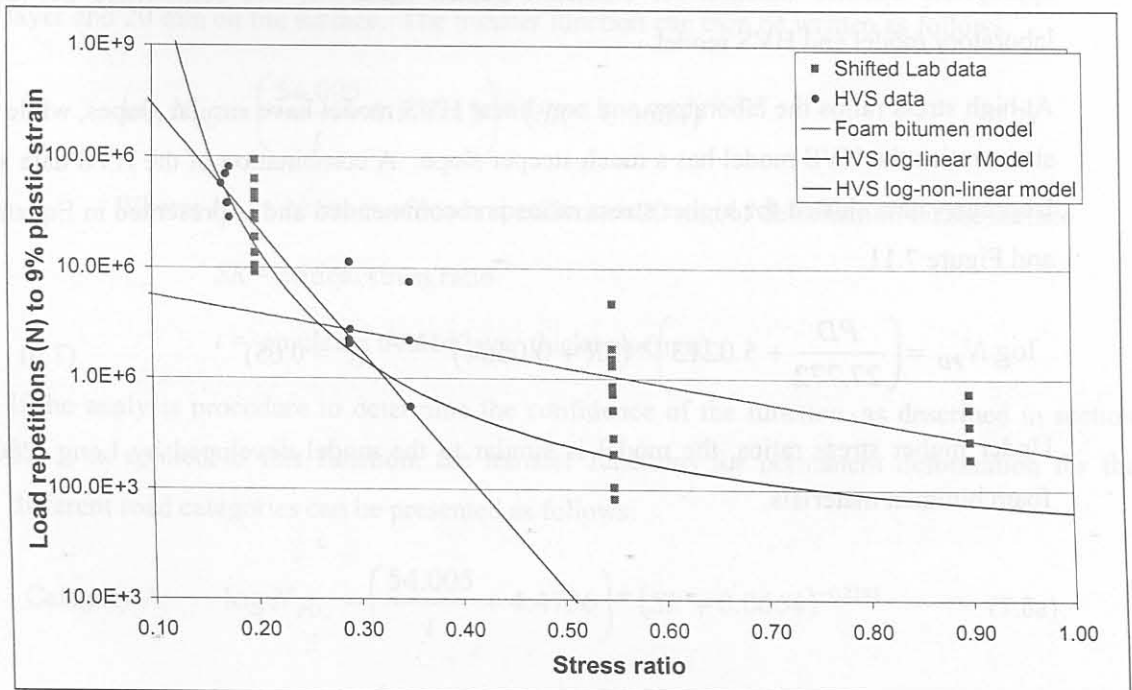
$$\log N = 9.089 + \frac{PD}{18.716} - 10.966SR \quad (r^2 = 0.98) \quad (7.4)$$

This function has a greater slope than the laboratory model. As mentioned, the material in the field does not seem to perform similar, under high stress ratios, to the material in the laboratory. A log-non-linear function can also be fitted with reasonable accuracy through the data as follows:

$$\log N = 3.725 + \frac{PD}{18.486} + \frac{0.598767}{SR} \quad (r^2 = 0.39) \quad (7.5)$$

This function gives very high load repetitions at low stress ratios and is not expected to be very accurate at low stress ratios. At high stress ratios, the function converges to the same slope as that of the laboratory and foam bitumen function.

These two functions are illustrated in Figures 7.9 and 7.10.



Function 7.9 HVS transfer functions compared to foam bitumen model.

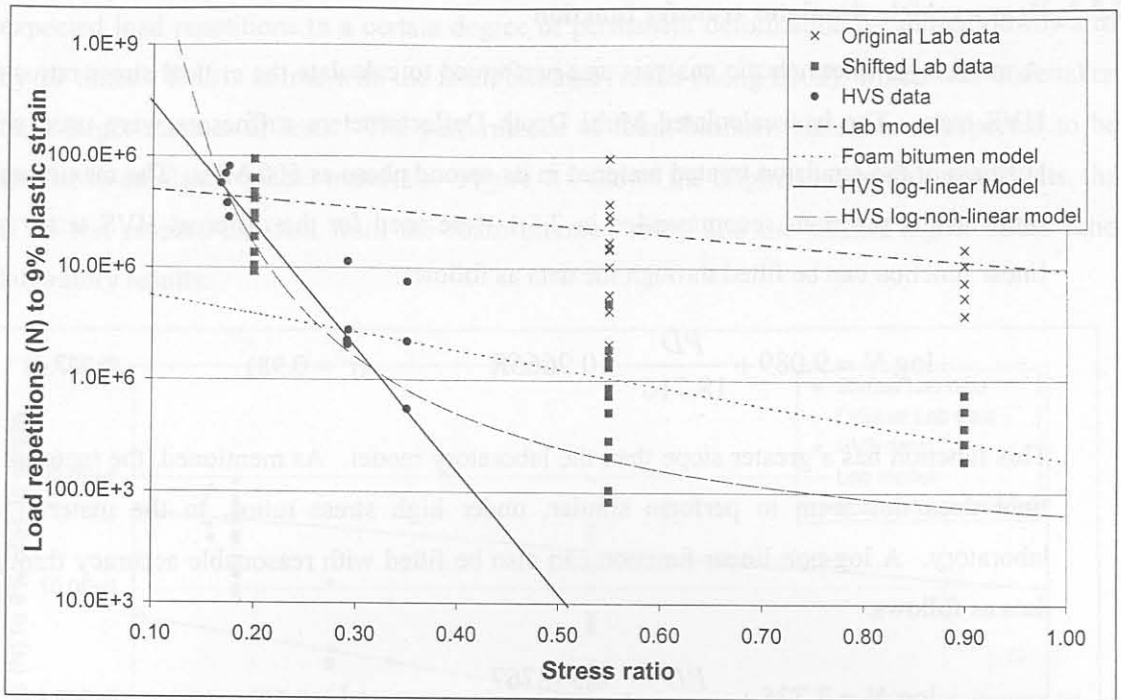


Figure 7.10 HVS transfer functions compared to original laboratory data, shifted laboratory data and foam bitumen model.

7.5.3 Permanent deformation transfer function

From the analysis of the laboratory test results and the HVS test results, it is assumed that the appropriate transfer function for emulsion treated materials, lies somewhere between the laboratory model and HVS model.

At high stress ratios the laboratory and non-linear HVS model have similar slopes, while at low stress ratios the HVS model has a much steeper slope. A combination of the HVS data and the laboratory data shifted for higher stress ratios is recommended and is presented in Equation 7.6 and Figure 7.11.

$$\log N_{PD} = \left(\frac{PD}{27.772} + 5.0213 \right) * (SR + 0.0664)^{-0.2313} \quad (r^2 = 0.65) \quad (7.6)$$

Under higher stress ratios, the model is similar to the model developed by Long (2001) for foam bitumen materials.

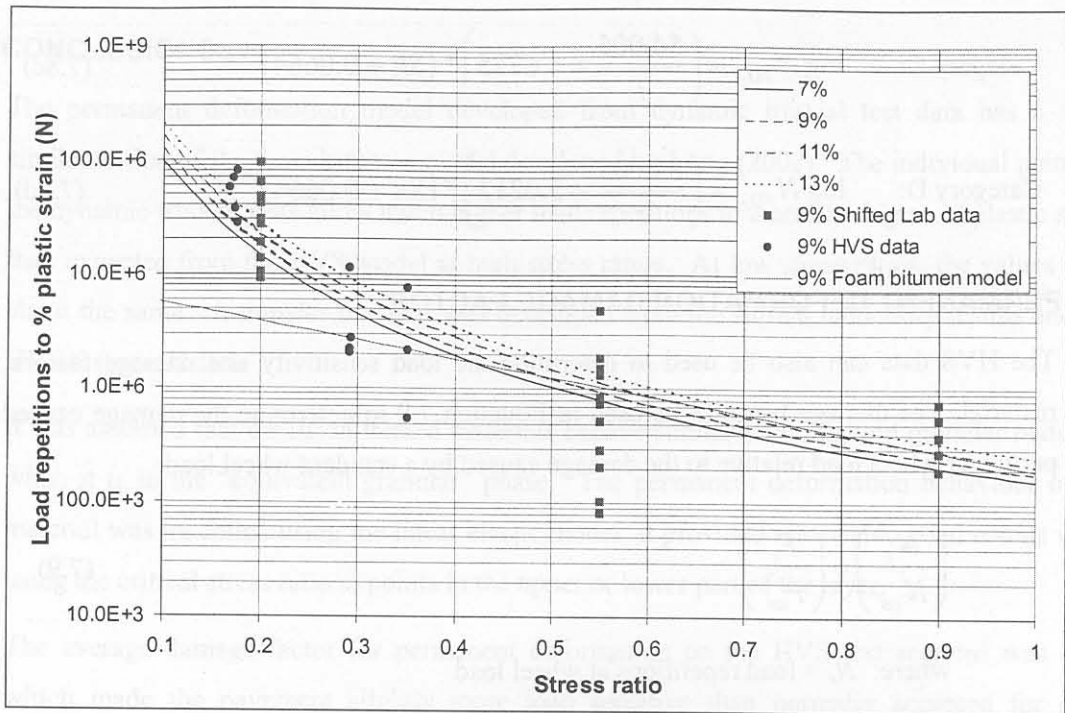


Figure 7.11 Transfer function for permanent deformation of emulsion treated materials

The TRH4 and the South African Mechanistic Pavement Design Method define the end of pavement life when the pavement reaches 20 mm of deformation or rutting on the surface. From the HVS test results discussed in Chapter 5, approximately 75 % of the total deformation of the pavement occurs within the base layer. This will allow 15 mm of deformation in a base layer and 20 mm on the surface. The transfer function can then be written as follows:

$$\log N_{PD} = \left(\frac{54.005}{t} + 5.0213 \right) * (SR + 0.0664)^{-0.2313} \quad (7.7)$$

Where: N_{PD} = Number of load repetitions to 20 mm of deformation on the surface

SR = critical stress ratio

t = emulsion treated layer thickness (mm)

If the analysis procedure to determine the confidence of the function, as described in section 6.5.1, is applied to this function, the transfer functions for permanent deformation for the different road categories can be presented as follows:

$$\text{Category A: } \log N_{PD_A} = \left(\frac{54.005}{t} + 4.4736 \right) * (SR + 0.0664)^{-0.2313} \quad (7.8a)$$

$$\text{Category B: } \log N_{PD_B} = \left(\frac{54.005}{t} + 4.5389 \right) * (SR + 0.0664)^{-0.2313} \quad (7.8b)$$

$$\text{Category C: } \log N_{PD_C} = \left(\frac{54.005}{t} + 4.6775 \right) * (SR + 0.0664)^{-0.2313} \quad (7.8c)$$

$$\text{Category D: } \log N_{PD_D} = \left(\frac{54.005}{t} + 5.0213 \right) * (SR + 0.0664)^{-0.2313} \quad (7.8d)$$

7.6 PERMANENT DEFORMATION DAMAGE FACTOR

The HVS data can also be used to determine the load sensitivity and damage factors for a material. The damage factor, n , is used in Equation 7.9 to determine the damage caused by a particular wheel load relative to the damage caused by a standard wheel load.

$$\left(\frac{N_x}{N_{std}} \right) = \left(\frac{P_x}{P_{std}} \right)^n \quad (7.9)$$

where: N_x = load repetitions at wheel load

N_{std} = load repetitions at standard wheel load

P_x = wheel load

P_{std} = standard wheel load

n = damage factor

Damage factors were calculated by relating a certain defect under a 80 kN and 100 kN wheel load to that defect under a 40 kN wheel load. The 40 kN HVS wheel load is equivalent to a 80 kN standard axle load. The damage factors calculated for permanent deformation are presented in Table 7.1.

The value published in this study was obtained from limited testing and could only be used as an interim guideline, until further research develops more definitive values.

Table 7.1 Permanent deformation life damage factors for emulsion-treated gravel

		40 kN wheel load (section 412A4)		
		MDD4	MDD8	MDD12
80 kN wheel load (section 410A4)	MDD4	5.77	4.89	5.50
	MDD12	5.58	4.70	5.31
100 kN wheel load (section 410B4)	MDD4	5.07	4.40	4.86
	MDD12	4.22	3.55	4.02
Average			4.82	
Std deviation			0.68	

7.7 CONCLUSIONS

The permanent deformation model developed from dynamic triaxial test data has a slope similar to that of the foam bitumen model developed by Long (2002). The individual points of the dynamic triaxial tests allow much higher load repetitions to a certain degree of plastic strain than expected from the HVS model at high stress ratios. At low stress ratios, the values were about the same. A transfer function was developed from the shifted laboratory results and the HVS test result data.

It was assumed that emulsion treated materials behave similarly to unbound granular materials when it is in the “equivalent granular” phase. The permanent deformation behaviour of the material was modelled using the linear elastic model. It provided reasonable good results when using the critical stress ratio at points in the upper or lower part of the layer.

The average damage factor for permanent deformation on the HVS test sections was 4.87, which made the pavement slightly more load sensitive than normally accepted for other pavement materials.

7.8 REFERENCES

- Barenberg EJ, (1971) *Behaviour and performance of aggregate-soil systems under repetitive loads*, Research Report PB 204 269, Department of Civil Engineering, University of Illinois, Urbana, Illinois, United States.
- Long FM, 2002, The development of *structural design models for foamed bitumen treated pavement layers*, Contract Report CR-2001/76, CSIR Transportek, Pretoria, South Africa.
- Maree JH, 1978, *Ontwerpparameters vir Klipslag in plaveisels*, MEng dissertation, University of Pretoria, Pretoria, South Africa.
- Maree JH, 1982, *Aspekte van die ontwerp en gedrag van padplaveisels met korrelmateriaalkroonlae*, PhD thesis, University of Pretoria, Pretoria, South Africa.
- Wolff H, 1992, *Elasto-plastic behaviour of granular pavement layers in South Africa*, PhD thesis, University of Pretoria, Pretoria, South Africa.

CHAPTER 8 THE STRUCTURAL DESIGN OF EMULSION TREATED MATERIALS

8.1 INTRODUCTION

The structural design of pavements is aimed at the protection of the subgrade by the provision of pavement layers in order to achieve a chosen level of service over a predetermined period. It considers factors of time, traffic loading, pavement materials, subgrade conditions, environmental details and economics. The main purpose of structural design is to obtain an objective rational estimate of the capacity of the pavement, with a certain level of confidence, to provide an acceptable service level without major structural distresses.

The TRH4:1996 (COLTO: 1996), South African Mechanistic Pavement Design Method, the Asphalt Institute method and the AASHTO design method are all methods that provide guidelines on the structural design of pavements. In South Africa the TRH4 and the South African Mechanistic Pavement Design Method are widely used in the design of new and rehabilitated pavements.

The models developed in this study will provide interim guidelines for the design of emulsion treated materials as pavement layers, using the principles of the TRH4 and the South African Mechanistic Pavement Design Method.

The TRH4 categorises roads into four categories. Category A roads are major interurban roads or interurban freeways that require a high level of service and reliability. Category B roads are interurban collectors, major rural roads and major industrial roads. These roads also require a high level of service and reliability. Category C roads are lightly trafficked rural and strategic roads, which have less traffic loading and require a lower level of service and reliability. Category D roads are light pavement structures, typically for rural access roads. These roads have a low traffic loading and require a low level of service. The four categories are summarised in Table 8.1.

Table 8.1 Definition of main road categories used in pavement design (COLTO: 1996, Jordaan: 1994)

ROAD CATEGORY				
	A	B	C	D
Description	Major interurban freeways and roads	Interurban collectors and major rural roads	Lifghtly trafficked rural roads, strategic roads	Light pavement structures, rural access roads
Importance:	Very important	Important	Less Important	Less important
Service Level:	Very high	High	Moderate	Moderate to low
TYPICAL PAVEMENT CHARACTERISTICS				
	RISK			
	Very Low	Low	Medium	High
Approximate design reliability	95	90	80	50
Equivalent traffic loading (E80/lane)	3 – 100 million over 20 years	0.3 – 10 million depending on design strategy	< 3 million depending on design strategy	< 1 million depending on design strategy
Typical pavement class	ES3 to ES100	ES1 to ES10	ES0.1 to ES3	ES0.1 to ES1
Daily traffic (e.v.u)	> 4 000	600 – 10 000	< 600	< 500
Construction riding quality: IRI (mm/m)	2.4 – 1.6	2.9 – 1.6	3.5 – 2.4	4.2 – 2.4
Terminal riding quality: IRI (mm/m)	3.5	4.2	4.5	5.1
Warning rut level (mm)	10	10	10	10
Terminal rut level (mm)	20	20	20	20
Area of road exceeding terminal condition (%)	5	10	20	50

Design traffic classes are divided into 7 groups depending on the number of standard 80 kN axles in the analysis period. A summary of the traffic classes is presented in Table 8.2.

Table 8.2 Traffic classes according to TRH4:1996

Traffic Class	Traffic loading range (E80's)
ES0.1	< 100 000
ES0.3	100 000 to 300 000
ES1	300 000 to 1 million
ES3	1 million to 3 million
ES10	3 million to 10 million
ES30	10 million to 30 million
ES100	30 million – 100 million

8.2 GENERAL PAVEMENT BEHAVIOUR

Pavement behaviour is a function of the initial construction composition of the pavement, the load carried by the pavement and the environment in which it operates. In addition to the as-built strength, pavement behaviour is also influenced by the behaviour of the materials in the various pavement layers. The type and behaviour of the material in the base layer of the pavement is of particular importance because it is close to the surface and distress in the base often reflects through to the surface of the road. It also has little protection in terms of material covering the layer and a relatively high quality and load-bearing strength is usually required from a base layer. The state of the materials in the pavement layers changes with time. The behaviour of pavements with different base layers differs slightly, but with a similar trend. The general behaviour is presented in Figure 8.2.

A detailed discussion of the behaviour of all the pavement materials can be found in the work of Jordaan (1994).

In general, a newly constructed pavement will have an initial phase where some densification will occur in the wheel tracks. This might not be the case with cemented and asphalt base pavements. Following this phase, the pavement will enter a stable phase during which little deformation or other distress occurs. The rate of increase in deformation, or other distresses, during this phase depends on the initial quality of the material. After the stable phase, the pavement will enter a phase where distresses and permanent deformation occur at an increasing rate. This may cause an increase in moisture content from water entering through cracks and without maintenance will result in failure of the layer.

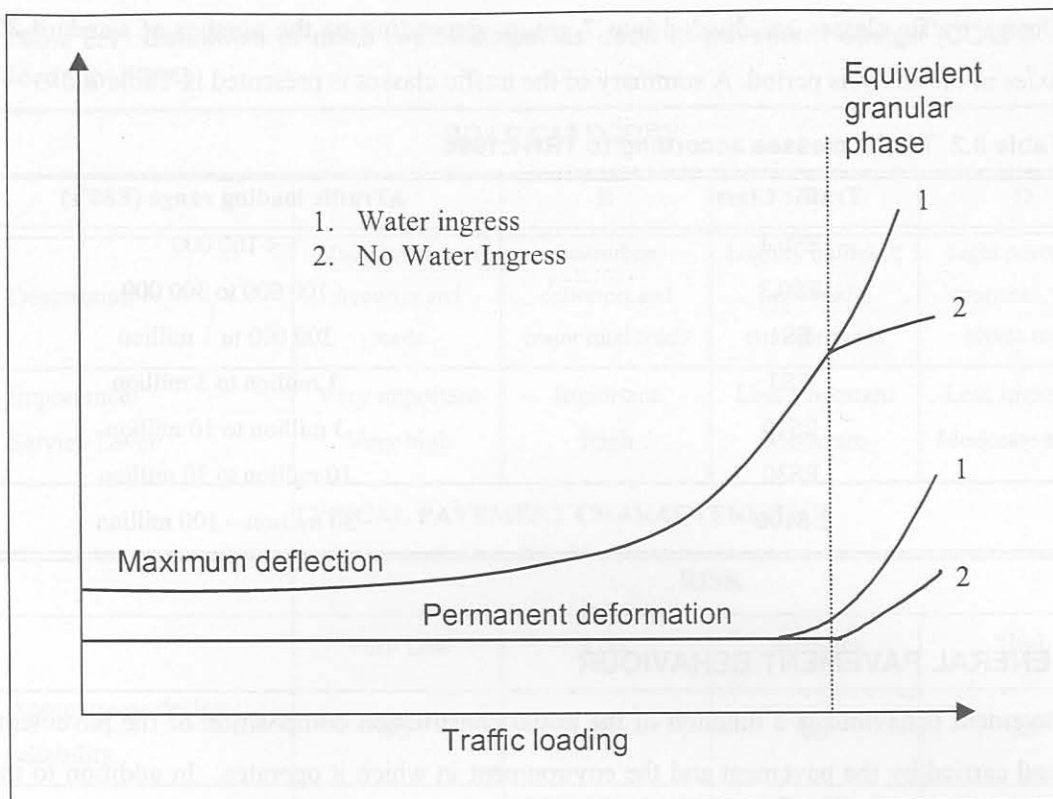


Figure 8.1 General behaviour of pavements (Freeme: 1983)

8.3 BEHAVIOUR OF EMULSION TREATED MATERIALS

The general behaviour of emulsion treated materials is similar to that of lightly cemented materials in the sense that emulsion treated materials also have a phased behaviour. As discussed in previous chapters, the first phase is a fatigue life phase similar to cemented materials, while the second phase is an “equivalent granular” phase, similar to granular unbound materials. The cement content of the emulsion treated material will determine the degree of resemblance to lightly cemented material. Higher cement contents will have behaviour similar to lightly cemented materials, while low cement contents will have either a high fatigue resistance or behaviour similar to granular material, depending on the net bitumen content.

In essence, the behaviour of emulsion treated material is a two-phase behaviour. The first phase being the fatigue life phase, which is characterised by a high resistance to permanent deformation and high elastic modulus. The second phase is known as the “equivalent” granular phase where the material behaves similarly to granular materials although it may still be physically intact. These different behaviour phases were discussed in detail in chapters 6 and 7.

8.4 MATERIAL CLASSIFICATION

In SABITA manual 21 (SABITA: 1999) emulsion treated materials are divided into two classes namely E1 and E2. This classification is based mainly on the material mix design. An E1 material would typically consist of parent materials of G1 to G3 or CTB quality materials with a residual bitumen content of less than 1 to 1.5 %. E2 type materials would typically consists of parent materials of G4 to G5 quality material with residual bitumen content of less than 1.8 %.

A new classification system for emulsion treated materials is proposed to take into account the influence of cement in the mix. Emulsion treated materials can be constructed with high or low cement content and with high or low net bitumen content. These variations have an effect on the strength and flexibility of the material. A classification system compatible with that of foam bitumen (Asphalt Academy: 2002) is proposed. Figure 8.2 gives an illustration of the four different combinations of emulsion treated materials.

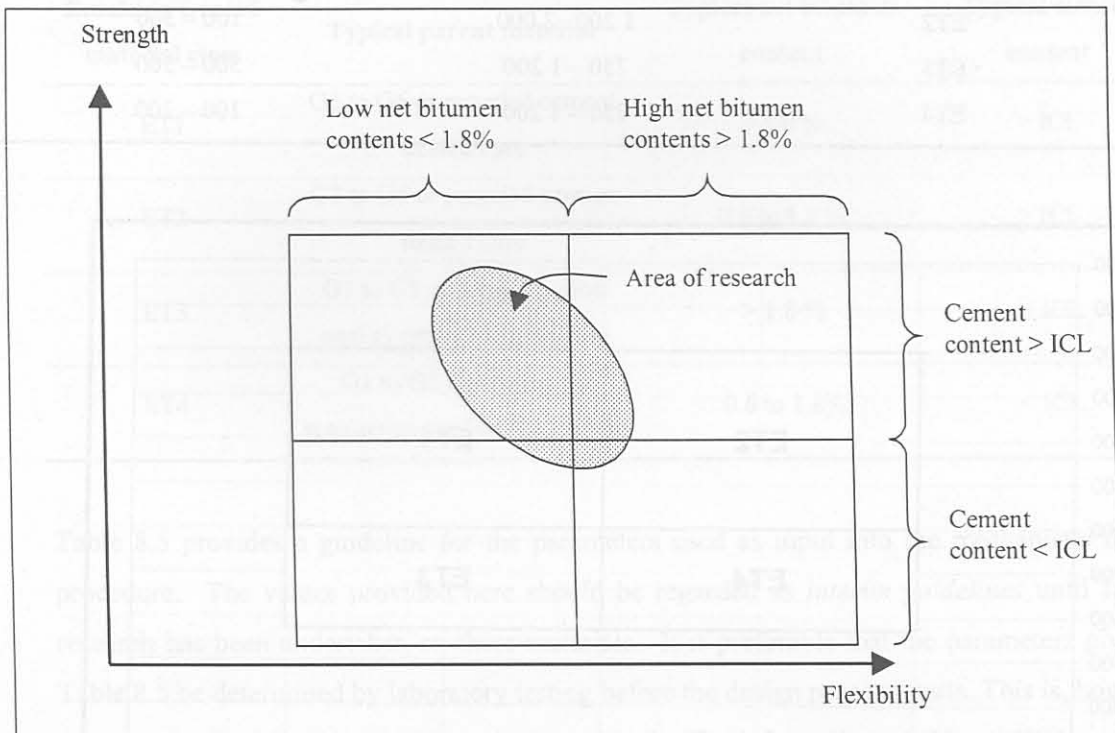


Figure 8.2 Illustration of different types of emulsion treated materials for structural design

The minimum Unconfined Compressive Strength (UCS) limits were set according to SABITA manual 21 (SABITA: 1999). The maximum UCS limits were selected by assuming that an emulsion treated material would not have maximum UCS values similar to that of a C4 lightly cemented material. The maximum value required for a C4 was then reduced by 1 000 kPa to obtain the maximum limit for emulsion treated materials. The above values were generated as

little research is available on desirable maximum allowable UCS for emulsion treated materials. A maximum limit is important to ensure that the layer is not built to such strength that the benefit of the emulsion in providing flexibility, is overshadowed by the cement in the mix.

Little information is available on the limits for the Indirect Tensile Strength (ITS) of emulsion treated material. Values of between 250 and 600 have been reported (Louw: 1997). Until further research provides better information, it is proposed that the guidelines used in foam bitumen be adopted. This may be applicable because of the similarity between foam bitumen and emulsion treated materials. The classification system and the UCS and ITS limits are presented in Figure 8.3 and Table 8.3.

Table 8.3 Proposed Classification of Emulsion treated materials

Material classification	UCS (kPa)	ITS (kPa) @ 23°C
ET1	1 200 – 2 000	300 – 500
ET2	1 200 – 2 000	100 – 300
ET3	750 – 1 200	300 – 500
ET4	750 – 1 200	100 – 300

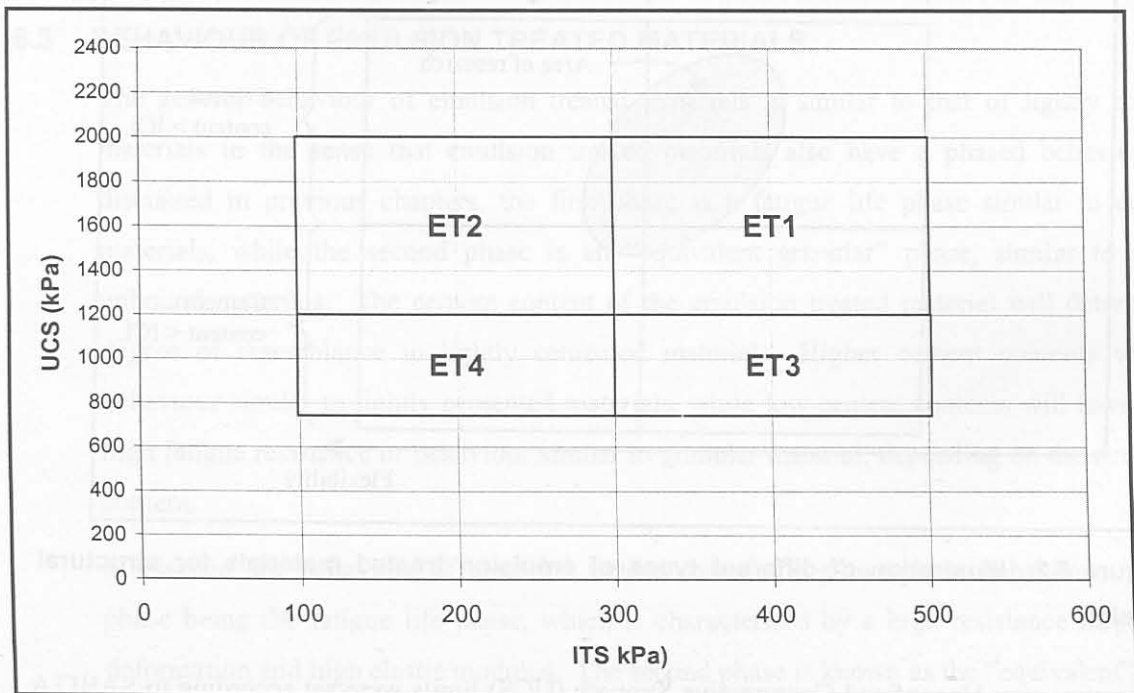


Figure 8.3 Proposed Classification of emulsion treated materials

Table 8.4 provides a summary of the typical composition of the different emulsion treated classes.

The different types of emulsion materials possible, provide the designer with a pavement structure which is either strong or flexible. The parent material available for emulsion treatment plays a role in the decision of the quantity of stabilising agent (cement, lime or emulsion) to be added, to obtain a predetermined level of performance. ET1 materials are therefore not necessarily superior to ET2 or ET3 materials, neither are ET4 materials only suitable for low volume roads. A G1 crushed stone material stabilised with no cement and 1.0 % bitumen emulsion, may be as good a product as stabilising a G4 material with 2 % cement and 3 % bitumen emulsion. In this case, the G1 stabilised material will be categorised as an ET4 material, while the G4 stabilised material will be categorised as an ET1 or ET3. The performance of materials which falls into the ET4 material class have not been researched and the structural design of these materials are excluded from this study. Experience (Bergh: 2001) has however shown that these material performed extremely well in practice.

Table 8.4 Typical composition of emulsion treated material per class

Emulsion treated material class	Typical parent material	Typical net bitumen content	Typical cement content
ET1	G3 to G6 or recycled cement treated base	> 1.8 %	> ICL
ET2	G3 to G6 or recycled cement treated base	0.6 to 1.8 %	> ICL
ET3	G1 to G5 or recycled good quality cement treated base	> 1.8 %	< ICL
ET4	G1 to G5 depending on requirements of traffic loading	0.6 to 1.8%	< ICL

Table 8.5 provides a guideline for the parameters used as input into the mechanistic design procedure. The values provided here should be regarded as *interim guidelines* until further research has been undertaken on these materials. It is preferable that the parameters given in Table 8.5 be determined by laboratory testing before the design process starts. This is, however, often expensive, time consuming and not practical. The information of C4 and EG5 materials is given for comparison only.

Initial stiffness: The initial stiffness is the elastic stiffness (elastic modulus) the material will have at the beginning of the fatigue life phase, i.e. just after construction. The initial stiffness is highly dependent on the cement stabilisation of the material and high cement content will increase the value.

Terminal stiffness: The terminal elastic stiffness is the stiffness the material will converge to when it reaches the end of its fatigue life. A value of 500 MPa has been backcalculated for the

material tested in this study, but the value will vary depending on the quality of the parent material and the amount of stabilisation. Better quality parent materials will have higher terminal stiffness values, while lower quality material will have lower stiffness values. The range of values proposed are a typical range in which terminal stiffnesses could lie and were estimated from the type of parent materials that would typically be used in emulsion stabilisation. The designer should familiarise himself with the parent material and select an appropriate stiffness accordingly.

Table 8.5 Proposed emulsion treated material properties for structural design

Property	ET1	ET2	ET3	ET4	C4	EG5
Initial Stiffness (MPa)	1 200 – 2 700 (1 800)	1 200 – 2 700 (1 800)	N/A ^(*)	N/A ^(*)	1 500 ^(a)	-
Terminal stiffness (MPa)	300 – 600 (500)	300 – 600 (500)	N/A ^(*)	N/A ^(*)	-	200 ^(a)
Poissons ratio	0.35 ^(b)	0.35 ^(b)	0.35 ^(b)	0.35 ^(b)	0.35	0.35
Strain at break ($\mu\epsilon$)	230	145	N/A ^(*)	N/A ^(*)	145 ^(a,c)	-
Cohesion (c) (kPa)	200 – 300 (250)	200 – 300 (250)	N/A ^(*)	N/A ^(*)	283 - 502 ^(d) 335 ^(e)	40
Friction angle (ϕ)	50°	50°	N/A ^(*)	N/A ^(*)	-	43°
c-term ^(g)	1 374	1 374	N/A ^(*)	N/A ^(*)	-	147 ^(a,f)
ϕ -term ^(h)	6.55	6.55	N/A ^(*)	N/A ^(*)	-	3.43 ^(a,f)

^(*) No research data available

^(a) Jordaan (1994)

^(b) Assumed value, not measured

^(c) de Beer (1985)

^(d) de Beer (1990)

^(e) Long et al (2001)

^(f) Moderate moisture condition

$$^{(h)} \phi_{term} = K \left(\tan^2 \left(45 + \frac{\phi}{2} \right) - 1 \right) \quad (8.1)$$

$$^{(i)} c_{term} = 2.K.c. \tan \left(45 + \frac{\phi}{2} \right) \quad (8.2)$$

Note. Values in brackets used in development of the design catalogue (Appendix F)

Strain at break: The strain at break gives an indication of the flexibility of the material. It is highly dependent on the cement and bitumen content. High bitumen content increases the value while an increase in cement content decreases the value. ET3 and ET4 materials should have a higher strain at break than ET1 and ET2 materials because of its lower cement content. ET1 and ET3 materials, however, would have a higher strain at break over ET2 and ET4 materials, because of their higher bitumen content. The values given in Table 8.5 are the average value expected for the specific type of emulsion treated material.

Cohesion and Friction angle: The cohesion and friction angle is the shear strength parameters, which determines the permanent deformation behaviour of the emulsion treated materials in the second behaviour phase, i.e. the “equivalent granular” phase. From the laboratory study, as well as studies by Maree (1978, 1982) and de Beer (1989), the friction angle is dependent on the parent material and is not sensitive to the addition of stabilising agents. A typical friction angle for emulsion treated materials is proposed in Table 8.5, which does not differ between the different types of emulsion treated materials. The cohesion is much more dependent on the addition of stabilising agents than the friction angle. From the laboratory study the addition of emulsion to a cemented material did not change the cohesion significantly. A typical range of values are proposed from the results of the laboratory study and the work done by Otte (1972) and De Beer (1989) on cemented materials.

8.5 MECHANISTIC ANALYSIS OF EMULSION TREATED PAVEMENT

8.5.1 Loading

The same principles as in TRH4 and in the South African Mechanistic Pavement Design Method apply. The load is a 40 kN dual wheel load with a tyre pressure of 620 kPa. The reason that the tyre pressure is 620 kPa is that it gives a uniform load contact area. That is also the value the transfer functions were calibrated for. The loaded area is assumed to be circular.

8.5.2 Layer thickness

The layer thickness of an emulsion treated material layer may vary between 125 mm and 300 mm. It does not seem practical to build a layer thinner than 125 mm because of construction tolerances, while layers thicker than 300 mm may be expensive and difficult to compact.

8.5.3 Mechanistic modelling of pavement behaviour

The mechanistic analysis and design procedure proposed in this study only considers emulsion treated materials. Other materials are discussed in the South African Mechanistic Pavement Design Method (Jordaan: 1994, Theyse et al 1996).

A pavement with an emulsion treated material should be analysed in two phases. The first phase being the fatigue life phase and the second phase the “equivalent” granular phase.

Fatigue

Fatigue cracking is primarily the result of cumulative damage caused by the bending of the layer under traffic loading. The horizontal tensile strain in an emulsion treated layer is used to determine the fatigue life of the pavement. The fatigue life is defined as the number of load repetitions until the elastic modulus reduces to a value of about 500 MPa or 25% of the initial stiffness. The fatigue criteria for the different road categories are as follows:

$$\text{Category A: } N_{f_A} = 10^{7.9183 - 1.2775 \left(\frac{\epsilon_t}{\epsilon_b} \right)} \quad (8.3a)$$

$$\text{Category B: } N_{f_B} = 10^{8.0331 - 1.2775 \left(\frac{\epsilon_t}{\epsilon_b} \right)} \quad (8.3b)$$

$$\text{Category C: } N_{f_C} = 10^{8.1747 - 1.2775 \left(\frac{\epsilon_t}{\epsilon_b} \right)} \quad (8.3c)$$

$$\text{Category D: } N_{f_D} = 10^{8.5066 - 1.2775 \left(\frac{\epsilon_t}{\epsilon_b} \right)} \quad (8.3d)$$

where: N_f = Number of load repetitions to end of fatigue life

ϵ_t = Maximum tensile strain at bottom of layer

ϵ_b = Strain at break

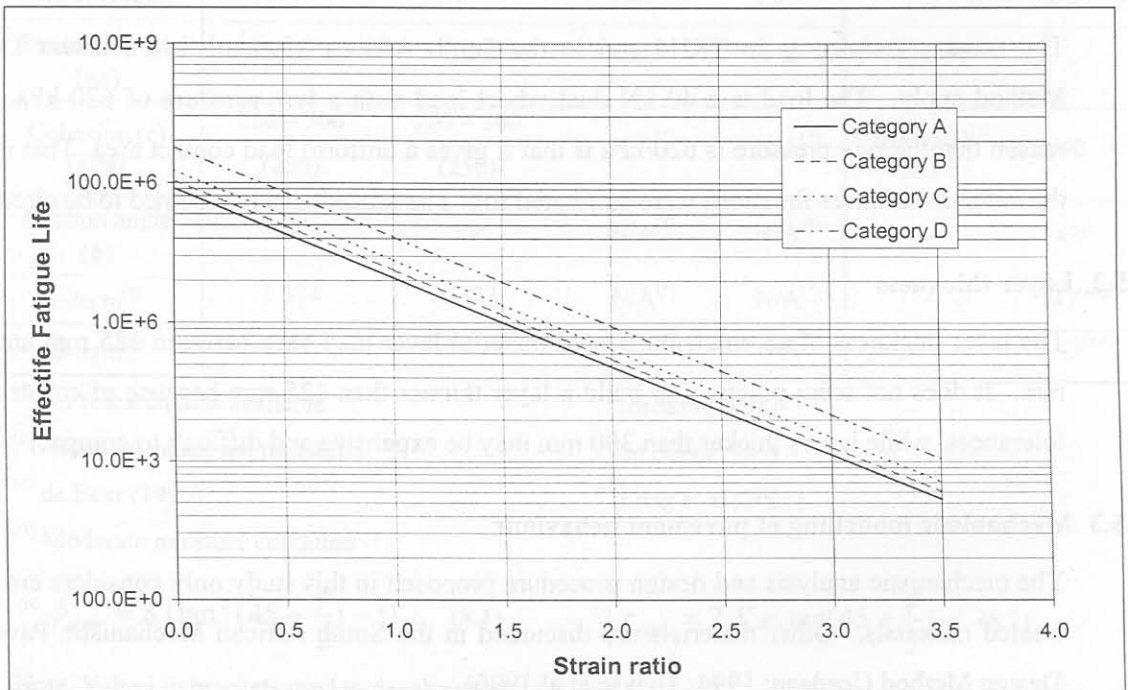


Figure 8.4 Effective fatigue transfer function for emulsion treated materials.

The maximum horizontal strain is not always at the bottom of the layer, and may be somewhere within the layer. Jordaan (1988) provided a procedure to test whether the maximum tensile strain is at the bottom of the layer.

The maximum horizontal tensile strain is at the bottom of the layer when:

$$\left(\frac{E_3}{E_2} \right)^2 h_c < K \quad (8.4)$$

$$\text{with: } h_c = h_1 \left(\frac{E_1}{E_3} \right)^{\frac{1}{3}} + h_2 \left(\frac{E_2}{E_3} \right)^{\frac{1}{3}} \quad (8.5)$$

where: E_1 = Elastic modulus of the asphalt layer (MPa)

E_2 = Elastic modulus of the emulsion treated layer (MPa)

E_3 = Elastic modulus of the supporting subbase layer (MPa)

h_1 = thickness of the asphalt layer (mm)

h_2 = thickness of the emulsion treated base layer (mm)

K = constant = 128

Procedure

- i) Determine the initial elastic properties of all pavement layers
- ii) Select an appropriate effective elastic modulus for the emulsion treated material from the recommended ranges in Table 8.5.
- iii) Use the modulus for all the pavement layers as determined in (i) and (ii) to determine the pavement response using an appropriate computer program
- iv) Determine whether the maximum tensile strain is at the bottom of the layer, using the procedure proposed by Jordaan (1988) described above. If not, a more detailed analysis of the layer is required.
- v) Determine the strain at break either from laboratory testing or using the guidelines in Table 8.5.
- vi) Use the appropriate transfer function for the category of road from Equations 8.3a to 8.3d to determine the effective fatigue life of the layer.

Permanent deformation ("equivalent granular" phase)

In the second phase the emulsion treated layer will be more susceptible to deformation. The stress state in the layer determines the permanent deformation behaviour of the layer. The failure criteria to 20 mm deformation on the surface for the different road categories is as follows:

$$\text{Category A: } \log N_{PD_A} = \left(\frac{54.005}{t} + 4.4736 \right) * (SR + 0.0664)^{-0.2313} \quad (8.6a)$$

$$\text{Category B: } \log N_{PD_B} = \left(\frac{54.005}{t} + 4.5389 \right) * (SR + 0.0664)^{-0.2313} \quad (8.6b)$$

Category C:
$$\log N_{PD_C} = \left(\frac{54.005}{t} + 4.6775 \right) * (SR + 0.0664)^{-0.2313} \quad (8.6c)$$

Category D:
$$\log N_{PD_D} = \left(\frac{54.005}{t} + 5.0213 \right) * (SR + 0.0664)^{-0.2313} \quad (8.6d)$$

where: N_f = Number of load repetitions to 20 mm deformation on surface

SR = Critical Stress ratio

t = thickness of the emulsion treated layer in mm.

$$SR = \frac{\sigma_1^a - \sigma_3}{\sigma_3 \left[\tan^2 \left(45^\circ + \frac{\phi}{2} \right) - 1 \right] + 2.c. \tan \left[45^\circ + \frac{\phi}{2} \right]} \quad (8.7)$$

or
$$SR = \frac{\sigma_1^a - \sigma_3}{\sigma_3 \cdot \phi_{term} + c_{term}} \quad (8.8)$$

where: SR = Stress ratio

ϕ = friction angle (measured in laboratory)

c = cohesion (kPa) (measured in laboratory)

ϕ_{term} = friction angle term from Table 8.5

c_{term} = cohesion term from Table 8.5

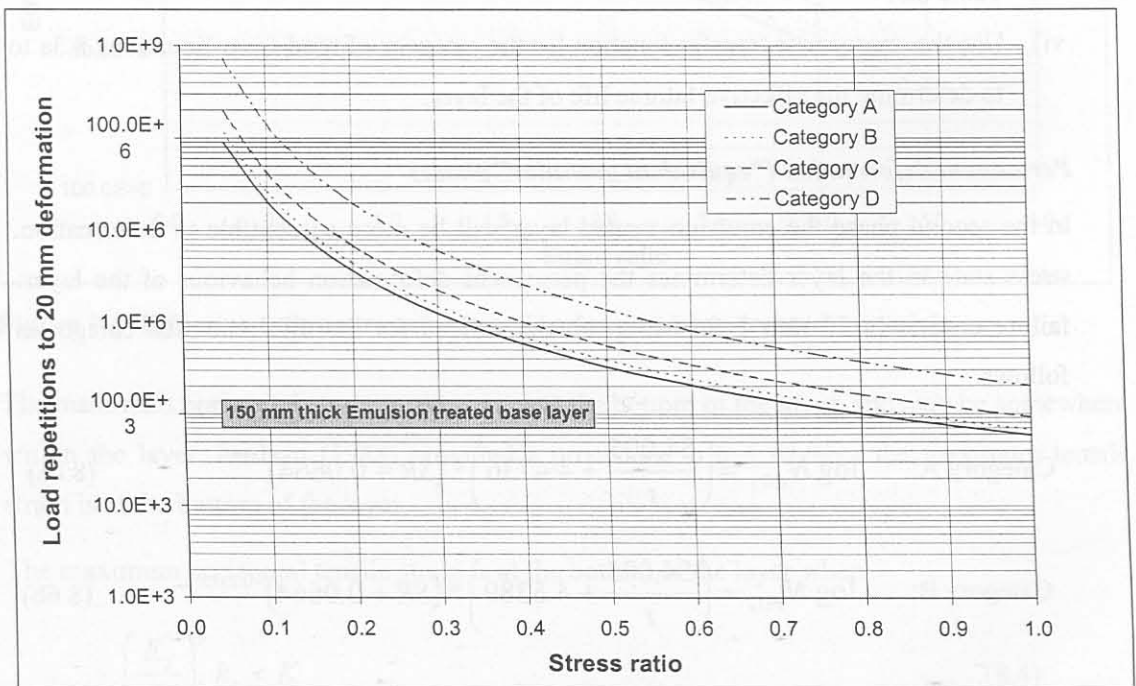


Figure 8.5 Permanent deformation transfer function for emulsion treated materials

Procedure

- i) Determine the initial elastic properties of all pavement layers in the second phase.
- ii) Select an appropriate effective elastic modulus for the emulsion treated material in its second phase (“equivalent” granular) from the recommended ranges in Table 8.5.
- iii) Use the modulus for all the pavement layers as determined in (i) and (ii) to determine the pavement response at the positions indicated in section 7.5.1 using an appropriate computer program
- iv) Use the procedure in section 7.5.1 to shift the minor principal stress if it is tensile.
- v) Calculate the stress ratio using Equation 8.7 or 8.8 by using the recommended values in Table 8.5, at the proposed positions as indicated in section 7.5.1.
- vi) Use the appropriate transfer function for the category of road from Equations 8.6a to 8.6b to calculate the bearing capacity of the layer to 20 mm of deformation on the surface.

The total life of the emulsion treated layer is the sum of the fatigue life and the bearing capacity to 20 mm deformation:

$$N = N_f + N_{PD} \quad (8.9)$$

Pavement life phases and residual life concept

The concept of pavement life phases has been introduced in the previous section. The phases are caused by changes taking place in pre-dominantly the emulsion treated layers in the pavement structure. The modulus of an emulsion treated layer is modelled as a constant value for the duration of a particular phase with a sudden change at the end of each phase.

The stresses and strains calculated during one phase, are not valid during the following phase. A structural analysis is therefore done for each phase with the applicable reduced moduli for the emulsion treated layer. The stresses and strains calculated for each phase will yield a predicted layer life for each layer during each phase. The transfer functions used for pavement design were developed for an initial condition of no distress. After phase 1, the predicted layer life for both phase 1 and 2 therefore becomes invalid but by combining the two values, an ultimate layer life may be calculated.

Consider the situation in Figure 8.6 where the layer life for each layer has been predicted for phase 1. At the end of phase 1, the modulus of the emulsion treated layer is suddenly reduced, resulting in higher stress/strain conditions in the other layers similar to an increase in loading on the pavement. The remaining part of the phase 1 predicted layer life for the other layers, or the residual life of the other layers is then reduced due to the increased stress conditions. The method assumes that the rate of decrease in the residual life of the other layers during the second phase, is equal to the ratio of the phase 1 predicted layer life to the phase 2 predicted

layer life for a particular layer, similar to a load equivalency factor. The only exception is the emulsion treated layer, which will start with a clean sheet for the second phase because there is a change in material state and therefore terminal condition. The predicted equivalent granular layer life for the original cemented layer will therefore be allocated to the emulsion treated layer in total for the second phase. Also note that if the top layer is a surfacing layer such as a surface seal or thin asphalt layer, then the predicted layer life for the top layer will not affect the ultimate pavement life. The reason for this is that surface maintenance should be done at regular intervals and it is not possible to design the thin asphalt surfacing layers for the total structural design life of the pavement structures, especially for high design traffic classes. The ultimate pavement life is calculated as the sum of the duration of phase 1 and the minimum adjusted residual life for phase 2 or the phase 2 predicted equivalent granular layer life for the original emulsion treated layer whichever is the smallest.

The process is extended along similar principles for a three phase analysis of a pavement structure incorporating an emulsion treated and cement-treated layers.

8.6 DESIGN CATALOGUE

A design catalogue, based on the mechanistic-empirical functions developed in this study is presented in Figures 8.7 and 8.8. The catalogue includes most of the factors that have to be considered by the designer. These include the road category and the design traffic loading over the design period. It should be used as an interim guideline and should not take precedence over the experience of the practitioner. The catalogue was, however, compared to other published catalogues on emulsion treated materials (de Beer and Grobler: 1994, Theyse: 1998). The pavement structures presented here are lighter than the pavement structures proposed by de Beer and Grobler (1994). This catalogue, however, agrees well with the catalogue proposed by Theyse (1998).

The catalogue allows the use of seals on roads with low design traffic volumes. It does not include practical considerations such as drainage, compaction or pavement cross-section. These aspects should be considered according to the TRH4 (COLTO: 1996).

The catalogue provides the use of ET1 and ET2 types of emulsion treated materials. No catalogue for ET3 and ET4 types of materials was developed.

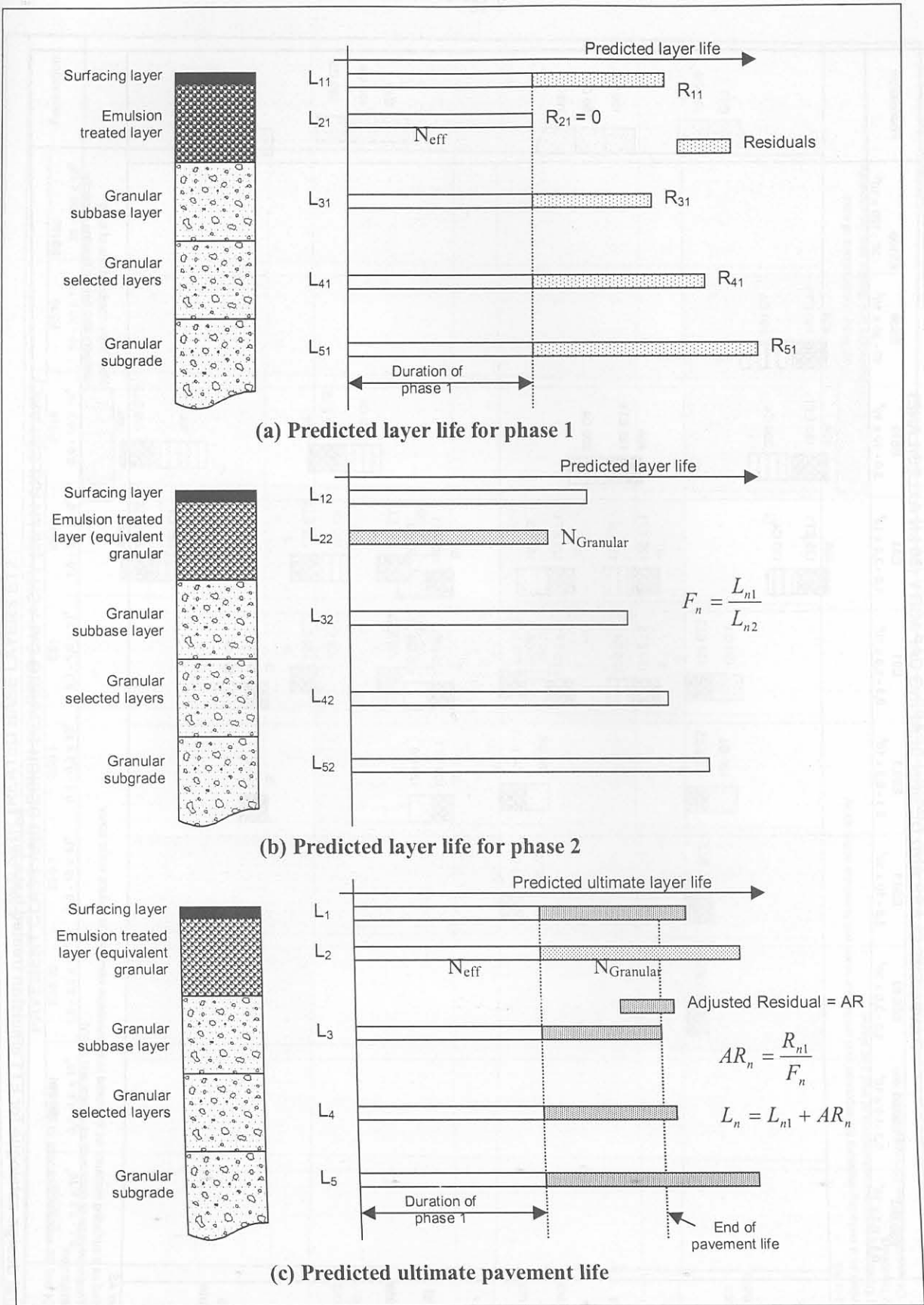


Figure 8.6 Calculating the ultimate pavement life for a pavement structure with emulsion treated layers

EMULSION TREATED BASE LAYERS ET1											
ROAD CATEGORY	PAVEMENT CLASS AND DESIGN BEARING CAPACITY (80 kN AXLES/LANE)										Foundation
	ES0.003 0,1 - 0,3 x 10 ⁴	ES0.01 0,3 - 1,0 x 10 ⁴	ES0.03 1,0 - 3,0 x 10 ⁴	ES0.1 3,0 - 10 x 10 ⁴	ES0.3 0,1 - 0,3 x 10 ⁶	ES1 0,3 - 1,0 x 10 ⁶	ES3 1,0 - 3,0 x 10 ⁶	ES10 3,0 - 10 x 10 ⁶	ES30 10 - 30 x 10 ⁶	ES100 30 - 100 x 10 ⁶	
A: Major interurban freeways and roads. (95% approximate design reliability)											
B: Interurban collectors and major rural roads. (90% approximate design reliability)						 	 				
C: Lightly trafficked rural roads and strategic roads. (80% approximate design reliability)											
D: Lightly pavement structures, rural access roads. (80% approximate design reliability)											

Symbol A denotes AG, AC or AS
 AO, AP may be recommended as a surfacing measure for improved skid resistance when wet to reduce water spray
 S denotes Double Surface Treatment (seal or combinations of seal and slurry)
 S1 denotes Single Surface Treatment
 * is Seal is used, increase C4 and G5 subbase thickness to 200 mm

Most likely combinations of road category and design bearing capacity

Figure 8.7 Structural design catalogue for ET1 emulsion treated base layers

ROAD CATEGORY	EMULSION TREATED BASE LAYERS ET2										Foundation
	PAVEMENT CLASS AND DESIGN BEARING CAPACITY (80 kN AXLES/LANE)										
	ES0.003 0,1 - 0,3 x 10 ⁴	ES0.01 0,3 - 1,0 x 10 ⁴	ES0.03 1,0 - 3,0 x 10 ⁴	ES0.1 3,0 - 10 x 10 ⁴	ES0.3 0,1 - 0,3 x 10 ⁶	ES1 0,3 - 1,0 x 10 ⁶	ES3 1,0 - 3,0 x 10 ⁶	ES10 3,0 - 10 x 10 ⁶	ES30 10 - 30 x 10 ⁶	ES100 30 - 100 x 10 ⁶	
A: Major interurban freeways and roads. (95% approximate design reliability)											
B: Interurban collectors and major rural roads. (90% approximate design reliability)					 	 					
C: Lightly trafficked rural roads and strategic roads. (80% approximate design reliability)											
D: Lightly pavement structures, rural access roads. (80% approximate design reliability)											

Symbol A denotes AG, AC or AS
 AO, AP may be recommended as a surfacing measure for improved skid resistance when wet to reduce water spray
 S denotes Double Surface Treatment (seal or combinations of seal and slurry)
 S1 denotes Single Surface Treatment
 * is Seal is used, increase C4 and G5 subbase thickness to 200 mm

Most likely combinations of road category and design bearing capacity

Figure 8.8 Structural design catalogue for ET2 emulsion treated base layers

8.7 REFERENCES

- Asphalt Academy, 2002, *The Design and Use of Foamed Bitumen Treated Materials*, Interim Technical Guideline TG2, Asphalt Academy, Pretoria, South Africa.
- Bergh AO, 2001, *Personal correspondence and communication*, Pretoria, South Africa.
- Committee of Land Transportation Officials (COLTO), 1996, *Structural design of flexible pavements for interurban and rural roads*, Draft TRH4:1996, Department of Transport, Pretoria, South Africa.
- Committee of State Road Authorities (CSRA), 1987, *Guidelines for Road Construction Materials*, TRH14:1987, Department of Transport, Pretoria.
- De Beer M and Grobler JE, 1993, *ETB': Heavy Vehicle Simulator (HVS) Evaluation of the Heilbron Sections*, South African Roads Board, Service Contract Report PR92/2/1, Pretoria, South Africa.
- De Beer M, 1985, Behaviour of cementitious subbase layers in bitumen base road structures in South Africa, MEng dissertation, University of Pretoria, Pretoria.
- De Beer M, 1989, Aspects of the design and behaviour of road structures incorporating lightly cemented layers, PhD Thesis, University of Pretoria, Pretoria.
- Freeme et al. 1983, *Evaluation of pavement behaviour for major rehabilitation of roads*, Technical Report RP/19/83, CSIR, Pretoria, South Africa.
- Jordaan GJ, 1988, *Analysis and developments of some pavement rehabilitation design methods*, PhD thesis, University of Pretoria, Pretoria, South Africa.
- Jordaan GJ, 1994, *The South African Mechanistic Pavement Rehabilitation Design Method*, Department of Transport, Research Report RR91/242, Pretoria, South Africa.
- Otte E, 1972, *Die Spannings en Vervormingseienskappe van Sementgestabiliseerde Materiale*, MSc(Eng) dissertation, University of Pretoria, Pretoria, South Africa.
- Long FM and Theyse HL, 2001, *Laboratory testing for the HVS Sections on Road P243-1*, Contract Report CR-2001/32, Transportek, CSIR, Pretoria, South Africa.
- Louw L, 1997, *ETB mix design: Summary of best practises*, Contract Report CR-96/079, CSIR Transportek, Pretoria, South Africa.
- Maree JH, 1978, *Ontwerpparameters vir klipslag in plaveisels*, MEng dissertation, University of Pretoria, Pretoria, South Africa.
- Maree JH, 1982, *Aspekte van die ontwerp an gedrag van padplaveisels met korrelmateriaalkroonlae*, PhD Thesis, University of Pretoria, Pretoria, South Africa.

SABITA, 1999, *ETB: The design and use of emulsion treated bases*, Manual 21, SABITA, Cape Town, South Africa.

Theyse HL, 1998, *Towards guidelines on the structural design of pavements with emulsion treated layers*, Transportek, CSIR, (CR-97/045), Pretoria, South Africa.

From the literature study, it is clear that mix design practices for emulsion treated materials are well established and researched, but do not provide enough input into the structural design and analysis process. This could be because no existing structural design method recognises the difference in emulsion treated material mixes. Structural design procedures are available and are widely used. A number of structural design methods for the structural design of emulsion treated materials exist. Most of these methods are empirical and focus on higher net bitumen content mixes. Mixes with high bitumen content are, however, not always economical in South Africa. Design methods on emulsion treated materials with lower net bitumen content are based on the behaviour of similar materials.

The objective of this study was to define the stress-strain behaviour and failure criteria of pavement layers treated with bitumen emulsion and to develop design equations for the relative mode of failure to any material. From the laboratory and Heavy Vehicle Massing (HVM) study, it was possible to define the life cycle behaviour and failure criteria, as well as a structural design procedure was developed for these types of materials.

9.1 CONCLUSIONS

- The amount and net bitumen content have an influence on the important engineering properties. If the amount of bitumen increases, the strength of the material increases but the flexibility decreases. An increase in net bitumen content will increase the flexibility but reduces the strength up to a point where the strength will start to increase again. The behaviour will then be visco-elastic similar to that of asphalt materials. Figure 9-1 illustrates this concept.
- The stiffness of the material depends on three parameters. These include the quality of the parent material, the cement content and the bitumen content. Stiffness values are expected to range between 1 000 MPa and 1 700 MPa depending on these parameters. This study includes only materials with net bitumen content of between 0.6 and 1.0 % and cement content between 1 and 2 %.

CHAPTER 9 CONCLUSIONS AND RECOMMENDATIONS

The conclusions and recommendations relevant to the particular chapter have been listed at the end of each chapter. This chapter contains the overall recommendations and conclusions from this study.

From the literature study, it is clear that mix design practices for emulsion treated materials are well established and researched, but do not provide much input into the structural design and analysis process. This could be because no existing structural design method recognises the difference in emulsion treated material mixes. Several mix design procedures are available and are widely used. A number of structural design methods for the structural design of emulsion treated materials exist. Most of these methods are empirical and focus on higher net bitumen content mixes. Mixes with high bitumen content are, however, not always economical in South Africa. Design methods on emulsion treated materials with lower net bitumen content are based on the behaviour of similar materials.

The objective of this study was to define the life cycle behaviour and failure criteria of pavement layers treated with bitumen emulsion and to develop transfer functions for the relative mode of failure to load repetitions. From the laboratory and Heavy Vehicle Simulator (HVS) study, it was possible to define the life cycle behaviour and transfer functions, as well as a structural design procedure were developed for these types of materials.

9.1 CONCLUSIONS

- The cement and net bitumen content have an influence on the important engineering properties. If the cement content increases, the strength of the material increases but the flexibility decreases. An increase in net bitumen content will increase the flexibility but reduces the strength up to a point where the strength will start to increase again. The behaviour will then be visco-elastic similar to that of asphalt materials. Figure 9.1 illustrates this concept.
- The stiffness of the material depends on three parameters. These include the quality of the parent material, the cement content and the bitumen content. Stiffness values are expected to range between 1 000 MPa and 2 700 MPa depending on these parameters. This study includes only materials with net bitumen content of between 0.6 and 3.0 % and cement content between 1 and 2 %.

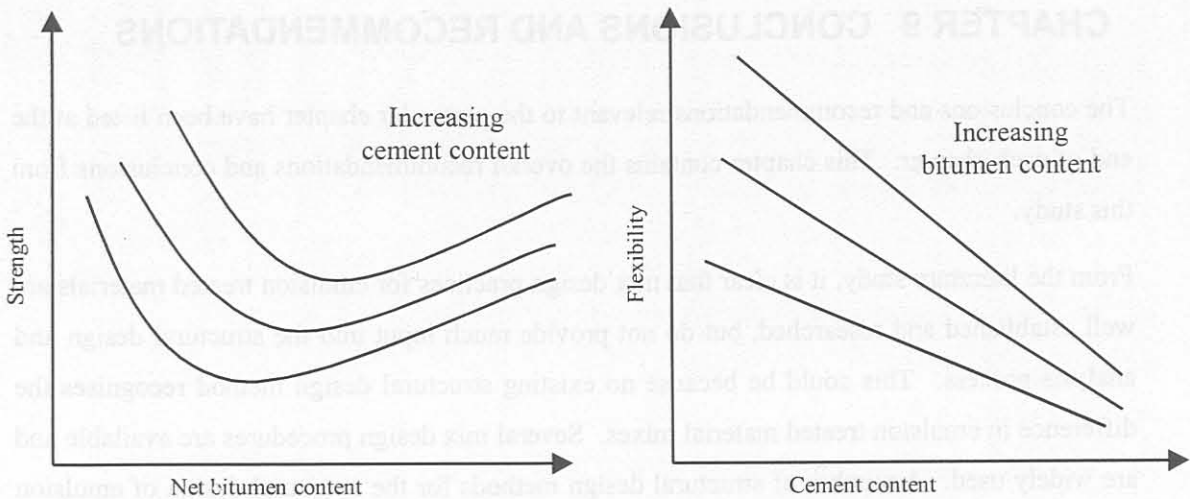


Figure 9.1 Influence of cement and net bitumen content on main engineering properties

- The Initial Consumption of Lime (ICL) is an important indicator of the behaviour of emulsion treated material. Below the ICL the cement acts mainly as an catalyst to assist in the breaking of the emulsion and does not contribute much to the strength of the material, as the cement is absorbed in the clay. Above the ICL the cement contributes significantly to the strength and limits the flexibility provided by the bitumen.
- The behaviour of an emulsion treated material is a two-phase behaviour. The first phase is similar to that of lightly cemented material, in the sense that it has an effective fatigue life. In the second phase the material will behave similarly to a granular material with a reduced resistance to permanent deformation.
- The strain at break (ϵ_b) can be obtained from the flexural beam test and depends largely on the cement and bitumen content of the mix.
- The shear stress parameters, internal friction angle (ϕ) and cohesion (c), can be obtained from static triaxial testing in the laboratory. The internal friction angle is influenced not much by a change in the cement or net bitumen content. The cohesion could vary between 200 and 300 kPa depending on the quality of the parent material, the cement content and the net bitumen content.
- Under HVS testing the backcalculated stiffness converges to a value of 500 MPa after a number of load repetitions. This was assumed to be the end of the fatigue life phase and the beginning of the “equivalent granular” phase. The terminal stiffness value also depends on the quality of the parent material, the cement content and the bitumen content. It is expected that the value could range between 400 and 600 MPa depending on the factors mentioned.
- The permanent deformation performance of the material considered was good under HVS testing. Less than 5 mm of permanent deformation was measured on all the test sections

after the termination of the tests. The introduction of water into the pavement decreased the permanent deformation resistance of the layer.

- Using the developed transfer functions, and the principles of the South African Mechanistic Pavement Design Method, it would be possible to model the behaviour of emulsion treated materials for rehabilitation analysis and design.
- A design catalogue was developed in accordance with the principles of the TRH4 and South African Mechanistic Pavement Design Method. The catalogue provides different pavement structures for different traffic classes and road categories.
- Material parameters, for the use in the mechanistic analysis process, have been derived in this study and should be used as a guideline only.

9.2 RECOMMENDATIONS

- The design method proposed in this study should be introduced as an *interim* guideline to the industry until such time as more knowledge on bitumen emulsion treated stabilised materials are obtained.
- Where possible, material properties should be measured in the laboratory and then entered into the structural design process. The material guidelines presented in Table 8.5 should only be used as a *guideline*.
- A database should be set up from projects, where emulsion treatment was used, to assist in the refining of material properties and to broaden the knowledge base to other material types.
- Mix design procedures should be refined to provide input into the structural design procedure.
- Laboratory studies on different cement and bitumen content should be extended to other types of materials.
- Field and HVS studies, on other types of materials and different cement and net bitumen content, are recommended to refine the proposed transfer functions. This may be expensive and should be a long term research objective.
- Finite element studies on the permanent deformation behaviour of emulsion treated materials should be investigated together with the use of elasto-plastic or other non-linear models. This will provide a better understanding and description of the behaviour of pavement structures, which involve emulsion treated materials.

A

A1. CBR test results

Sample no	Bitumen content (%)	Moulding Density (kg/m ³)	Moulding Moisture content (%)	Swell (%)	CBR		
					2.54 mm	2.00 mm	1.02 mm
1009/01a	0.6	1991	12.2	0.0	18.1	16.7	18.0
1009/01b	0.6	1947	12.2	0.0	18.6	17.6	18.4
1009/01c	0.6	1974	12.2	0.0	19.0	18.3	19.3
1009/01s	1.0	1940	12.7	0.0	12.0	15.0	18.5
1009/01b	1.8	1963	12.7	0.0	14.3	15.4	21.2
1009/01c	1.8	1952	12.7	0.0	12.0	14.3	16.8
1109/01a	3.0	1952	10.7	0.0	14.1	17.2	2.9
1109/01b	3.0	1952	10.7	0.0	14.1	17.2	45.2
1109/01c	3.0	1906	10.7	0.0	14.1	17.2	42.1

APPENDIX A. LABORATORY TEST RESULTS

A1. California Bearing Ratio (CBR)

A2 Unconfined compressive Strength (UCS)

A3. Indirect Tensile Strength (ITS)

A4. Flexural Beam Tests

A5 Static Triaxial Tests

A6 Dynamic Triaxial Tests

A1. CBR test results

Sample no	Bitumen content (%)	Moulding Density (kg/m ³)	Moulding Moisture content (%)	Swell (%)	CBR		
					2.54 mm	2.05 mm	7.62 mm
10/09/01a	0.6	1 991	12.2	0.0	12.1	16.7	19.0
10/09/01b	0.6	1 947	12.2	0.0	16.6	17.6	18.4
10/09/01c	0.6	1 974	12.2	0.0	13.0	16.3	19.3
4/09/01a	1.8	1 940	12.7	0.0	12.9	15.6	18.9
4/09/01b	1.8	1 968	12.7	0.0	14.4	18.4	21.7
4/09/01c	1.8	1 952	12.7	0.0	10.9	14.9	16.9
11/09/01a	3.0	1 982	10.7	0.0	14.2	17.2	2.3
11/09/01b	3.0	1 979	10.7	0.2	30.7	43.2	45.2
11/09/01c	3.0	1 996	10.7	0.0	30.4	38.2	42.1

A2. UCS test results

Sample no	Cement content (%)	Bitumen content (%)	Moulding Density (kg/m ³)	Moulding Moisture content (%)	UCS (kPa)
10/09/01a	0	0.6	1 947	12.6	174
10/09/01b	0	0.6	1 980	12.6	137
10/09/01c	0	0.6	1 980	12.6	165
3/09/01g	0	1.8	1 950	11.9	131.6
3/09/01h	0	1.8	1 941	11.9	142.5
3/09/01i	0	1.8	1 924	11.9	120.6
11/09/01a	0	3.0	1 964	11.1	285
11/09/01b	0	3.0	1 938	11.1	280
11/09/01c	0	3.0	1 964	11.1	384
3/09/01a	1	0.6	1 964	12.5	543
3/09/01b	1	0.6	1 943	12.5	510
3/09/01c	1	0.6	1 945	12.5	592
5/09/01d	1	1.8	1 944	12.0	548
5/09/01e	1	1.8	1 949	12.0	543
5/09/01f	1	1.8	1 943	12.0	543
7/09/01a	1	3.0	1 976	10.0	724
7/09/01b	1	3.0	1 991	10.0	658
7/09/01c	1	3.0	1 971	10.0	981

A3. ITS test results

Sample no	Cement content (%)	Bitumen content (%)	Moulding Density (kg/m ³)	Moulding Moisture content (%)	ITS (kPa)
10/09/01d	0	0.6	1 942	12.6	16.4
10/09/01e	0	0.6	1 963	12.6	16.4
10/09/01f	0	0.6	1 972	12.6	16.4
3/09/01a	0	1.8	1 953	12.3	16.4
3/09/01b	0	1.8	1 936	12.3	29.6
3/09/01c	0	1.8	1 949	12.3	26.3
11/09/01d	0	3.0	1 950	11.1	32.9
11/09/01e	0	3.0	1 966	11.1	36.2
11/09/01f	0	3.0	1 978	11.1	32.9
3/09/01d	1	0.6	1 918	12.3	49.3
3/09/01e	1	0.6	1 977	12.3	59.2
3/09/01f	1	0.6	1 932	12.3	59.2
5/09/01g	1	1.8	1 965	12.0	65.8
5/09/01h	1	1.8	1 915	12.0	65.8
5/09/01i	1	1.8	1 945	12.0	62.5
7/09/01d	1	3.0	1 945	10.0	131.6
7/09/01e	1	3.0	1 954	10.0	115.1
7/09/01f	1	3.0	1 957	10.0	161.2

A4. Flexural beam test results

													B e a m	
													←-----→	
Sample no	Binder	Cement	Wet Mass	Height	width	length	LVDT#1	LVDT#1	LVDT#2	LVDT#2	Comments	Moisture	Failure	
	(%)	(%)	(g)	(mm)	(mm)	(mm)	Strain	Stress	Strain	Stress		(%)	(mm)	
Betb1-1	0.0	1.0	5715	75	75	450	144	53	53	54		10.4	260	
Betb1-1x	0.0	1.0	5715	76	75	450	Data looks incorrect					10.7	205	
Betb1-3	0.0	1.0	5705	76	75	450	129	30	129	30		10.3	265	
Betb1-5	0.0	1.0	5685	76	75	450	72	29	46	33		11.0	165	
Betb2-6	1.8	0.0	5665	75	75	450	Broke under 2kg load					10.4	200	
Betb2-4	1.8	0.0	5665	75	75	450	Broke under own weight					10.4	210	
Betb2-3	1.8	0.0	5645	75	75	450	Broke under 2kg load					10.2	140	
Betb2-2	1.8	0.0	5730	75	75	450	Broke under 2kg load					10.0	285	
Betb3-1	1.8	1.0	5660	75	75	450	632	32	599	32		10.2	250	
Betb3-3	1.8	1.0	5720	75	75	450	200	18	231	18		10.2	260	
Betb3-9	1.8	1.0	5715	75	75	450	255	26	313	25		10.0	230	
Betb3-11	1.8	1.0	5690	75	75	450	229	26	229	25	Stone (b)	9.4	240	
Betb4-6	0.6	0.0	5680	75	75	450	Broke under 2kg load					10.2	210	
Betb4-16	0.6	0.0	5680	76	75	450	Broke under 2kg load					10.3	160	
Betb4-18	0.6	0.0	5675	76	75	450	Broke under 2kg load under both load platforms					10.1	150 / 310	
Betb4-26	0.6	0.0	5680	76	75	450	Broke under 2kg load					10.7	150	
Betb5-1	3.0	1.0	5680	75	75	450	Broke under 2kg load				Stone (b)	9.6	160	
Betb5-10	3.0	1.0	5680	75	75	450	633	37	1189	37		8.6	240	
Betb5-13	3.0	1.0	5665	75	75	450	601	68	601	68		8.4	280	
Betb5-14	3.0	1.0	5670	75	75	450	462	64	549	64	Stone (b)	7.8	285	
Betb6-5	3.0	0.0	5620	75	75	450	Tested but no load change from loadcell					8.2	310	
Betb6-8	3.0	0.0	5615	75	75	450	Broke under 2kg load after 20 -30 seconds					8.6	210	
Betb6-12	3.0	0.0	5615	75	75	450	Broke under 2kg load after 20 -30 seconds					8.5	215	
Betb6-15	3.0	0.0	5610	75	75	450	Broke under 2kg load after 20 -30 seconds				Stone (b)	9.3	195	

(b) = bottom

A5. Static triaxial test results

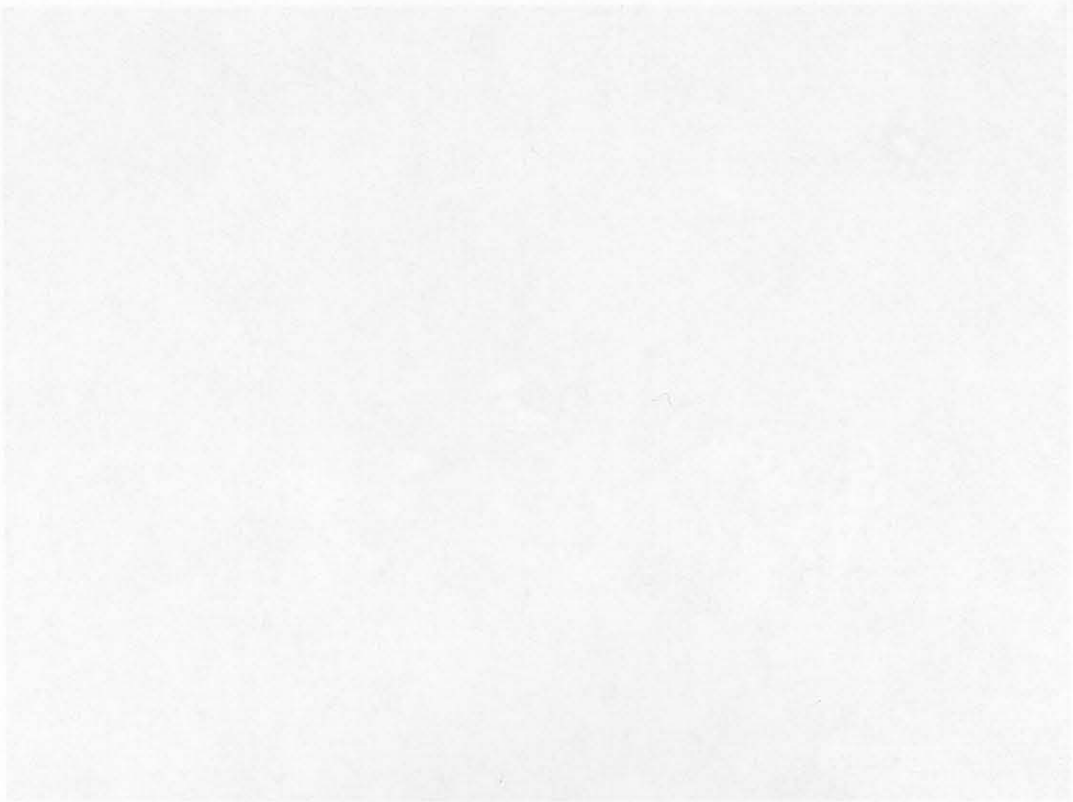
 MDD: 1971
 OMC: 12.5
 ARD: 2.7770

Sample #	Dry density (kg/cub m)	Compaction (%)	Moisture Content (MC) (%)	Saturation (%)	Residual Binder Content (%)	Confining stress (kPa)	Static test results						Cohesion and friction angle	Actual MC (%)	Actual Dry density (kg/cub m)	Compaction (%)	Compaction Average	Saturation (%)	Saturation Average
							Failure load kN	Failure stress (kPa)	Stiffness (MPa)	Sigma 1 (kPa)	p (kPa)	q (kPa)							
ETF01	1870	67.3%	13	74.3%	1.8%	22	36.3	1998	474	2020	1021	999	543.0 32.5	10.48	1974	71.1%	70.4%	63.2%	64.5%
ETF02	94.9					80	40.8	2246	398	2326	1203	1123		11.19	1960	70.6%		67.1%	
ETF03						140	41.1	2264	482	2404	1272	1132		10.76	1936	69.7%		63.7%	
ETF04						200	44.0	2427	285	2627	1413.5	1213.5		10.77	1944	70.0%		64.0%	
ETF05	1870	67.3%	8	45.7%	1.8%	20	30.8	1700	357	1720	870	850	328.6 46.5	10.56	1930	69.5%	69.5%	62.3%	59.0%
ETF06	94.9					80	39.3	2167	442	2247	1163.5	1083.5		9.99	1923	69.2%		58.7%	
ETF07						140	43.1	2377	307	2517	1328.5	1188.5		9.99	1943	70.0%		59.4%	
ETF08						200	48.3	2664	438	2864	1532	1332		9.45	1923	69.2%		55.6%	
ETF09	2030	73.1%	10	75.5%	1.8%	20	45.8	2524	419	2544	1282	1262	458.0 48.3	10.50	2022	72.8%	73.2%	64.9%	62.8%
ETF10	103.0					80	52.2	2878	514	2958	1519	1439		8.66	2041	73.5%		54.1%	
ETF11						140	50.8	2801	494	2941	1540.5	1400.5		10.74	2011	72.4%		66.0%	
ETF12						200	53.0	2922	904	3122	1661	1461		10.57	2051	73.9%		66.3%	
ETF13	2030	73.1%	6	45.3%	1.8%	20	45.6	2513	350	2533	1276.5	1256.5	370.0 54.8	9.77	2026	73.0%	72.4%	60.5%	58.2%
ETF14	103.0					80	55.3	3050	707	3130	1605	1525		10.14	1985	71.5%		61.6%	
ETF15						140	51.9	2858	707	2998	1569	1429		8.87	2017	72.6%		54.7%	
ETF16						200	63.5	3500		3700	1950	1750		9.09	2012	72.5%		55.9%	

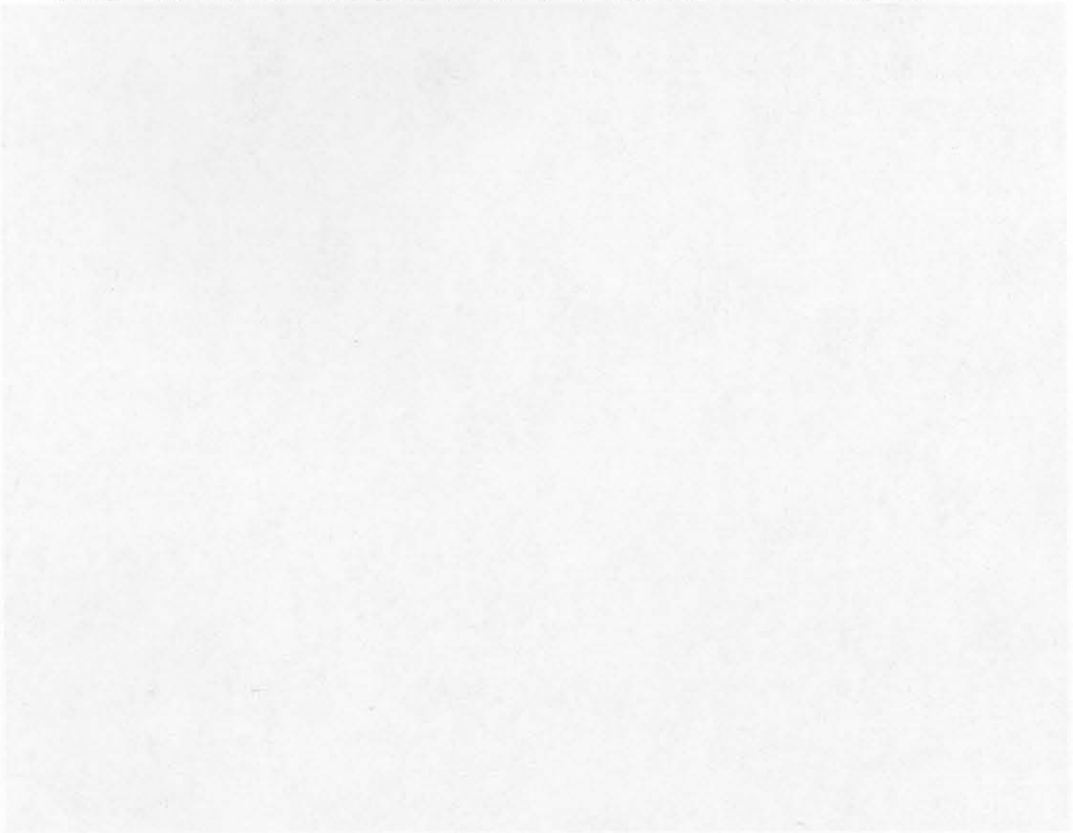
Sample #	Dry density (kg/cub m)	Compaction (%)	Moisture Content (MC) (%)	Saturation (%)	Residual Binder Content (%)	Confining stress (kPa)	Failure load (kN)	Failure stress (kPa)	Stiffness (MPa)	Sigma 1 (kPa)	p (kPa)	q (kPa)	Cohesion and friction angle	Actual MC (%)	Actual Dry density (kg/cub m)	Compaction (%)	Compaction Average	Saturation (%)	Saturation Average
ETF01	1870	67.3%	13	74.3%	1.8%	22	36.3	1998	474	2020	1021	999	543.0 32.5	10.48	1974	71.1%	70.4%	63.2%	64.5%
ETF02	94.9					80	40.8	2246	398	2326	1203	1123		11.19	1960	70.6%		67.1%	
ETF03						140	41.1	2264	482	2404	1272	1132		10.76	1936	69.7%		63.7%	
ETF04						200	44.0	2427	285	2627	1413.5	1213.5		10.77	1944	70.0%		64.0%	
ETF05	1870	67.3%	8	45.7%	1.8%	20	30.8	1700	357	1720	870	850	328.6 46.5	10.56	1930	69.5%	69.5%	62.3%	59.0%
ETF06	94.9					80	39.3	2167	442	2247	1163.5	1083.5		9.99	1923	69.2%		58.7%	
ETF07						140	43.1	2377	307	2517	1328.5	1188.5		9.99	1943	70.0%		59.4%	
ETF08						200	48.3	2664	438	2864	1532	1332		9.45	1923	69.2%		55.6%	
ETF09	2030	73.1%	10	75.5%	1.8%	20	45.8	2524	419	2544	1282	1262	458.0 48.3	10.50	2022	72.8%	73.2%	64.9%	62.8%
ETF10	103.0					80	52.2	2878	514	2958	1519	1439		8.66	2041	73.5%		54.1%	
ETF11						140	50.8	2801	494	2941	1540.5	1400.5		10.74	2011	72.4%		66.0%	
ETF12						200	53.0	2922	904	3122	1661	1461		10.57	2051	73.9%		66.3%	
ETF13	2030	73.1%	6	45.3%	1.8%	20	45.6	2513	350	2533	1276.5	1256.5	370.0 54.8	9.77	2026	73.0%	72.4%	60.5%	58.2%
ETF14	103.0					80	55.3	3050	707	3130	1605	1525		10.14	1985	71.5%		61.6%	
ETF15						140	51.9	2858	707	2998	1569	1429		8.87	2017	72.6%		54.7%	
ETF16						200	63.5	3500		3700	1950	1750		9.09	2012	72.5%		55.9%	

A6. Dynamic triaxial tests

Sample	Relative density (%)	Saturation (%)	Confining stress (kPa)	Dynamic test conditions			Actual MC (%)	Actual Dry density (kg/cub m)	Sample height (mm)	LVDT #1				LVDT #2			
				Load kN	Stress (kPa)	Stress Ratio				a	m	b	c	a	m	b	c
ETF18	74.00	82.20	80	21.6	1189.7	0.55	10.4	2055	303					0.44	1.84E-06	1.00	0.00
ETF19	74.25	85.69	80	35.3	1946.8	0.90	10.7	2062	304	1.08	1.77E-06	0.62	0.00	1.16	2.45E-06	1.00	0.00
ETF20	74.97	90.68	140	8.4	460.4	0.20	10.9	2082	301	0.28	4.27E-07	1.00	0.07	0.51	2.57E-06	0.93	0.02
ETF21	74.47	89.91	140	23.0	1266.1	0.55	11.1	2068	303	0.28	1.80E-06	0.70	0.02	0.33	1.80E-06	0.53	0.01
ETF22	72.85	80.47	140	37.6	2071.9	0.90	10.8	2023	304					1.18	3.50E-06	1.10	0.01
ETF23	73.93	61.42	80	7.5	413.7	0.20	7.8	2053	302	0.41	2.86E-07	1.00	0.00	0.43	5.64E-07	0.85	0.01
ETF24	73.82	67.34	80	20.6	1137.8	0.55	8.6	2050	300	0.90	9.93E-07	0.80	0.01	1.20	2.50E-06	0.95	0.01
ETF25	74.32	64.31	80	33.8	1861.8	0.90	8	2064	300	2.45	6.47E-06	0.78	0.01	1.51	1.59E-07	1.00	0.05
ETF27	74.54	67.48	140	23.8	1311.9	0.55	8.3	2070	300	1.10	2.69E-07	0.90	0.00	0.94	7.00E-07	0.72	0.00
ETF28	75.19	61.43	140	39.0	2146.8	0.90	7.3	2088	300	2.00	4.54E-06	0.98	0.01				
ETF29	77.93	92.15	80	10.4	575.6	0.20	9.4	2164	305	0.37	6.55E-07	1.05	0.00	0.53	8.84E-07	0.85	0.01
ETF30	78.54	82.31	80	28.7	1582.9	0.55	8.1	2181	304					1.15	8.69E-07	0.85	0.01
ETF32	76.13	99.17	140	11.7	646.4	0.20	11.2	2114	307	0.79	1.44E-06	0.95	0.01	0.42	1.00E-06	1.01	0.01
ETF33	75.77	98.10	140	32.3	1777.6	0.55	11.3	2104	305	2.12	1.22E-05	0.72	0.00	2.00	1.55E-05	0.71	0.02
ETF35	77.42	78.08	80	11.1	610.0	0.20	8.2	2150	305					0.18	3.00E-06	0.60	0.00
ETF36	77.49	86.06	80	30.4	1677.5	0.55	9	2152	303	1.06	1.55E-06	0.95	0.01				
ETF38	77.35	80.61	140	13.0	717.4	0.20	8.5	2148	305	0.35	2.00E-06	0.63	0.00				
ETF39	77.49	75.54	140	35.8	1972.9	0.55	7.9	2152	305					1.63	4.50E-06	1.30	0.03



APPENDIX B. OPTICAL MICROSCOPE PICTURES



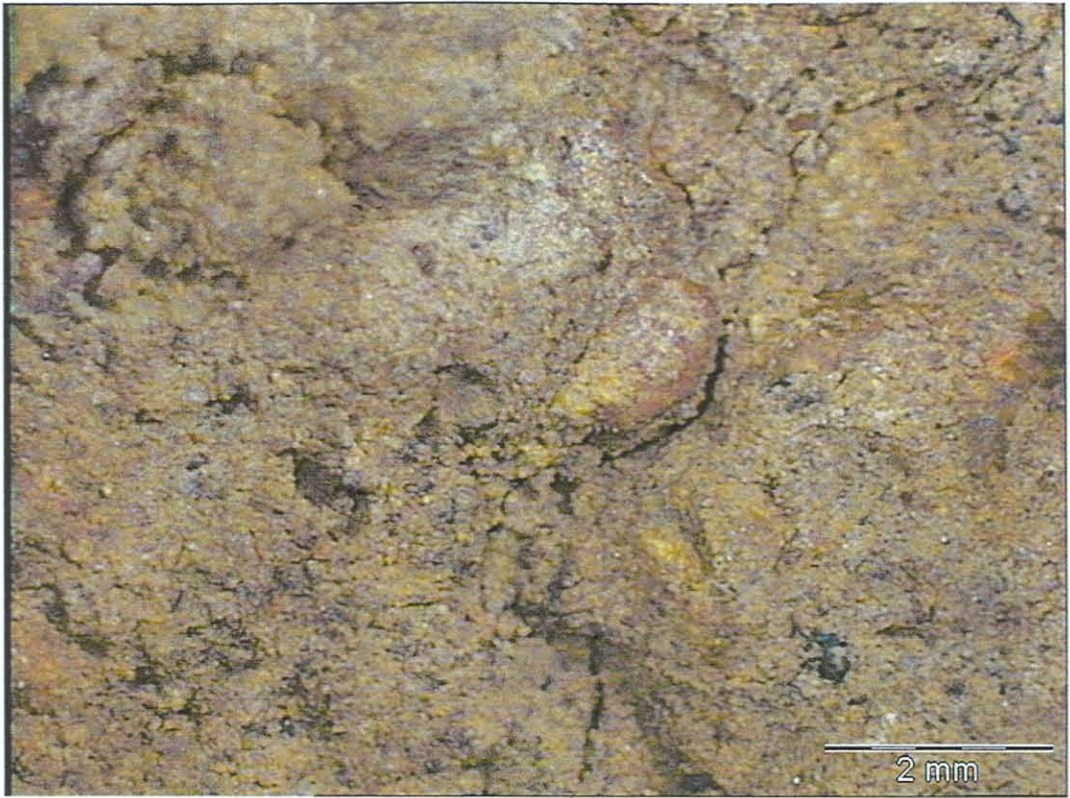
Photograph A2: 0.5% w/v solution, 0% carbon, 30x magnification



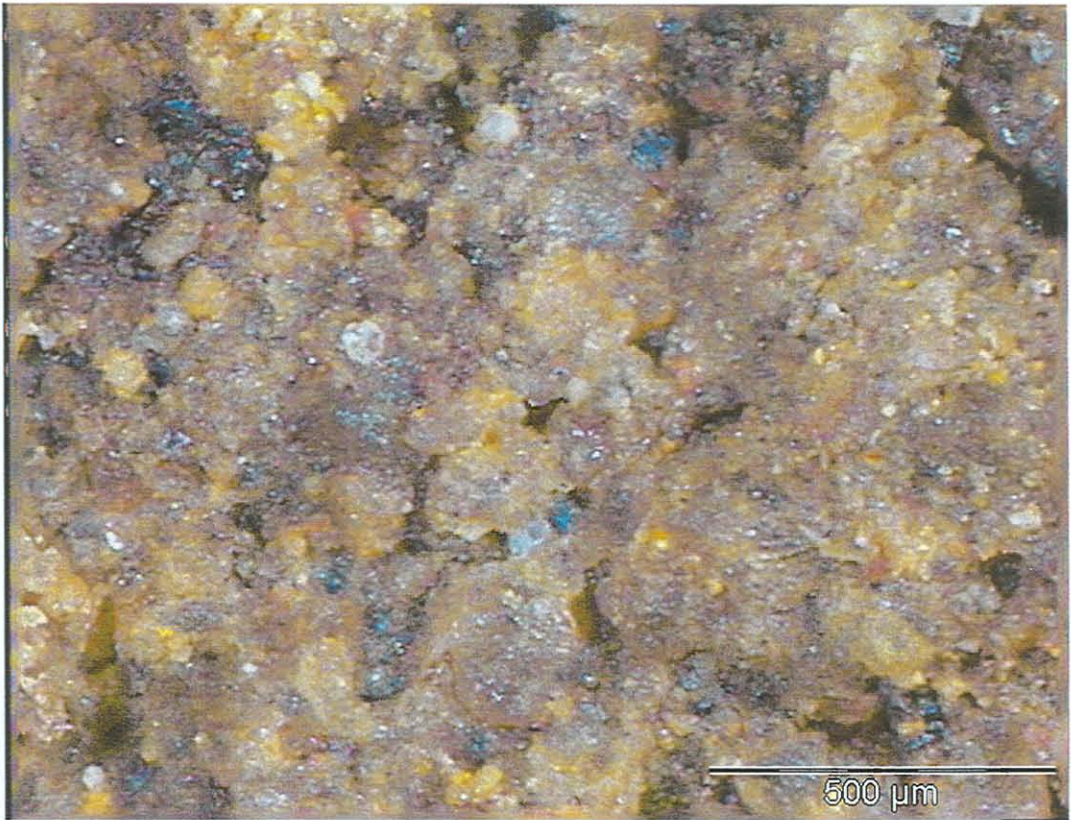
Photograph A1. 0.6 % net bitumen, 0% cement, 7x magnification



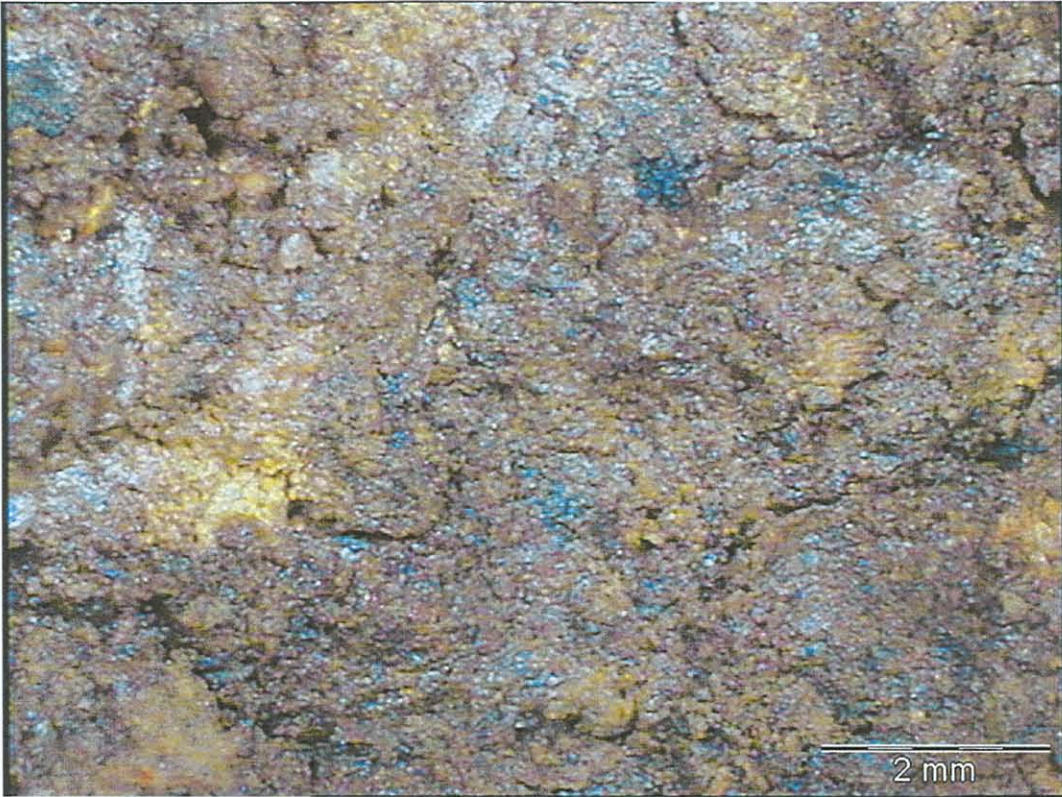
Photograph A2. 0.6 % net bitumen, 0% cement, 50x magnification



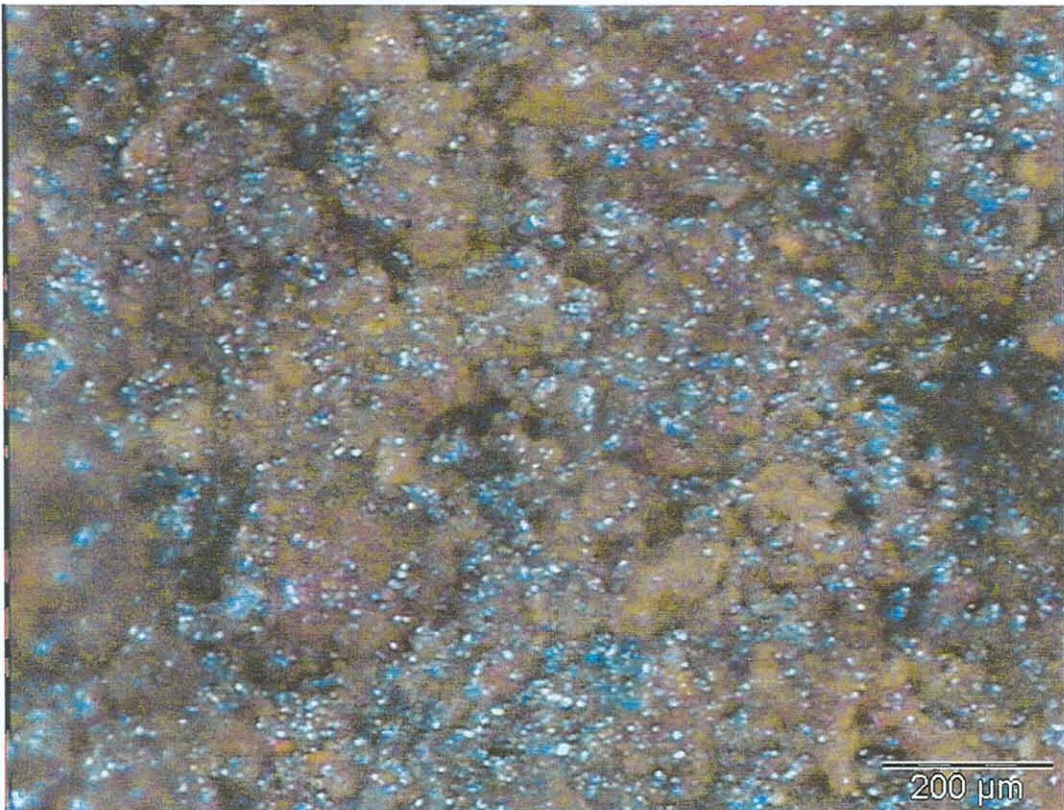
Photograph A3. 0.6 % emulsion, 1% cement, 7x magnification



Photograph A4. 0.6 % emulsion, 1% cement, 40x magnification



Photograph A5. 1.8% net bitumen, 0% cement, 7x magnification



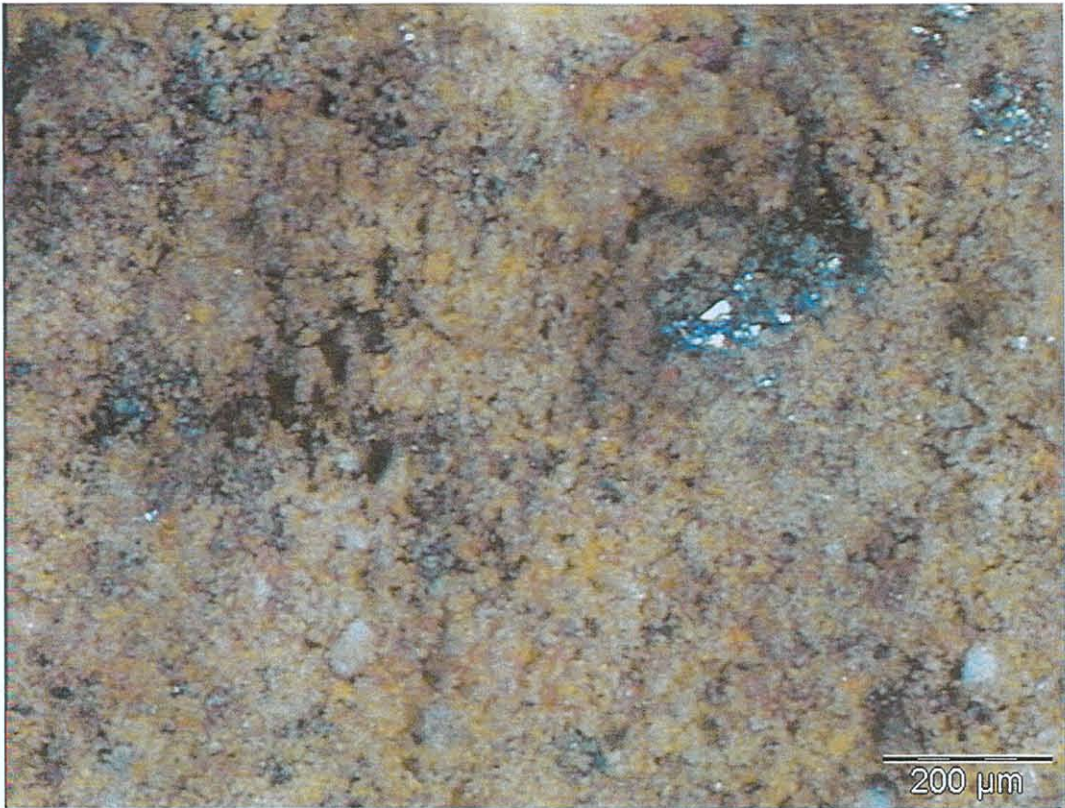
Photograph A6. 1.8% net bitumen, 0% cement, 50x magnification (sample very wet)



Photograph A7. 1.8% net bitumen, 1% cement, 7x magnification



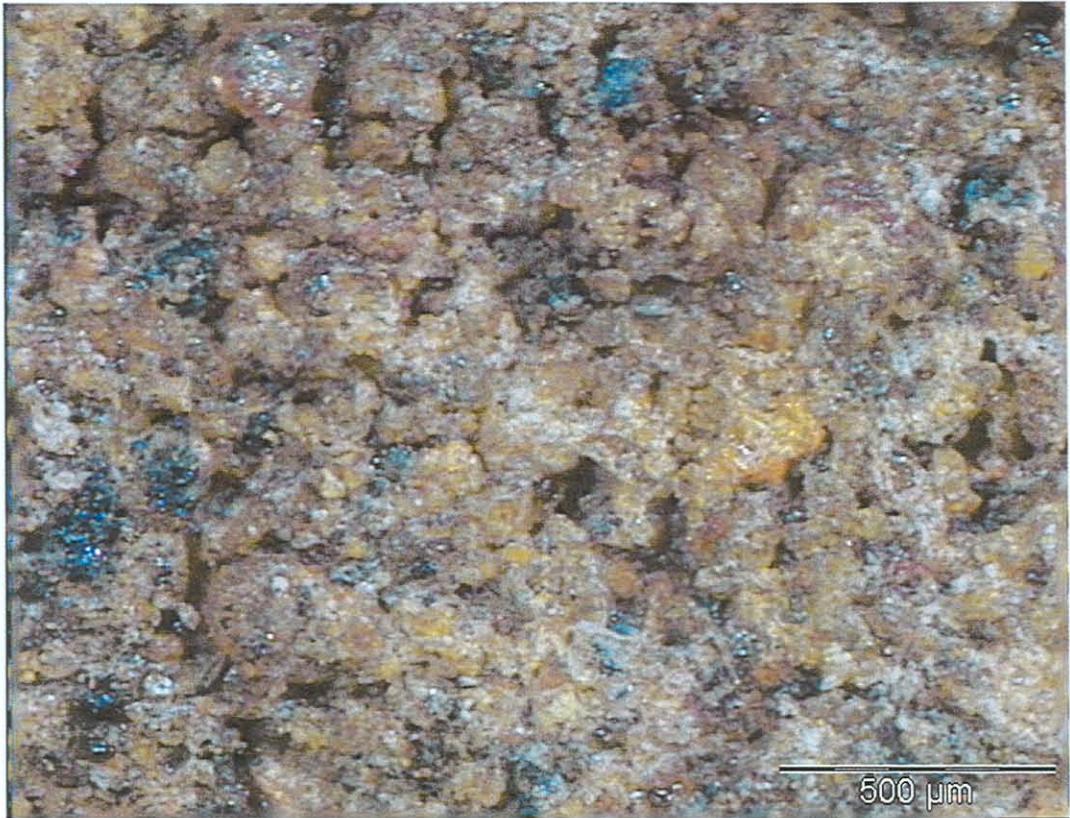
Photograph A8. 1.8% net bitumen, 1% cement, 40x magnification



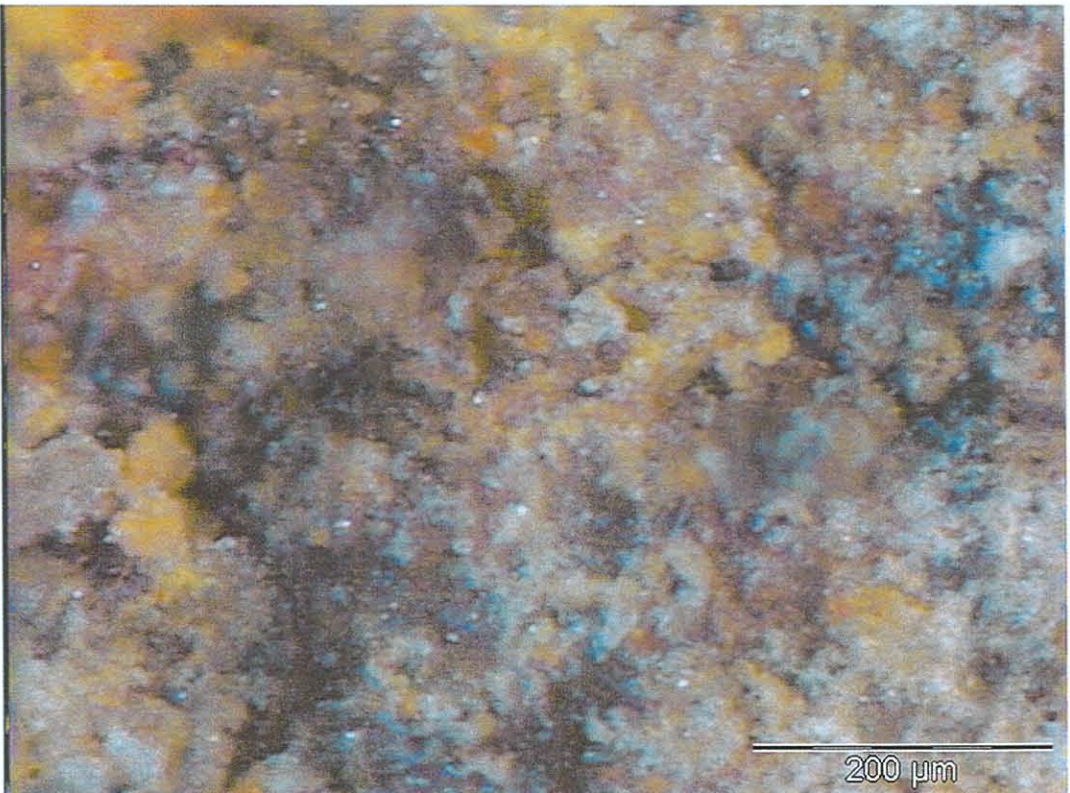
Photograph A9. 1.8% net bitumen, 1% cement, 50x magnification



Photograph A10. 1.8% net bitumen, 2% cement, 7x magnification



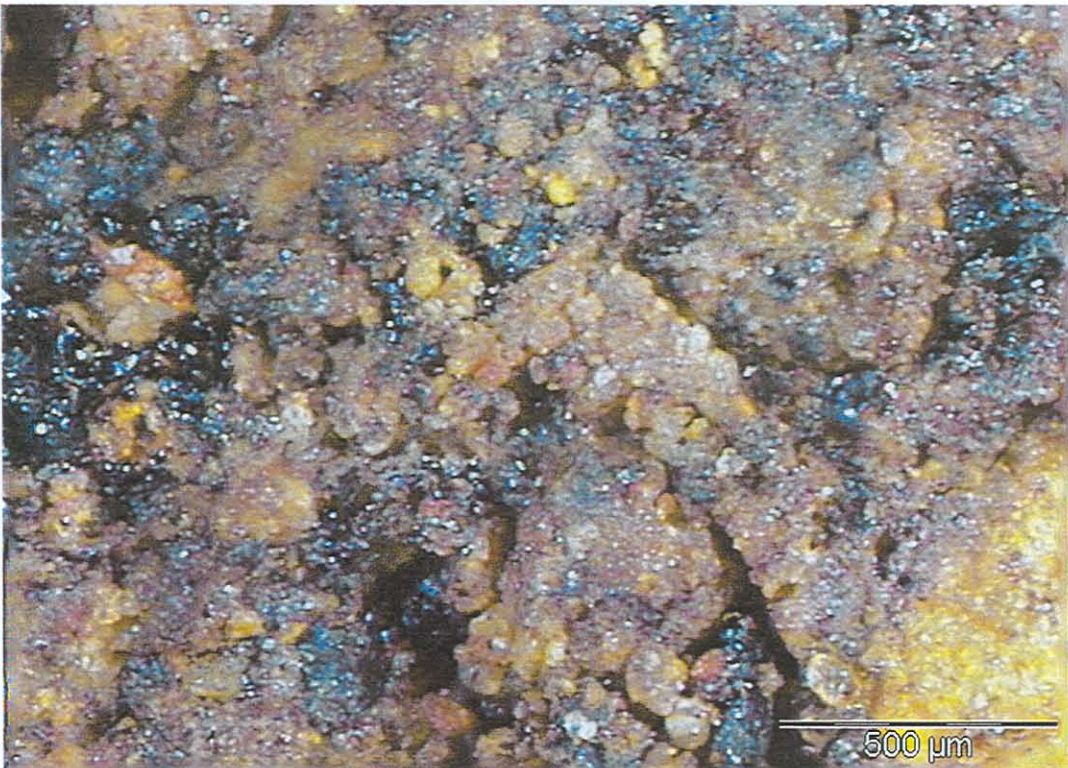
Photograph A11. 1.8% net bitumen, 2% cement, 32x magnification



Photograph A12. 1.8% net bitumen, 2% cement, 90x magnification



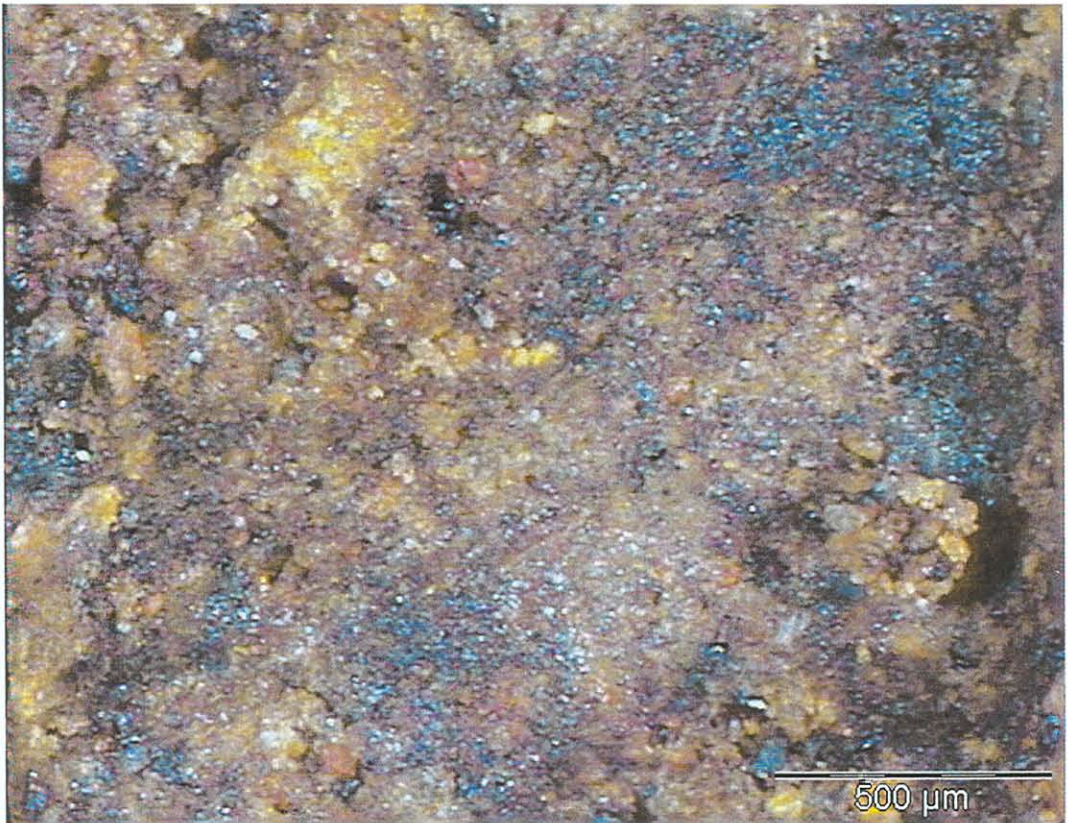
Photograph A13. 3.0% net bitumen, 0% cement, 7x magnification



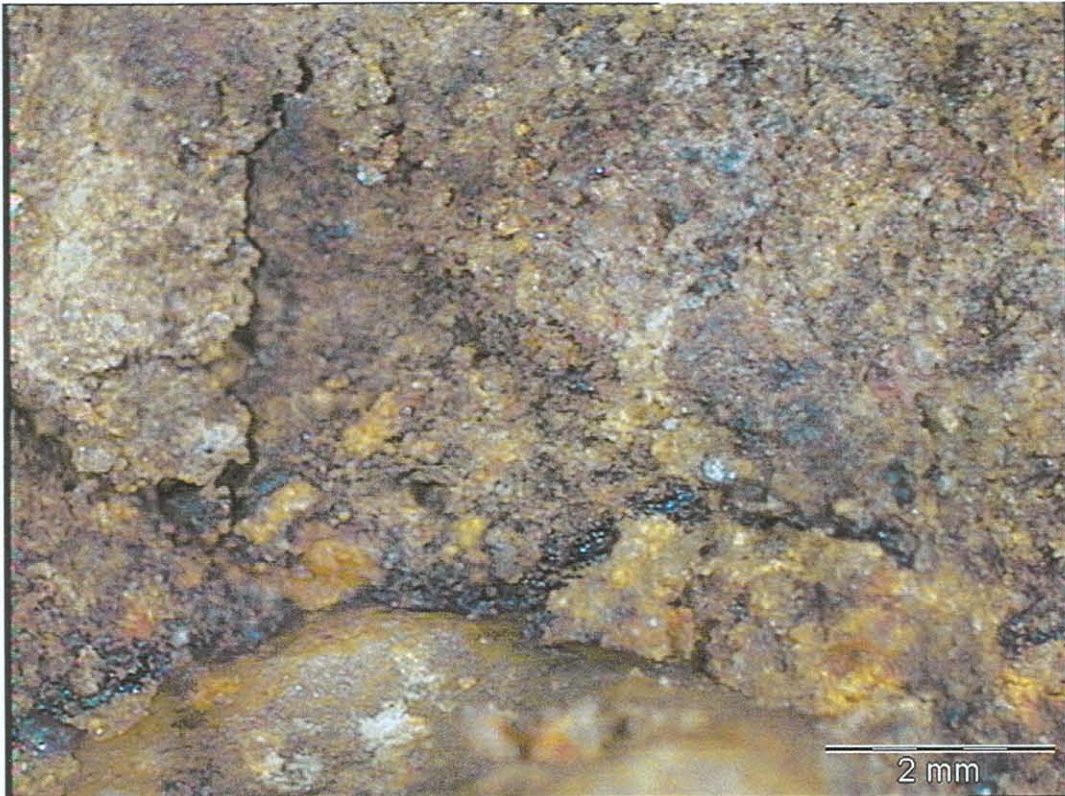
Photograph A14. 3.0% net bitumen, 0% cement, 32x magnification



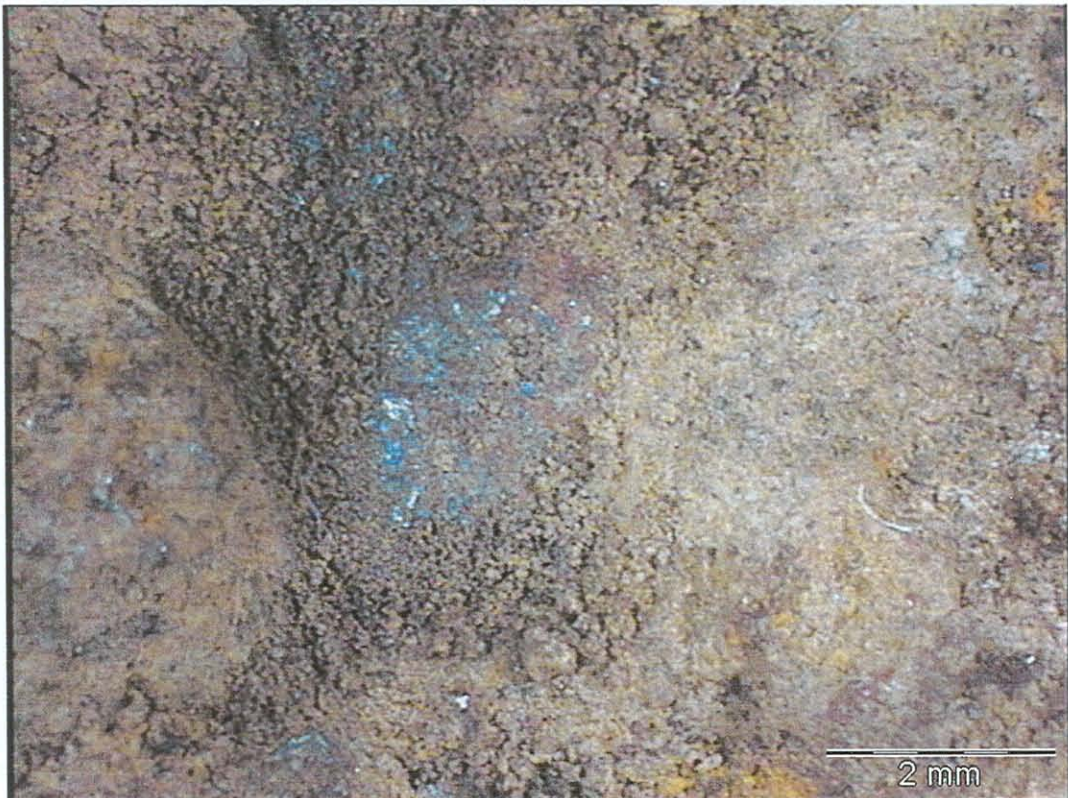
Photograph A15. 3.0% net bitumen, 1% cement, 7x magnification



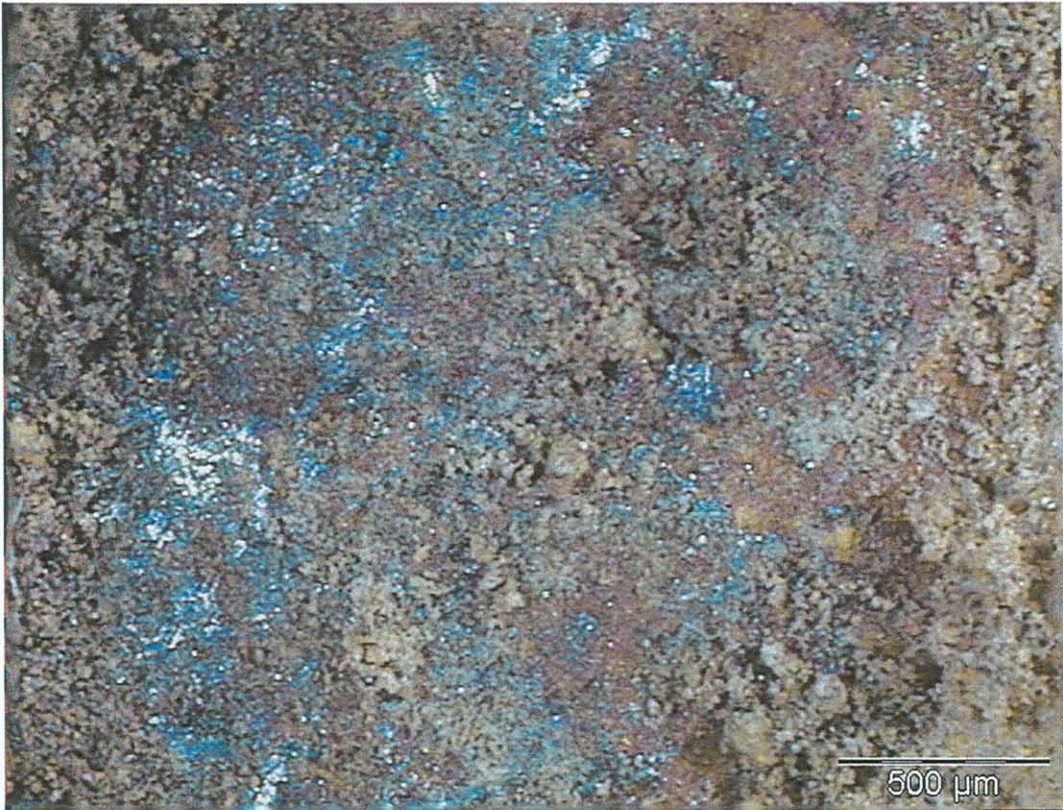
Photograph A16. 3.0% net bitumen, 1% cement, 32x magnification



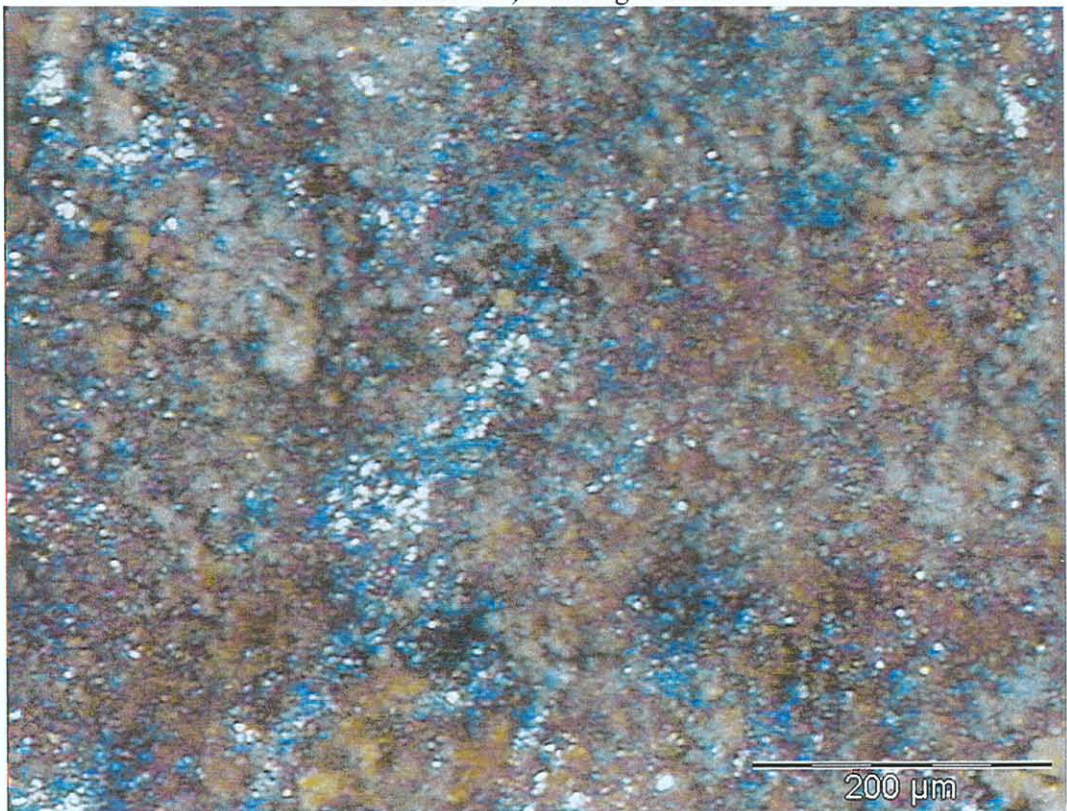
Photograph A17. 3.0% net bitumen, 1% cement, 7x magnification (note bitumen film around bigger aggregate)



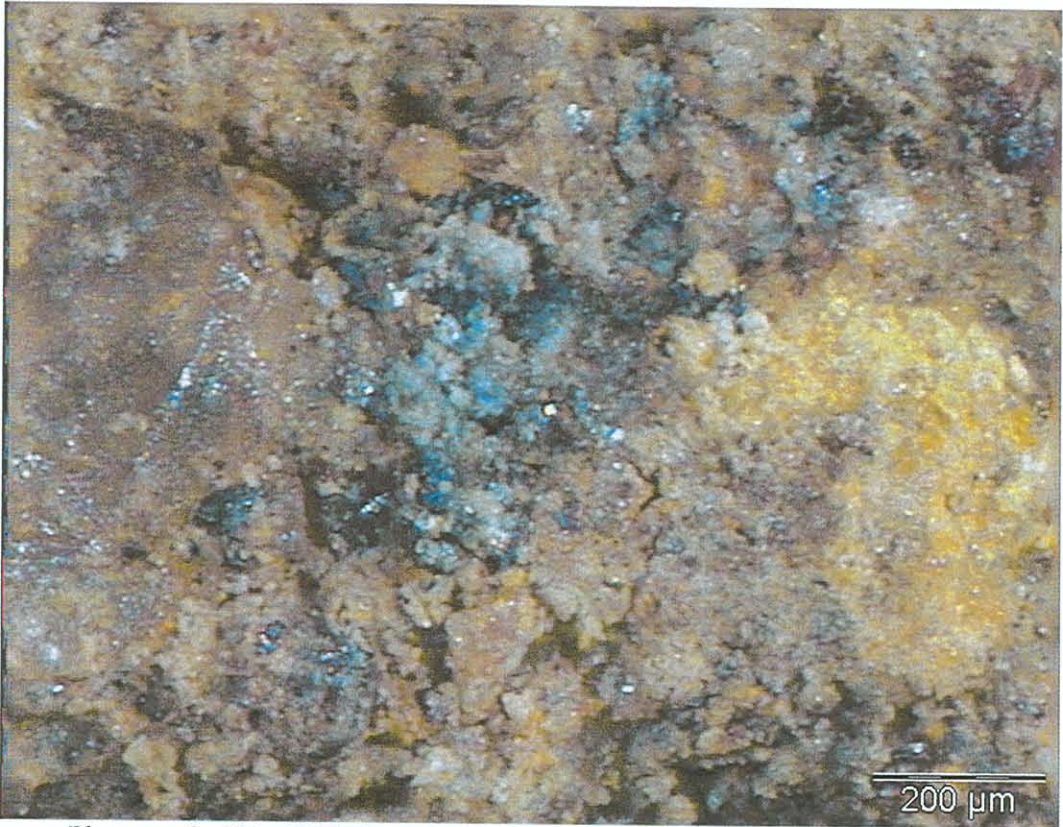
Photograph 18. HVS site sample. Aggregate coated with bitumen, 7x magnification



Photograph 19. HVS site sample. Aggregate coated with bitumen. (Some of the binder has been rubbed off) 25x magnification



Photograph A20. HVS site sample. Aggregate coated with bitumen. (Some of the binder has been rubbed off) 90x magnification



Photograph A21. HVS site sample. Bitumen with cement, 50x magnification

HVS / SVN NUMBER 4		TEST PROGRAM			km :- 14.310 - 14.318		TEST LOAD 80kN		Start Date 26/09/2000		
Base ETB		Section no. 410A4			Road No. P243-1		Tyre Pressure 800 kPa		Dual Wheel		
REPETITIONS	DATE	DISK NO.	WHEEL TRAFFIC LOAD KN	PROFILO-METER	MDD LOADS KN ALONG C/L	RSD LOADS KN ALONG C/L	RSD LOADS KN AT 200 TS	RSD LOADS KN AT 200 CS	PHOTOS	TEMPERATURE THERMOCOUPLES	MDD Depths & Positions
				MP 0 to 15	Points 4 & 12	MP 3 to 13	MP 4,6,8,10,12	MP 4,6,8,10,12		13 CS & TS	4
ON SITE CALIBRATION OF ALL INSTRUMENTS				PROF	MDD's	RSD					topcap
N10	26/09/2000	251	80	YES	40,80	40,80	40,80	40,80	YES	0 & 40 mm	275mm
50	26/09/2000	252	80	NO	40	40	No	No	NO		450mm
200	26/09/2000	253	80	NO	40	40	No	No	NO		650mm
1000	27/09/2000	254	80	YES	40	40	40	40	NO		850mm
3000	27/09/2000	255	80	YES	40	40	40	40	NO		
5000	28/09/2000	256	80	YES	40	40	40	40	NO		
7500	28/09/2000	257	80	YES	40	40	40	40	NO		
10000	29/09/2000	258	80	YES	40,80	40,80	40,80	40,80	YES	Telephone numbers	
15000	03/10/2000	259	80	YES	40	40	40	40	NO	Willie Diederiks	0823776940
20000	04/10/2000	260	80	YES	40,80	40,80	40,80	40,80	YES	Louw Du Plessis	(012) 841-2922
25000	05/10/2000	261	80	YES	40	40	40	40	NO	Wynand Steyn	(012) 841-2634
28000	05/10/2000	262	80	YES	40	40	40	40	NO	Wynand Steyn	(H)(012) 567-4685
33400	06/10/2000	263	80	YES	40	40	40	40	NO	Wynand Steyn	0822199704
37000	06/10/2000	264	80	YES	40,80	40,80	40,80	40,80	YES	Colin Fisher	(012) 841-3960
43800	07/10/2000	265	80	YES	40	40	40	40	NO	SPECIAL NOTES	
47500	07/10/2000	266	80	YES	40	40	40	40	NO	Tyre Pressure @ 800kPa & 40 kN load	
57619	08/10/2000	267	80	YES	40,80	40,80	40,80	40,80	YES	Monitor Cracks & take Photos	
87000	10/10/2000	268	80	YES	40	40	40	40	NO	Test is to be DONE DRY	
117700	12/10/2000	269	80	YES	40	40	40	40	NO	Write down PD values Daily	
190300	17/10/2000	270	80	YES	40,80	40,80	40,80	40,80	YES	All measurements mailed to cfisher@csir.co.za within 24hrs.	
233000	20/10/2000	271	80	YES	40	40	40	40	NO	STRATA READINGS AT LOADS	
295617	27/10/2000	272	80	YES	40,80	40,80	40,80	40,80	YES	ALL STRATA POINTS	
										HAPPY TESTING	

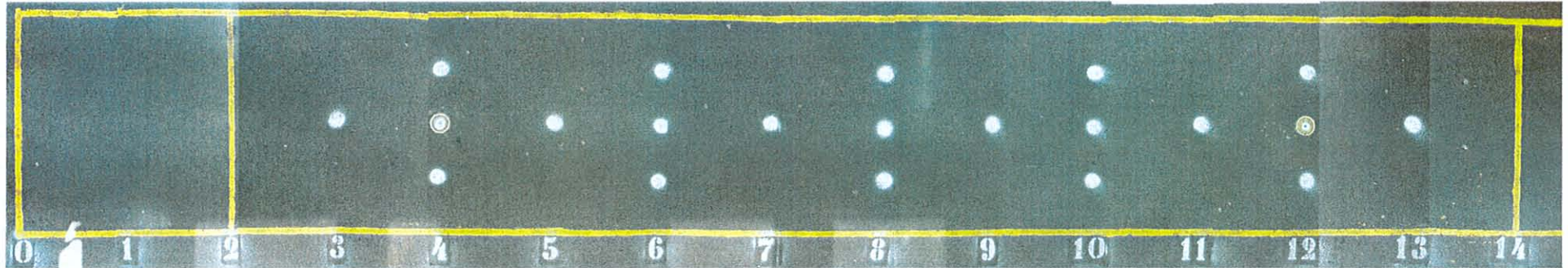
Structure Description	20 AC / 250ETB , 250 G6
Section Objectives	EVALUATION OF THE ETB

HVS / SVN NUMBER 4		TEST PROGRAM				km :- 14.310 - 14.318		TEST LOAD 100kN		Start Date 30/10/2000	
Base ETB		Section no. 410B4			Road No. P243-1			Tyre Pressure 850 kPa		Dual Wheel	
REPETITIONS	DATE	DISK NO.	WHEEL TRAFFIC LOAD kN	PROFILO-METER MP 0 to 15	MDD LOADS kN ALONG C/L 4 & 12	RSD LOADS kN ALONG C/L MP 3 to 13	RSD LOADS kN AT 200 TS MP 4,6,8,10,12	RSD LOADS kN AT 200 CS MP 4,6,8,10,12	PHOTOS	TEMPERATURE THERMOCOUPLES 5 CS & TS 0 & 40 mm	MDD Depths & Positions 4 & 12 topcap 275mm 450mm 650mm 850mm
ON SITE CALIBRATION OF ALL INSTRUMENTS				PROF	MDD's	RSD					
N10	31/10/2000	273	100	YES	40,80	40,80	40,80	40,80	YES		
50	31/10/2000	274	100	NO	40	40	No	No	NO		
200	31/10/2000	275	100	NO	40	40	40	40	NO		
1000	01/11/2000	276	100	YES	40	40	40	40	NO		
2000	01/11/2000	277	100	YES	40	40	40	40	NO		
3000	01/11/2000	278	100	YES	40	40	40	40	NO		
4000	02/11/2000	279	100	YES	40	40	40	40	NO	Telephone numbers <i>Willie Diederiks</i> 0823776940 <i>Louw Du Plessis</i> (012) 841-2922 <i>Wynand Steyn</i> (012) 841-2634 <i>Wynand Steyn</i> (H)(012) 567-4685 <i>Wynand Steyn</i> 0822199704 <i>Colin Fisher</i> (012) 841-3960	
6000	02/11/2000	280	100	YES	40	40	40	40	NO		
8000	02/11/2000	281	100	YES	40	40	40	40	NO		
10000	07/11/2000	282	100	YES	40,80	40,80	40,80	40,80	YES		
39600	09/11/2000	283	100	YES	40	40	40	40	NO		
50000	10/11/2000	284	100	YES	40	40	40	40	NO		
70000	14/11/2000	285	100	YES	40,80	40,80	40,80	40,80	YES		
80000	15/11/2000	286	100	YES	40	40	40	40	NO	SPECIAL NOTES Tyre Pressure @ 850kPa & 40 kN load Monitor Cracks & take Photos Test is to be DONE DRY Write down PD values Daily All measurements mailed to cfisher@csir.co.za within 24hrs. STRATA READINGS AT LOADS ALL STRATA POINTS HAPPY TESTING	
100000	16/11/2000	287	100	YES	40,80	40,80	40,80	40,80	YES		
129544	20/11/2000	288	100	YES	40	40	40	40	NO		
171500	23/11/2000	289	100	YES	40,80	40,80	40,80	40,80	YES		
185407	28/11/2000	290	100	YES	40,80	40,80	40,80	40,80	YES		
Structure Description		20 AC / 250 ETB , 250 G6									
Section Objectives		EVALUATION OF THE ETB									

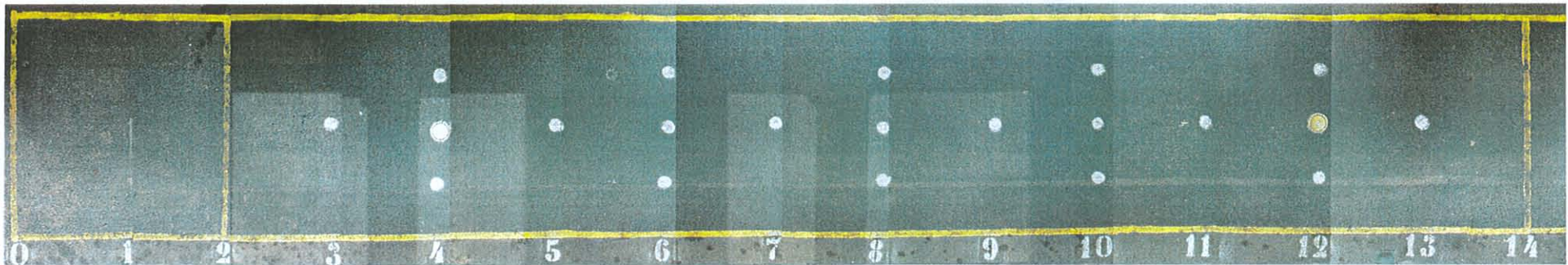
HVS / SVN NUMBER 4		TEST PROGRAM					TEST LOAD	40kN	Start Date 04/07/2001		
Base ETB		Section no. 412A4			Road No. P243-1		Tyre Pressure 620 kPa		Dual Wheel		
REPETITIONS	DATE	DISK NO.	WHEEL TRAFFIC LOAD kN	PROFILO-METER	MDD LOADS kN ALONG C/L	RSD LOADS kN ALONG C/L	RSD LOADS kN AT 200 TS	RSD LOADS kN AT 200 CS	PHOTOS	TEMPERATURE THERMOCOUPLES	MDD Depths & Positions 4, 8, 12
ON SITE CALIBRATION OF ALL INSTRUMENTS				PROF	MDD's	RSD					
N10	04/07/2001	31	40	YES	40	40	40	40	YES	4 & 12 CS & TS	topcap 275mm
2000	05/07/2001	32	40	YES	40	40	40	40		0 & 25 mm	450mm
5000	06/07/2001	33	40	YES	40	40	40	40			650mm
10000	09/07/2001	34	40	YES	40	40	40	40			850mm
15000	10/07/2001	35	40	YES	40	40	40	40			
20000	11/07/2001	35	40	YES	40	40	40	40		Telephone numbers	
40000	13/07/2001	36	40	YES	40	40	40	40			
60000	16/07/2001	37	40	YES	40	40	40	40		Louw Du Plessis	(012) 841-2922
175395	24/07/2001	38	40	YES	40	40	40	40		Wynand Steyn	(012) 841-2634
300814	15/08/2001	39	40	YES	40	40	40	40		Wynand Steyn	(H)(012) 567-4685
401700	22/08/2001	40	40	YES	40	40	40	40		Colin Fisher	(012) 841-3960
490800	29/08/2001	41	40	YES	40	40	40	40		SPECIAL NOTES	
597900	06/09/2001	42	40	YES	40	40	40	40		Monitor Cracks & take Photos	
695000	20/09/2001	43	40	YES	40	40	40	40		Test is to be DONE DRY	
827100	03/10/2001	44	40	YES	40	40	40	40		Write down PD values Daily	
957121	11/10/2001	45	40	YES	40	40	40	40			
1019700	15/10/2001	46	80	YES	40	40	40	40			
1052100	18/10/2001	47	80	YES	40, 80	40, 80	40	40			
1128700	24/10/2001	48	80	YES	40, 80	40, 80	40	40			
1226000	21/10/2001	49	80	YES	40, 80	40, 80	40	40	YES		
1321700 wet	06/11/2001	50	80	YES	40/80	40/80	40	40	YES		

Structure Description	20 AC / 250 Emulsion Treated Base (ETB) , 250 G6
Section Objectives	EVALUATION OF THE FOAMED BITUMEN BASE & ETB

Crack Pattern: Section 410A4 (80 kN)

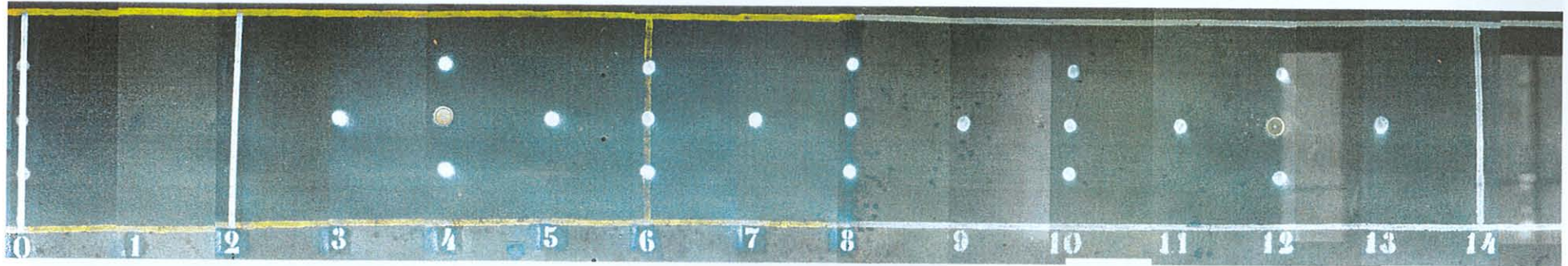


Repetitions = 10

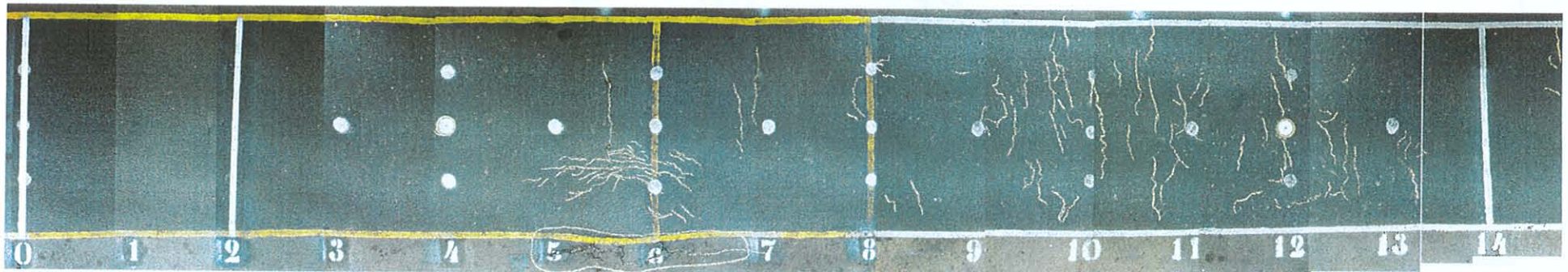


Repetitions = 295 617

Crack Pattern: Section 410B4 (100 kN)

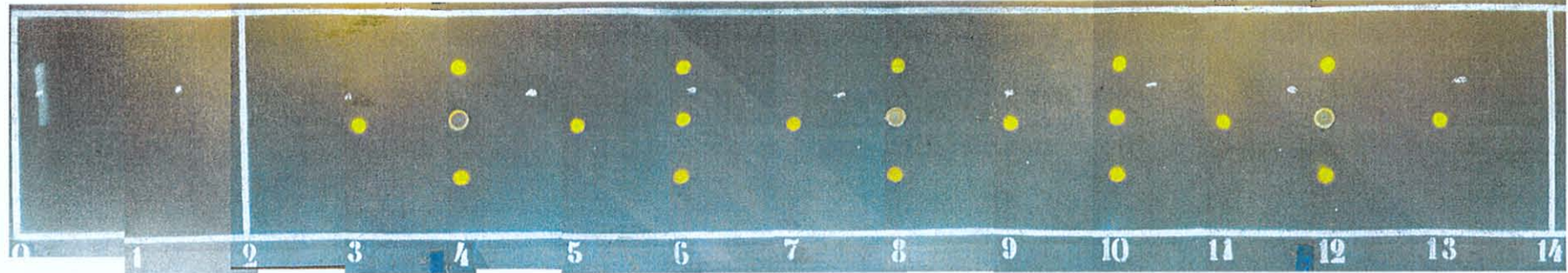


Repetitions = 10

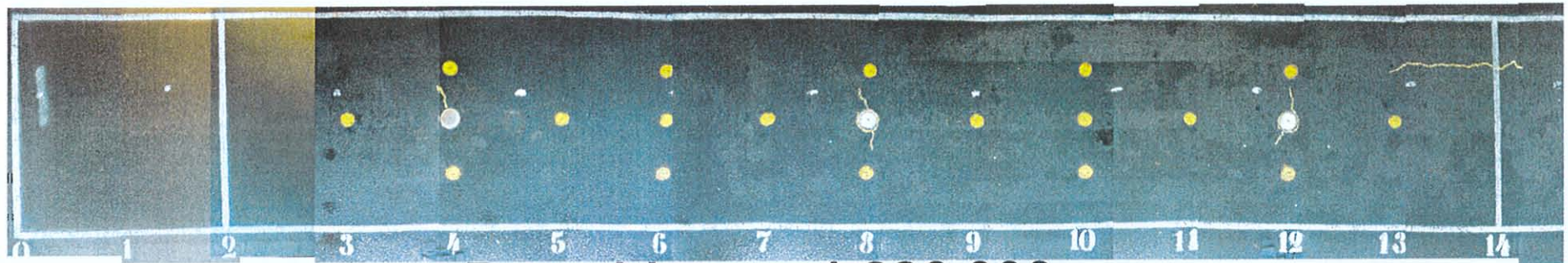


Repetitions = 129 544

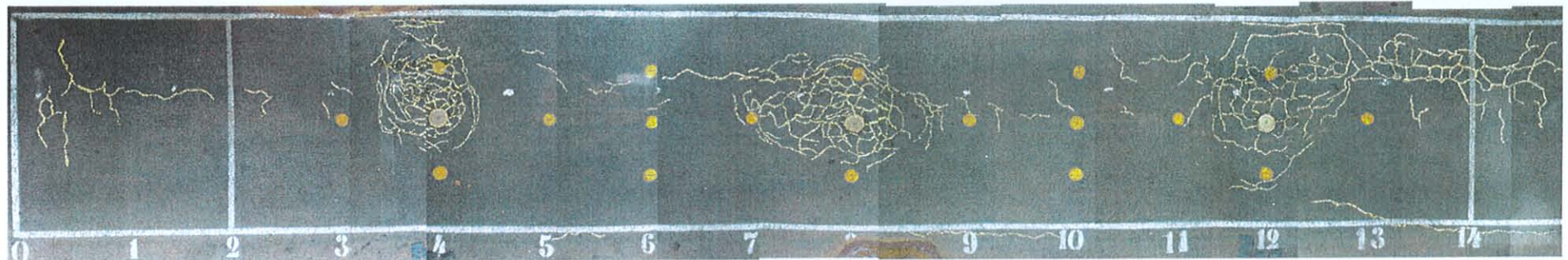
Crack Pattern: Section 412A4 (40 kN)



Repetitions = 10

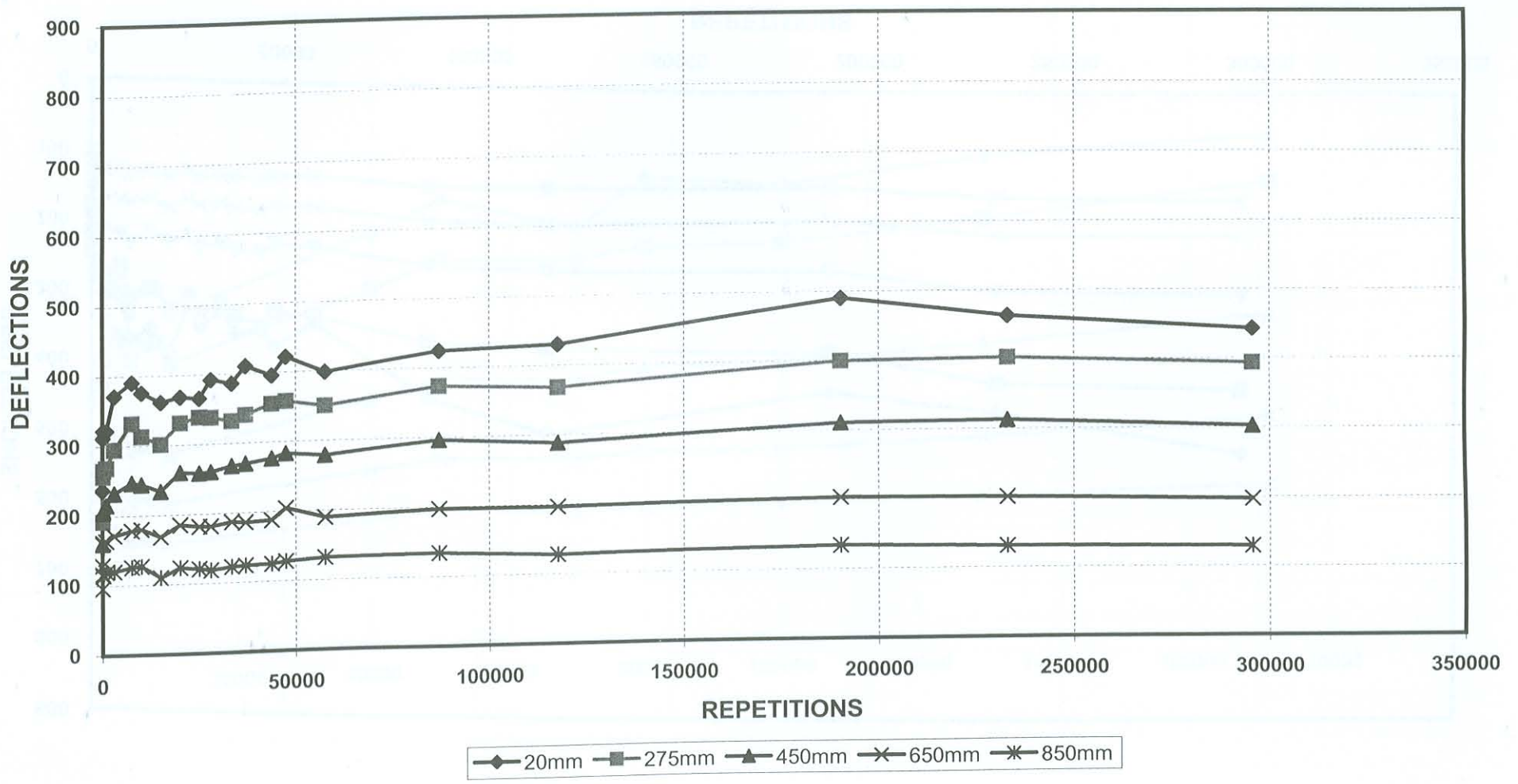


Repetitions = 1 226 000



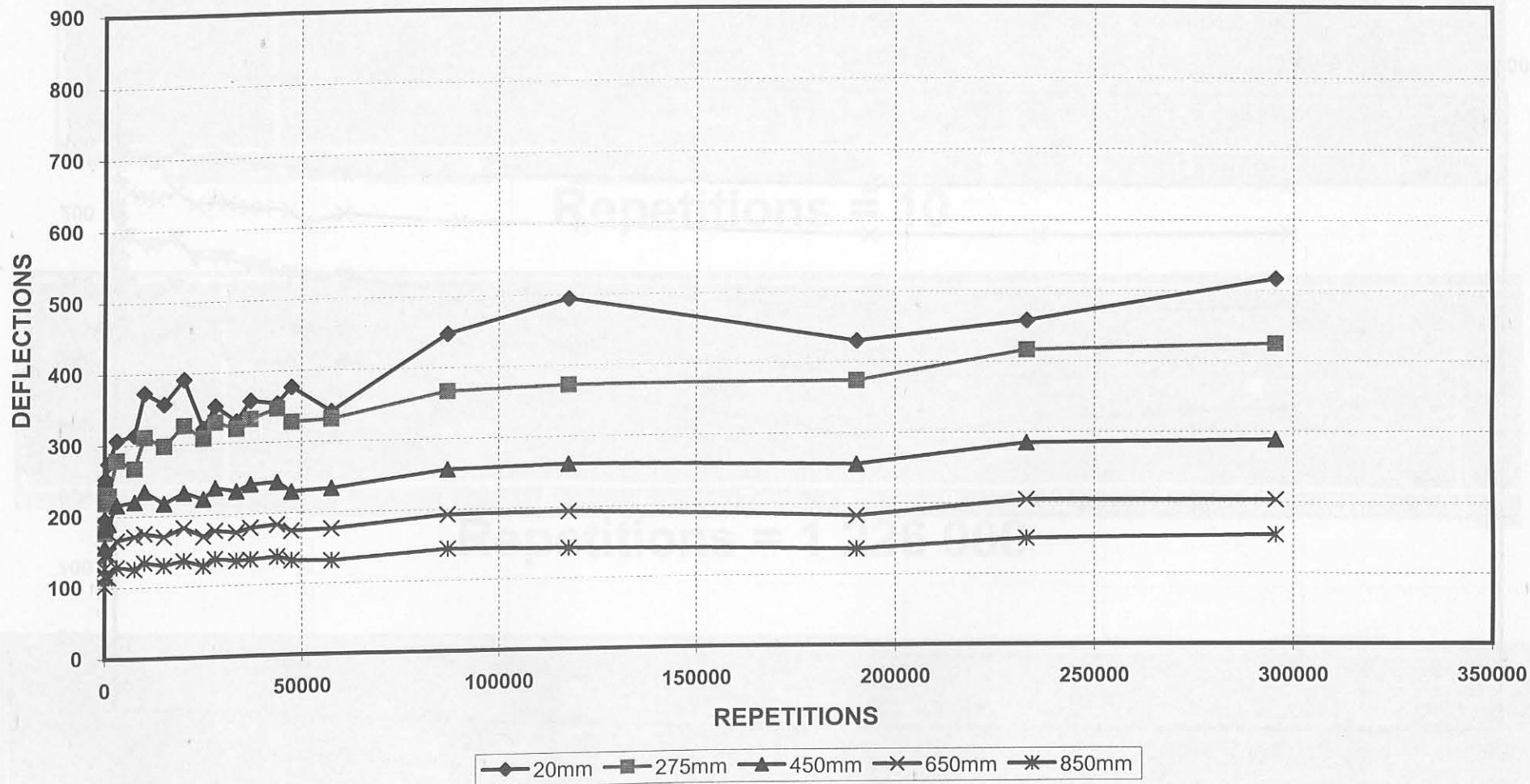
Repetitions = 1 321 700

MDD 4 DEFLECTION AT 40kN ON SECTION 410A4 (250 ETB)

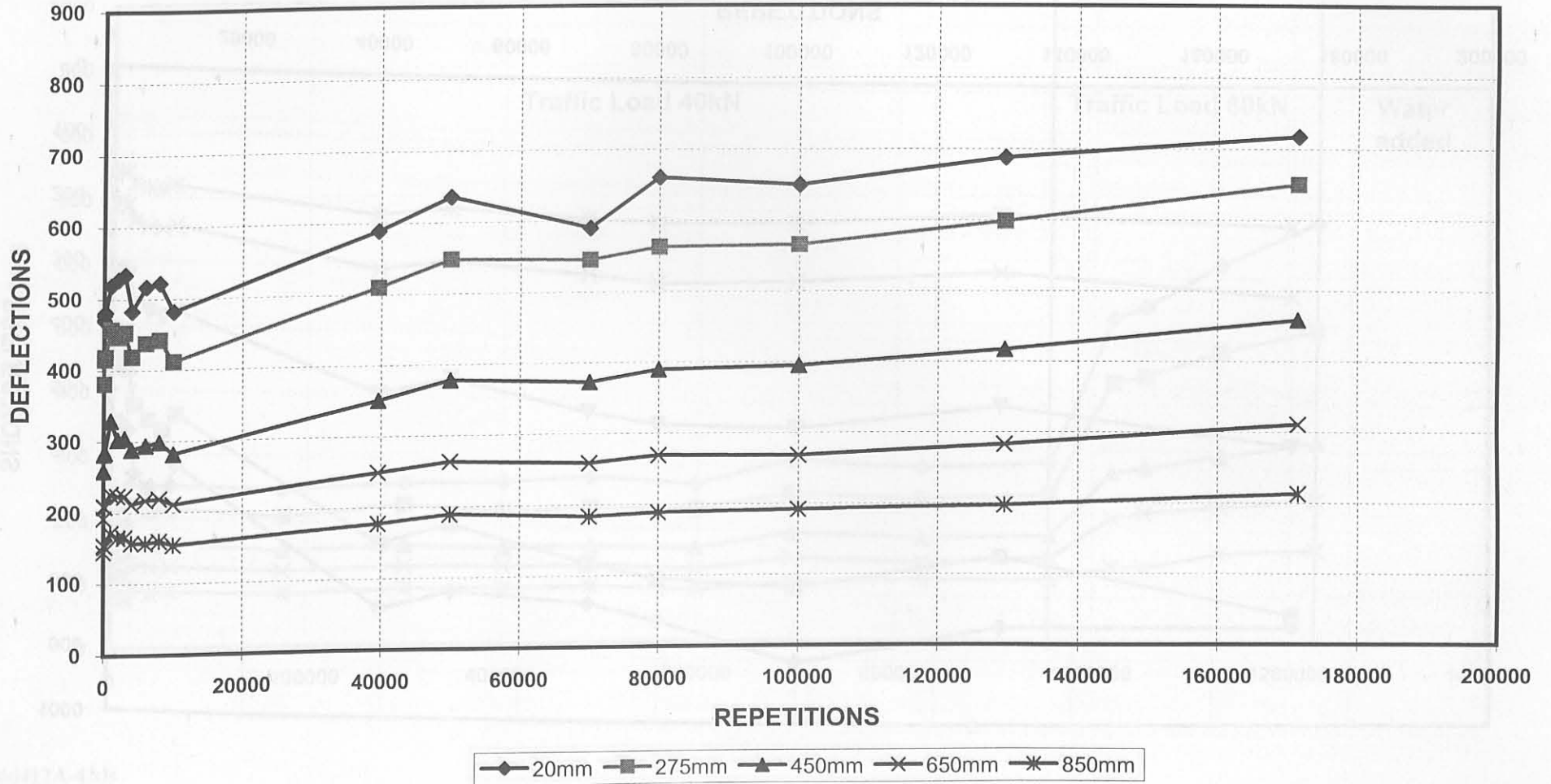


Crack Pattern: Section 412A4 (40 kN)

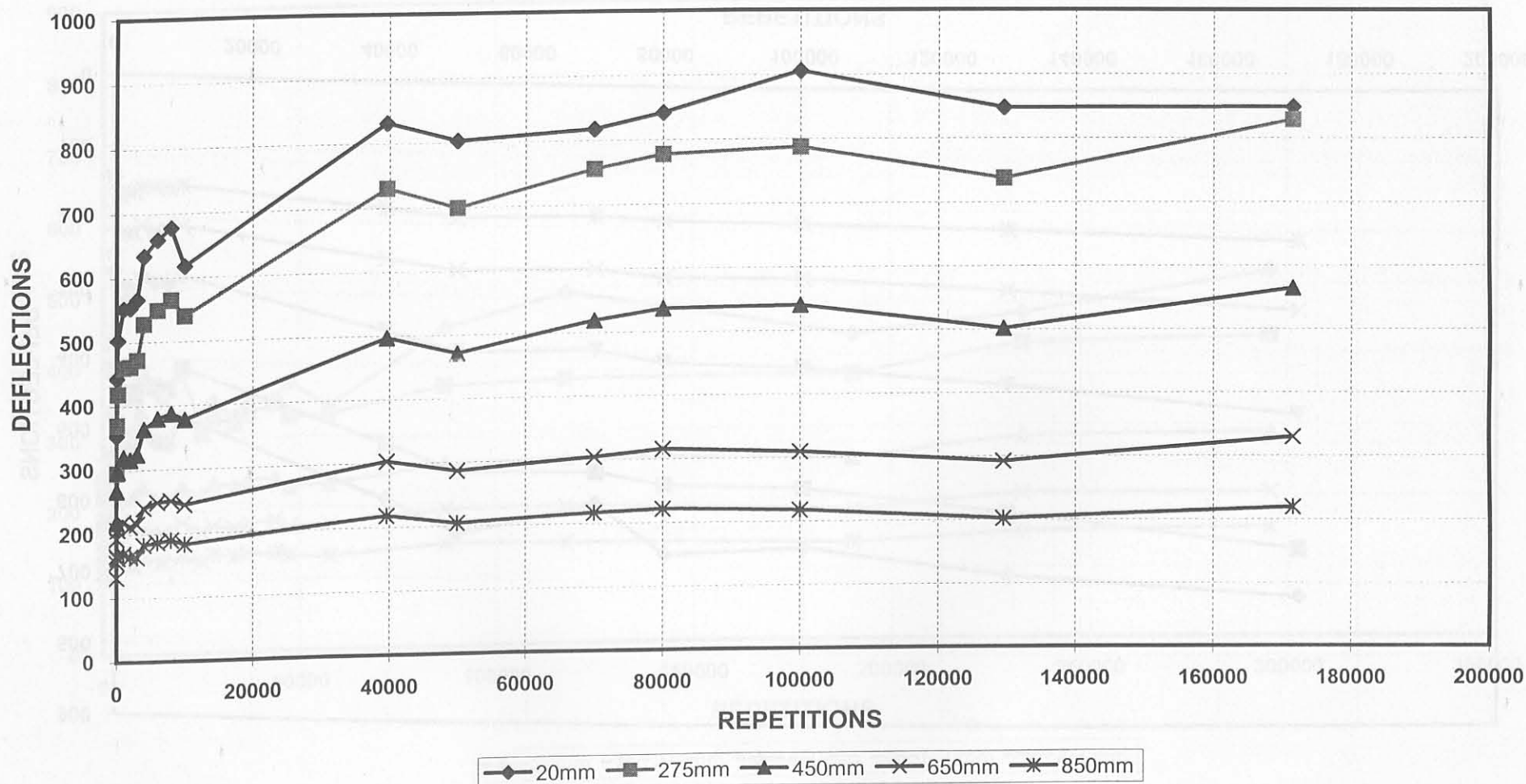
MDD 12 DEFLECTION AT 40kN ON SECTION 410A4 (250 ETB)



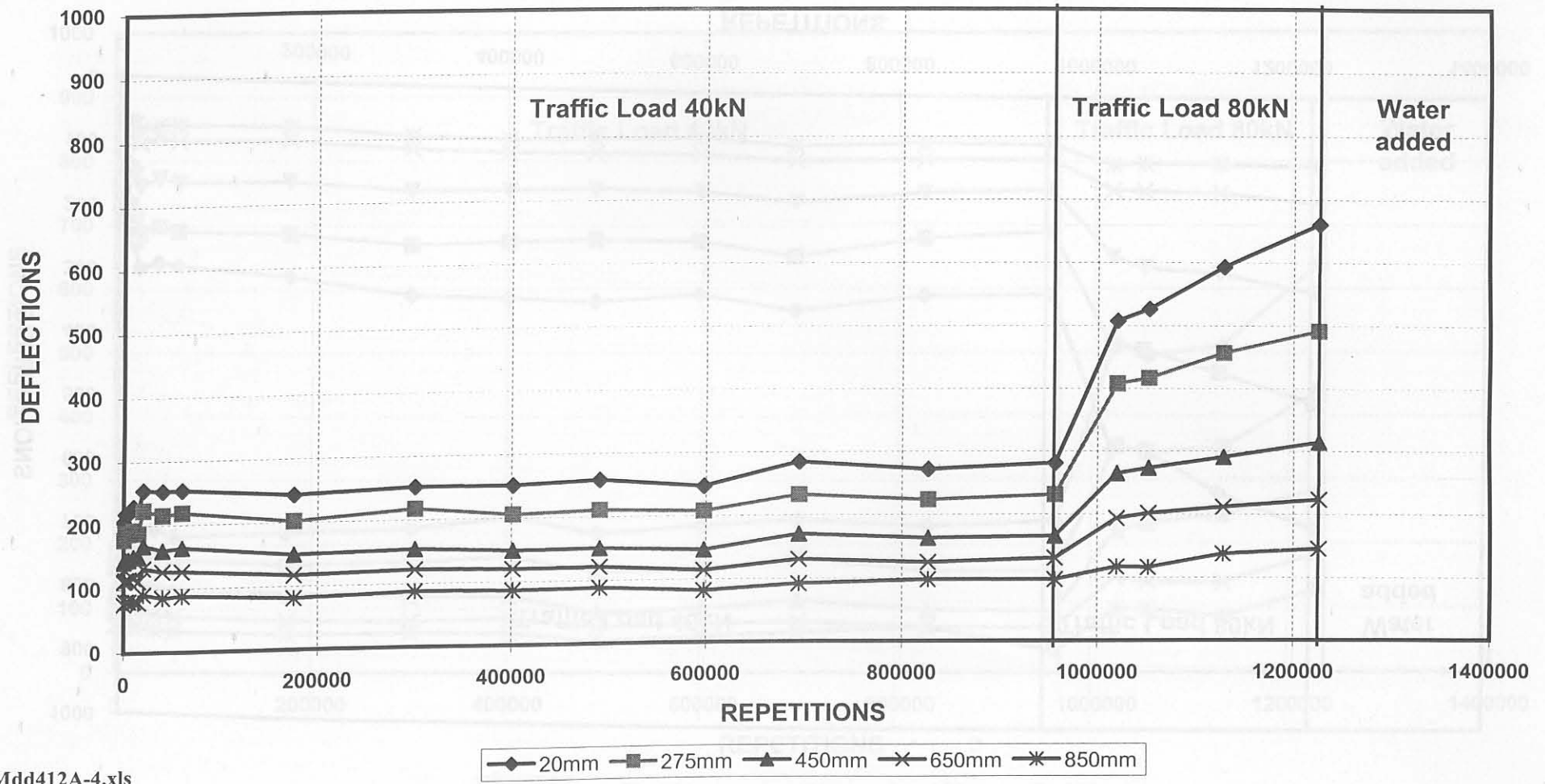
MDD 4 DEFLECTION AT 40kN ON SECTION 410B4 (250 ETB)



MDD 12 DEFLECTION AT 40kN ON SECTION 410B4 (250 ETB)

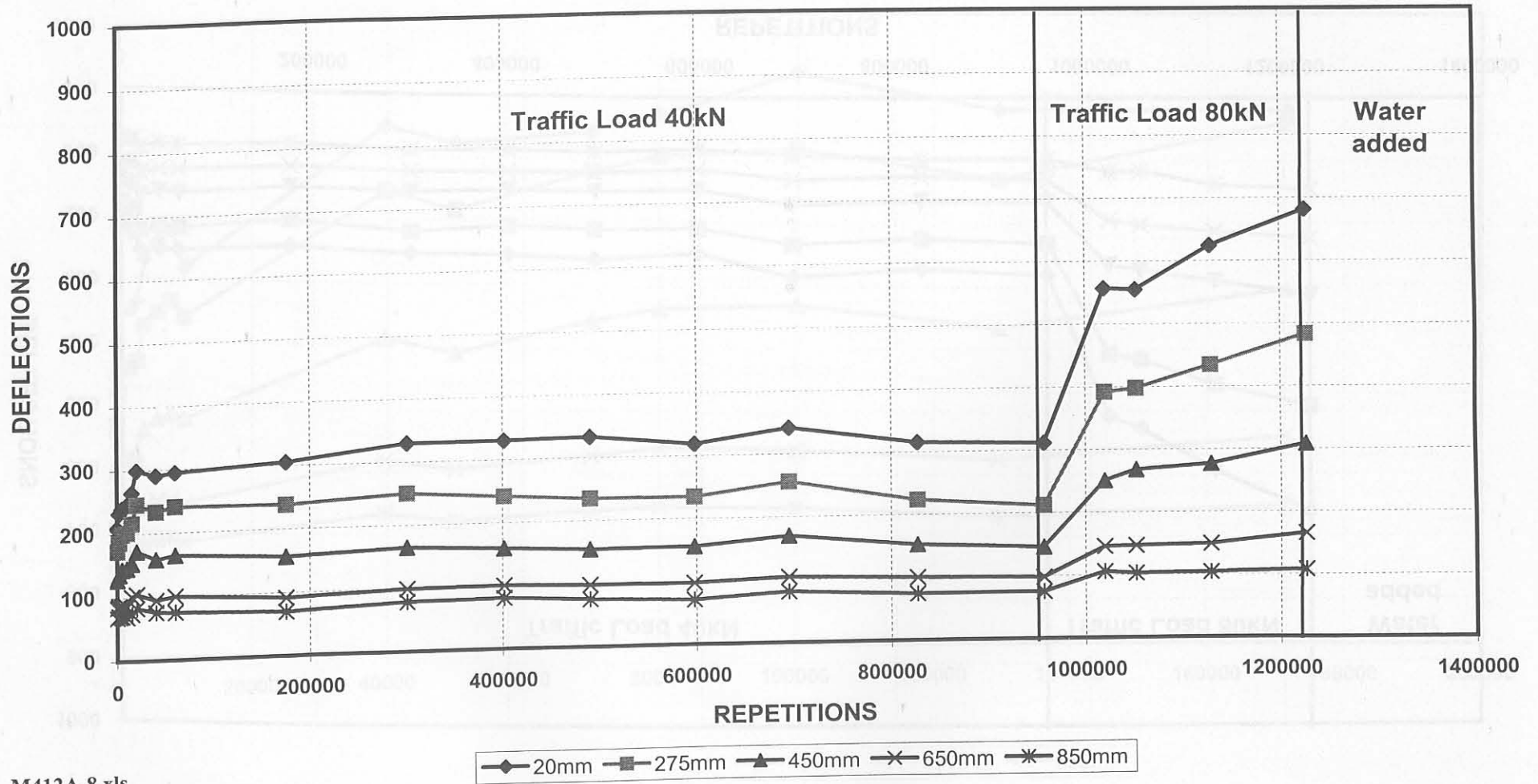


MDD 4 DEFLECTION AT 40kN ON SECTION 412A4 (250 ETB)

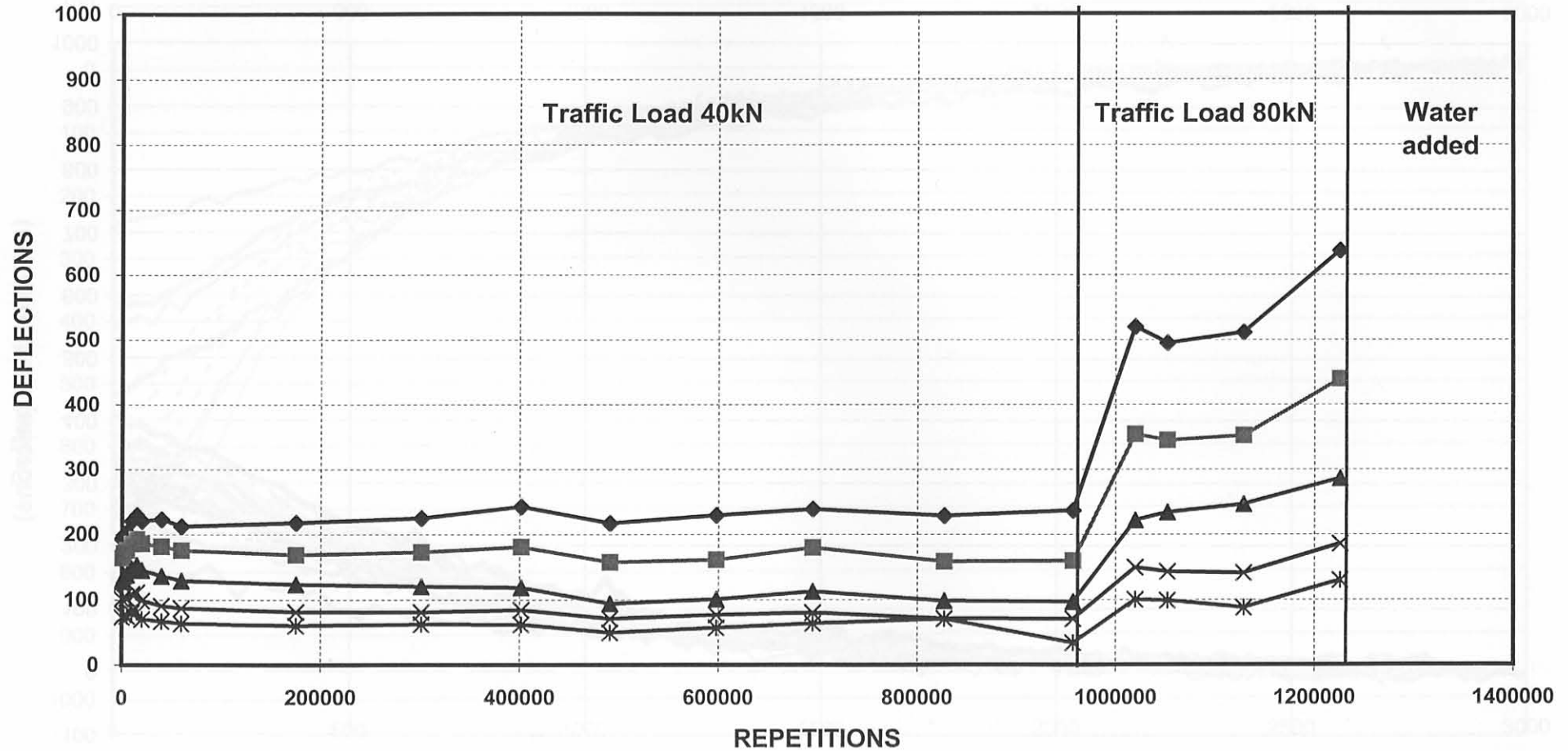


Mdd412A-4.xls

MDD 8 DEFLECTION AT 40kN ON SECTION 412A4 (250 ETB)

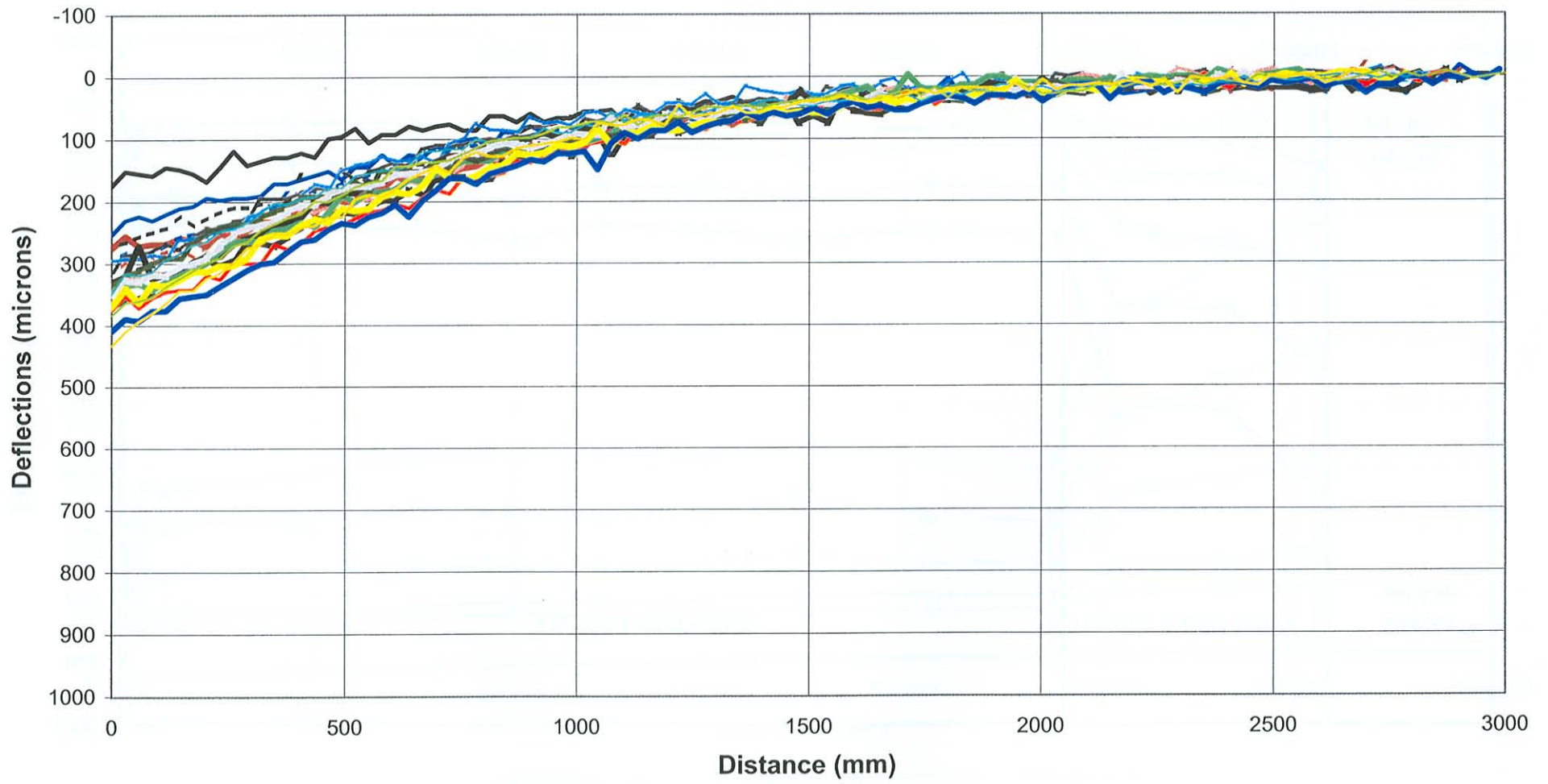


MDD 12 DEFLECTION AT 40kN ON SECTION 412A4 (250 ETB)



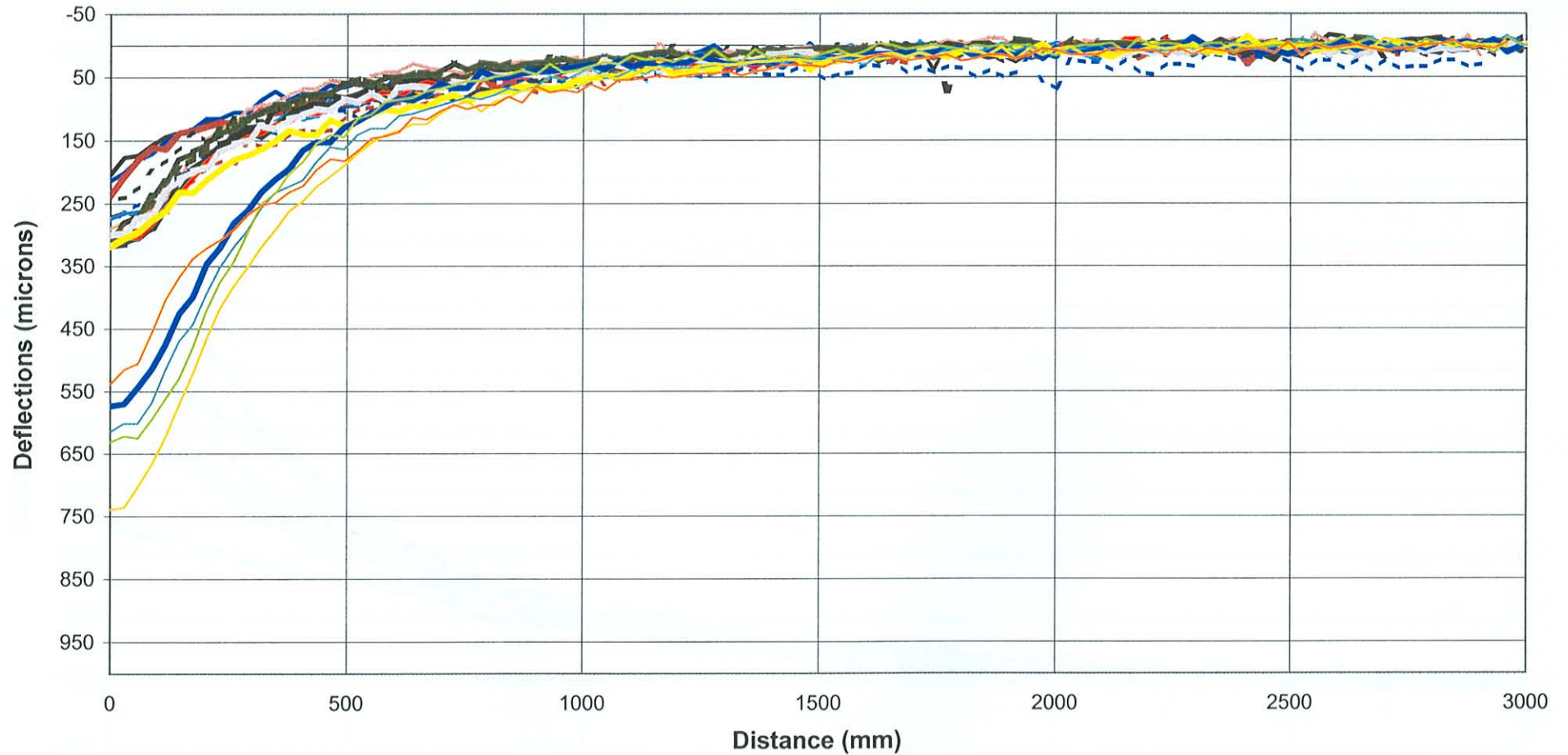
—◆— 20mm —■— 275mm —▲— 450mm —×— 650mm —*— 850mm

Section 410A4 RSD at Point 8 CentreLine Test Load 40kN



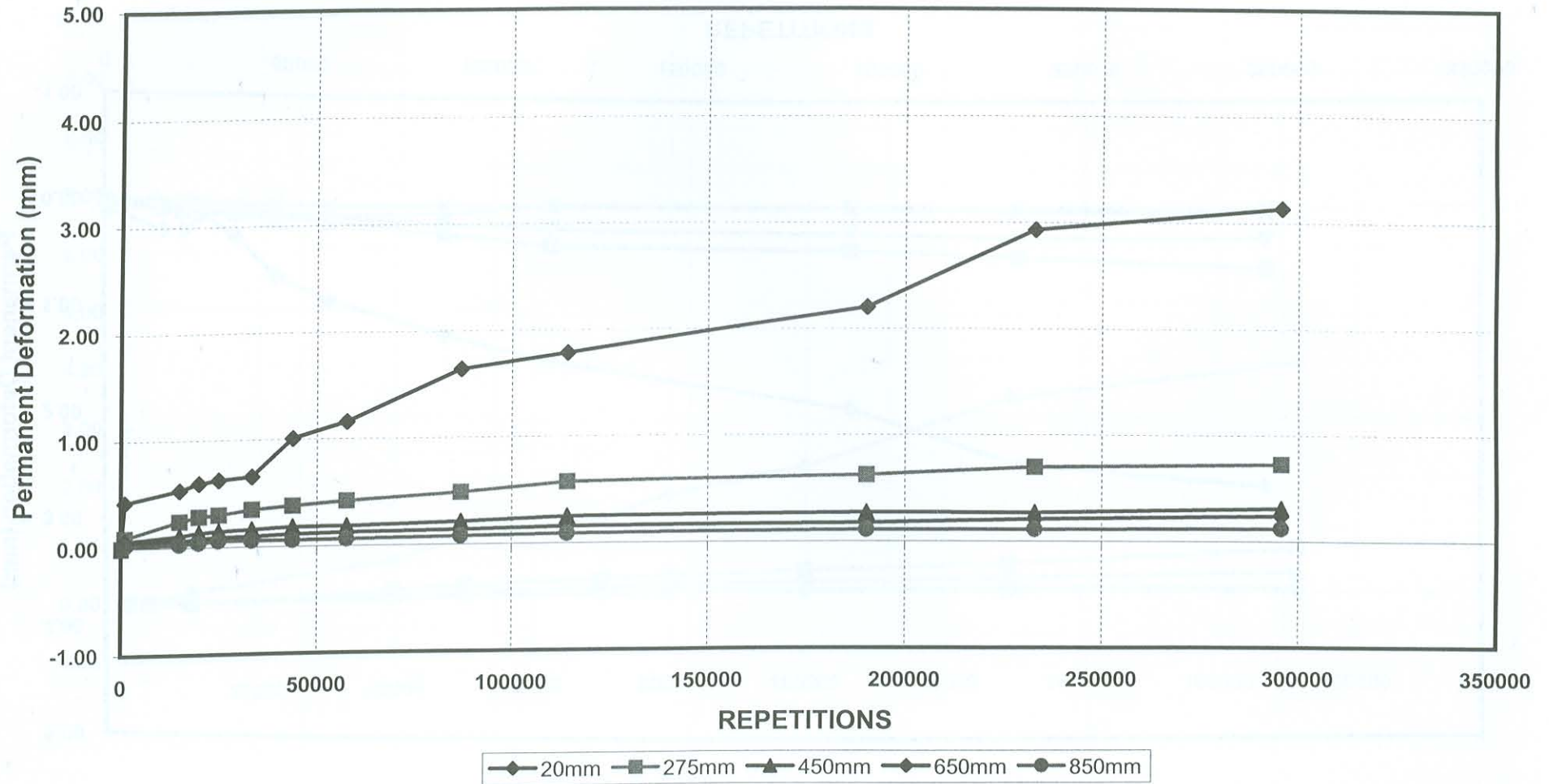
- | | | | | | | | | | |
|-------|-------|-------|-------|-------|-------|-------|--------|--------|--------|
| 10 | 50 | 200 | 1000 | 3000 | 5000 | 7500 | 10000 | 20000 | 25000 |
| 28000 | 33400 | 37000 | 43800 | 47500 | 57619 | 87000 | 117700 | 190300 | 233000 |

Section 412A4 RSD at Point 8 CentreLine Test Load 40kN

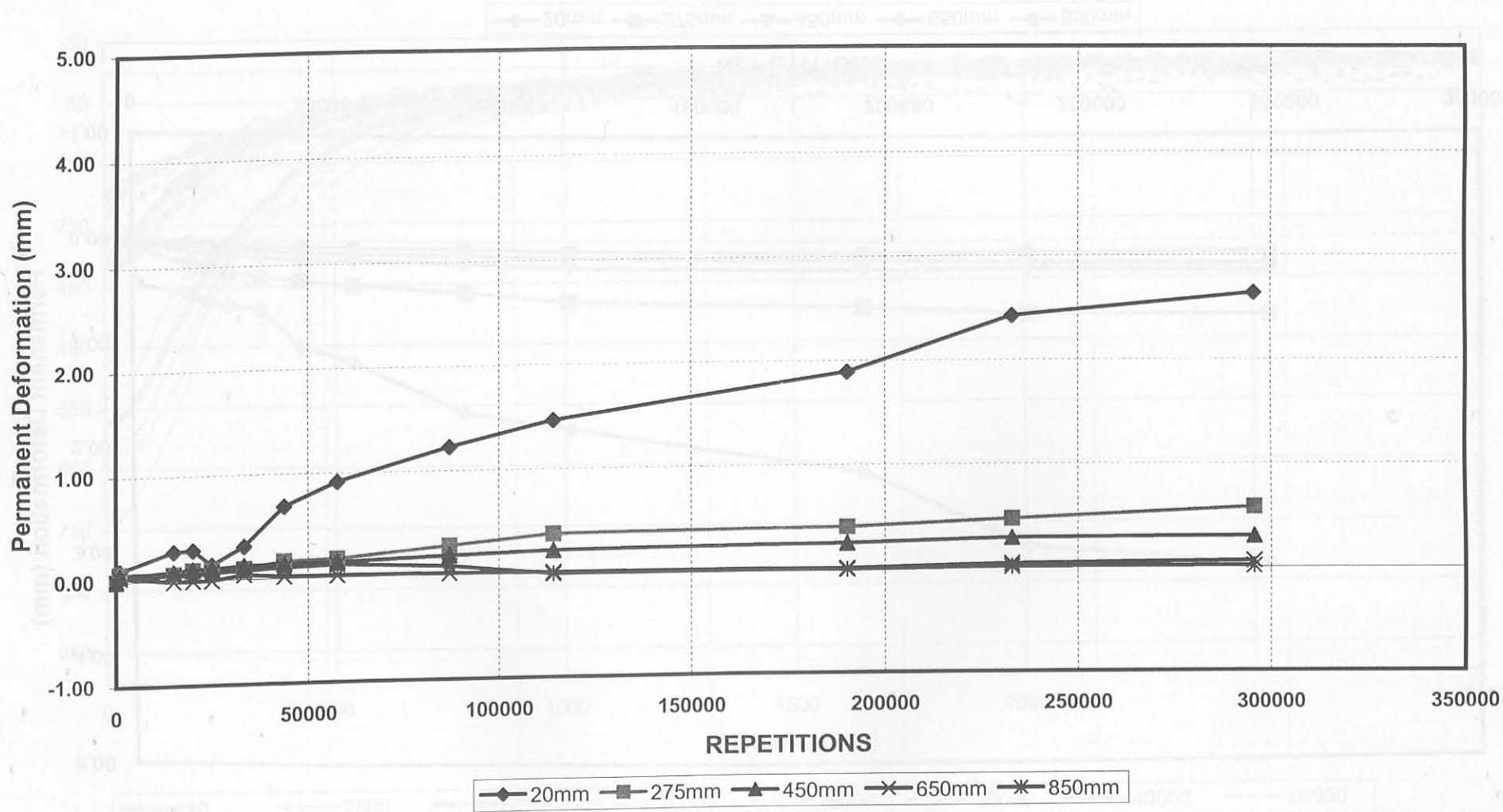


10	2000	5000	10000	15000	20000	40000	60000
175395	300814	401700	490800	597900	695000	827100	957121
1019700	1052100	1128700	1226000	1321700			

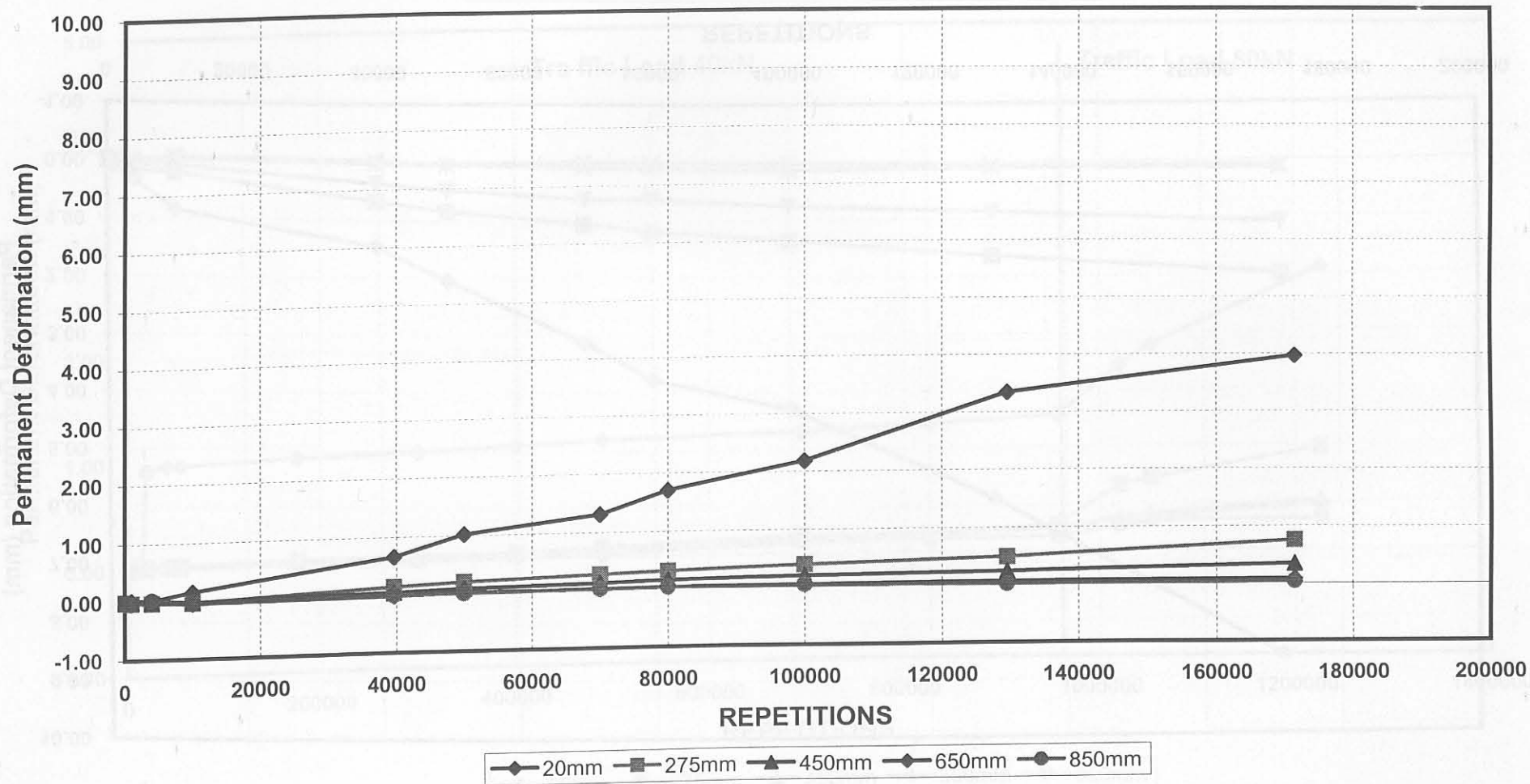
MDD 4 Permanent Deformation SECTION 410A4 (250 ETB)



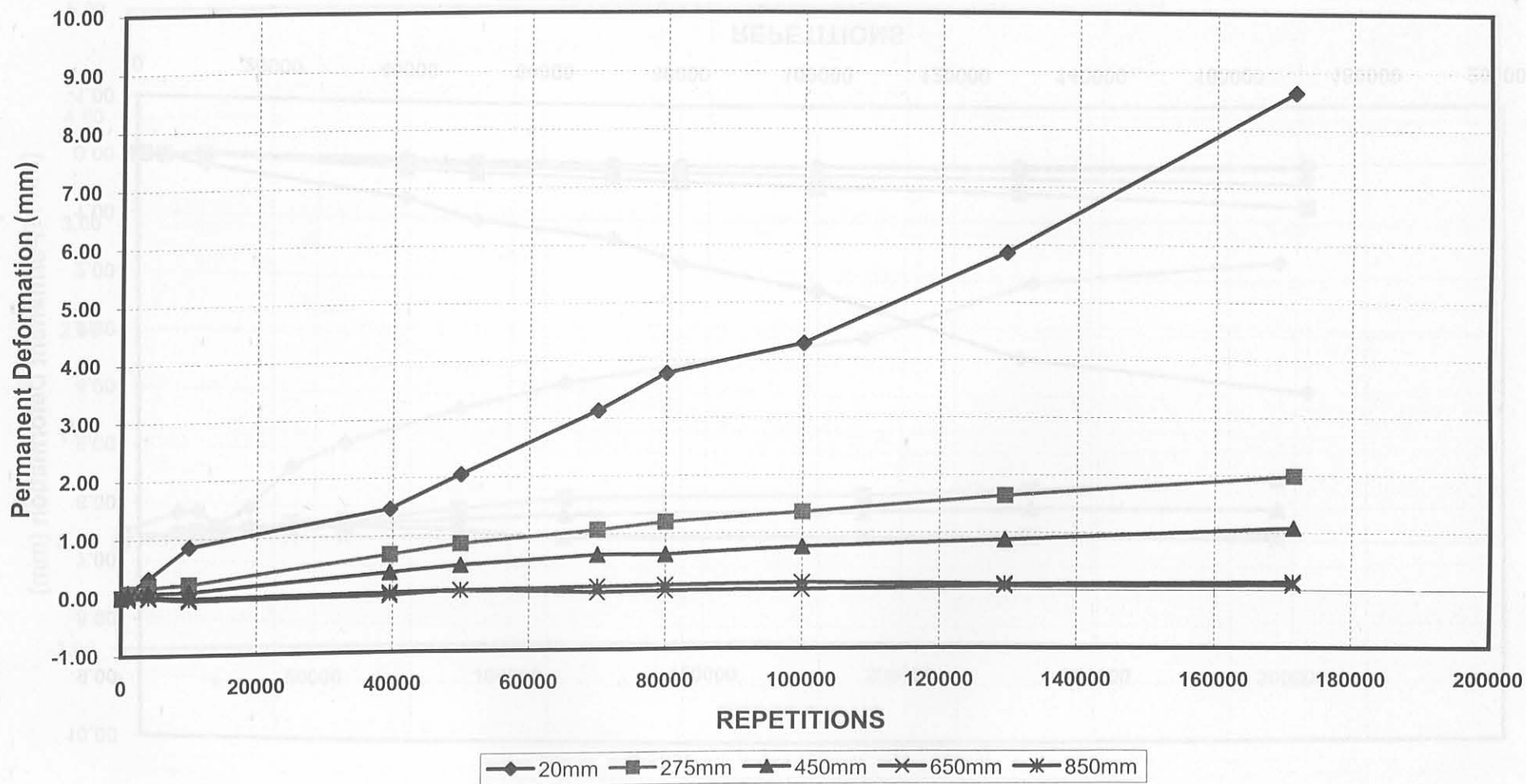
MDD 12 Permanent Deformation SECTION 410A4 (250 ETB)



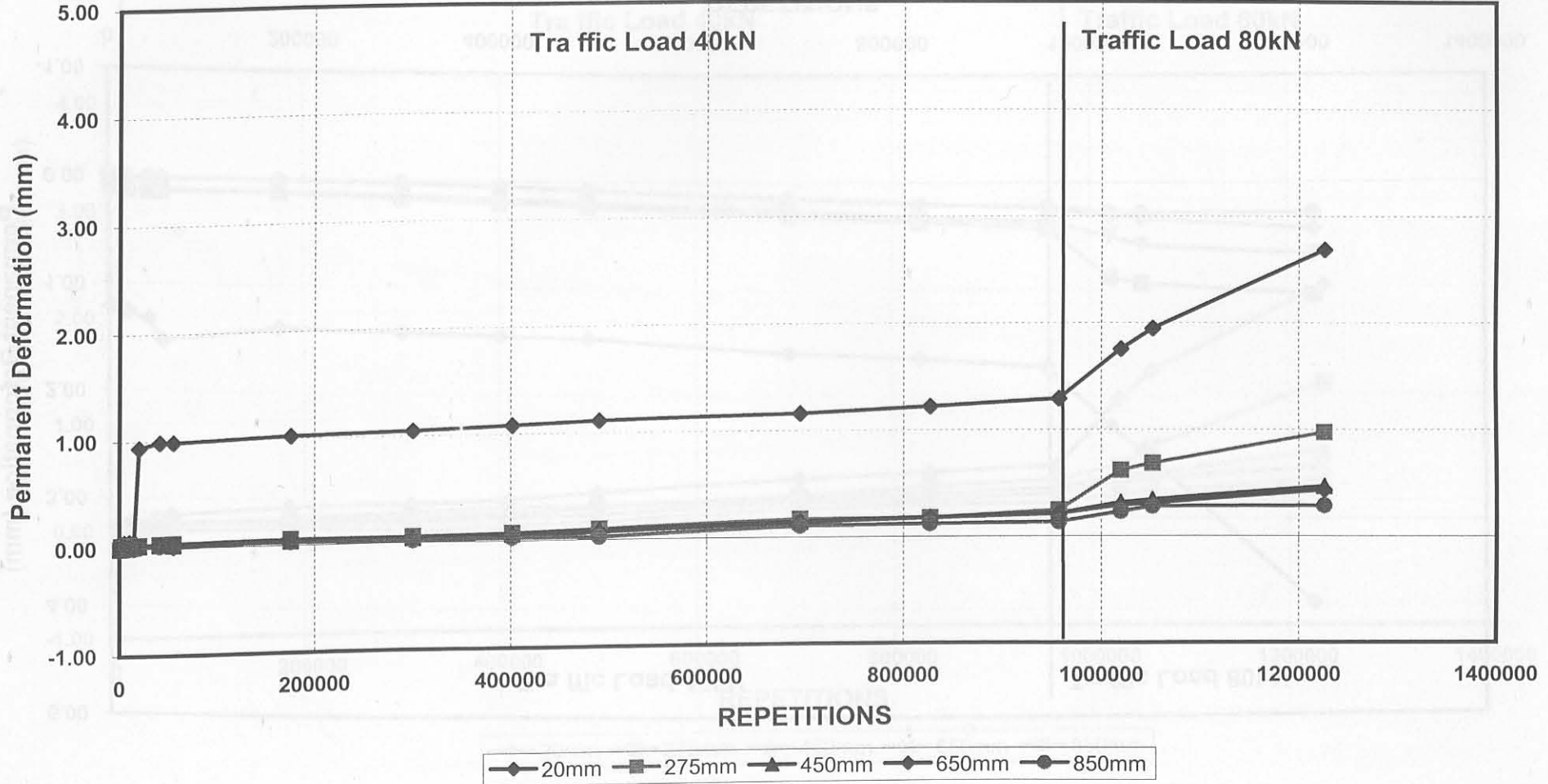
MDD 4 Permanent Deformation SECTION 410B4 (250 ETB)



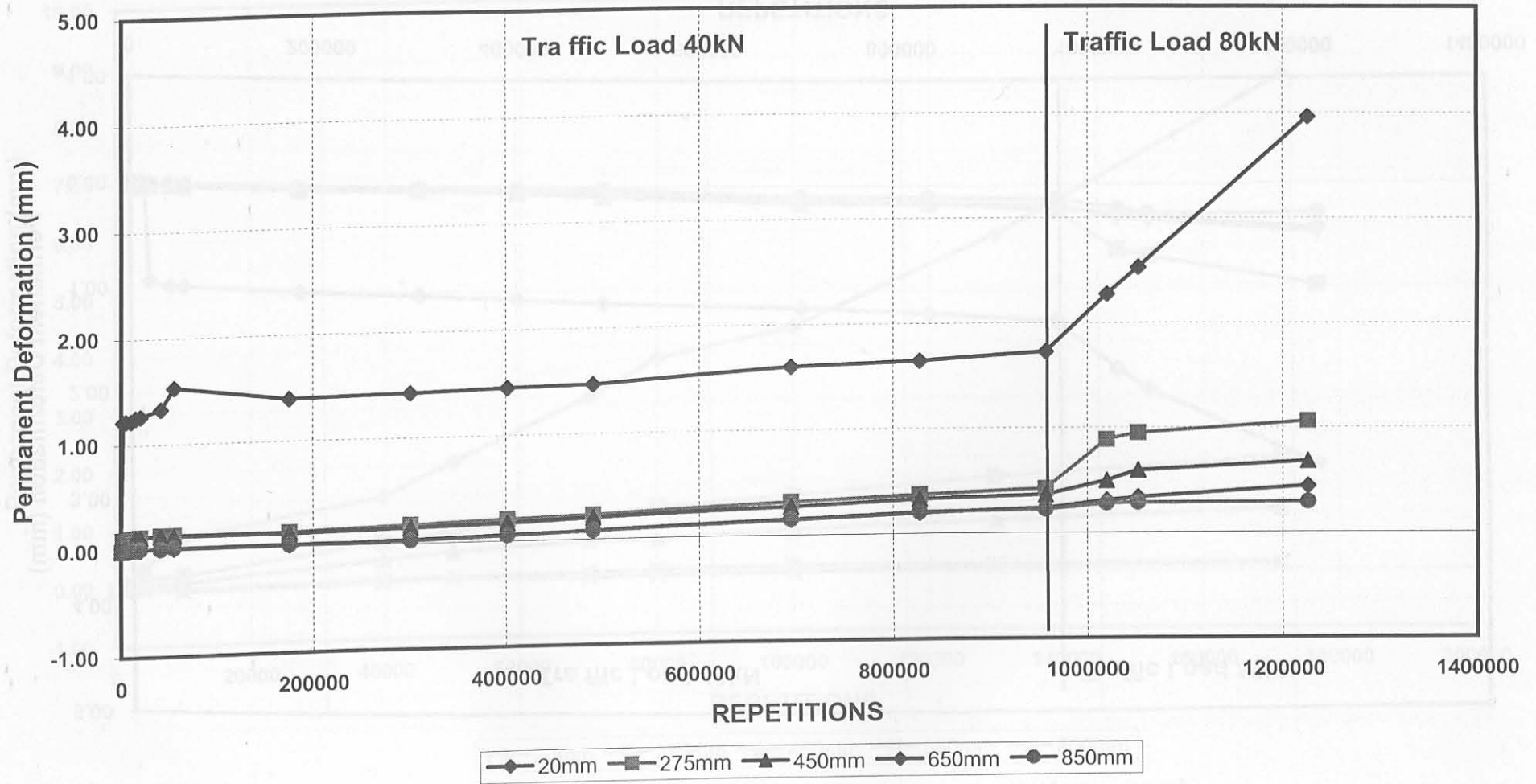
MDD 12 Permanent Deformation SECTION 410B4 (250 ETB)



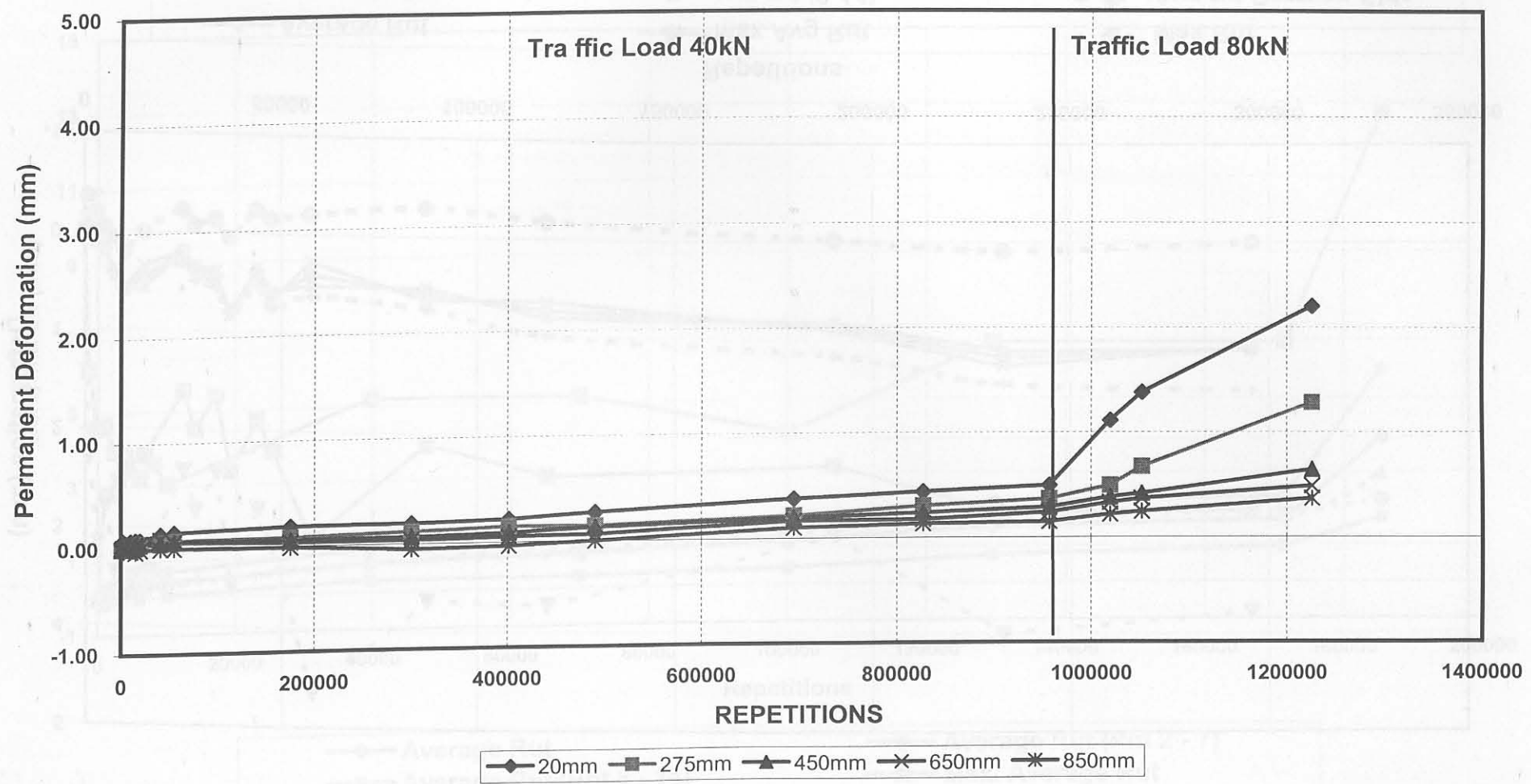
MDD 4 Permanent Deformation SECTION 412A4 (250 ETB)



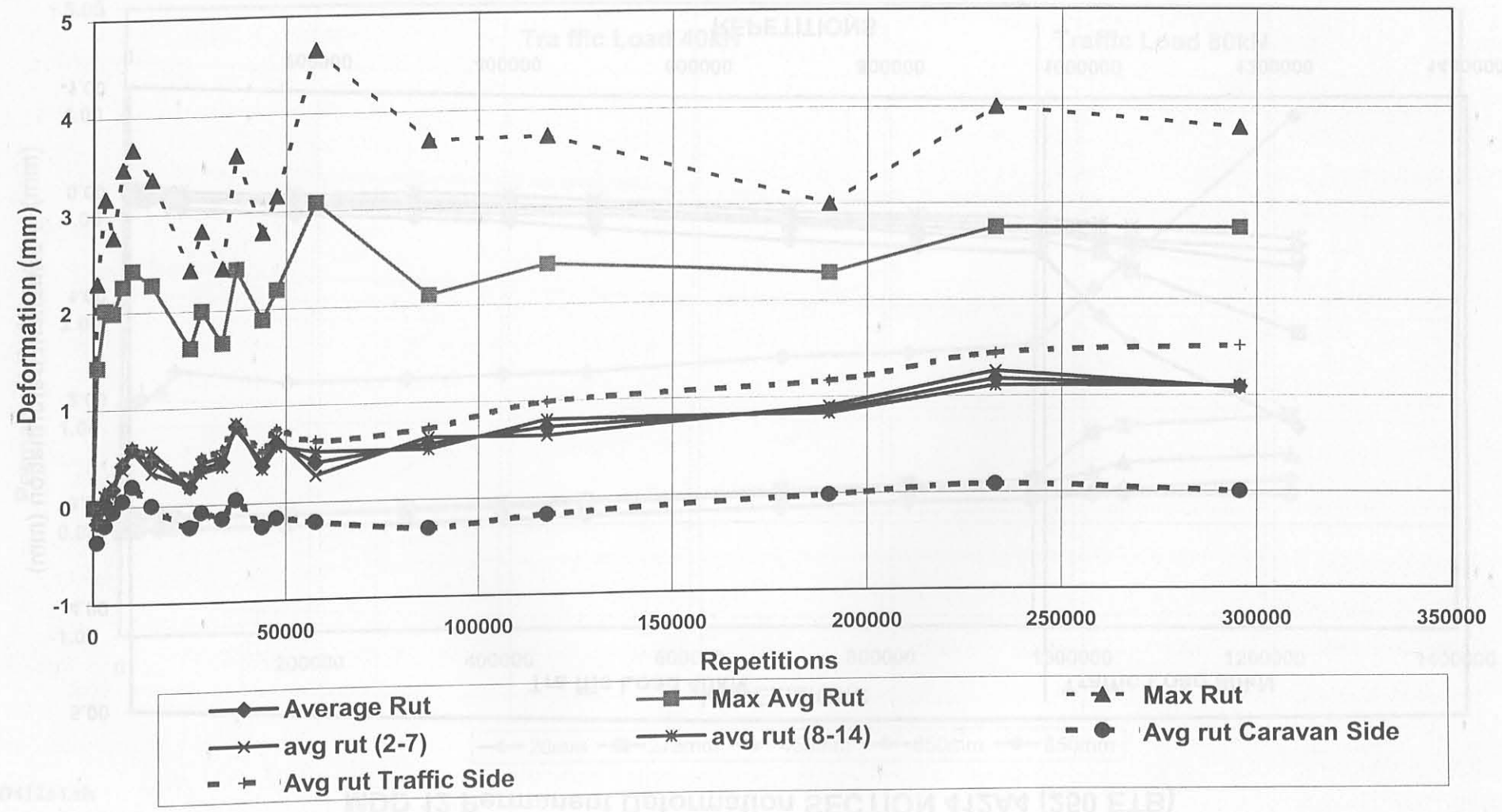
MDD 8 Permanent Deformation SECTION 412A4 (250 ETB)



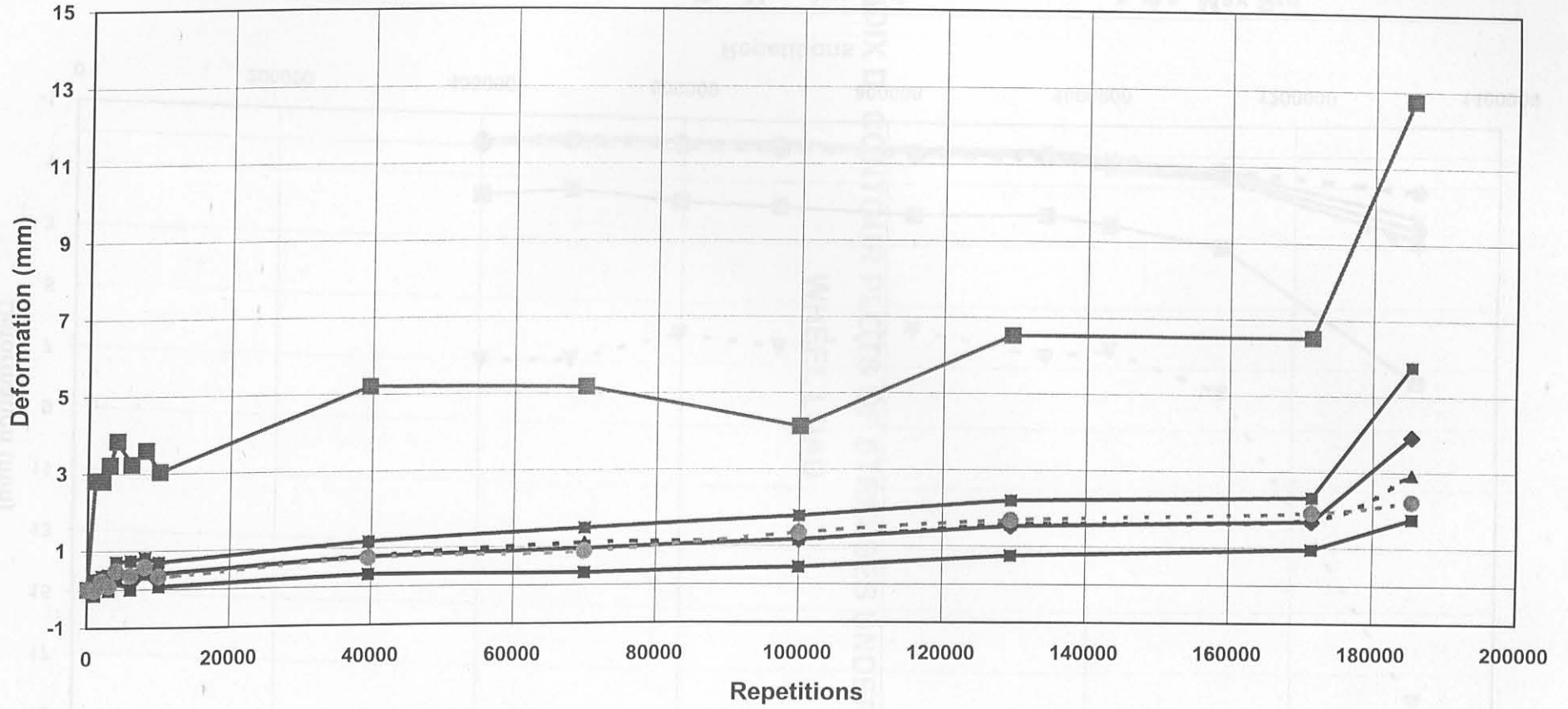
MDD 12 Permanent Deformation SECTION 412A4 (250 ETB)



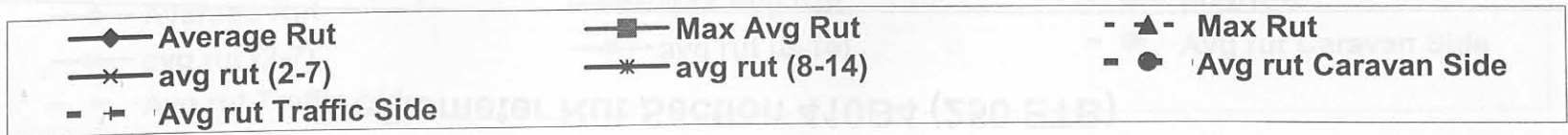
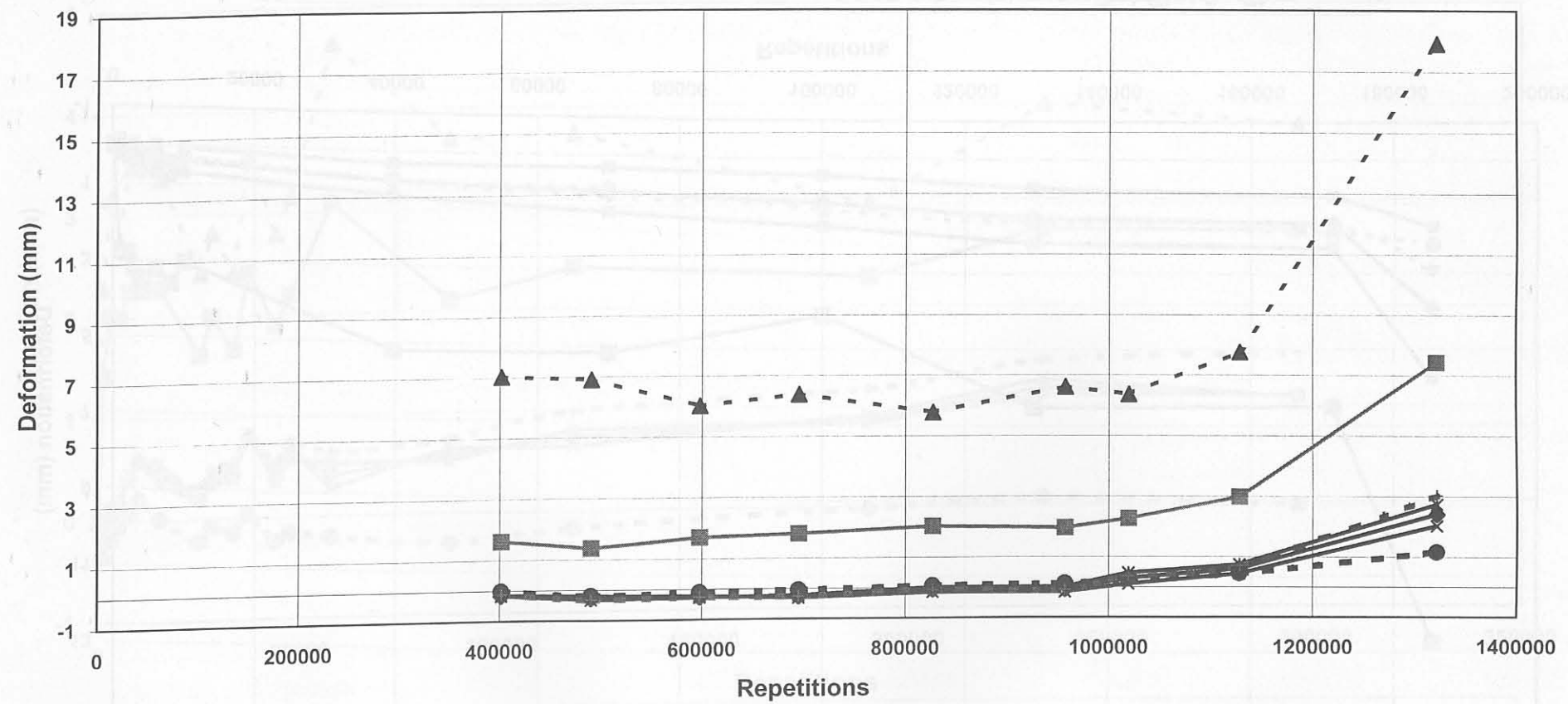
Profilometer Rut Section 410A4 (250 ETB)



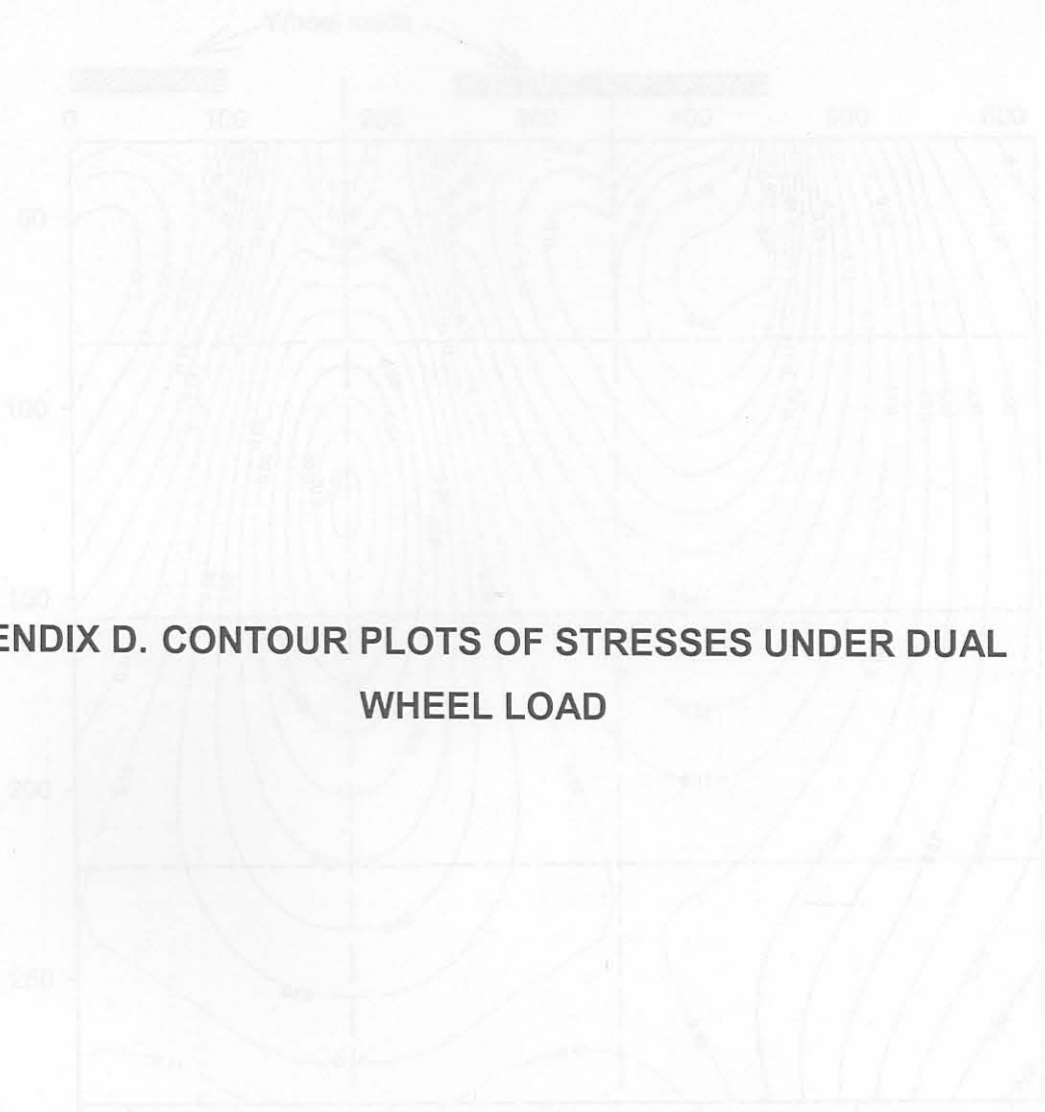
Profilometer Rut Section 410B4 (250 ETB)



Profilometer Rut Section 412A4 (250 ETB)

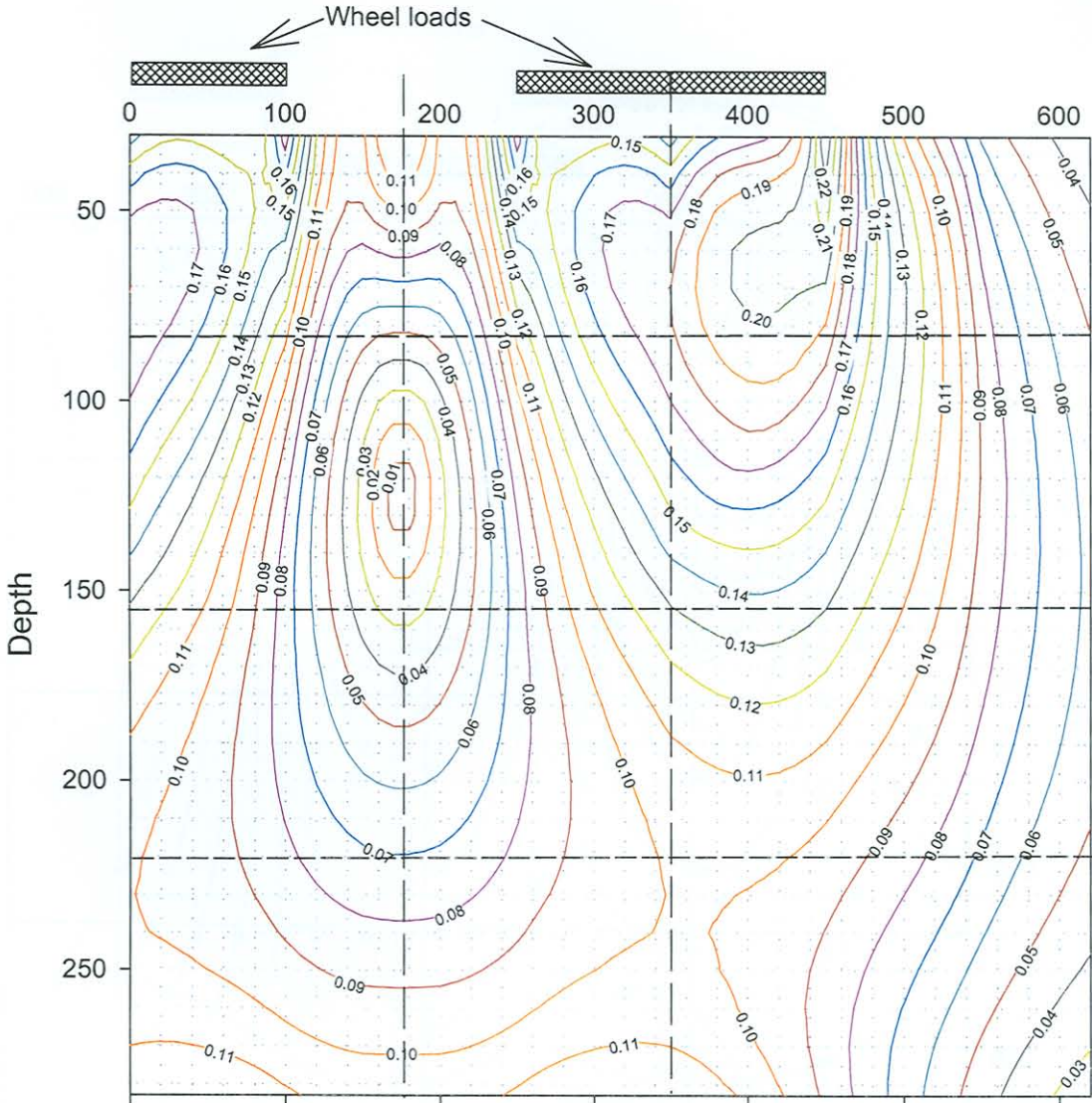


Stress Ratio under 40 kN, 600kPa dual wheel load

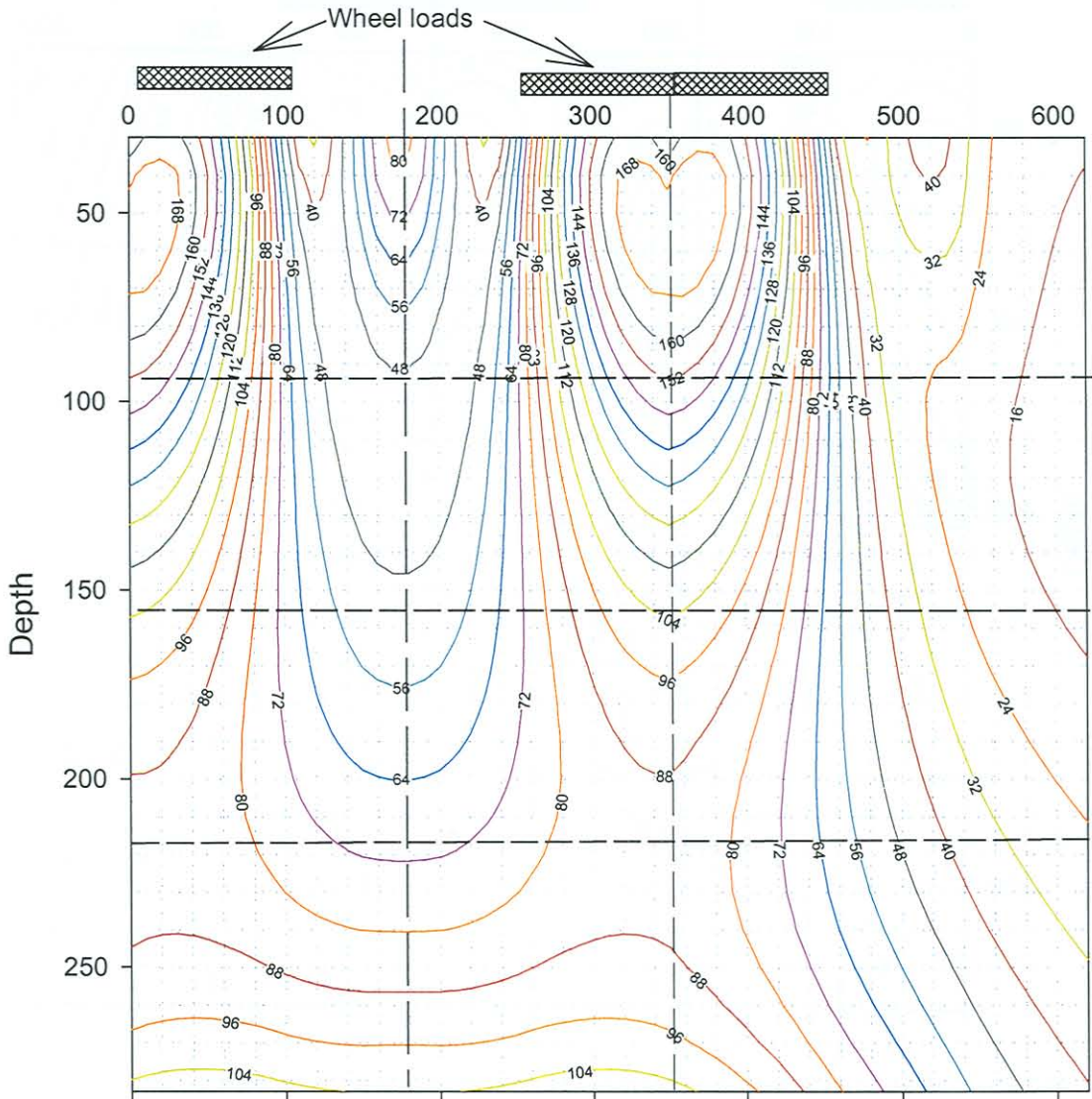


APPENDIX D. CONTOUR PLOTS OF STRESSES UNDER DUAL WHEEL LOAD

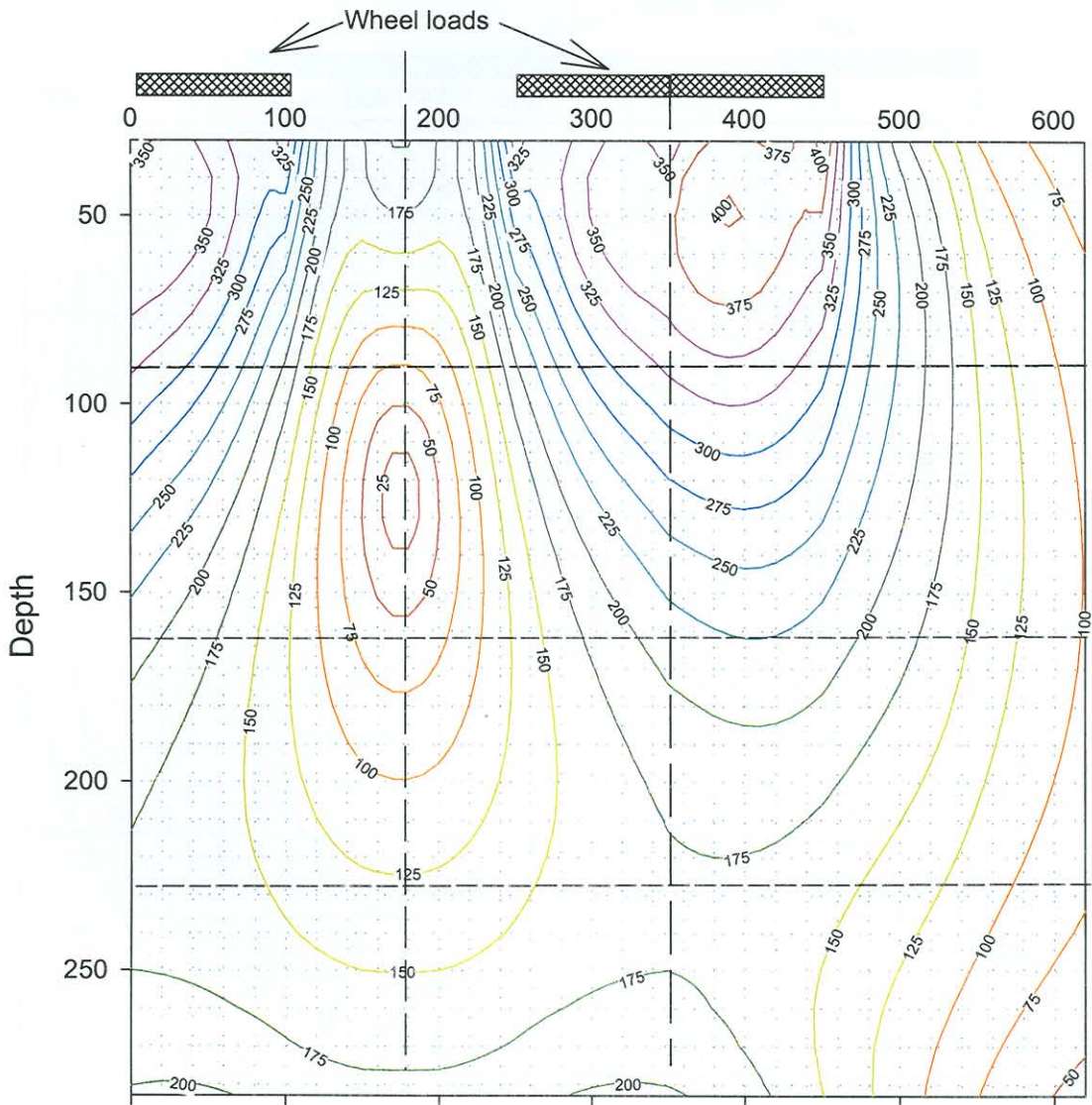
Stress Ratio under 40 kN, 680kPa dual wheel load



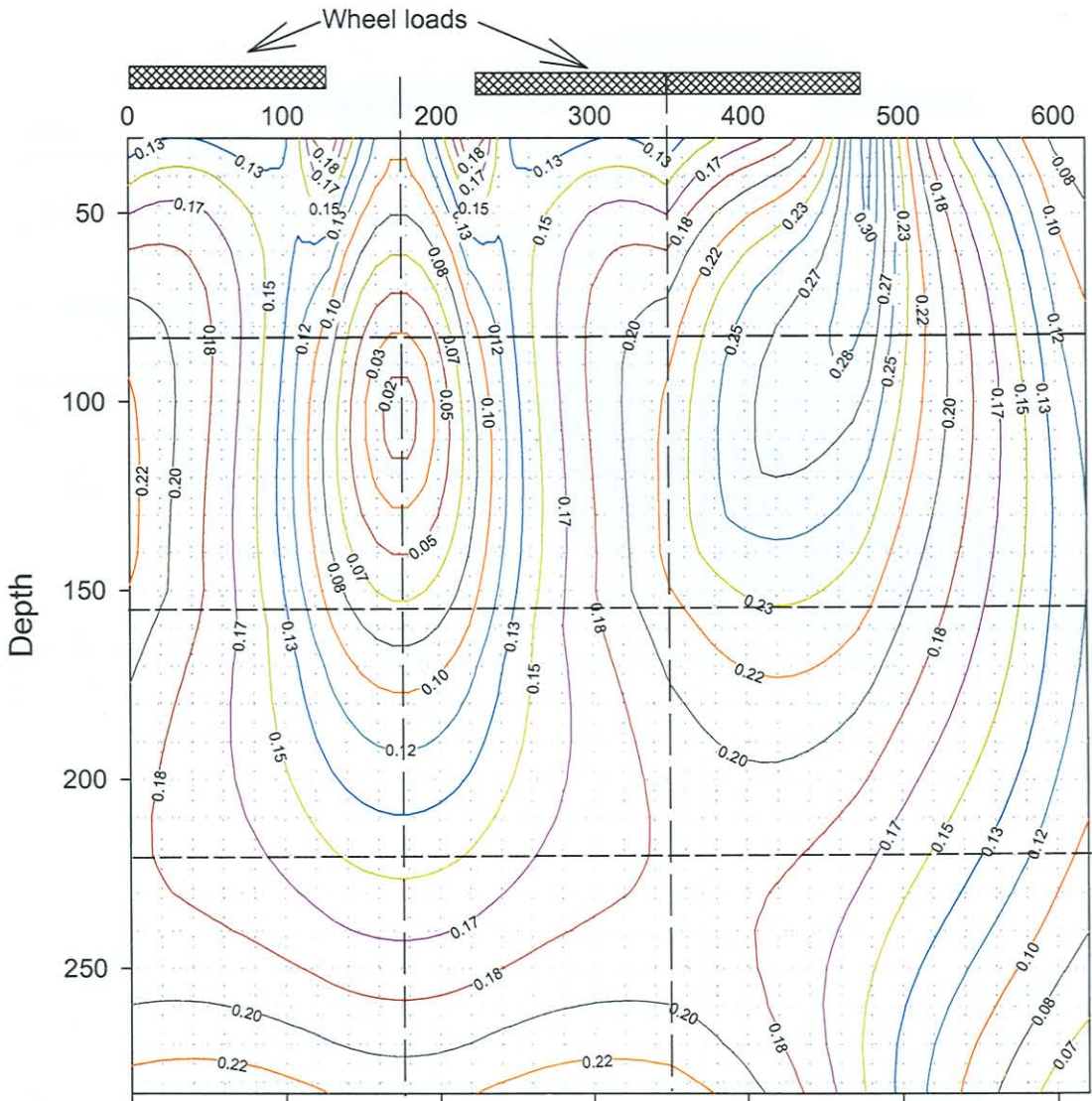
Octahedral shear stress under 40 kN, 680 kPa dual wheel load



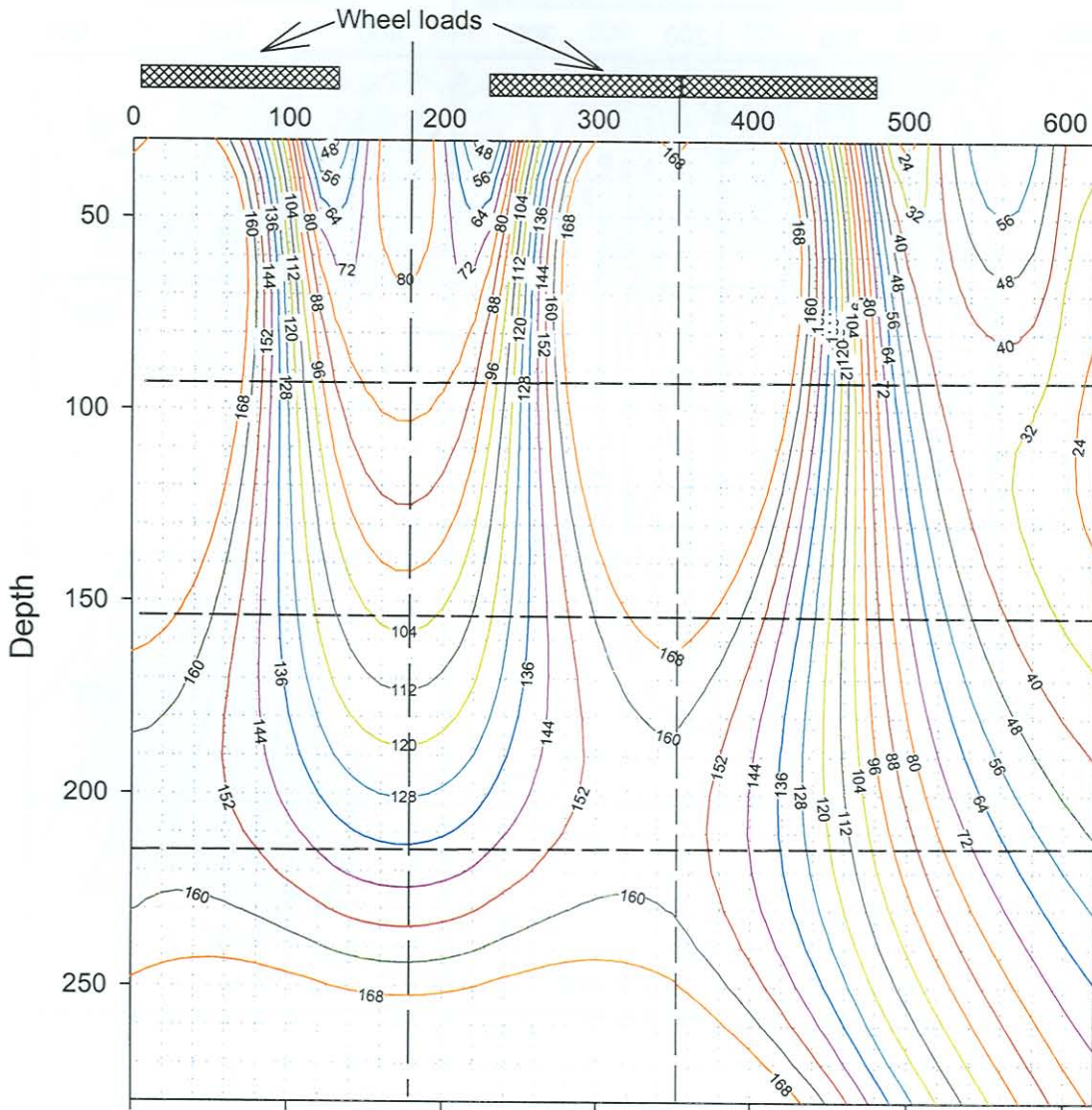
Deviator stress under 40 kN, 680 kPa dual wheel load



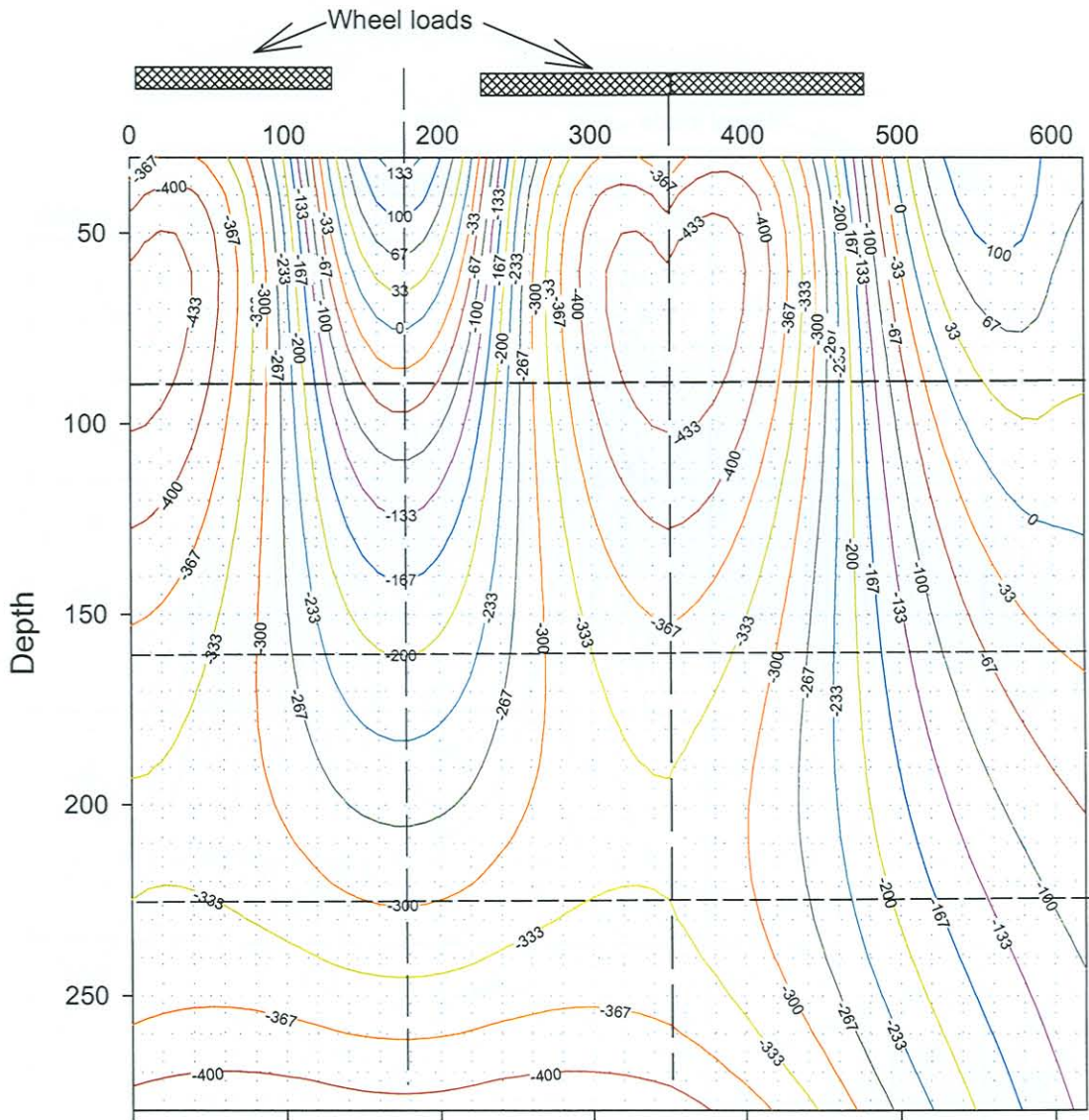
Stress Ratio under 80 kN, 800kPa dual wheel load



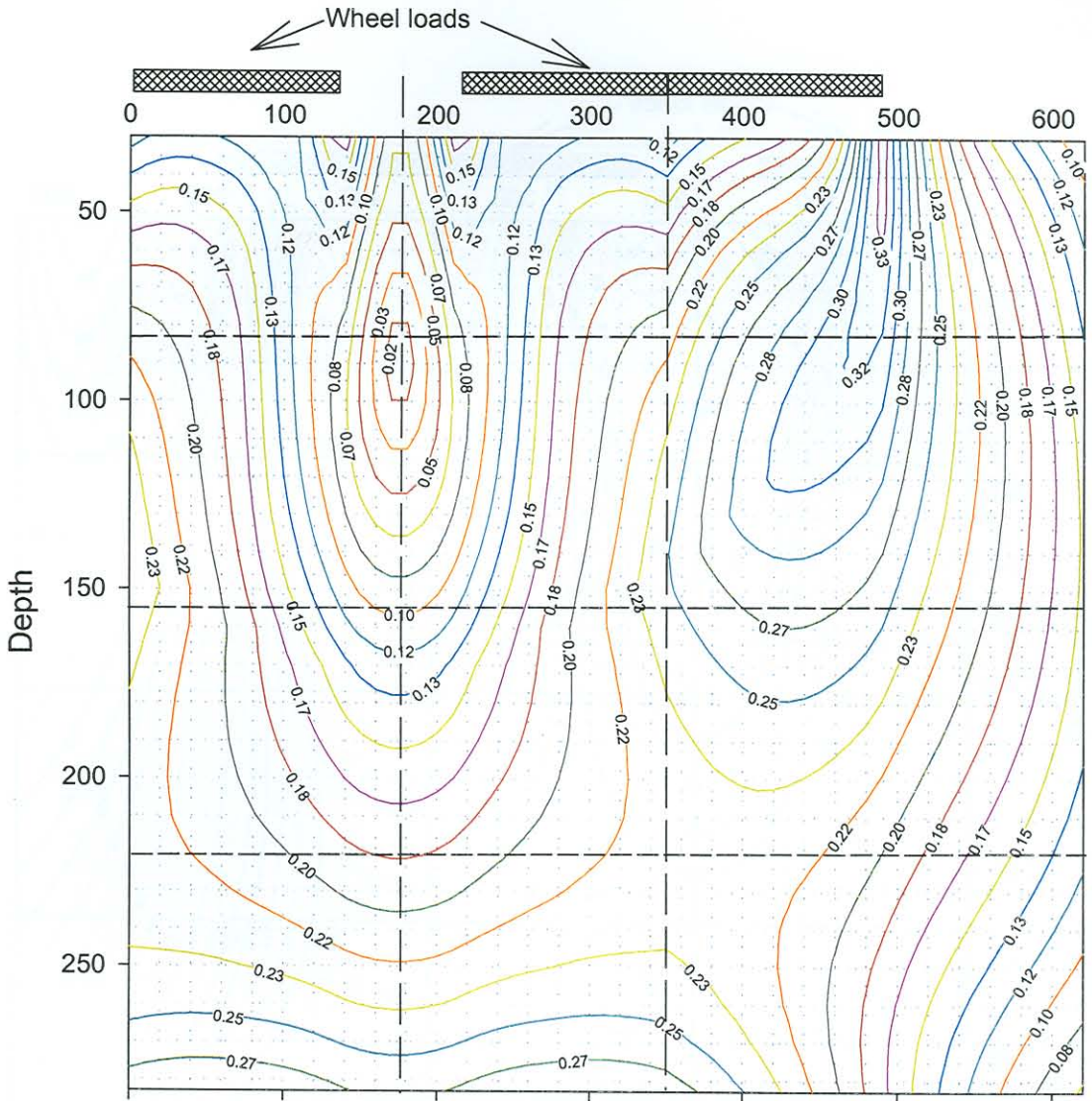
Octahedral shear stress under 80 kN, 800 kPa dual wheel load



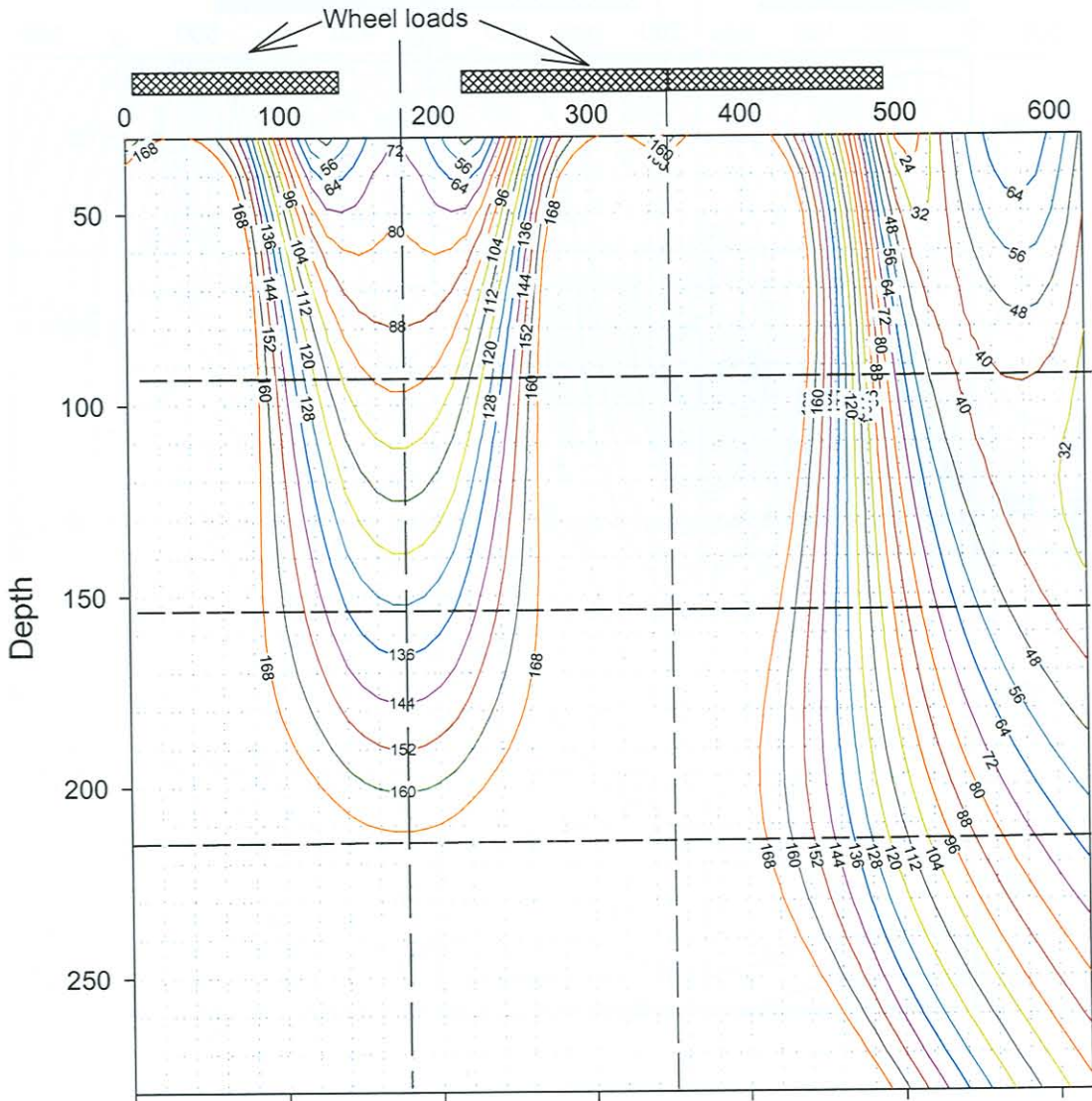
Deviator stress under 80 kN, 800 kPa dual wheel load



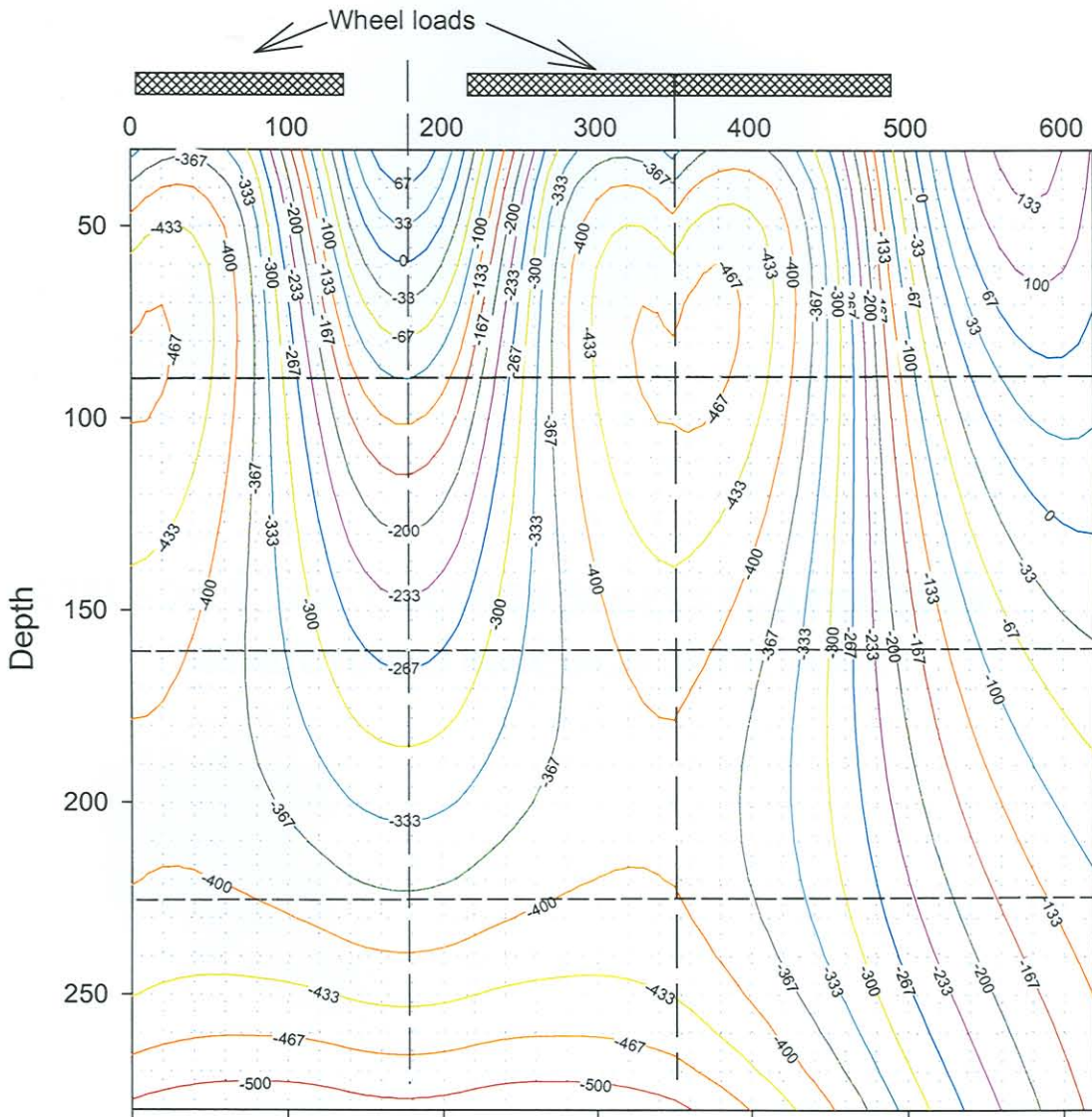
Stress Ratio under 100 kN, 850kPa dual wheel load



Octahedral shear stress under 100 kN, 850 kPa dual wheel load



Deviator stress under 100 kN, 850 kPa dual wheel load



APPENDIX E. CALCULATION SHEETS FOR PAVEMENT STRUCTURES IN DESIGN CATALOGUE

Emulsion treated bases - Design catalogue

ETB1

ET1 Bases

Road category = A

Expected pavement life = 11.8E+6

	Phase 1				Phase 2				Phase 3				Phase 4											
	Thickness	Layer characteristics			E moduli	eb/phi	c/A	poisson	Layer characteristics			E moduli	eb/phi	c/A	poisson	Layer characteristics								
		E moduli	eb/phi	c/A					E moduli	eb/phi	c/A					E moduli	eb/phi	c/A	E moduli	eb/phi	c/A	poisson		
AC Surfacing	40	3000			0.35				3000				0.35					3000				0.35		
ET1 Base	150	1800	230		0.35				1800	230			0.35					500	6.55	1374		0.35		
125 C4	125	1500	145		0.35				1500	145			0.35					225	2.8	100		0.35		
125 C4	125	1500	145		0.35				225	2.8	100		0.35					225	2.8	100		0.35		
G7 Selected	150	120		36.3	0.35				120		36.3		0.35					120		36.3		0.35		
G9 Subbase	inf	70																						
	Critical parameters				Critical parameters				Critical parameters				Critical parameters											
	S1	S3	ev/et		S1	S3	ev/et		S1	S3	ev/et		S1	S3	ev/et									
AC Surfacing			26				21				16				176									
ET1 Base			44				58				174													
125 C4			41				105		61.45	-5.71			88.03	-11.43										
125 C4			70		30.37	-9.65			39.66	-10.78			51.21	-16.31										
G7 Selected			171				214				274				352									
	Expected layer life (E80's)				Expected layer life (E80's)				Expected layer life (E80's)				Expected layer life (E80's)											
	Neff	FOS	SF	Nt	Neff	FOS	SF	Nt	Neff	FOS/SR	SF	Nt	Neff	FOS/SR	SF	Nt								
AC Surfacing	14.4E+9			1.75	25.2E+9			1.75	75.2E+9	172.9E+9			1.75	302.5E+9			809.6E+3			1.75	1.4E+6			
ET1 Base	47.2E+6			1	47.2E+6			1	39.5E+6	9.0E+6			1	9.0E+6				0.21453			9.0E+6			
125 C4	2.9E+6			1.1567779	3.4E+6			1.1567779	1.4E+6		1.4889815			22.9E+6				1.005429			22.9E+6			
125 C4	1.9E+6			1.1567779	2.2E+6			2.4987506	9.8E+9		1.9825535			441.5E+6				1.481043			441.5E+6			
G7 Selected					93.3E+12				9.9E+12					836.6E+9							836.6E+9			
	Neff	R	EG	Fn	AR	L	Neff	R	EG	Fn	AR	L	Neff	R	EG	Fn	AR	L	Neff	R	EG	Fn	AR	L
AC Surfacing	2.2E+6	25.2E+9	000.0E+0	0.3352104	75.2E+9	75.2E+9	2.7E+6	75.2E+9	000.0E+0	0.2486473	302.5E+9	302.5E+9	11.0E+6	302.5E+9	000.0E+0	213534.7	1.4E+6	12.5E+6						
ET1 Base	2.2E+6	45.0E+6	000.0E+0	1.1960818	37.6E+6	39.8E+6	2.7E+6	37.1E+6	000.0E+0	4.4496531	8.3E+6	11.0E+6	11.0E+6	000.0E+0	3.0E+6		3.0E+6	14.1E+6						
125 C4	2.2E+6	1.1E+6	000.0E+0	2.4888795	460.3E+3	2.7E+6	2.7E+6	000.0E+0	22.9E+6		22.9E+6	25.6E+6	11.0E+6	14.5E+6	000.0E+0	20.33252	713.9E+3	11.8E+6						
125 C4	2.2E+6	000.0E+0	9.8E+9	9.8E+9	9.8E+9	9.8E+9	2.7E+6	9.8E+9	000.0E+0	22.12361	441.3E+6	444.0E+6	11.0E+6	433.0E+6	000.0E+0	20.37161	21.3E+6	32.3E+6						
G7 Selected	2.2E+6	93.3E+12	000.0E+0	9.4227275	9.9E+12	9.9E+12	2.7E+6	9.9E+12	000.0E+0	11.840444	836.6E+9	836.6E+9	11.0E+6	836.5E+9	000.0E+0	12.24397	68.3E+9	68.3E+9						

Emulsion treated bases - Design catalogue

ETB35

Road category = A Expected pavement life = 7.3E+6

	Thickness	Phase 1				Phase 2				Phase 3			
		Layer characteristics				Layer characteristics				Layer characteristics			
		E moduli	eb/phi	c/A	poisson	E moduli	eb/phi	c/A	poisson	E moduli	eb/phi	c/A	poisson
AC Surfacing	40	3000			0.35	3000			0.35	3000			0.35
ET1 Base	150	1800	230		0.35	1800	145		0.35	500	6.55	1374	0.35
150 C4	200	1500	145		0.35	200	2.8	100	0.35	200	2.8	100	0.35
150 G7	150	120		36.3	0.35	120		36.3	0.35	120		36.3	0.35
G9 Subgrade	inf	70		36.3	0.35	70		36.3	0.35	70		36.3	0.35
		Critical parameters				Critical parameters				Critical parameters			
		S1	S3	ev/et		S1	S3	ev/et		S1	S3	ev/et	
AC Surfacing				19				10				170	
ET1 Base				48				183		373.83	34.71		
150 C4				93		47.19	-13.79			66.69	-20.26		
150 G7				193				305				399	
G9 Subgrade				274				406				495	
		Expected layer life (E80's)				Expected layer life (E80's)				Expected layer life (E80's)			
		Neff	FOS	SF	Nt	Neff	FOS	SF	Nt	Neff	FOS/SR	SF	Nt
AC Surfacing		71.7E+9			1.75	1.9E+12			1.75	966.8E+3			1.75
ET1 Base		44.8E+6			1	2.0E+6			1		0.2117713		
150 C4		1.4E+6		1.8923436	2.6E+6		1.6398819				1.1500863		
150 G7					27.8E+12								56.5E+6
G9 Subgrade					836.6E+9								286.4E+9
													16.4E+9
		Expected pavement life (E80's)											
		Neff	R	EG	Fn	AR	L	Neff	R	EG	Fn	AR	L
AC Surfacing		2.6E+6	125.6E+9	000.0E+0	0.03744876	3.4E+12	3.4E+12	4.5E+6	3.4E+12	000.0E+0	1981502	1.7E+6	6.2E+6
ET1 Base		2.6E+6	42.2E+6	000.0E+0	22.1658509	1.9E+6	4.5E+6	4.5E+6	000.0E+0	3.2E+6		3.2E+6	7.7E+6
150 C4		2.6E+6	000.0E+0	56.5E+6		56.5E+6	59.2E+6	4.5E+6	54.6E+6	000.0E+0	19.760681	2.8E+6	7.3E+6
150 G7		2.6E+6	27.8E+12	000.0E+0	97.1460851	286.4E+9	286.4E+9	4.5E+6	286.4E+9	000.0E+0	14.680286	19.5E+9	19.5E+9
G9 Subgrade		2.6E+6	836.6E+9	000.0E+0	51.0216745	16.4E+9	16.4E+9	4.5E+6	16.4E+9	000.0E+0	7.2587226	2.3E+9	2.3E+9

Emulsion treated bases - Design catalogue

ETB6

ET1 Bases

Road category = A

Expected pavement life =

3.0E+6

	Thickness	Phase 1				Phase 2				Phase 3			
		Layer characteristics				Layer characteristics				Layer characteristics			
		E moduli	eb/phi	c/A	poisson	E moduli	eb/phi	c/A	poisson	E moduli	eb/phi	c/A	poisson
AC Surfacing	40	3000			0.35	3000			0.35	3000			0.35
ET1 Base	125	1800	230		0.35	1800	145		0.35	500	6.55	1374	0.35
150 C4	150	1500	145		0.35	200	2.8	100	0.35	200	2.8	100	0.35
150 G7	150	120		36.3	0.35	120		36.3	0.35	120		36.3	0.35
G9 Subgrade	inf	70		36.3	0.35	70		36.3	0.35	70		36.3	0.35
		Critical parameters				Critical parameters				Critical parameters			
		S1	S3	ev/et		S1	S3	ev/et		S1	S3	ev/et	
AC Surfacing				19				14				182	
ET1 Base				60				212		385.68	32.38		
150 C4				116		65.15	-11.99			89.93	-20.22		
150 G7				198				284				346	
G9 Subgrade				274				406				495	
		Expected layer life (E80's)				Expected layer life (E80's)				Expected layer life (E80's)			
		Neff	FOS	SF	Nt	Neff	FOS	SF	Nt	Neff	FOS/SR	SF	Nt
AC Surfacing		71.7E+9			1.75	125.6E+9			1.75	599.2E+9			1.2E+6
ET1 Base		38.5E+6			1	38.5E+6			1	1.1E+6			3.4E+6
150 C4		1.0E+6		1.363013		1.4E+6		1.2963443		7.2E+6		0.2227492	700.1E+3
150 G7						21.5E+12				584.5E+9		0.9078529	81.1E+9
G9 Subgrade						836.6E+9				16.4E+9			2.3E+9
		Expected pavement life (E80's)											
		Neff	R	EG	Fn	AR	L	Neff	R	EG	Fn	AR	L
AC Surfacing		1.4E+6	125.6E+9	000.0E+0	0.20954107	599.2E+9	599.2E+9	2.5E+6	599.2E+9	000.0E+0	502071.04	1.2E+6	3.6E+6
ET1 Base		1.4E+6	37.1E+6	000.0E+0	34.23988	1.1E+6	2.5E+6	2.5E+6	000.0E+0	3.4E+6		3.4E+6	5.9E+6
150 C4		1.4E+6	000.0E+0	7.2E+6		7.2E+6	8.6E+6	2.5E+6	6.1E+6	000.0E+0	12.238699	499.6E+3	3.0E+6
150 G7		1.4E+6	21.5E+12	000.0E+0	36.8579773	584.5E+9	584.5E+9	2.5E+6	584.5E+9	000.0E+0	7.2040808	81.1E+9	81.1E+9
G9 Subgrade		1.4E+6	836.6E+9	000.0E+0	51.0216745	16.4E+9	16.4E+9	2.5E+6	16.4E+9	000.0E+0	7.2581716	2.3E+9	2.3E+9

Emulsion treated bases - Design catalogue

Road category = B Expected pavement life = 7.0E+6

ETB7

	Thickness	Phase 1				Phase 2				Phase 3			
		Layer characteristics				Layer characteristics				Layer characteristics			
		E moduli	eb/phi	c/A	poisson	E moduli	eb/phi	c/A	poisson	E moduli	eb/phi	c/A	poisson
AC Surfacing	40	3000			0.35	3000			0.35	3000			0.35
ET1 Base	125	1800	230		0.35	1800	145		0.35	500	6.55	1374	0.35
200 C4	200	1500	145		0.35	200	2.8	100	0.35	200	2.8	100	0.35
150 G7	150	120		36.38	0.35	120		36.38	0.35	120		36.38	0.35
G9 Subgrade	inf	70		36.38	0.35	70		36.38	0.35	70		36.38	0.35
		Critical parameters				Critical parameters				Critical parameters			
		S1	S3	ev/et		S1	S3	ev/et		S1	S3	ev/et	
AC Surfacing				22				15				182	
ET1 Base				53				208		386.67	33.67		
200 C4				94		60.2	-9.56			81.18	-15.86		
150 G7				228				363				456	
G9 Subgrade				225				361				432	
		Expected layer life (E80's)				Expected layer life (E80's)				Expected layer life (E80's)			
		Neff	FOS	SF	Nt	Neff	FOS	SF	Nt	Neff	FOS/SR	SF	Nt
AC Surfacing		38.6E+9			1.75	67.5E+9			1.75	479.9E+9			1.4E+6
ET1 Base		54.8E+6			1	54.8E+6			1	1.6E+6	0.221381		4.3E+6
200 C4		1.8E+6		1.892344		3.4E+6	1.433486			27.7E+6	1.030503		2.5E+6
150 G7						6.3E+12				60.4E+9			6.2E+9
G9 Subgrade						7.2E+12				63.8E+9			10.6E+9
		Expected pavement life (E80's)				Expected pavement life (E80's)				Expected pavement life (E80's)			
		Neff	R	EG	Fn	AR	L	Neff	R	EG	Fn	AR	L
AC Surfacing		3.4E+6	67.5E+9	000.0E+0	0.1407162	479.9E+9	479.9E+9	4.9E+6	479.9E+9	000.0E+0	354987.9	1.4E+6	6.3E+6
ET1 Base		3.4E+6	51.4E+6	000.0E+0	34.5279894	1.5E+6	4.9E+6	4.9E+6	000.0E+0	4.3E+6		4.3E+6	9.2E+6
200 C4		3.4E+6	000.0E+0	27.7E+6		27.7E+6	31.1E+6	4.9E+6	26.2E+6	000.0E+0	12.60741	2.1E+6	7.0E+6
150 G7		3.4E+6	6.3E+12	000.0E+0	104.644831	60.4E+9	60.4E+9	4.9E+6	60.4E+9	000.0E+0	9.786032	6.2E+9	6.2E+9
G9 Subgrade		3.4E+6	7.2E+12	000.0E+0	113.043823	63.8E+9	63.8E+9	4.9E+6	63.8E+9	000.0E+0	6.022664	10.6E+9	10.6E+9

Emulsion treated bases - Design catalogue

ETB14

Road category = B Expected pavement life = 2.4E+6

	Thickness	Phase 1				Phase 2				Phase 3			
		Layer characteristics				Layer characteristics				Layer characteristics			
		E moduli	eb/phi	c/A	poisson	E moduli	eb/phi	c/A	poisson	E moduli	eb/phi	c/A	poisson
ET1 Base	125	1800	230		0.35	500	6.55	1374	0.35				
150 G5 Sbase	150	200	3.5	120	0.35	200	3.5	120	0.35				
150 G7 SSG	150	120		36.38	0.35	120		36.38	0.35				
G9 Subgrade	inf	70		36.38	0.35	70		36.38	0.35				
		Critical parameters				Critical parameters				Critical parameters			
		S1	S3	ev/et		S1	S3	ev/et		S1	S2	ev/et	
ET1 Base				303		466.78	41.77						
150 G5 Sbase		93.93	-19.19			138.49	-20.79						
150 G7 SSG				542				718					
G9 Subgrade				551				679					
		Expected layer life (E80's)				Expected layer life (E80's)				Expected layer life (E80's)			
		Neff	FOS	SF	Nt	Neff	FOS/SR	SF	Nt	Neff	FOS	SF	Nt
ET1 Base		2.2E+6			1	2.2E+6			2.8E+6				
150 G5 Sbase			1.06082		3.0E+6		0.257958		468.1E+3				
150 G7 SSG					1.1E+9		0.75339		65.9E+6				
G9 Subgrade					930.0E+6				115.2E+6				
		Expected pavement life (E80's)											
		Neff	R	EG	Fn	AR	L	Neff	R	EG	Fn	AR	L
ET1 Base		2.2E+6	000.0E+0	2.8E+6		2.8E+6	5.1E+6	2.4E+6	2.7E+6	000.0E+0	#DIV/0!	#DIV/0!	#DIV/0!
150 G5 Sbase		2.2E+6	720.2E+3	000.0E+0	6.3E+0	113.9E+3	2.4E+6	2.4E+6	000.0E+0	000.0E+0	#DIV/0!	#DIV/0!	#DIV/0!
150 G7 SSG		2.2E+6	1.1E+9	000.0E+0	16.6E+0	65.7E+6	68.0E+6	2.4E+6	65.6E+6	000.0E+0	#DIV/0!	#DIV/0!	#DIV/0!
G9 Subgrade		2.2E+6	927.8E+6	000.0E+0	8.1E+0	114.9E+6	117.1E+6	2.4E+6	114.8E+6	000.0E+0	#DIV/0!	#DIV/0!	#DIV/0!

Emulsion treated bases - Design catalogue

Road category = B Expected pavement life = 1.2E+6

ETB29

	Thickness	Phase 1				Phase 2				Phase 3			
		Layer characteristics				Layer characteristics				Layer characteristics			
		E moduli	eb/phi	c/A	poisson	E moduli	eb/phi	c/A	poisson	E moduli	eb/phi	c/A	poisson
ET1 Base	125	1800	230		0.35	1800	145		0.35	500	6.55	1374	0.35
150 C4	150	1500	145		0.35	200	2.8	100	0.35	200	2.8	100	0.35
150 G7	150	120		36.38	0.35	120		36.38	0.35	120		36.38	0.35
G9 Subgrade	inf	70		36.38	0.35	70		36.38	0.35	70		36.38	0.35
		Critical parameters				Critical parameters				Critical parameters			
		S1	S3	ev/et		S1	S3	ev/et		S1	S3	ev/et	
ET1 Base				60				303		466	41.77		
150 C4				164		92.93	-19.19			138.49	-20.79		
150 G7				341				542				718	
G9 Subgrade				356				551				679	
		Expected layer life (E80's)				Expected layer life (E80's)				Expected layer life (E80's)			
		Neff	FOS	SF	Nt	Neff	FOS	SF	Nt	Neff	FOS/SR	SF	Nt
ET1 Base		50.1E+6			1	231.0E+3			1	231.0E+3			2.8E+6
150 C4		670.0E+3		1.363013	913.2E+3		0.891902				0.627825		220.4E+3
150 G7					112.8E+9								65.9E+6
G9 Subgrade					73.4E+9								115.2E+6
		Expected pavement life (E80's)				Expected pavement life (E80's)				Expected pavement life (E80's)			
		Neff	R	EG	Fn	AR	L	Neff	R	EG	Fn	AR	L
ET1 Base		913.2E+3	49.2E+6	000.0E+0	216.907023	226.8E+3	1.1E+6	1.1E+6	000.0E+0	2.8E+6		2.8E+6	4.0E+6
150 C4		913.2E+3	000.0E+0	1.1E+6		1.1E+6	2.0E+6	1.1E+6	847.7E+3	000.0E+0	9.018003	94.0E+3	1.2E+6
150 G7		913.2E+3	112.8E+9	000.0E+0	102.907985	1.1E+9	1.1E+9	1.1E+6	1.1E+9	000.0E+0	16.65749	65.8E+6	67.0E+6
G9 Subgrade		913.2E+3	73.4E+9	000.0E+0	78.8889197	930.0E+6	930.9E+6	1.1E+6	929.8E+6	000.0E+0	8.083559	115.0E+6	116.2E+6

Emulsion treated bases - Design catalogue

ETB9

Road category = B

Expected pavement life = 846.4E+3

	Thickness	Phase 1				Phase 2				Phase 3			
		E moduli	eb/phi	c/A	poisson	E moduli	eb/phi	c/A	poisson	E moduli	eb/phi	c/A	poisson
ET1 Base	125	1800	230		0.35	1800	145		0.35	500	6.55	1374	0.35
150 C4	125	1500	145		0.35	200	2.8	100	0.35	200	2.8	100	0.35
150 G7	150	120		36.38	0.35	120		36.38	0.35	120		36.38	0.35
G9 Subgrade	inf	70		36.38	0.35	70		36.38	0.35	70		36.38	0.35
		Critical parameters				Critical parameters				Critical parameters			
		S1	S3	ev/et		S1	S3	ev/et		S1	S3	ev/et	
ET1 Base				67				309		468.6	41.69		
150 C4				185		97.6	-21.84			148.29	-24.45		
150 G7				394				584				811	
G9 Subgrade				402				590				733	
		Expected layer life (E80's)				Expected layer life (E80's)				Expected layer life (E80's)			
		Neff	FOS	SF	Nt	Neff	FOS	SF	Nt	Neff	FOS/SR	SF	Nt
ET1 Base		45.8E+6			1	45.8E+6			1	204.5E+3			2.8E+6
150 C4		496.9E+3		1.156778	574.8E+3		0.83724		774.1E+3		0.259194		2.8E+6
150 G7					26.6E+9				519.8E+6		0.578905		164.4E+3
G9 Subgrade					21.8E+9				469.3E+6				19.5E+6
		Expected pavement life (E80's)				Expected pavement life (E80's)				Expected pavement life (E80's)			
		Neff	R	EG	Fn	AR	L	Neff	R	EG	Fn	AR	L
ET1 Base		574.8E+3	45.2E+6	000.0E+0	224.003729	201.9E+3	776.7E+3	776.7E+3	000.0E+0	2.8E+6		2.8E+6	3.6E+6
150 C4		574.8E+3	000.0E+0	774.1E+3		774.1E+3	1.3E+6	776.7E+3	572.1E+3	000.0E+0	8.206803	69.7E+3	846.4E+3
150 G7		574.8E+3	26.6E+9	000.0E+0	51.1877751	519.8E+6	520.4E+6	776.7E+3	519.6E+6	000.0E+0	26.70242	19.5E+6	20.2E+6
G9 Subgrade		574.8E+3	21.8E+9	000.0E+0	46.3724013	469.3E+6	469.9E+6	776.7E+3	469.1E+6	000.0E+0	8.77081	53.5E+6	54.3E+6

Emulsion treated bases - Design catalogue

Road category = C Expected pavement life = 1.6E+6

ETB11

	Thickness	Phase 1				Phase 2				Phase 3			
		Layer characteristics				Layer characteristics				Layer characteristics			
		E moduli	eb/phi	c/A	poisson	E moduli	eb/phi	c/A	poisson	E moduli	eb/phi	c/A	poisson
ET1 Base	125	1800	230		0.35	500	6.55	1374	0.35				
150 G6 Sbase	150	150	2.32	84	0.35	150	2.32	84	0.35				
150 G7 SSG	150	120		36.47	0.35	120		36.47	0.35				
G9 Subgrade	inf	70		36.47	0.35	70		36.47	0.35				
		Critical parameters				Critical parameters				Critical parameters			
		S1	S3	ev/et		S1	S3	ev/et		S1	S2	ev/et	
ET1 Base				338		475.09	35.55						
150 G6 Sbase		89.96	-8.1			135.43	-10.75						
150 G7 SSG				547				731					
G9 Subgrade				570				708					
		Expected layer life (E80's)				Expected layer life (E80's)				Expected layer life (E80's)			
		Neff	FOS	SF	Nt	Neff	FOS/SR	SF	Nt	Neff	FOS	SF	Nt
ET1 Base		2.0E+6			1	2.0E+6			3.6E+6				
150 G6 Sbase			0.856618				0.273541		302.2E+3				
150 G7 SSG							0.574634		67.7E+6				
G9 Subgrade									93.3E+6				
		Expected pavement life (E80's)											
		Neff	R	EG	Fn	AR	L	Neff	R	EG	Fn	AR	L
ET1 Base	Fail	1.6E+6	342.7E+3	000.0E+0	548.8E-3	624.6E+3	2.3E+6	1.6E+6	624.6E+3	000.0E+0	#DIV/0!	#DIV/0!	#DIV/0!
150 G6 Sbase		1.6E+6	000.0E+0	302.2E+3		302.2E+3	1.6E+6	1.6E+6	000.0E+0	000.0E+0	#DIV/0!	#DIV/0!	#DIV/0!
150 G7 SSG		1.6E+6	1.2E+9	000.0E+0	18.2E+0	67.6E+6	69.3E+6	1.6E+6	67.6E+6	000.0E+0	#DIV/0!	#DIV/0!	#DIV/0!
G9 Subgrade		1.6E+6	813.5E+6	000.0E+0	8.7E+0	93.1E+6	94.7E+6	1.6E+6	93.1E+6	000.0E+0	#DIV/0!	#DIV/0!	#DIV/0!

Emulsion treated bases - Design catalogue

ETB30

Road category = C

Expected pavement life = 741.0E+3

	Thickness	Phase 1				Phase 2				Phase 3			
		Layer characteristics				Layer characteristics				Layer characteristics			
		E moduli	eb/phi	c/A	poisson	E moduli	eb/phi	c/A	poisson	E moduli	eb/phi	c/A	poisson
ET1 Base	125	1800	230		0.35	500	6.55	1374	0.35				
150 G6 Sbase	150	150	2.32	75	0.35	150	2.32	75	0.35				
150 G7 SSG	150	120		36.47	0.35	120		36.47	0.35				
G9 Subgrade	inf	70		36.47	0.35	70		36.47	0.35				
		Critical parameters				Critical parameters				Critical parameters			
		S1	S3	ev/et		S1	S3	ev/et		S1	S2	ev/et	
ET1 Base				342		476.29	35.6						
150 G6 Sbase		94.6	-8.97			145.21	-12.1						
150 G7 SSG				579				822					
G9 Subgrade				608				762					
		Expected layer life (E80's)				Expected layer life (E80's)				Expected layer life (E80's)			
		Neff	FOS	SF	Nt	Neff	FOS/SR	SF	Nt	Neff	FOS	SF	NI
ET1 Base		1.9E+6			1	1.9E+6			3.6E+6				
150 G6 Sbase			0.724148						168.0E+3				
150 G7 SSG									21.0E+6				
G9 Subgrade									44.7E+6				
		Expected pavement life (E80's)				Expected pavement life (E80's)				Expected pavement life (E80's)			
		Neff	R	EG	Fn	AR	L	Neff	R	EG	Fn	AR	L
ET1 Base		741.0E+3	1.1E+6	000.0E+0	524.9E-3	2.2E+6	2.9E+6	741.0E+3	2.2E+6	000.0E+0	#DIV/0!	#DIV/0!	#DIV/0!
150 G6 Sbase	Fail	741.0E+3	000.0E+0	168.0E+3		168.0E+3	741.0E+3	741.0E+3	000.0E+0	000.0E+0	#DIV/0!	#DIV/0!	#DIV/0!
150 G7 SSG		741.0E+3	696.2E+6	000.0E+0	33.3E+0	20.9E+6	21.7E+6	741.0E+3	20.9E+6	000.0E+0	#DIV/0!	#DIV/0!	#DIV/0!
G9 Subgrade		741.0E+3	426.8E+6	000.0E+0	9.6E+0	44.6E+6	45.4E+6	741.0E+3	44.6E+6	000.0E+0	#DIV/0!	#DIV/0!	#DIV/0!

Emulsion treated bases - Design catalogue

ETB33

Road category = C

Expected pavement life = 311.4E+3

	Thickness	Phase 1				Phase 2				Phase 3			
		Layer characteristics				Layer characteristics				Layer characteristics			
		E moduli	eb/phi	c/A	poisson	E moduli	eb/phi	c/A	poisson	E moduli	eb/phi	c/A	poisson
ET1 Base	100	1800	230		0.35	500	6.55	1374	0.35				
150 G6 Sbase	125	150	2.32	75	0.35	150	2.32	75	0.35				
150 G7 SSG	150	120		36.47	0.35	120		36.47	0.35				
G9 Subgrade	inf	70		36.47	0.35	70		36.47	0.35				
		Critical parameters				Critical parameters				Critical parameters			
		S1	S3	ev/et		S1	S3	ev/et		S1	S2	ev/et	
ET1 Base				412		505.95	36.38						
150 G6 Sbase		121.51	-7.88			180.11	-8.84						
150 G7 SSG				714				976					
G9 Subgrade				714				847					
		Expected layer life (E80's)				Expected layer life (E80's)				Expected layer life (E80's)			
		Neff	FOS	SF	Nt	Neff	FOS/SR	SF	Nt	Neff	FOS	SF	Nt
ET1 Base		769.7E+3			1	769.7E+3			4.2E+6				
150 G6 Sbase			0.579643			311.4E+3			104.1E+3				
150 G7 SSG						85.7E+6			3.8E+6				
G9 Subgrade						85.7E+6			15.5E+6				
		Expected pavement life (E80's)											
		Neff	R	EG	Fn	AR	L	Neff	R	EG	Fn	AR	L
ET1 Base		311.4E+3	458.2E+3	000.0E+0	185.3E-3	2.5E+6	2.8E+6	311.4E+3	2.5E+6	000.0E+0	#DIV/0!	#DIV/0!	#DIV/0!
150 G6 Sbase	Fail	311.4E+3	000.0E+0	104.1E+3		104.1E+3	311.4E+3	311.4E+3	000.0E+0	000.0E+0	#DIV/0!	#DIV/0!	#DIV/0!
150 G7 SSG		311.4E+3	85.4E+6	000.0E+0	22.8E+0	3.7E+6	4.1E+6	311.4E+3	3.7E+6	000.0E+0	#DIV/0!	#DIV/0!	#DIV/0!
G9 Subgrade		311.4E+3	85.4E+6	000.0E+0	5.5E+0	15.5E+6	15.8E+6	311.4E+3	15.5E+6	000.0E+0	#DIV/0!	#DIV/0!	#DIV/0!

Emulsion treated bases - Design catalogue

Road category = D Expected pavement life = 747.2E+3

ETB13

	Thickness	Phase 1				Phase 2				Phase 3			
		Layer characteristics				Layer characteristics				Layer characteristics			
		E moduli	eb/phi	c/A	poisson	E moduli	eb/phi	c/A	poisson	E moduli	eb/phi	c/A	poisson
ET1 Base	100	1800	230		0.35	500	6.55	1374	0.35				
150 G7 Sbase	150	120	1.4	60	0.35	120	1.4	60	0.35				
G9 Subgrade	inf	70		36.7	0.35	70		36.7	0.35				
		Critical parameters				Critical parameters				Critical parameters			
		S1	S3	ev/et		S1	S3	ev/et		S1	S2	ev/et	
ET1 Base				466		521	30.48						
150 G7 Sbase		103.91	-10.8			153.29	-15.83						
G9 Subgrade				1004				1328					
		Expected layer life (E80's)				Expected layer life (E80's)				Expected layer life (E80's)			
		Neff	FOS	SF	Nt	Neff	FOS/SR	SF	Nt	Neff	FOS	SF	Nt
ET1 Base		828.5E+3			1	828.5E+3	0.31171		9.2E+6				
150 G7 Sbase			0.523058		747.2E+3		0.354778		272.3E+3				
G9 Subgrade					4.8E+6				293.8E+3				
		Expected pavement life (E80's)				Expected pavement life (E80's)				Expected pavement life (E80's)			
		Neff	R	EG	Fn	AR	L	Neff	R	EG	Fn	AR	L
ET1 Base		747.2E+3	81.2E+3	000.0E+0	89.9E-3	903.3E+3	1.7E+6	747.2E+3	903.3E+3	000.0E+0	#DIV/0!	#DIV/0!	#DIV/0!
150 G7 Sbase		747.2E+3	000.0E+0	272.3E+3		272.3E+3	747.2E+3	747.2E+3	000.0E+0	000.0E+0	#DIV/0!	#DIV/0!	#DIV/0!
G9 Subgrade	Fail	747.2E+3	4.1E+6	000.0E+0	16.4E+0	248.2E+3	995.4E+3	747.2E+3	248.2E+3	000.0E+0	#DIV/0!	#DIV/0!	#DIV/0!

Emulsion treated bases - Design catalogue

ETB31

 Road category = D Expected pavement life = 140.4E+3

	Thickness	Phase 1				Phase 2				Phase 3			
		Layer characteristics				Layer characteristics				Layer characteristics			
		E moduli	eb/phi	c/A	poisson	E moduli	eb/phi	c/A	poisson	E moduli	eb/phi	c/A	poisson
ET1 Base	125	1800	230		0.35	500	6.55	1374	0.35				
150 G9 Sbase	150	70	0	36.3	0.35	70	0	36.3	0.35				
G10 Subgrade	inf	70		36.7	0.35	70		36.7	0.35				
		Critical parameters				Critical parameters				Critical parameters			
		S1	S3	ev/et		S1	S3	ev/et		S1	S2	ev/et	
ET1 Base				441		504.45	20.24						
150 G9 Sbase				1304				2416					
G10 Subgrade				822				1293					
		Expected layer life (E80's)				Expected layer life (E80's)				Expected layer life (E80's)			
		Neff	FOS	SF	Nt	Neff	FOS/SR	SF	Nt	Neff	FOS	SF	Nt
ET1 Base		1.1E+6			1		0.321399		6.2E+6				
150 G9 Sbase					140.4E+3				294.5E+0				
G10 Subgrade					35.6E+6				383.7E+3				
		Expected pavement life (E80's)											
		Neff	R	EG	Fn	AR	L	Neff	R	EG	Fn	AR	L
ET1 Base		140.4E+3	1.0E+6	000.0E+0	185.3E-3	5.4E+6	5.5E+6	140.4E+3	5.4E+6	000.0E+0	#DIV/0!	#DIV/0!	#DIV/0!
150 G9 Sbase	Fail	140.4E+3	000.0E+0	294.5E+0		294.5E+0	140.4E+3	140.4E+3	000.0E+0	000.0E+0	#DIV/0!	#DIV/0!	#DIV/0!
G10 Subgrade		140.4E+3	35.4E+6	000.0E+0	92.7E+0	382.2E+3	522.6E+3	140.4E+3	382.2E+3	000.0E+0	#DIV/0!	#DIV/0!	#DIV/0!

Emulsion treated bases - Design catalogue

Road category = A Expected pavement life = 5.9E+6

ETB1

ET2 Bases

	Phase 1				Phase 2				Phase 3				Phase 4							
	Thickness	Layer characteristics			E moduli	Layer characteristics			E moduli	Layer characteristics			E moduli	Layer characteristics						
		E moduli	eb/phi	c/A		poisson	E moduli	eb/phi		c/A	poisson	E moduli		eb/phi	c/A	poisson	E moduli	eb/phi	c/A	poisson
AC Surfacing	40	3000			0.35	3000			0.35	3000			0.35	3000			0.35			
ET2 Base	150	1800	145		0.35	1800	145		0.35	1800	145		0.35	500	6.55	1374	0.35			
125 C4	125	1500	145		0.35	1500	145		0.35	225	2.8	100	0.35	225	2.8	100	0.35			
125 C4	125	1500	145		0.35	225	2.8	100	0.35	225	2.8	100	0.35	225	2.8	100	0.35			
G7 Selected	150	120		36.3	0.35	120		36.3	0.35	120		36.3	0.35	120		36.3	0.35			
G9 Subbase	inf	70																		
		Critical parameters				Critical parameters				Critical parameters				Critical parameters						
		S1	S3	ev/et		S1	S3	ev/et		S1	S3	ev/et		S1	S3	ev/et				
AC Surfacing				26				21				16					176			
ET2 Base				44				58				174					375.29			
125 C4				41				105		61.45	-5.71						88.03			
125 C4				70		30.37	-9.65			39.66	-10.78						51.21			
G7 Selected				171				214				274					352			
		Expected layer life (E80's)					Expected layer life (E80's)					Expected layer life (E80's)					Expected layer life (E80's)			
		Neff	FOS	SF	Nt	Neff	FOS	SF	Nt	Neff	FOS/SR	SF	Nt	Neff	FOS/SR	SF	Nt			
AC Surfacing		14.4E+9			1.75	25.2E+9			1.75	75.2E+9			1.75	302.5E+9			1.75			
ET2 Base		33.9E+6		1	33.9E+6	43.0E+9		1	25.5E+6	2.4E+6		1	2.4E+6		0.21453		3.0E+6			
125 C4		2.9E+6		1.1567779	3.4E+6	25.5E+6		1.1567779	1.4E+6	1.4889815		22.9E+6		1.005429		1.3E+6				
125 C4		1.9E+6		1.1567779	2.2E+6	1.2E+6		2.4987506	9.8E+9	1.9825535		441.5E+6		1.481043		21.8E+6				
G7 Selected					93.3E+12				9.9E+12			836.6E+9				68.3E+9				
		Neff	R	EG	Fn	AR	L	Neff	R	EG	Fn	AR	L	Neff	R	EG	Fn	AR	L	
AC Surfacing		2.2E+6	25.2E+9	000.0E+0	0.3352104	75.2E+9	75.2E+9	2.7E+6	75.2E+9	000.0E+0	0.2486473	302.5E+9	302.5E+9	4.9E+6	302.5E+9	000.0E+0	213534.7	1.4E+6	6.3E+6	
ET2 Base		2.2E+6	31.7E+6	000.0E+0	1.3284488	23.9E+6	26.1E+6	2.7E+6	23.4E+6	000.0E+0	10.747623	2.2E+6	4.9E+6	4.9E+6	000.0E+0	3.0E+6	3.0E+6	3.0E+6	7.9E+6	
125 C4		2.2E+6	1.1E+6	000.0E+0	2.4888795	460.3E+3	2.7E+6	2.7E+6	000.0E+0	22.9E+6		22.9E+6	25.6E+6	4.9E+6	20.7E+6	000.0E+0	20.33252	1.0E+6	5.9E+6	
125 C4		2.2E+6	000.0E+0	9.8E+9		9.8E+9	9.8E+9	2.7E+6	9.8E+9	000.0E+0	22.12361	441.3E+6	444.0E+6	4.9E+6	439.2E+6	000.0E+0	20.37161	21.6E+6	26.4E+6	
G7 Selected		2.2E+6	93.3E+12	000.0E+0	9.4227275	9.9E+12	9.9E+12	2.7E+6	9.9E+12	000.0E+0	11.840444	836.6E+9	836.6E+9	4.9E+6	836.6E+9	000.0E+0	12.24397	68.3E+9	68.3E+9	

Emulsion treated bases - Design catalogue

ETB6

ET2 Bases Road category = A

Expected pavement life = 2.9E+6

	Thickness	Phase 1				Phase 2				Phase 3			
		Layer characteristics				Layer characteristics				Layer characteristics			
		E moduli	eb/phi	c/A	poisson	E moduli	eb/phi	c/A	poisson	E moduli	eb/phi	c/A	poisson
AC Surfacing	40	3000			0.35	3000			0.35	3000			0.35
ET2 Base	125	1800	145		0.35	1800	145		0.35	500	6.55	1374	0.35
150 C4	150	1500	145		0.35	200	2.8	100	0.35	200	2.8	100	0.35
150 G7	150	120		36.3	0.35	120		36.3	0.35	120		36.3	0.35
G9 Subgrade	inf	70		36.3	0.35	70		36.3	0.35	70		36.3	0.35
		Critical parameters				Critical parameters				Critical parameters			
		S1	S3	ev/et		S1	S3	ev/et		S1	S3	ev/et	
AC Surfacing				19				14				182	
ET2 Base				60				212		385.68	32.38		
150 C4				116		65.15	-11.99			89.93	-20.22		
150 G7				198				284				346	
G9 Subgrade				274				406				495	
		Expected layer life (E80's)				Expected layer life (E80's)				Expected layer life (E80's)			
		Neff	FOS	SF	Nt	Neff	FOS	SF	Nt	Neff	FOS/SR	SF	Nt
AC Surfacing		71.7E+9			1.75 125.6E+9	342.4E+9			1.75 599.2E+9	681.9E+3			1.75 1.2E+6
ET2 Base		24.5E+6			1 24.5E+6	1.1E+6			1 1.1E+6		0.2227492		3.4E+6
150 C4		1.0E+6		1.363013	1.4E+6		1.2963443		7.2E+6		0.9078529		700.1E+3
150 G7					21.5E+12				584.5E+9				81.1E+9
G9 Subgrade					836.6E+9				16.4E+9				2.3E+9
		Expected pavement life (E80's)											
		Neff	R	EG	Fn	AR	L	Neff	R	EG	Fn	AR	L
AC Surfacing		1.4E+6	125.6E+9	000.0E+0	0.20954107	599.2E+9	599.2E+9	2.4E+6	599.2E+9	000.0E+0	502071.04	1.2E+6	3.6E+6
ET2 Base		1.4E+6	23.2E+6	000.0E+0	21.8359662	1.1E+6	2.4E+6	2.4E+6	000.0E+0	3.4E+6		3.4E+6	5.9E+6
150 C4		1.4E+6	000.0E+0	7.2E+6		7.2E+6	8.6E+6	2.4E+6	6.1E+6	000.0E+0	12.238699	501.5E+3	2.9E+6
150 G7		1.4E+6	21.5E+12	000.0E+0	36.8579773	584.5E+9	584.5E+9	2.4E+6	584.5E+9	000.0E+0	7.2040808	81.1E+9	81.1E+9
G9 Subgrade		1.4E+6	836.6E+9	000.0E+0	51.0216745	16.4E+9	16.4E+9	2.4E+6	16.4E+9	000.0E+0	7.2581716	2.3E+9	2.3E+9

Emulsion treated bases - Design catalogue

ETB7

Road category = B

Expected pavement life = 7.0E+6

	Thickness	Phase 1				Phase 2				Phase 3			
		Layer characteristics				Layer characteristics				Layer characteristics			
		E moduli	eb/phi	c/A	poisson	E moduli	eb/phi	c/A	poisson	E moduli	eb/phi	c/A	poisson
AC Surfacing	40	3000			0.35	3000			0.35	3000			0.35
ET2 Base	125	1800	145		0.35	1800	145		0.35	500	6.55	1374	0.35
200 C4	200	1500	145		0.35	200	2.8	100	0.35	200	2.8	100	0.35
150 G7	150	120		36.38	0.35	120		36.38	0.35	120		36.38	0.35
G9 Subgrade	inf	70		36.38	0.35	70		36.38	0.35	70		36.38	0.35
		Critical parameters				Critical parameters				Critical parameters			
		S1	S3	ev/et		S1	S3	ev/et		S1	S3	ev/et	
AC Surfacing				22				15				182	
ET2 Base				53				208		386.67	33.67		
200 C4				94		60.2	-9.56			81.18	-15.86		
150 G7				228				363				456	
G9 Subgrade				225				361				432	
		Expected layer life (E80's)				Expected layer life (E80's)				Expected layer life (E80's)			
		Neff	FOS	SF	Nt	Neff	FOS	SF	Nt	Neff	FOS/SR	SF	Nt
AC Surfacing		38.6E+9			1.75	67.5E+9			1.75	479.9E+9			1.75
ET2 Base		36.8E+6			1	36.8E+6			1	1.6E+6	0.221381		1.6E+6
200 C4		1.8E+6		1.892344		3.4E+6	1.433486			27.7E+6	1.030503		27.7E+6
150 G7						6.3E+12				60.4E+9			60.4E+9
G9 Subgrade						7.2E+12				63.8E+9			63.8E+9
		Expected pavement life (E80's)											
		Neff	R	EG	Fn	AR	L	Neff	R	EG	Fn	AR	L
AC Surfacing		3.4E+6	67.5E+9	000.0E+0	0.1407162	479.9E+9	479.9E+9	4.9E+6	479.9E+9	000.0E+0	354987.9	1.4E+6	6.2E+6
ET2 Base		3.4E+6	33.4E+6	000.0E+0	23.2061689	1.4E+6	4.9E+6	4.9E+6	000.0E+0	4.3E+6		4.3E+6	9.1E+6
200 C4		3.4E+6	000.0E+0	27.7E+6		27.7E+6	31.1E+6	4.9E+6	26.2E+6	000.0E+0	12.60741	2.1E+6	7.0E+6
150 G7		3.4E+6	6.3E+12	000.0E+0	104.644831	60.4E+9	60.4E+9	4.9E+6	60.4E+9	000.0E+0	9.786032	6.2E+9	6.2E+9
G9 Subgrade		3.4E+6	7.2E+12	000.0E+0	113.043823	63.8E+9	63.8E+9	4.9E+6	63.8E+9	000.0E+0	6.022664	10.6E+9	10.6E+9

Emulsion treated bases - Design catalogue

ETB8

Road category = B

Expected pavement life = 1.5E+6

	Thickness	Phase 1				Phase 2				Phase 3			
		Layer characteristics				Layer characteristics				Layer characteristics			
		E moduli	eb/phi	c/A	poisson	E moduli	eb/phi	c/A	poisson	E moduli	eb/phi	c/A	poisson
ET2 Base	150	1800	145		0.35	500	6.55	1374	0.35				
150 G5 Sbase	150	200	3.5	120	0.35	200	3.5	120	0.35				
150 G7 SSG	150	120		36.38	0.35	120		36.38	0.35				
G9 Subgrade	inf	70		36.38	0.35	70		36.38	0.35				
		Critical parameters				Critical parameters				Critical parameters			
		S1	S3	ev/et		S1	S3	ev/et		S1	S2	ev/et	
ET2 Base				256		443.4	-39.09						
150 G5 Sbase		75.05	-18.41			115.24	-21.86						
150 G7 SSG				466				625					
G9 Subgrade				477				614					
		Expected layer life (E80's)				Expected layer life (E80's)				Expected layer life (E80's)			
		Neff	FOS	SF	Nt	Neff	FOS/SR	SF	Nt	Neff	FOS	SF	Nt
ET2 Base		599.3E+3			1 599.3E+3		0.351157		989.8E+3				
150 G5 Sbase			1.283972		11.3E+6		0.875274		972.4E+3				
150 G7 SSG					5.0E+9				263.8E+6				
G9 Subgrade					3.9E+9				315.0E+6				
		Expected pavement life (E80's)											
		Neff	R	EG	Fn	AR	L	Neff	R	EG	Fn	AR	L
ET2 Base		599.3E+3	000.0E+0	989.8E+3		989.8E+3	1.6E+6	1.5E+6	69.0E+3	000.0E+0	#DIV/0!	#DIV/0!	#DIV/0!
150 G5 Sbase		599.3E+3	10.7E+6	000.0E+0	11.6E+0	920.8E+3	1.5E+6	1.5E+6	000.0E+0	000.0E+0	#DIV/0!	#DIV/0!	#DIV/0!
150 G7 SSG		599.3E+3	5.0E+9	000.0E+0	18.8E+0	263.7E+6	264.3E+6	1.5E+6	262.8E+6	000.0E+0	#DIV/0!	#DIV/0!	#DIV/0!
G9 Subgrade		599.3E+3	3.9E+9	000.0E+0	12.5E+0	315.0E+6	315.6E+6	1.5E+6	314.0E+6	000.0E+0	#DIV/0!	#DIV/0!	#DIV/0!

Emulsion treated bases - Design catalogue

ETB29

Road category = B Expected pavement life = 1.2E+6

	Thickness	Phase 1				Phase 2				Phase 3			
		Layer characteristics				Layer characteristics				Layer characteristics			
		E moduli	eb/phi	c/A	poisson	E moduli	eb/phi	c/A	poisson	E moduli	eb/phi	c/A	poisson
ET2 Base	125	1800	145		0.35	1800	145		0.35	500	6.55	1374	0.35
150 C4	150	1500	145		0.35	200	2.8	100	0.35	200	2.8	100	0.35
150 G7	150	120		36.38	0.35	120		36.38	0.35	120		36.38	0.35
) Subgrade	inf	70		36.38	0.35	70		36.38	0.35	70		36.38	0.35
		Critical parameters				Critical parameters				Critical parameters			
		S1	S3	ev/et		S1	S3	ev/et		S1	S3	ev/et	
ET2 Base				60				303		466	41.77		
150 C4				164		92.93	-19.19			138.49	-20.79		
150 G7				341				542				718	
) Subgrade				356				551				679	
		Expected layer life (E80's)				Expected layer life (E80's)				Expected layer life (E80's)			
		Neff	FOS	SF	Nt	Neff	FOS	SF	Nt	Neff	FOS/SR	SF	Nt
ET2 Base		32.0E+6			1 32.0E+6	231.0E+3			1 231.0E+3		0.257485		2.8E+6
150 C4		670.0E+3		1.363013	913.2E+3		0.891902		1.1E+6		0.627825		220.4E+3
150 G7					112.8E+9				1.1E+9				65.9E+6
) Subgrade					73.4E+9				930.0E+6				115.2E+6
		Expected pavement life (E80's)				Expected pavement life (E80's)				Expected pavement life (E80's)			
		Neff	R	EG	Fn	AR	L	Neff	R	EG	Fn	AR	L
ET2 Base		913.2E+3	31.0E+6	000.0E+0	138.329177	224.4E+3	1.1E+6	1.1E+6	000.0E+0	2.8E+6		2.8E+6	4.0E+6
150 C4		913.2E+3	000.0E+0	1.1E+6		1.1E+6	2.0E+6	1.1E+6	850.1E+3	000.0E+0	9.018003	94.3E+3	1.2E+6
150 G7		913.2E+3	112.8E+9	000.0E+0	102.907985	1.1E+9	1.1E+9	1.1E+6	1.1E+9	000.0E+0	16.65749	65.8E+6	66.9E+6
) Subgrade		913.2E+3	73.4E+9	000.0E+0	78.8889197	930.0E+6	930.9E+6	1.1E+6	929.8E+6	000.0E+0	8.083559	115.0E+6	116.2E+6

Emulsion treated bases - Design catalogue

Road category = B

Expected pavement life = 844.9E+3

ETB9

	Thickness	Phase 1				Phase 2				Phase 3			
		Layer characteristics				Layer characteristics				Layer characteristics			
		E moduli	eb/phi	c/A	poisson	E moduli	eb/phi	c/A	poisson	E moduli	eb/phi	c/A	poisson
ET2 Base	125	1800	145		0.35	1800	145		0.35	500	6.55	1374	0.35
150 C4	125	1500	145		0.35	200	2.8	100	0.35	200	2.8	100	0.35
150 G7	150	120		36.38	0.35	120		36.38	0.35	120		36.38	0.35
G9 Subgrade	inf	70		36.38	0.35	70		36.38	0.35	70		36.38	0.35
		Critical parameters				Critical parameters				Critical parameters			
		S1	S3	ev/et		S1	S3	ev/et		S1	S3	ev/et	
ET2 Base				67				309		468.6	41.69		
150 C4				185		97.6	-21.84			148.29	-24.45		
150 G7				394				584				811	
G9 Subgrade				402				590				733	
		Expected layer life (E80's)				Expected layer life (E80's)				Expected layer life (E80's)			
		Neff	FOS	SF	Nt	Neff	FOS	SF	Nt	Neff	FOS/SR	SF	Nt
ET2 Base		27.7E+6			1 27.7E+6	204.5E+3			1 204.5E+3		0.259194		2.8E+6
150 C4		496.9E+3		1.156778	574.8E+3		0.83724		774.1E+3		0.578905		164.4E+3
150 G7					26.6E+9				519.8E+6				19.5E+6
G9 Subgrade					21.8E+9				469.3E+6				53.6E+6
		Expected pavement life (E80's)				Expected pavement life (E80's)				Expected pavement life (E80's)			
		Neff	R	EG	Fn	AR	L	Neff	R	EG	Fn	AR	L
ET2 Base		574.8E+3	27.1E+6	000.0E+0	135.551225	200.3E+3	775.0E+3	775.0E+3	000.0E+0	2.8E+6		2.8E+6	3.6E+6
150 C4		574.8E+3	000.0E+0	774.1E+3		774.1E+3	1.3E+6	775.0E+3	573.8E+3	000.0E+0	8.206803	69.9E+3	844.9E+3
150 G7		574.8E+3	26.6E+9	000.0E+0	51.1877751	519.8E+6	520.4E+6	775.0E+3	519.6E+6	000.0E+0	26.70242	19.5E+6	20.2E+6
G9 Subgrade		574.8E+3	21.8E+9	000.0E+0	46.3724013	469.3E+6	469.9E+6	775.0E+3	469.1E+6	000.0E+0	8.77081	53.5E+6	54.3E+6

Emulsion treated bases - Design catalogue

Road category = B Expected pavement life = 662.5E+3

ETB14

	Thickness	Phase 1				Phase 2				Phase 3			
		Layer characteristics				Layer characteristics				Layer characteristics			
		E moduli	eb/phi	c/A	poisson	E moduli	eb/phi	c/A	poisson	E moduli	eb/phi	c/A	poisson
ET2 Base	125	1800	145		0.35	500	6.55	1374	0.35				
150 G5 Sbase	150	200	3.5	120	0.35	200	3.5	120	0.35				
150 G7 SSG	150	120		36.38	0.35	120		36.38	0.35				
G9 Subgrade	inf	70		36.38	0.35	70		36.38	0.35				
		Critical parameters				Critical parameters				Critical parameters			
		S1	S3	ev/et		S1	S3	ev/et		S1	S2	ev/et	
ET2 Base				303		466.78	41.77						
150 G5 Sbase		93.93	-19.19			138.49	-20.79						
150 G7 SSG				542				718					
G9 Subgrade				551				679					
		Expected layer life (E80's)				Expected layer life (E80's)				Expected layer life (E80's)			
		Neff	FOS	SF	Nt	Neff	FOS/SR	SF	Nt	Neff	FOS	SF	Nt
ET2 Base		231.0E+3			1 231.0E+3		0.257958		2.8E+6				
150 G5 Sbase			1.06082		3.0E+6		0.75339		468.1E+3				
150 G7 SSG					1.1E+9				65.9E+6				
G9 Subgrade					930.0E+6				115.2E+6				
		Expected pavement life (E80's)				Expected pavement life (E80's)				Expected pavement life (E80's)			
		Neff	R	EG	Fn	AR	L	Neff	R	EG	Fn	AR	L
ET2 Base		231.0E+3	000.0E+0	2.8E+6		2.8E+6	3.0E+6	662.5E+3	2.4E+6	000.0E+0	#DIV/0!	#DIV/0!	#DIV/0!
150 G5 Sbase		231.0E+3	2.7E+6	000.0E+0	6.3E+0	431.6E+3	662.5E+3	662.5E+3	000.0E+0	000.0E+0	#DIV/0!	#DIV/0!	#DIV/0!
150 G7 SSG		231.0E+3	1.1E+9	000.0E+0	16.6E+0	65.9E+6	66.1E+6	662.5E+3	65.4E+6	000.0E+0	#DIV/0!	#DIV/0!	#DIV/0!
G9 Subgrade		231.0E+3	929.8E+6	000.0E+0	8.1E+0	115.1E+6	115.4E+6	662.5E+3	114.7E+6	000.0E+0	#DIV/0!	#DIV/0!	#DIV/0!

Emulsion treated bases - Design catalogue

Road category = C Expected pavement life = 430.6E+3

ETB11

	Thickness	Phase 1				Phase 2				Phase 3			
		Layer characteristics				Layer characteristics				Layer characteristics			
		E moduli	eb/phi	c/A	poisson	E moduli	eb/phi	c/A	poisson	E moduli	eb/phi	c/A	poisson
ET2 Base	125	1800	145		0.35	500	6.55	1374	0.35				
150 G6 Sbase	150	150	2.32	84	0.35	150	2.32	84	0.35				
150 G7 SSG	150	120		36.47	0.35	120		36.47	0.35				
G9 Subgrade	inf	70		36.47	0.35	70		36.47	0.35				
		Critical parameters				Critical parameters				Critical parameters			
		S1	S3	ev/et		S1	S3	ev/et		S1	S2	ev/et	
ET2 Base				338		475.09	35.55						
150 G6 Sbase		89.96	-8.1			135.43	-10.75						
150 G7 SSG				547				731					
G9 Subgrade				570				708					
		Expected layer life (E80's)				Expected layer life (E80's)				Expected layer life (E80's)			
		Neff	FOS	SF	Nt	Neff	FOS/SR	SF	Nt	Neff	FOS	SF	Nt
ET2 Base		157.3E+3			1 157.3E+3		0.273541		3.6E+6				
150 G6 Sbase			0.856618		1.6E+6		0.574634		302.2E+3				
150 G7 SSG					1.2E+9				67.7E+6				
G9 Subgrade					815.2E+6				93.3E+6				
		Expected pavement life (E80's)											
		Neff	R	EG	Fn	AR	L	Neff	R	EG	Fn	AR	L
ET2 Base	Fail	157.3E+3	000.0E+0	3.6E+6		3.6E+6	3.8E+6	430.6E+3	3.3E+6	000.0E+0	#DIV/0!	#DIV/0!	#DIV/0!
150 G6 Sbase		157.3E+3	1.5E+6	000.0E+0	5.4E+0	273.2E+3	430.6E+3	430.6E+3	000.0E+0	000.0E+0	#DIV/0!	#DIV/0!	#DIV/0!
150 G7 SSG		157.3E+3	1.2E+9	000.0E+0	18.2E+0	67.7E+6	67.9E+6	430.6E+3	67.5E+6	000.0E+0	#DIV/0!	#DIV/0!	#DIV/0!
G9 Subgrade		157.3E+3	815.0E+6	000.0E+0	8.7E+0	93.2E+6	93.4E+6	430.6E+3	93.0E+6	000.0E+0	#DIV/0!	#DIV/0!	#DIV/0!

Emulsion treated bases - Design catalogue

ETB30

Road category = C Expected pavement life = 280.2E+3

	Thickness	Phase 1				Phase 2				Phase 3			
		Layer characteristics				Layer characteristics				Layer characteristics			
		E moduli	eb/phi	c/A	poisson	E moduli	eb/phi	c/A	poisson	E moduli	eb/phi	c/A	poisson
ET2 Base	125	1800	145		0.35	500	6.55	1374	0.35				
150 G6 Sbase	150	150	2.32	75	0.35	150	2.32	75	0.35				
150 G7 SSG	150	120		36.47	0.35	120		36.47	0.35				
G9 Subgrade	inf	70		36.47	0.35	70		36.47	0.35				
		Critical parameters				Critical parameters				Critical parameters			
		S1	S3	ev/et		S1	S3	ev/et		S1	S2	ev/et	
ET2 Base				342		476.29	35.6						
150 G6 Sbase		94.6	-8.97			145.21	-12.1						
150 G7 SSG				579				822					
G9 Subgrade				608				762					
		Expected layer life (E80's)				Expected layer life (E80's)				Expected layer life (E80's)			
		Neff	FOS	SF	Nt	Neff	FOS/SR	SF	Nt	Neff	FOS	SF	Nt
ET2 Base		145.1E+3			1 145.1E+3		0.274201		3.6E+6				
150 G6 Sbase			0.724148		741.0E+3		0.476766		168.0E+3				
150 G7 SSG					697.0E+6				21.0E+6				
G9 Subgrade					427.5E+6				44.7E+6				
		Expected pavement life (E80's)				Expected pavement life (E80's)				Expected pavement life (E80's)			
		Neff	R	EG	Fn	AR	L	Neff	R	EG	Fn	AR	L
ET2 Base	Fail	145.1E+3	000.0E+0	3.6E+6		3.6E+6	3.7E+6	280.2E+3	3.5E+6	000.0E+0	#DIV/0!	#DIV/0!	#DIV/0!
150 G6 Sbase		145.1E+3	595.9E+3	000.0E+0	4.4E+0	135.1E+3	280.2E+3	280.2E+3	000.0E+0	000.0E+0	#DIV/0!	#DIV/0!	#DIV/0!
150 G7 SSG		145.1E+3	696.8E+6	000.0E+0	33.3E+0	21.0E+6	21.1E+6	280.2E+3	20.8E+6	000.0E+0	#DIV/0!	#DIV/0!	#DIV/0!
G9 Subgrade		145.1E+3	427.4E+6	000.0E+0	9.6E+0	44.7E+6	44.8E+6	280.2E+3	44.6E+6	000.0E+0	#DIV/0!	#DIV/0!	#DIV/0!

Emulsion treated bases - Design catalogue

Road category = C Expected pavement life = 127.4E+3

ETB33

	Thickness	Phase 1				Phase 2				Phase 3			
		Layer characteristics				Layer characteristics				Layer characteristics			
		E moduli	eb/phi	c/A	poisson	E moduli	eb/phi	c/A	poisson	E moduli	eb/phi	c/A	poisson
ET2 Base	100	1800	145		0.35	500	6.55	1374	0.35				
150 G6 Sbase	125	150	2.32	75	0.35	150	2.32	75	0.35				
150 G7 SSG	150	120		36.47	0.35	120		36.47	0.35				
G9 Subgrade	inf	70		36.47	0.35	70		36.47	0.35				
		Critical parameters				Critical parameters				Critical parameters			
		S1	S3	ev/et		S1	S3	ev/et		S1	S2	ev/et	
ET2 Base				412		505.95	36.38						
150 G6 Sbase		121.51	-7.88			180.11	-8.84						
150 G7 SSG				714				976					
G9 Subgrade				714				847					
		Expected layer life (E80's)				Expected layer life (E80's)				Expected layer life (E80's)			
		Neff	FOS	SF	Nt	Neff	FOS/SR	SF	Nt	Neff	FOS	SF	Nt
ET2 Base		35.1E+3			1 35.1E+3		0.291244		4.2E+6				
150 G6 Sbase			0.579643		311.4E+3		0.39693		104.1E+3				
150 G7 SSG					85.7E+6				3.8E+6				
G9 Subgrade					85.7E+6				15.5E+6				
		Expected pavement life (E80's)											
		Neff	R	EG	Fn	AR	L	Neff	R	EG	Fn	AR	L
ET2 Base	Fail	35.1E+3	000.0E+0	4.2E+6		4.2E+6	4.2E+6	127.4E+3	4.1E+6	000.0E+0	#DIV/0!	#DIV/0!	#DIV/0!
150 G6 Sbase		35.1E+3	276.4E+3	000.0E+0	3.0E+0	92.4E+3	127.4E+3	127.4E+3	000.0E+0	000.0E+0	#DIV/0!	#DIV/0!	#DIV/0!
150 G7 SSG		35.1E+3	85.7E+6	000.0E+0	22.8E+0	3.8E+6	3.8E+6	127.4E+3	3.7E+6	000.0E+0	#DIV/0!	#DIV/0!	#DIV/0!
G9 Subgrade		35.1E+3	85.7E+6	000.0E+0	5.5E+0	15.5E+6	15.6E+6	127.4E+3	15.4E+6	000.0E+0	#DIV/0!	#DIV/0!	#DIV/0!

Emulsion treated bases - Design catalogue

ETB12

Road category = D

Expected pavement life = 750.0E+3

	Thickness	Phase 1				Phase 2				Phase 3			
		Layer characteristics				Layer characteristics				Layer characteristics			
		E moduli	eb/phi	c/A	poisson	E moduli	eb/phi	c/A	poisson	E moduli	eb/phi	c/A	poisson
ET2 Base	125	1800	145		0.35	500	6.55	1374	0.35				
150 G7 Sbase	150	120	1.45	70	0.35	120	1.45	70	0.35				
G9 Subgrade	inf	70		36.7	0.35	70		36.7	0.35				
		Critical parameters				Critical parameters				Critical parameters			
		S1	S3	ev/et		S1	S3	ev/et		S1	S2	ev/et	
ET2 Base				382		487.4	31.05						
150 G7 Sbase		81.11	-10.26			124.1	-16.74						
G9 Subgrade				834				1125					
		Expected layer life (E80's)				Expected layer life (E80's)				Expected layer life (E80's)			
		Neff	FOS	SF	Nt	Neff	FOS/SR	SF	Nt	Neff	FOS	SF	Nt
ET2 Base		138.4E+3			1	138.4E+3			8.4E+6				
150 G7 Sbase			0.766116						639.2E+3				
G9 Subgrade									1.5E+6				
		Expected pavement life (E80's)											
		Neff	R	EG	Fn	AR	L	Neff	R	EG	Fn	AR	L
ET2 Base	Fail	138.4E+3	000.0E+0	8.4E+6		8.4E+6	8.6E+6	750.0E+3	7.8E+6	000.0E+0	#DIV/0!	#DIV/0!	#DIV/0!
150 G7 Sbase		138.4E+3	3.1E+6	000.0E+0	5.0E+0	611.6E+3	750.0E+3	750.0E+3	000.0E+0	000.0E+0	#DIV/0!	#DIV/0!	#DIV/0!
G9 Subgrade		138.4E+3	30.6E+6	000.0E+0	19.9E+0	1.5E+6	1.7E+6	750.0E+3	924.8E+3	000.0E+0	#DIV/0!	#DIV/0!	#DIV/0!

Emulsion treated bases - Design catalogue

ETB13

Road category = D Expected pavement life = 288.3E+3

	Thickness	Phase 1				Phase 2				Phase 3			
		Layer characteristics				Layer characteristics				Layer characteristics			
		E moduli	eb/phi	c/A	poisson	E moduli	eb/phi	c/A	poisson	E moduli	eb/phi	c/A	poisson
ET2 Base	100	1800	145		0.35	500	6.55	1374	0.35				
150 G7 Sbase	150	120	1.4	60	0.35	120	1.4	60	0.35				
G9 Subgrade	inf	70		36.7	0.35	70		36.7	0.35				
		Critical parameters				Critical parameters				Critical parameters			
		S1	S3	ev/et		S1	S3	ev/et		S1	S2	ev/et	
ET2 Base				466		521	30.48						
150 G7 Sbase		103.91	-10.8			153.29	-15.83						
G9 Subgrade				1004				1328					
		Expected layer life (E80's)				Expected layer life (E80's)				Expected layer life (E80's)			
		Neff	FOS	SF	Nt	Neff	FOS/SR	SF	Nt	Neff	FOS	SF	Nt
ET2 Base		25.2E+3			1	25.2E+3			9.2E+6				
150 G7 Sbase			0.523058		747.2E+3		0.354778		272.3E+3				
G9 Subgrade					4.8E+6				293.8E+3				
		Expected pavement life (E80's)											
		Neff	R	EG	Fn	AR	L	Neff	R	EG	Fn	AR	L
ET2 Base	Fail	25.2E+3	000.0E+0	9.2E+6		9.2E+6	9.2E+6	288.3E+3	8.9E+6	000.0E+0	#DIV/0!	#DIV/0!	#DIV/0!
150 G7 Sbase		25.2E+3	722.0E+3	000.0E+0	2.7E+0	263.1E+3	288.3E+3	288.3E+3	000.0E+0	000.0E+0	#DIV/0!	#DIV/0!	#DIV/0!
G9 Subgrade		25.2E+3	4.8E+6	000.0E+0	16.4E+0	292.2E+3	317.4E+3	288.3E+3	29.1E+3	000.0E+0	#DIV/0!	#DIV/0!	#DIV/0!

Emulsion treated bases - Design catalogue

Road category = D Expected pavement life = 42.0E+3

ETB31

	Thickness	Phase 1				Phase 2				Phase 3			
		Layer characteristics				Layer characteristics				Layer characteristics			
		E moduli	eb/phi	c/A	poisson	E moduli	eb/phi	c/A	poisson	E moduli	eb/phi	c/A	poisson
ET2 Base	125	1800	145		0.35	500	6.55	1374	0.35				
150 G9 Sbase	150	70	0	36.3	0.35	70	0	36.3	0.35				
G10 Subgrade	inf	70		36.7	0.35	70		36.7	0.35				
		Critical parameters				Critical parameters				Critical parameters			
		S1	S3	ev/et		S1	S3	ev/et		S1	S2	ev/et	
ET2 Base				441		504.45	20.24						
150 G9 Sbase				1304				2416					
G10 Subgrade				822				1293					
		Expected layer life (E80's)				Expected layer life (E80's)				Expected layer life (E80's)			
		Neff	FOS	SF	Nt	Neff	FOS/SR	SF	Nt	Neff	FOS	SF	Nt
ET2 Base		41.8E+3			1		0.321399		6.2E+6				
150 G9 Sbase					140.4E+3				294.5E+0				
G10 Subgrade					35.6E+6				383.7E+3				
		Expected pavement life (E80's)											
		Neff	R	EG	Fn	AR	L	Neff	R	EG	Fn	AR	L
ET2 Base	Fail	41.8E+3	000.0E+0	6.2E+6		6.2E+6	6.2E+6	42.0E+3	6.2E+6	000.0E+0	#DIV/0!	#DIV/0!	#DIV/0!
150 G9 Sbase		41.8E+3	98.5E+3	000.0E+0	476.6E+0	206.8E+0	42.0E+3	42.0E+3	000.0E+0	000.0E+0	#DIV/0!	#DIV/0!	#DIV/0!
G10 Subgrade		41.8E+3	35.5E+6	000.0E+0	92.7E+0	383.3E+3	425.1E+3	42.0E+3	383.1E+3	000.0E+0	#DIV/0!	#DIV/0!	#DIV/0!

Emulsion treated bases - Design catalogue

ETB34

Road category = D Expected pavement life = 4.3E+3

	Thickness	Phase 1				Phase 2				Phase 3			
		Layer characteristics				Layer characteristics				Layer characteristics			
		E moduli	eb/phi	c/A	poisson	E moduli	eb/phi	c/A	poisson	E moduli	eb/phi	c/A	poisson
ET2 Base	100	1800	145		0.35	500	6.55	1374	0.35				
150 G9 Sbase	150	70	0	36.3	0.35	70	0	36.3	0.35				
G10 Subgrade	inf	70		36.7	0.35	70		36.7	0.35				
		Critical parameters				Critical parameters				Critical parameters			
		S1	S3	ev/et		S1	S3	ev/et		S1	S2	ev/et	
ET2 Base				553		323.18	-213.22						
150 G9 Sbase				1708				3065					
G10 Subgrade				1009				1360					
		Expected layer life (E80's)				Expected layer life (E80's)				Expected layer life (E80's)			
		Neff	FOS	SF	Nt	Neff	FOS/SR	SF	Nt	Neff	FOS	SF	Nt
ET2 Base		4.3E+3			1	4.3E+3							
150 G9 Sbase							0.390393						4.6E+6
G10 Subgrade													27.3E+0
													231.5E+3
		Expected pavement life (E80's)											
		Neff	R	EG	Fn	AR	L	Neff	R	EG	Fn	AR	L
ET2 Base	Fail	4.3E+3	000.0E+0	4.6E+6		4.6E+6	4.6E+6	4.3E+3	4.6E+6	000.0E+0	#DIV/0!	#DIV/0!	#DIV/0!
150 G9 Sbase		4.3E+3	5.1E+3	000.0E+0	346.3E+0	14.8E+0	4.3E+3	4.3E+3	000.0E+0	000.0E+0	#DIV/0!	#DIV/0!	#DIV/0!
G10 Subgrade		4.3E+3	4.6E+6	000.0E+0	19.8E+0	231.3E+3	235.6E+3	4.3E+3	231.3E+3	000.0E+0	#DIV/0!	#DIV/0!	#DIV/0!